The role of the Tousled Like Kinases in genome stability and mammalian development

Helena González Burón

Memòria presentada per

Helena González Burón

per obtenir el grau de doctor per la Universitat de Barcelona en el Programa de Doctorat de BIOMEDICINA al 2014.

Aquest treball ha estat realitzat a l'Institut de Recerca Biomèdica de Barcelona sota la direcció del Dr. Travis H. Stracker (Genomic Instability and Cancer Lab) i porta el títol:

The role of the Tousled Like Kinases in genome stability and mammalian development.

Travis H. Stracker
Director de la tesi

Helena González Burón
Doctorant

Para Á y Á

SAMUEL: (Alzándose.) Me llamo Samuel y el tiempo... se me va.
MARIONETA I: ¿Así que se le va el tiempo?
SAMUEL: Un poco.
MARIONETA I: ¿y por qué no lo retiene?
SAMUEL: ¿Al tiempo?
MARIONETA I: Claro.
SAMUEL: No es fácil.
MARIONETA I: Usted le dice...
SAMUEL: ¿A quién?
MARIONETA I: Al tiempo. (Pausa.) Usted le dice.... (Como buscando algo.) Señor Tiempo, ¿acepta una tertulia?
SAMUEL: ¿Una tertulia con el tiempo?
MARIONETA I: ¿Y por qué no?

Fragmento de "La Navaja", E. Quiles

Acknowledgements.

I would like to thank my supervisor, **Travis Stracker**, for believing in my potential and driving my transformation from a student to a scientist. Thanks to **Joan Guinovart**, IRB director, for his continuous support in both, scientific and artistic projects.

Thanks to all the members of the Genomic Instability and Cancer Lab for their help, especially **Phillip and Aida** for sharing TLKs nightmares and affairs. And thanks to the eternal smile of **Joana** (the lab is brighter with you).

Thanks **to Marta Vilaseca** for her never-ending lists of "potential" TLK-interactors (we corroborated one!). To **Julien, Lidia and Anna,** the SPIM team, for bringing a whole new 3dimension into my PhD. Thanks to **Jaume and Sonia** for all the support and help with FACs and sortings. And especial thanks to **Tanya Yates** for her constant advise with english during my thesis writing.

Deep thanks to **Mireia Bes**, friend and advisor, because her energy and creativity make the scientific world a much better place to stay.

A **Loren y Jaime**, porque las vidas pueden ser paralelas. A **Andrés**, por abrir y cerrar esta etapa en Barcelona. A **Iban, Dani, Nico, Bego y Claudia** por mantener el mundo balanceado y ser ejemplos a seguir.

A los escenarios y los focos a los que algún día pusimos el nombre de **Etón o Albricias**. A esos 12 científicos de **TBVT** que también creen que el arte puede cambiar el mundo.

A **Ángel y Ángela** por enseñarme a apuntar al sol, por dejar bien claro que la felicidad no se negocia, por la energía y los ánimos incondicionales para alcanzar cualquier meta que me proponga.

Y especial/esencialmente a **Oriol**, motor para seguir descubriendo que la felicidad no es lo que ellos dicen, que los límites no son los que ellos ponen, que somos y seremos unos raros invencibles, que tenemos todo en nuestras manos.

List of Abbreviations

293T	Human embryonic kidney-293-transformed
3D	Three dimension
53BP1	P53 binding protein 1
9-1-1	Rad9-Rad1-Hus1
A	Adenine
APS	Ammonium persulpha
Asf1	Anti-silencing factor-1
ATM	Ataxia telangiectasia mutated
ATR	Ataxia-telangiectasia mutated and Rad3-related
bp	Base pair
BRCA2	Breast cancer type 2 susceptibility protein
BrdU	Bromodeoxyuridine
BSA	Bovine serum albumin
C	Cytosine
C-terminus	Carboxyl-terminus
CAF-1	Chromatin assembly factor-1
CaR	Calcium-sensing receptor
Cdk	Cyclin-dependent kinase
CdkI	Cyclin-dependent kinas inhibitors
cDNA	Complementary DNA
CFS	Common fragile sites
Chk1	Checkpoint kinase 1
Chk2	Checkpoint kinase 2
CIN	Chromosomal instability
CLP	Common lymphoid progenitor
CMP	Common myeloid progenitor
CNIO	Centro Nacional de Investigaciones Oncológicas
CNS	Central Nervous System
Co-ip	Co-immunoprecipitation
CPT	Camptothecin
CSR	Class switch recombination
CtIP	CtBP-interacting protein
DAPI	4',6-diamidino-2-phenylindole
Dc	Decidua
DDR	DNA damage response
DDT	Dichlorodiphenyltrichloroethane
DMSO	Dimethyl sulfoxide
DNA	Deoxyribonucleic acid
DNA-PKs	DNA-dependent protein kinase catalytic subunit
dNTP	Deoxynucleotide 5' triphosphate
DSB	Double strand break
E	Embryonic day
EDTA	Ethylenediaminetetra-acetic acid
EGF	Epidermal growth factor
FACS	Fluorescence activated cell sorting
FBS	Foetal bovine serum
FGF	Fibroblast growth factor
FRT	Flp Recombinase Target
G	Guanine
G1	Growth phase 1
G2	Growth phase 2
GCR	Gross chromosomal rearrangement

GFP	Green fluorescent protein
Gy	Gray (unit of ionizing radiation)
H	Histone
H&E	Hematoxilin & Eosin
HDAC	Histone deacetylase
HEPES	4-(2-Hydroxyethyl)piperazine-1-ethanesulfonic acid
HIRA	Histone cell cycle Regulator A
HR	Homologous recombination
HRP	Horseradish peroxidase
HSC	Hematopoietic stem cells
HU	Hydroxyurea
IF	Immunfluorescence
IHC	Immunohistochemistry
IP	Immunoprecipitation
IR	Ionizing radiation
kb	Kilobase pair
KD	kinase dead
kDa	KiloDalton
KO	Knock-out
Lb	Labyrint
LC-MS	Liquid chromatography–mass spectrometry
LC8	Dynein light chain 8
Lin	Lineage
LOH	Loss of heterozygosity
LoxP	Locus of crossover of P1
LSK	lin-, c-kit+, Sca+
LT-HSC	Long-term HSC
LT-HSC	Long-term Haematopoietic Stem Cells
M	Mitosis
Mb	Megabase
MCM	Minichromosome maintenance
Mec1	Mitosis entry checkpoint mutant 1
MEFs	Mouse embryonic fibroblasts
MMS	Methyl methanesulfonate
MMTV-Pymt	MMTV driven polyoma middle-T antigen
MOB	Mps one binder.
MRN	Mre11-Rad50-Nbs1
mRNA	messenger ribonucleic acid
N-terminus	Amino-terminus
Nbs1	Nijmegen breakage syndrome 1
NCBI	National centre for Biotechnology Information
NER	Nucleotide excision repair
ng	Nanogram
NGS	Next generation sequencing
NHEJ	Non-homologous end joining
nm	Nanometer
nM	Nanomolar
NTP	Nucleotide triphosphate
ORC	Origin recognition complex
ORF	Open reading frame
P	Phosphorylated/phosphate
PAGE	Polyacrylamide gel electrophoresis
PBS	Phosphate buffer saline
PBST	PBS supplemented with Tween 20
PCNA	Proliferating cell nuclear antigen
PCR	Polymerase chain reaction

PEI	Polyethylenimine
pH	Power of hydrogen
PI	Propidium iodide
PI3K	Phosphoinositide-3 kinase
PIKK	Phosphatidylinositol 3'-kinase related kinase
PIPES	Piperazine-N,N"-bis(2-ethanesulfonic acid)
PKA	Protein kinase A
PMSF	Phenylmethylsulfonylfluoride
Pol	DNA-dependant DNA polymerase
PP1	Protein phosphatase 1
PTM	Post-translational modifications
Rad53	Radiation sensitive mutant 53
Rcf	Relative centrifugal force
RNA	Ribonucleic acid
RNAP	RNA polymerase
RPA	Replication protein A
RPE	Retinal pigment epithelial
Rpm	Revolutions per minute
S-phase	Synthesis-phase
s.d.	Standard deviation
Sca-1	Stem cell antigen 1
SCD	SQ/TQ cluster domain
SDS	Sodium dodecyl sulfate
SDS-PAGE	Sodium dodecyl sulfate polyacrylamide gel electrophoresis
siRNA	Small interfering ribonucleic acid
SNP	Single nucleotide polymorphism
ssDNA	Single-strand DNA
ST-HSC	Short-term HSC
SV40	Simian Virus 40
TAE	Tris/acetate/EDTA
TAP	Tandem Affinity Purification
TBS	Tris-buffered saline (Tris/borate/EDTA)
TE	Tris/EDTA
TEMED	Tetramethylethylenediamine
TF	Transcription factor
TGC	Trophoblast gigant cells
TLK1 (Tlk1)	Tousled like protein 1 (PROTEIN/ gene)
TLK2 (Tlk2)	Tousled like protein 2 (PROTEIN/ gene)
Tls	Tousled gene
Topo	Topoisomerase
Tp	Trophoblast
Tris	Tris[hydroxymethyl]aminomethane
Tween-20	Polyoxyethylene-sorbitan monolaurate
U	Units of enzyme activity
UV	Ultra violet
WT	Wildtype

Table of contents

Introduction

1. Genome integrity and human disease.

1.1. Genome integrity is actively maintained.

The main task that cells must carry out is to ensure their own survival and to transmit their genetic information to the next generation with high fidelity. However, all living cells are constantly being threatening by many types of DNA lesions produced by their own metabolism and processess or by exogenous environmental agents.

Cells have developed robust mechanisms to detect and repair DNA lesions that can compromise DNA stability. To maintain genome integrity, cells activate a signal transduction network that can arrest cell cycle after detecting the lesion, amplify the signal, activate repair of the DNA and modulate other processes such as transcription and translation. Altogether this response is called the DNA Damage Response (DDR) [1]. In addition to the repair of genotoxic lesions, the DDR is also necessary for several physiological processes, such as V(D)J recombination, class switch recombination and meiosis that involve the programmed generation of DNA breaks. Thus, the DDR needs to be tightly controlled to regulate cellular homeostasis in a variety of contexts such as growth, differentiation and development. Accordingly, these repair tools are precisely regulated, preventing access to DNA at an inappropriate time or place that could give rise to a loss of DNA integrity.

1.2. Genome integrity is important to prevent disease

The maintenance of genome stability requires the coordination of several overlapping pathways involving many different proteins. Defects in the machinery involved in DDR leads to an accumulation of DNA lesions that can give rise to disease phenotypes. The most prevalent ones include neurodegeneration, microcephaly, infertility, immune deficiency and cancer.

1.1.1 Neurodevelopmental disorders

The DDR plays a critical role during early brain development. In this regard, a wide number of DDR syndromes display microcephaly, a reduced head circumference resulting from defective proliferation of neuroprogenitor cells during fetal development, or neurodegeneration, the progressive loss of neurons in early life..

Human neurodegenerative disorders associated with DDR defects include Ataxia Telangiestasia (A-T) and A-T like disorder (ATLD) caused by mutations in the *ATM* and *MRE11* genes respectively. The protein products of these genes play apical roles in detecting and signaling DNA breaks and will be discussed in more detail later. In these syndromes, the cerebellum is the primary target of neurodegeneration. Since the cerebellum is primarily responsible for motor coordination, these DDR-associated syndromes are characterized by profound ataxia (defective motor coordination).

Microcephaly is a feature of Nijmegen breakage syndrome (*NBS*), NBS like disease (*NBSLD*), Seckel syndrome, primary microcephaly (PM) and Ligase 4 syndrome. Most of these syndromes display defective defective development of the cortex and patients suffer from mild to severe mental retardation and learning and memory deficits..

In addition to facilitating the development of the nervous system, the DDR is important for maintaining neuronal homeostasis. Given that neurons display limited capacity of replacement, they must overcome DNA damage lesions throughout our lifetime. This situation dictates that neurons rely heavily on intact DDR processes. In general, neurons exhibit high levels of metabolic activity, associated with generation of reactive oxygen species (ROS) that can cause DNA damage. In addition, their high transcription and translation rates also increase the potential for DNA damage. Thus, the DDR is crucial for development and homeostasis of the central nervous system (CNS).

1.1.2 Infertility.

Another feature associated with human diseases caused by DDR mutations is infertility. During gametogenesis many components of DDR are of particular importance for proper strand exchange during meiosis. In this process, Double Strand Breaks (DSB) are generated in a controlled manner by a meiosis-specific topoisomerase-like enzyme Spo11 [2] together with a number of other proteins. Failure in the generation, regulation or resolution of meiotic DSBs leads to a meiotic recombination failure that provokes cell death and eventually infertility.

1.1.3 Immune deficiency.

DSBs and single strand breaks (SSBs) are also introduced in a programmed manner during the development of antigen receptors in the immune system, that includes V(D)J recombination, class switch recombination (CSR) and somatic hypermutation (SHM).

Deficiency in DDR proteins that act in these molecular mechanisms compromise the generation of mature B- and T-cells and dampen the immune systems ability to improve antigen recognition. For example, Severe Combined Immunodeficiency (SCID), is characterized by defects in both B and T cell development due to defects in the process of V(D)J recombination. This failure is due to defects in key players in the generation and resolution of DSB, such as RAG1, RAG2 and DNA-PKs [3-5]. Less severe forms of immunodeficiency are also manifested when other DDR proteins are affected, such as in NBS and ATLD where mutations in Nbs1 or Mre11, impair the process of CSR [6,7]. In this case, patients show an increase in the sensitivity of infectious diseases. Even more, there is ample evidence that failure to resolve breaks generated in V(D)J and CSR recombination lead to aberrant chromosomal translocations seen in leukemic cells[8,9].

1.1.4 Cancer.

A well established hallmark of cancer is genomic instability [10]. For instance, genomic instability in lymphoid tumours frequently corresponds to chromosomal translocations, where proto-oncogene loci are fused to those of antigen receptors. In addition, mismatch repair defects cause microsatellite instability that predisposes to colorectal and endometrial carcinomas. Furthermore, chromosomal instability is seen in most sporadic solid tumours [11]. In this sense, the DDR influences tumor progression in multiple ways. Several inheritated cancers exhibit mutations in DDR genes that drive genomic instability that is likely to be responsible for cancer development. Some of the best-documented examples are germline mutations in breast cancer susceptibility genes (BRCA1 and BRCA2), NBS1, Werner syndrome helicase (WRN), Bloom syndrome helicase (BLM) and the Fanconi anemia genes all of which are linked to the repair of DNA. All of these mutations leads to an instable genotype and predispose to the development of several types of cancer [12-14]. DDR failure also appears in sporadic cancers, and is still not well understood if it is a cause or a consequence of tumor progression. This issue will be further discussed later in this introduction.

2. The DNA damage response.

Damage to the genetic material of each living cell is a continuous threat to both the ability to faithfully transmit genetic information to the offspring as well as its own survival. Several types of DNA damage are provoked by different genotoxic agents (Figure 1). To protect the genome against DNA damage, cells have developed a robust

DNA-damage response (DDR) that activates reversible cell cycle checkpoints, leading to cell cycle arrest in order to provide time for DNA repair [15]. This regulatory mechanism allows cells to sense many types of damage and activate a proper response. It usually consists of the recruitment of repair proteins with several enzymatic activities that repair damage by chemically modifying the DNA. The DDR is a complex signal transduction network, which can be divided into three parts: first damage detection by sensors; then transmission of the information through transducers; finally, the receipt of the signal by the effectors, which execute various cellular functions that represent a choreographed response that protects the cell and lessens the threat to the organism [1,10]. When damage is severe or in certain cellular contexts, cells can trigger a permanent cell cycle arrest, known as senescence or programmed cell death that leads to apoptosis[16]. These mechanisms ensure that damaged DNA will not be propogated and play important roles in tumor suppression and development.

2.1. Sources of DNA damage and type of lesions.

Genome integrity is constantly challenged both by environmental agents and by metabolic products that can induce DNA damage. In this section we will divide these two types of DNA damage in endogenous and exogenous (environmental) sources.

1.1.5 Endogenous sources of DNA damage.

DNA damage can arise spontaneously during DNA metabolism. DNA lesions can appear as a result of dNTP misincorporation during DNA replication, interconversion between DNA bases caused by deamination, loss of DNA bases following DNA depurination, and modification of DNA bases by alkylation [17]. Additionally, reactive oxygen species (ROS) produced from normal cellular metabolism can oxidize DNA bases and promote DNA breakage. Cells also fix topological problems due to DNA unwinding during transcription, replication, and chromosome segregation. Unwinding is essential for the relaxation of supercoiled DNA, and this issue is solved by DNA topoisomerases. These enzymes introduce single strand breaks in DNA (type I topoisomerases) or double strand breaks (type II topoisomerases), and thus they produce the relaxation of the DNA structure, which corresponds to an energetically more stable state. These strand breaks are protected by covalent binding to proteins, and do not generate a DDR. Also, the DNA damage checkpoints monitor the proper activity of these enzymes in order to ensure a normal chromosome segregation and

chromosome stability [18]. However, although being a highly regulated mechanism, the potential DNA damage that can be caused by Topoisomerases has been used as a powerful molecular tool in cancer chemotherapy and several anticancer drugs directly target these enzymes.

In addition, one specially threatening situation for genomic integrity is the collision of replication machinery with transcription machinery at highly transcribed genes [19]. In fact, the highest pausing of the replication fork has been described to occur at the ORFs of highly transcribed genes [20]. These regions of fork pausing exhibit high levels of recombination, which can potentially, lead to chromosome rearrangements. Chromosome topology can also stall or slow replication forks during DNA synthesis. In this regard, these DNA regions may be composed of difficult sequences to replicate, such as repetitive sequences that can form DNA secondary structures like hairpins of G-quadraplexes. These regions are prone to accumulate DNA breaks and are known as common fragile sites (CFS).

Further more, DNA breaks are also required during physiological processes such as immunity acquisition and gametogenesis. DSB are the starting point of chromosomal rearrangements required for generate a diverse repertoire of antigen-specific receptors in the immune system[5]. In an analogous way, in meiotic recombination Spo11 introduces DSB that enables a correct chromatid exchange[2].

1.1.6 Exogenous sources of DNA damage

In addition to the DNA damage produced by normal cellular processes, cells can receive insults from exogenous sources. Environmental DNA damage can be produced by physical or chemical agents. Physical genotoxic agents include ionizing radiation (IR) can induce oxidation of DNA bases and generate single and double strand breaks (SSBs and DSBs, respectively); ultraviolet (UV) light which produces DNA damage by covalent binding of pyrimidines, causing damage in one strand of the DNA. These dimers of pyrimidines interfere with replication, stalling replication forks due to helical distortions. Chemical agents are used in cancer chemotherapy and lead to a variety of DNA lesions: The mutagen MMS (methyl methanesulfonate) generates mutations by methylation of DNA bases, which causes mispairing in DNA synthesis and therefore point mutations; Topoisomerase inhibitor camptothecin (CPT) repress topoisomerase I and induce DNA damage by trapping covalent topoisomerase- DNA complexes; Bleomycin produces DSB, and hydroxyurea inhibits the ribonucleotide reductase

enzyme, causing a depletion of nucleotides, which in turn leads to replication fork stalling. All these types of damage are illustrated in figure 1.

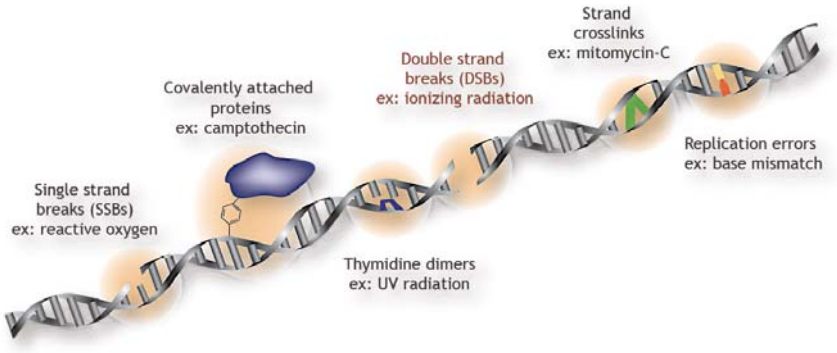

Figure 1 : Types of DNA damage caused by endogenous or exogenous DNA damaging agents

2.2. Initiation and propagation of the DDR.

For DNA repair and DNA damage signaling to occur, the DNA lesion must first be detected. Sensors perform surveillance and signaling duties, in that they initially detect abnormalities in DNA and emit signals that recruit other signaling and repair factors to the damaged DNA. Damage to genomic DNA stimulates functionally diverse cellular responses that affect fundamental cellular processes. To modify cellular responses in order to deal with the damage, there are several downstream pathways that amplify the signal, spreading the information through a wide variety of cellular effectors. This signaling can be divided in two key events: cascades of protein modifications carry out by transducers and chromatin rearrangements that serve as a platform for repair proteins.

1.1.7 Sensor proteins and DNA damage detection

Since a wide variety of DNA lesions can activate the DDR, the question of what senses DNA lesions is crucial to understand the activation mechanisms. For instance, DSBs are recognized by the MRE11 complex, which consists of meiotic recombination 11 (MRE11), RAD50 and NBS1 (also known as nibrin), and leads to the activation of ATM in conjunction with other proteins [21]. ATM activation promotes cell-cycle checkpoint activation and regulates DNA repair (Figure 2). In the case of replication blocks, DNA polymerases stall, the MCM replicative helicases continue DNA unwinding ahead of the replication fork, leading to the generation of ssDNA, which binds to the single

strand-binding protein complex RPA. This complex of ssDNA-RPA acts as a catalysis for the activation of additional DDR kinases ATR and Chk1 [22].

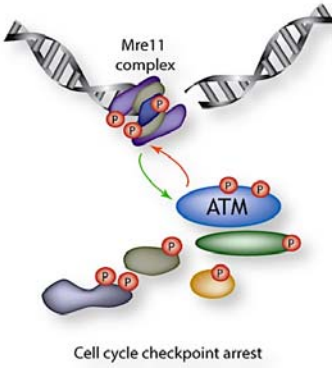

Figure 2. DNA Damage Response in the presence of DSB. Recognition of DSB by MRE11 and signal transduction through ATM and effector proteins

1.1.8 Transducers and post-translational modification (PTM).

After lesion recognition, several response pathways are initiated by members of the phospho-inositide kinase (PIK)-related kinase family (PIKKs), which include ataxia-telangiectasia mutated (ATM), DNA-dependent protein kinase catalytic subunit (DNA-PKcs) and ataxia-telangiectasia-and-RAD3-related (ATR). Damage leads to the activation of these kinases in the presence of adaptor proteins such as Nijmegen breakage syndrome 1 (NBS1), Ku70/80 and ATRIP, respectively. ATM and DNA-PK respond primarily to DSBs and associated changes in chromatin density. ATR is activated by the formation of replication protein A (RPA)-coated single-stranded DNA (reviewed in [23]) that can be formed after replication fork stalling. However, these functional distinctions between ATM and ATR are not absolute and, in many cases, both kinases participate in checkpoint control pathways in response to a genotoxic insult. In addition, DNA-PKcs, has overlapping substrate specificity with ATM and ATR and variably contributes to checkpoint signaling in mammalian cells [24].

Upon activation, PIKKs phosphorylate and activate the transducer kinases Chk1 and Chk2, where ATM activates mainly Chk2, and ATR activates mainly Chk1 [15]. Both Chk1 and Chk2 activate cell cycle checkpoints by phosphorylating members of a protein phosphatase family known as Cdc25 [25]. Phosphorylation of Cdc25 targets it for degradation and, consequently, Cyclin dependent kinases (Cdks) normally activated by Cdc25-mediated dephosphorylation remain inactive and cell cycle progression is halted [25,26]. Chk1 and Chk2, together with PIK-related kinases, also activate and recruit p53, a transcription factor that has predominant roles in the transcriptional activation of genes

associated with cell cycle arrest, DNA repair, senescence and apoptosis; thus p53 is considered to be a major effector and is an important tumor suppressor [27-29].

In addition to p53, Chk1, Chk2, and PIKKs activate and recruit various other proteins to sites of DNA damage. Many of these proteins are involved in facilitate the reorganization of the chromatin or DNA in the vicinity of the lesion in order to facilitate signaling and repair.

2.3. Cell cycle checkpoint responses

The cell cycle is an ordered progression through phases that leads to cell division, which can be divided into two basic processes: DNA replication and DNA segregation. During S-phase, DNA synthesis takes place to fully replicate the double stranded molecule of DNA. During cell division, the replicated material is segregated into two daughter cells. Two gap phases precede S and M phases; in G1 the cell prepares for DNA synthesis, and in G2 the cell prepares for the mitotic division that takes places in M-phase. Together, G1, S, and G2 phase are referred to as interphase.

1.1.9 Regulation of cell cycle progression.

Progression through each phase of the cell cycle is under the strict control of various molecules named cyclins, cyclin-dependent kinases (Cdks) and Cdks inhibitors (CdkI), all of them regulated primarily by phosphorylation and dephosphorylation events [30]. Cyclin levels oscillate during the cell cycle as a result of variations in transcription and ubiquitin- mediated degradation [30,31]. The cyclins interact with CDKs and activate their kinase activity, which plays a crucial role in regulating cell cycle progression. Cdk activity is negatively regulated by association with CdkIs. Specific cyclin/Cdk complexes become activated in different phases of the cell cycle. For instance cyclin D/Cdk4-6 complexes initiate the progression through G1 by the phosphorylation of substrates (ex. Retinoblastoma proteins) that lead to the transcription of genes that are essential for DNA synthesis and subsequent cell cycle progression. Similarly, cyclin E/Cdk2 complex is important for G1/S transition, cyclin A/Cdk1 acts during S-phase progression and cyclin B/Cdk1 is important for the progression through G2/M. Consequently, the regulation of cyclin levels through the cell cycle is essential and has to be tightly controlled to allow the ordered progression through the different phases.

1.1.10 Cell cycle checkpoints

In addition to DNA repair, the DDR initiates cell cycle checkpoint responses in dividing cells. Cell cycle checkpoints are unprogrammed pauses in the cell cycle that are induced by alterations in DNA. These pauses serve to give cells time to repair the damage before the start of mitosis. The cell has three major cell cycle checkpoints that can be triggered in response to DNA damage: G1/S, intra-S, and G2/M (Figure 4**)** [32,33]. Activation of these checkpoints arrests the cell cycle in order to give further time for signaling and repair events to deal with the genetic lesion. Upon completion of repair, progression through the cell cycle resumes, thereby ensuring that DNA lesions are not duplicated and segregated during S and M phases. Failure of the cell to complete repair before replication or chromosomal segregation can lead to chromosomal damage. Under certain conditions, cell cycle checkpoints and DNA damage signaling result in an irreversible withdrawal from the cell cycle known as senescence.

G1/S checkpoint: The induction of DNA damage during the G1 phase of the cell cycle prevents cells to enter S phase, in a process named G1/S checkpoint. This checkpoint is dependent on the activities of the ATM and ATR protein kinases, which are activated in response to distinct and partially overlapping types of DNA damage (Figure 3). G1/S checkpoint is comprised of “rapid” and “delayed” phases that initiate and sustain checkpoint arrest, respectively.

The rapid phase of the G1/S checkpoint is a protein synthesis-independent response that acutely inhibits the activity of cyclin E/A-Cdk2, thus preventing the early steps required for firing DNA replication forks. The delayed G1/S checkpoint response is a protein synthesis dependent process that relies on the upregulation of CKIs, including p21Waf1/Cip1 to inhibit Cdk activity. This delayed pathway is critically dependent on the p53 tumor suppressor.

Intra-S checkpoint: This checkpoint is activated when replication forks encounter a DSB or other fork-obstructing lesion. Thus, the fork can undergo a process termed replication fork collapse whereby the replication complex dissociates from the fork. Collapsed replication forks can promote genome instability and chromosomal rearrangements [34,35]. Therefore, the intra-S checkpoint is characterized by several functions. These include delaying the firing of uninitiated DNA replication origins; protecting DNA replication forks that have stalled; and delaying mitosis until S-phase damage has been repaired and DNA replication has been completed. Generally, intra-

S-phase checkpoints require the ATR-Chk1 pathway, but there is significant overlap between ATR- and ATM-dependent signaling elements, with the precise pathways of S-phase checkpoint arrest being dictated by the type of the lesion. However, this is a poorly characterize checkpoint and its relation with human diseases remains unclear.

G2/M checkpoint: The G2/M checkpoint represents a temporary G2 delay that suppresses mitotic entry following an overt DNA-damaging insult. It is a highly sensitive response; in budding yeast the introduction of a single persistent DSB is sufficient to activate it [36-38]. G2/M checkpoint arrest begins with DNA damage detection and activation of the apical DNA damage-signaling kinases ATM and ATR. Chk1 plays a critical role in this checkpoint activation in response to a variety of genotoxic stimuli (Figure 3). Chk1 can target Cdc25 phosphatases, leading to the inactivation of Cdks and the suppression of mitotic entry [39,40]. Some mutations in ATM substrates can impair G2/M checkpoint arrest, resulting in tumor predisposition. This observation indicates that G2/M checkpoint is important for tumor suppression[41].

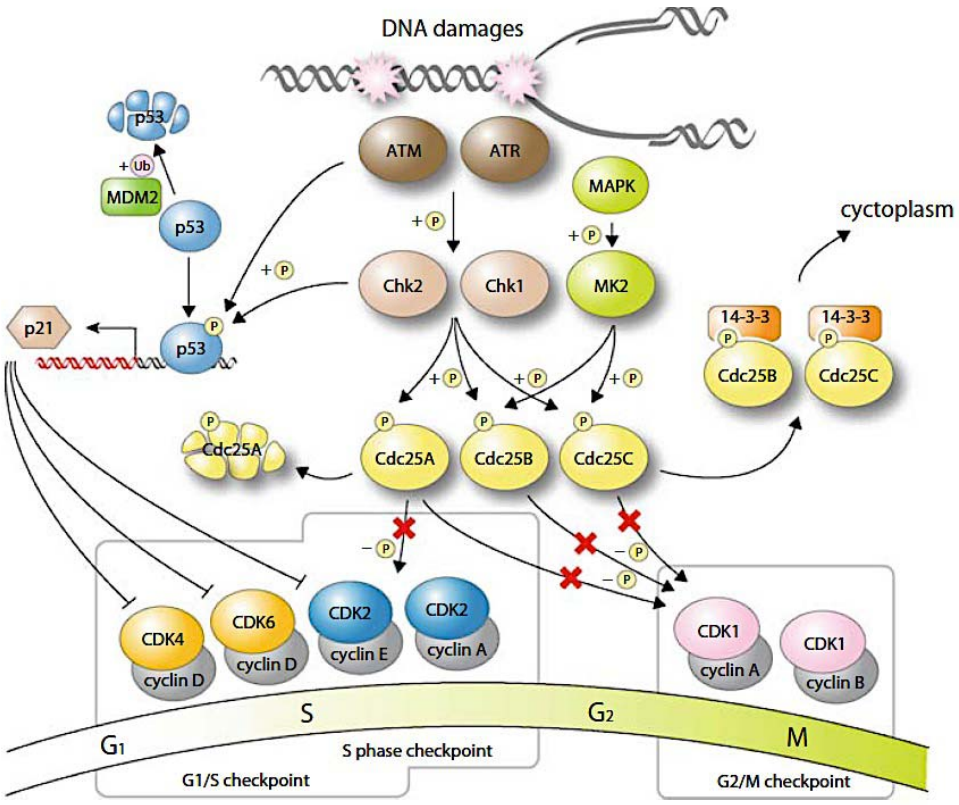

Figure 3: Simplified view of DNA damage-induced cell cycle checkpoint pathways

2.4. DNA Repair pathways

The DDR detects and respond to multiple types of lesions in DNA. Among these, DNA double-strand breaks (DSBs) represent dangerous lesions as they can initiate cytotoxic or cytostatic events. Their inaccurate repair can lead to mutations, chromosome translocations, or the generation of repair products that are toxic to the cell[42]. In mammalian cells there are two major repair pathways of DSB, namely non-homologous end joining (NHEJ) and homologous recombination or homology directed repair (HDR). The induction of NHEJ or HDR depends on the cell-cycle phase (Figure 4). NHEJ is the major pathway for the repair of DSBs that arise during G0 and G1 [43]. In addition, NHEJ is responsible for the repair of programmed DSBs generated during V(D)J recombination [44,45]. In contrast, HDR functions only in late S and G2 when an intact sister chromatid is available to act as a template for repair. As HDR uses a template to repair the lesion, is substantially less error-prone than NHEJ, which typically results in the deletion or addition of DNA sequences at the junction of repair, thus potentially resulting in errors. HDR is initiated when DSBs are recognized and resected by nuclease activities, resulting in 3' ssDNA overhangs, that are coated by RAD51. This nucleoprotein filament can invade the sister chromatid and use it as a template. One of the main functions of HDR is the repair of endogenous DSBs produced when replication forks collapse [45,46]

Deficiencies in DSB repair pathways have been linked to chromosomal instability, DNA damage sensitivity, immunodeficiency, infertility and predisposition to cancer and other human pathologies[10].

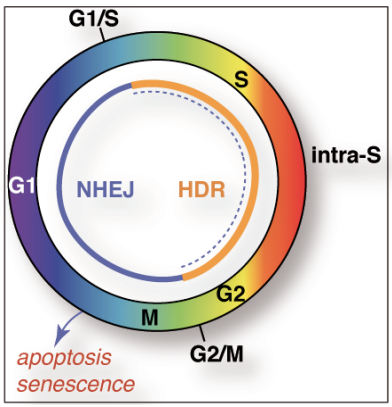

Figure 4. Schematic representation of checkpoints and preferred repair pathways in response to DNA damage in the context of the cell cycle.

1.1.11 DNA metabolism and repair pathway choice

To maintain a balance between NHEJ and HDR pathways is crucial to preserve genome stability. The mechanisms that influence the election of one or another are still under study. Recent studies pointed out that the factors 53BP1 and BRCA1 are pivotal regulators of pathway choice.

53BP1 contributes to NHEJ by interacting with chromatin at DSB and inhibiting DNA resection crucial for HDR [47]. The 53BP1 protein needs to oligomerize through Tudor domains that mediates its accumulation in DBS via interaction with H4-K20me2 histone modification.

As cells enter in S phase, this resection inhibition is antagonized by the action of BRCA1, which participates in the removal of 53BP1 in S/G2 phases and allowing resection [48,49]. It has been also hypothesize that the genomic instability present in cells with BRCA1 mutations comes from the failure to exclude 53BP1 from DSB during S-phase[49].

1.1.11.1 HDR and DNA resection

In S and G2 phases of the cell cycle, checkpoint responses and DNA repair coordination depend on DNA resection at the DSB to form ssDNA[50]. DNA end resection is regulated by the Mre11 complex and ATM through CtIP, which associates with BRCA1 and is a target of its E3 ligase activity. BRCA1 ubiquitinates CtIP, facilitating its association with damage sites and activation of resection activities[51]. Following CtIP association, resection is initiated by the Mre11 complex that generates an internal nick with its endonuclease activities and resects towards the end using 3'-5' exonuclease activity. This initiation is followed by long DNA resection performed by Exo1 or DNA2 exonucleases, which perform nucleolytic resection 5'-3'. Together with the action of BLM helicase, long ssDNA overhangs arise, that are coated by RPA. ssDNA-RPA complexes serve as a platform to recruit several cofactors, particularly ATRIP, that facilitate the activation of ATR and Chk1.

For efficient DNA resection, the chromatin structure is modulated in the vicinity of DSBs. Nucleosomes, core particles that comprise 164 DNA base pairs organized around an octamer consisting of two copies of each highly conserved histone protein - H2A, H2B, H3 and H4, need to be removed from the regions of resection, and replaced after DNA repair has been completed. Studies in yeast revealed that nucleosome

depletion occurs in a region spanning at least 2 kb on either side of the break[52]. This nucleosome removal during DDR is a particularly important issue in regions of highly compacted chromatin. In fact, mutations in tumoral cells occur more frequently in heterochromatin regions, that presents a barrier for the correct repair of DNA.

1.1.11.2 Chromatin and histone modifications in the DDR

How chromatin can undergo rapid decondensation at regions of DNA repair is still an open question. It has been suggested ATM targets phosphorylation is a key event for relaxation of chromatin at DSB[53], promoting the relocation of chromatin compactation proteins, such as Kap1, HDACs and Heterochromatin Protein 1 (HP1)[54-56]. One of the substrates of ATM is H2AX at Ser 136 [57], and this histone mark promotes the recruitment and retention of mentioned DDR proteins for repair completion. Bidirectional spreading of γH2AX away from DNA breaks helps to amplify the checkpoint signal [58] and contributes to delineate a chromatin region to which the DDR is active. Indeed, γH2AX mediate the localization of ubiquitin ligases and SUMO-ligases that, among other substrates, can modify H2AX itself. These modifications are crucial for the recruitment of many other factors modulating the DDR signal[59]. For instance, sumoylation of γH2AX is essential for the recruitment of 53BP1. In this regard, chromatin modification is not only essential for nucleosome redistribution and DNA access but also as platform and signal for DDR pathways.

Thus, it's clear that removal of H2AX histone marks is crucial for the resolution of the repair. The first step is to replace the phosphorylated form of H2AX for an unphosphorylated one, followed by the dephosphorylation of the soluble fraction [60,61]. Thus, it seems that depending the factors surrounding DSB, chromatin can either be relaxed or compacted.

H2AX is not the only histone modified by PTMs in response to DNA damage. Many other enzymes that modify different histones are regulated by the DDR. These include enzymes that regulate phosphorylation, acetylation, methylation, ubiquitination, poly(ADP-ribosyl)ation (PARylation), and SUMOylation of different histone molecules. Some histone modifications alter the packing of nucleosomes. For instance, histone-tail acetylation destabilizes the folding of chromatin into higher-order structures [62]. Interestingly, following the initial recruitment of histone acetylases (HATs), several histone deacetylases (HDACs) associate with chromatin near DSBs, and a clear decrease in histone acetylation takes place upon completion of repair [63]. In order to

prevent inappropriate gene activation, HDACs may act to restore chromatin higher-order structure after DSB repair.

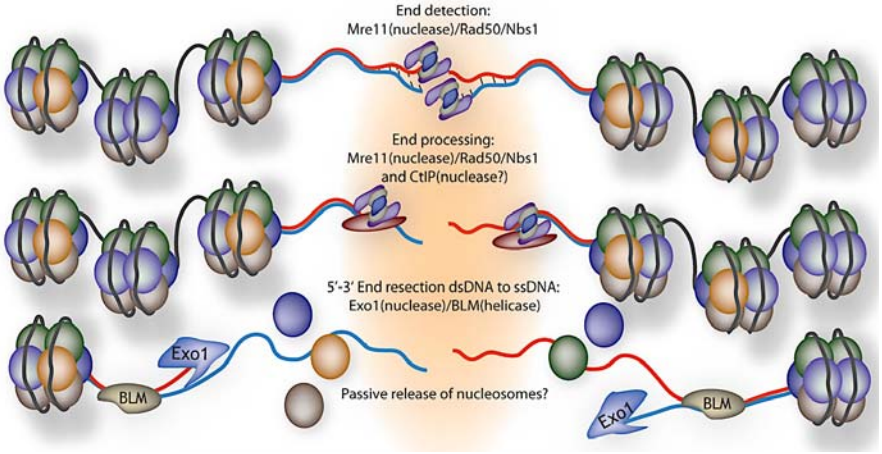

Figure 5: DSB recognition and end processing. The resection of dsDNA into ssDNA can extend over 2kb in yeast.

However many other histone modifications have been identified to control cellular signaling without an evident role in chromatin compactation. Two key PTMs occurring on histone H4 that function in the DDR are histone H4K16 acetylation and H4K20 methylation. Acetylation of H4K16 occurs upon DNA damage and is mediated by the HATs TIP60 and MOF[60,64]. Importantly, depletion of either HAT results in defective HR and NHEJ. The precise mechanism of how acetylation of H4K16 promotes DSB repair also remains elusive.

Methylation of histone H4K20 is another well-established histone mark associated with the DDR, which creates a binding site for the Tudor-domain region of the DDR protein 53BP1[65]. H3K36me2 (H3 Lys36 dimethylation) is also induced by DNA damage. Furthermore, impairment of this specific histone methylation resulted in defective loading of the NHEJ factor Ku as well as the DSB repair. Histone H3 acetylations, particularly Lys9 and Lys56, were deacetylated upon DNA damage in a cell-cycle independent manner, indicating that they directly respond to DNA damage induction[66,67]. The HDACs are rapidly recruited to DSBs and, under normal conditions, co-regulate H3K56Ac and H4K16Ac levels[66]. Importantly, such regulation appears to be important for DSB repair because depletion of HDAC1 and HDAC2 impaired DNA repair, especially NHEJ, and rendered cells hypersensitive to DSB-inducing agents[66]

1.1.12 Regulation of transcription at DSB.

The DDR must deal with serious threats by quickly responses that comprises a vast array of cellular complexes. This response cannot be dependent on the production of new proteins –a time consuming response- but in contrast it must lay on existing resources used for the cause. This means that DDR pulls proteins out of the cellular roles to act in this context. For instance, introduction of DSB disrupts physical integrity of chromatin and it must lead to the inhibition of numerous processes that occurs in the context of chromatin structure such as gene transcription. At the surroundings of DSB chromatin is decondensed, which is an activator of gene-transcription. To avoid unwanted gene expression, transcriptional activity is largely repressed in regions surrounding DSB, processed previously called DNA DSB-induced silencing in Cis (DISC)[68]. Notably, DISC coincides with two hallmarks of transcriptional repression: Stalling and degradation of RNA polymerases (RNAP) and spread of chromatin modifications to inhibit other transcriptional factors[69], both of them driven by ATM activity. RNA polymerase I and II (RNAPI & II)-dependent transcription is silenced in proximal regions to DSB in ATM dependent manner[68]. RNPAI & II transcriptional silencing correlates with the ubiquitination of histone H2A (uH2A), histone mark that requires active ATM for its maintenance.

On the other hand, RNF20-RNF40 heterodimer promotes transcription in the by the monoubiquitination of H2B (uH2B). This histone mark helps to shape the chromatin in a transcriptional context. Importantly, RNF20-RNF40 interacts physically with and it's substrate of ATM and uH2B promoted by RNF20-RNF40 is required for DNA repair. uH2B serves as a catalysis for further histone modifications that recruits SNF2 and other chromatin remodeling proteins[70] that disassemble chromatin structure to make DNA accessible for repair proteins. This pathway is the typical example of how DDR call to action proteins that regulates other processes in unprovoked cells.

However, one question that remains to be answered is how chromatin can become more accessible for DDR proteins but, at the same time, become inaccessible for transcription factors.

In addition, is also important to understand the mechanisms that reestart transcription at repair sites after repair is completed. Recent studies shed light to the importance of HIRA in de novo deposition of histones at repair sites, which is essential for the

reactivation of transcription after repair[71]. But which marks carry these histones and for how long they stay in newly repair chromatin will be matter of future investigations.

1.1.12.1 ATP-dependent chromatin remodeling and histone chaperones.

ATP-dependent chromatin remodelers are crucial factors involved in DNA replication, repair and transcriptional regulation. Chromatin remodelers can slide nucleosomes along DNA and evict nucleosomes from chromatin [72]. Chromatin remodeling complexes of the SWI2/SNF2 family share a catalytic subunit that contains an ATPase/helicase domain. Specific functional domains outside the ATPase/helicase region in these catalytic subunits determine the classification of chromatin remodelers in the four subfamilies of SWI/SNF, ISWI, CHD, and INO80 of the SWI2/SNF2 superfamily [72,73]. For instance, in yeast, ATP-dependent nucleosome remodeler INO80 promotes histone removal from the site of a DSB [74,75] to allow 5'-3' strand resection. The ISWI was suggested to exchange modified histones after repair, while SWI/SNF may facilitate clearance of nucleosomes prior to Rad51-mediated strand invasion. Recently, a poorly characterized ATP-dependent chromatin remodeler in yeast, Fun30, has been reported to promote DNA resection in an Exo1 and Dna2-dependent pathways by remodeling chromatin[76]. Even more, downregulation of Fun30 human homolog, SMARCAD1, increased sensitivity to DNA damage and exhibit RPA hyperloading, indicating impaired resection[76].

Histones are constantly exchanged throughout the cell cycle in a replication-dependent and independent manner. During replication, nucleosomes are disassembled ahead of the replication fork and are rapidly assembled on newly synthesized DNA to maintain chromosomal integrity. In the same way, nucleosomes are remodeled and reassembled following gene transcription and DNA repair [77]

Histone chaperones are key proteins in multiple steps of nucleosome formation. Histone chaperones deliver histones to DNA during chromatin assembly, in addition to removing histones from DNA to facilitate chromatin disassembly. These chaperones bind to the positively charged histones and shield their charge from the highly negatively charged DNA [78]. In budding yeast, several histone chaperones involved in regulation of chromatin integrity have been identified [79]. Histone chaperones that bind preferentially to histones H3/H4 include Asf1, CAF-1 (chromatin assembly factor 1), HIR (histone regulator), Spt6 and Rtt106 [80-85]. Furthermore, FACT (facilitates chromatin transcription), Nap1 and Vps75 associate with all four histone core [86-88]. All these

histone chaperones have been demonstrated to play diverse roles in the regulation of chromatin including the maintenance of histone pools, the regulation of histone deposition and exchange and the facilitation of PTMs and some are-well known regulators of DNA repair processes [77].

2.5. Resolution of the DDR.

1.1.13 Checkpoint silencing

To ensure cells do not enter mitosis prematurely, checkpoints act on cell cycle machinery to ultimately control CDK activity. After detection of DNA damage and activation of ATM and ATR, Cdc25 is rapidly inhibited by Chk1, leading to decreased CDK activity and cell cycle arrest before mitosis. After completion of DNA repair, the checkpoint must be released. Chk1 activation is extremely rapid, and the magnitude of activation is saturated at relatively low levels of DNA damage. However, the duration of the checkpoint arrest is clearly dose-dependent, suggesting that regulation of Chk1 activation-inactivation must be extremely precise. Numerous phosphatases and ubiquitin ligases have been identified that negatively regulate Chk1 activity. In this regard, ATR mediated Chk1 phosphorylation is antagonize by Protein Phosphatase 2A circuit (PP2A) [89]. Moreover, after completion of DNA repair, Chk1 can also be a target for degradation, as ATR can also activate ubiquitin ligases that target Chk1 for degradation[90].

1.1.14 Chromatin assembly and cell cycle resumption.

In addition to Chk1 inactivation, the restoration of chromatin is thought to be crucial for checkpoint recovery. This is evident in the ‘‘Access-Repair-Restore’’ model[91], in which it was proposed that not only was the relaxation of chromatin important during the repair process, but also in the reconstitution of pre-existing chromatin structure after successful repair. Indeed, in yeast, a central component of cell cycle resumption is the reestablishment of nucleosomes on repaired regions that have been rendered nucleosome free due to resection and repair processes. This epigenetic restoration comprises several steps including removal of acetyl marks, dephosphorylation of γH2AX and nucleosome restoration at repair sites.

Following the initial recruitment of histone acetylases (HATs), several HDACs associate with chromatin near DSBs, and a clear decrease in histone acetylation takes place upon completion of repair[63]. HDACs could act to restore chromatin higher-order

structure following DSB repair to prevent inappropriate gene activation. In addition, reduction of chromatin plasticity may be essential to inactivate the DNA-damage response by inhibiting further recruitment of checkpoint mediators that directly bind to constitutive histone marks, such as H3K79me3 and H4K20me3 [60,92,93]

As already discussed, one of the most intensively studied histone modifications associated with DSB repair is the phosphorylation of histone H2AX variants. Clearance of this histone mark is crucial for the resumption of the cell cycle. The first step is to replace the phosphorylated form of H2AX for an unphosphorylated one, that imediated by histone remodeling complexes, such as SWR1. Following displacement of chromatin, H2AX as part of the soluble fraction is dephosphorylated by phosphatase complexes [60,61].

Nucleosome deposition is specifically mediated by histone chaperones that play a crucial role in the restoration of epigenetic information following repair. For instance, H3-H4 incorporation during the repair of UV lesions by Nucleotide Excision Repair (NER) is mediated by CAF-1,[94] even though NER only involves relatively short patches of DNA synthesis (30 nucleosides). Moreover, CAF-1-mediated histone deposition likely contributes to chromatin restoration following a wide range of repair processes, as it is directly recruited to sites of single-strand breaks and DSBs that are marked by γH2AX[94,95]

Several studies in yeast point out Asf1 as an important player in chromatin rearrangements at repair sites[96]. Asf1 has been shown to be required for cell cycle resumption by promoting the incorporation of acetylated histones H3 and H4 in newly repaired regions. Moreover, Asf1 is linked to checkpoint control as it is an interactor of the yeast Rad53 checkpoint kinase that plays similar roles to the mammalian Chk1[80]. In mammals, it has been shown that Chk1 does not interact directly with Asf1 but can regulate its function through Tousled like kinase 1 (TLK1) [97,98]. In mammalian cells there are two TLK proteins, TLK1 and TLK2, that interact with each other and with Asf1. TLK1 has been shown to be a target of ATM/ATR dependent Chk1 activity after DNA damage and TLK2 may be a direct target of ATM/ATR although this has not been clearly demonstrated[97]. This regulation of TLKs by damage-induced kinases suggests a mechanism that could coordinate repair with the deposition of chromatin and facilitate checkpoint resolution.

Chromatin restoration mechanisms are key steps to prevent CIN and epigenetic

instability. Deregulation of chromatin maintenance mechanisms presents a threat that can contribute to cellular ageing and cancer.

3. The DDR in the etiology of cancer.

3.1. Oncogene-Induced DNA Damage Model: an inducible barrier.

Chromosomal instability is a hallmark of cancer cells and chromosomal rearrangements, chromosomal loss or gain, translocations and increased mutagenesis are all evident in different types of cancer. The DDR plays an important protective mechanism by activating death by apoptosis or senescence in response to CIN and both of these pathways are commonly suppressed during cancer progression. In many precancerous lesions, an active DDR is evident as increased nuclear DDR protein foci and increased phosphorylation of histone H2AX, ataxia telangiectasia (ATM), Chk2, and p53, have been readily observed[99,100] In addition, markers of apoptosis and senescence are higher in early stage lesions. In later stage invasive lesions, an attenuation of the DDR has been observed, correlating with mutations in key DDR effectors such as p53 and ATM. Thus, with respect to the DDR, tumoral development can be described divided into two main stages: the precancerous state, where there is evidence of DSB production, DDR activation and high rates of apoptosis and senescence, followed by the cancerous lesion, where the proliferation levels peaks, corresponding with a sharp decrease in the senescence and apoptosis rates and DDR markers.

The concept of the DDR as a tumorigenesis barrier acting in precancerous lesions contrasts with earlier models, which considered that precancerous lesions were less aggressive than cancers simply because they had fewer oncogenic mutations. DDR as a tumorigenesis barrier model suggests that the less aggressive nature of precancerous lesions is in part due to the tumorigenesis barrier imposed by the DNA damage checkpoints[100-102].

An open question is what generates DSBs in these cancer cells. A key feature that many cancer cells share is the activation of oncogenes. Most oncogenes deregulate entry into the cell cycle and do so by directly or indirectly enhancing the activities of Cdks that function in the G1 and S phases of the cell cycle[103,104]. In yeast, deregulation of Cdk activity compromises DNA replication and leads to formation of DNA DSBs and

genomic instability.[105] In the same way, oncogenes may induce a replication stress that can culminate in the production of DSB lesions due to unscheduled DNA replication[99,102].

Replication stress is defined as a systemic state in the cell that leads to collapse of DNA replication forks, that leads to a dissociation of the replication proteins (replisome), inhibiting the progression of the DNA synthesis and giving rise to DNA lesions at collapsed forks, especially DSB. This replication collapse occurs more frequently in specific loci called common fragile sites (CFS) (see 3.2).

Thus, the DDR model proposes that genomic instability is driven by oncogenic stress leading to replication stress, fork collapse and DSBs. This situation activates senescence and apoptosis in the precancerous lesions. Nevertheless, the genomic instability produced by replication stress is considered critical for cancer development because it can stimulate the accumulation of mutations necessary to become a cancer cell (Figure 6: Oncogenic induded DNA damage model for cancer progression. Taken from Bartkova et al, 2006[102].)

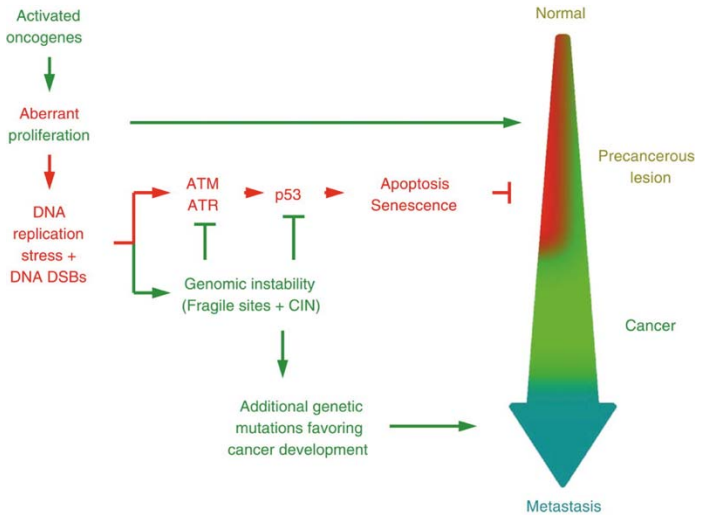

Figure 6: Oncogenic induded DNA damage model for cancer progression. Taken from Bartkova et al, 2006[102].

3.2. The role of fragile sites in chromosome stability.

Common fragile sites (CFS) are non-randomly distributed loci on DNA prone to breakage under conditions of mild replication stress. They are considered to precede the instability in the other genomic regions and in this sense, be a driving force in

cancer progression. The molecular basis of the CFSs are still not well defined, but normally involve chromosome topology that stalls or slows replication forks during DNA synthesis. In this regard, these DNA regions may be composed of difficult sequences to replicate, such as repetitive sequences that can form DNA secondary structures like hairpins of G-quadraplexes. Several inducers of CFS are known, and all of them can potentially stop elongation of DNA replication, and even concentrations that partially inhibit replication without arresting the cell cycle can lead to CFS. The most typical inducer of increased CFS expression is aphidicolin, an inhibitor of the replicative DNA polymerases.

Consistent with the fact that CFS are induced during replication stress, the maintenance of CFS stability relies on the ATR-dependent checkpoint, together with a number of proteins that work in the recovery of stalled replication forks. Indeed, ATR disruption, but not the related kinase ATM, greatly increases chromosome instability at CFS, both under unperturbed replication and treatment with aphidicolin[106,107].

The activity of the ATR target Chk1 is essential to suppress CFS breakage. Chk1 suppresses late replication origin firing and arrests cell cycle progression to provide cells the adequate time to resolve the problem[108]. Indeed, Chk1 mutants exhibit an increase in CFS expression after fork stalling. In addition to cell cycle regulation, Chk1 has been implicated also in maintaining replication fork integrity following replication inhibition. Indeed, Chk1 inhibition or genetic downregulation leads to accumulation of DSB in S-phase cells.

To resolve stalled fork replication intermediates and secondary DNA structures in order to avoid DNA breakage, ATR-mediated regulation of DNA helicases may be a key event. Downregulation of the WRN RecQ family helicase leads to gaps and constrictions in metaphase chromosomes, as well as the loss of telomeres that have a propensity to form G-quadraplexes, either upon aphidicolin treatment or under unperturbed conditions[109]. Another helicase implicated in CFS expression is BLM, as Bloom's syndrome patients (BLM deficient) show spontaneous aberrations in fragile sites involved in cancer rearrangements[110].

Moreover, the replication checkpoint could protect CFS integrity by promoting the repair of underreplicated DNA regions in late S/G2 through the regulation of HDR repair[111]. Indeed, DSB proteins such as BRCA1 and Rad51 are involved in processing replication fork lesions and ultimately important to prevent CFS breakage.

In addition, alterations in the chromatin status has been implicating in CFS expression. Some studies reveal that chromatin at CFS is more compact, maybe indicating a barrier for the progression of the replication fork that results in a collapse of the replisome[112]. (In the Bartek NCB paper they also manipulate condensing to demonstrate this point)

Therefore, the data reported clearly suggest that the pathways responding to replication fork stalling may function, perhaps at multiple levels, as an integral part of the mechanism regulating the integrity of the fragile genomic regions and preventing oncogenesis.

1.1.15 Replication fork progression and chromatin.

Chromatin represents a barrier for the progression of the replication fork. In order to allow smooth progression of the replisome, cells contain specialized complexes involved in nucleosome disassembly ahead of and reassembly behind the replication fork to reestablish chromatin conformation during DNA replication. In addition, during this nucleosome deposition in the nascent DNA, the epigenetic information needs to be maintained. Thus, it is also required to effectively maintain the pattern of DNA methylation status, a correct supply of histones and an accurate integration of histone PTMs.

There are several histone chaperones that are known to be involved in nucleosome assembly during DNA replication (Figure 7). Nucleosome assembly occurs in a stepwise manner, with assembly of (H3/H4)2 tetramer followed by the addition of H2A/H2B dimers. Histones H3 and H4 are rapidly transferred to the heterotrimeric chaperone chromatin assembly factor 1 (CAF-1) that shown direct interaction with PCNA[113]. CAF-1 is involved in depositing histones onto both newly replicated DNA strands to form chromatin. This transport pathway involves many other chaperons that work cooperatively, including NASP1, HSP90 and Asf1[114-116]. Asf1 is a key histone H3-H4 chaperone and loss of function causes severe replication defects and loss of chromatin integrity[117]. Asf1 can interact with CAF-1 and with the helicase MCM2-7[118] to facilitate histone deposition.. If replication is arrested in response to genotoxic insults, Asf1 acts as a buffer to store excess histones that cannot be incorporated into chromatin[117]. A further coordination between FACT remodelling complex and NAP1 promotes deposition of H2A/H2B dimers[119].

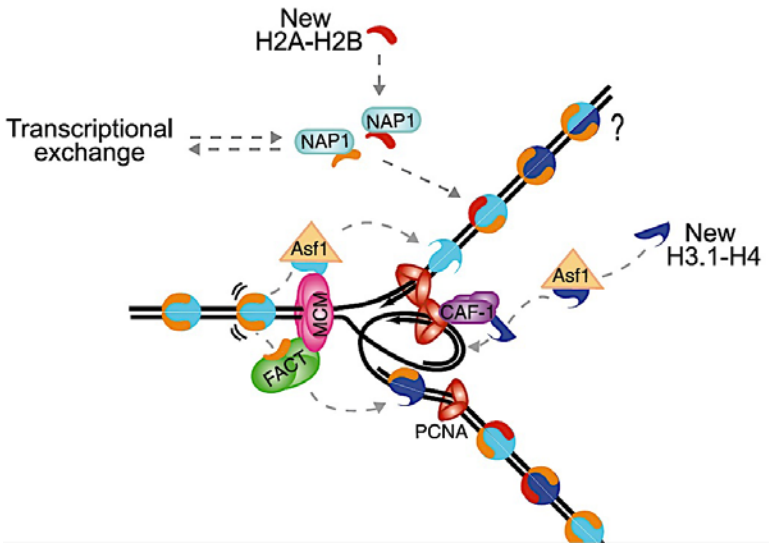

Figure 7: MCM2-7 is an helicase complex that works ahead of the replication fork, unwinding DNA and promoting nucleosome disruption. On nascent DNA nucleosome assembly occurs in a stepwise manner, with deposition of (H3/H4)2,-mediated by CAF-1 via recruitment to PCNA- followed by the adition of H2A/H2B dimers – NAP-1 mediated-. Taken from Groth, 2009 [120]

Understanding the mechanisms that underlie nucleosome regulation at the replication fork can give insights into how defects in chromatin maintenance can promote genome instability. Indeed, in yeast, impaired nucleosome assembly can lead to replication fork collapse, DNA damage and chromosomal rearrangements[121]. In humans, mutations in codanin1, a protein that regulates Asf1 function, is associated with a rare type of anemia involving replication defects and chromatin abnormalities[122].

As chromatin represents a barrier for fork progression, impairment in the regulation of chromatin disassembly and re-assembly during replication can lead to fork collapse and DNA damage. Furthermore, as HDR is a mechanism commonly used to repair DNA during fork collapse, and this mechanism needs large DNA resection and nucleosome disassembly, problems in chromatin remodelling complexes can also trigger expression of CFS due to a failure in the efficiency of HDR or the proper regulation of compaction.

3.3. Targeting DDR proteins in cancer treatment.

Independently of the factor that drives genome instability in cancer cells, DNA repair pathways and cell cycle control processes are crucial for genomic stability and tumor cell biology. Many cancer cells lack one or other aspect of the DDR as a result of selective pressures operating during tumor development. This characteristic has been used to selectively target cancer cells, and most therapies attempt to manipulate the DDR to selectively induce tumor cell death through catastrophic genomic instability. In fact, apart from surgery, the most prevalent cancer treatments are radiotherapy and chemotherapies that involve inducing DNA damage (Table 1).

Cancer treatment	*Types of DNA lesions induced*
Radiotherapy and radiomimetics Ionizing radiation Bleomycin	SSBs, DSB, base damage
Monofunctional alkylators Alkylsulphonates Nitrosourea compounds Temozolomide	Base damage, replication lesions, bulky DNA
Bifunctional alkylators Nitrogen mustard Mitomycin C Cisplatin	DSBs, DNA crosslinks, replication lesions, bulky DNA adducts
Antimetabolites **5**-Fluorouracil Thiopurines Folate analogues	Cytotoxic metabolite, inhibits base pairing leading to base damage and replication lesions
Topoisomerase inhibitors Camptothecins (Topo I) Etoposide (Topo II) Anthracyclines (Topo II)	DSBs, SSBs, replication lesions; anthracyclines also generate free radicals
Replication inhibitors Aphidicolin Hydroxyurea	DSBs, replication lesions

Table 1: Examples of DNA-damaging drugs used to treat cancer. These DNA damaging agents can be also used in combination with inhibitors of DDR pathways inhibitors, such as ATR, ATM or checkpoint kinases inhibitors.

Although these therapies generate toxicity in healthy tissues, they are often efficient. In part, this observation reflects that most cancer cells show an impaired DDR and that they are able to proliferate more rapidly than most normal cells (S phase is a particularly vulnerable time for DNA-damage exposure). It has therefore been speculated that DDR inhibition might enhance the effectiveness of radiotherapy and DNA-damaging chemotherapies; in this regard, various DDR-inhibitory drugs are in pre-clinical and clinical development to test this premise [123].

1.1.16 Synthetic lethalities in cancer treatment.

Different DNA-repair pathways can overlap in function, and one pathway can sometimes compensate for defects in another. As discussed above, cancer cells

sometimes lack one aspect of the DDR. To treat these tumoral cells, the therapies normally involve unspecific generation of DNA damage.

However, knowing the DDR pathway that is impaired in cancer cells, the compensatory pathways that remain active can be considered as a target for inhibition. These strategies are known as synthetic lethalities - Synthetic cell lethality defines a genetic interaction in which the inhibition of the function 2 or more genes leads to cell death[124], although the impairment of only 1 of them is not lethal (**Figure 8**a)-. There are several examples of these kinds of synthetic lethalities in cancer therapy. A number of lethal combinations have been discovered using small interfering RNA (siRNA) and chemical screens. A paradigm for this is provided by drugs targeting the enzyme PARP1 and checkpoint activators such as ATM/ATR/CHK1/CHK2.

1.1.16.1 PARP1 inhibitors

PARP1 is a key player in Base Excision repair (BER) of single strand breaks (SSBs). Notably, PARP inhibitors are relatively non-toxic to normal cells but are strikingly cytotoxic towards HDR-defective cells, particularly those impaired in BRCA1 or BRCA2 (**Figure 8**b)90,91. BRCA proteins have multiple cellular functions and are important for the repair of DSBs by HDR. In the absence of functional BRCA proteins, cells use alternative forms of DNA repair, such as BER. By inhibition of PARP1, BRCA deficient cells become highly sensitive to DNA damage, as both repair pathways are missfunctional (**Figure 8**b). Significantly, some sporadic breast, ovarian, prostate, pancreatic and other tumours also possess HDR defects due to mutation or epigenetic inactivation of HDR components. In this regard, PARP inhibitors might be more broadly applicable. Furthermore, as other DDR pathways are frequently impaired in cancers, there may be additional situations where DDR inhibitors would display selective antitumour effects.

1.1.16.2 ATR/ATM/Chk1/Chk2 Inhibitors.

Cancer cells with activated oncogenes generate replication stress at much greater levels than normal cells. According to the prevailing model (see 3.1), DDR is activated in precancerous lesions by accumulation of DSBs during replication stress. The DDR triggers primary barriers, such as checkpoint arrest, apoptosis or senescence, which can be overcome by mutations in cancer cells. As the replication stress continues in cancer cells, there is an expansion in the number of genetic lesions and, therefore, an increase in the number of oncogenic mutations.

A current therapeutic approach is the inhibition or disruption of ATM/ATR pathway to exacerbate the levels of replication stress and promote cell death. Moreover, ATR inhibition can sensitize cancer cells to DNA damage to a higher degree than normal cells. Consistent with this idea, ATR or Chk1 inhibition is highly effective in killing Myc-induced cells, that show a clear increase in DNA damage due to replicative stress[125]. Comparably, a combination of Ras activation with complete ATR suppression resulted in significant tumor cell killing[126]. Similarly, ATM inhibition results in a significant radiosensitization of cancer cells[127].

In this case, the concept of synthetic lethality can be exploited by combining ATR/Chk1 inhibitors with other modifiers of DDR pathways, such as Parp1 inhibitors[128].

1.1.16.3 Chromatin modifiers inhibition.

Histone deacetylases are enzymes that have been involved in the regulation of gene transcription. However, there is growing evidence that histone acetylation is involved in a larger number of pathways, including DDR. Indeed, several class I and class II HDACs (HDAC1–4) have been shown to promote DNA repair[66,129-131]. Thus, (HDACs) also represent targets for the inhibition of DNA repair, leading to the use of HDAC inhibitors chemosensitizers. The same principle is also applied to class III HDACs or the sirtuin family of deacetylases, of which SIRT1[132,133] and SIRT6[134,135] have been broadly reported to promote DNA repair. SIRT6 has recently been shown to facilitate HR by deacetylating CtBP-interacting protein (CtIP). Consequently depletion of SIRT6 sensitizes cells to DNA damaging agents[134] .Furthermore, activation of SIRT1 seems to be especially detrimental for BRCA1-deficient tumour cells, possibly because it downregulates the apoptosis inhibitor survivin[136].

In general, most current inhibitors of epigenetic modifiers lack target specificity, and genome-wide alterations may result in adverse effects on the tumours or increase side effects when combined with chemotherapy. A better insight into the mechanisms through which these compounds sensitize to chemotherapy may lead to the identification of relevant target genes and ultimately yield more selective therapeutic strategies.

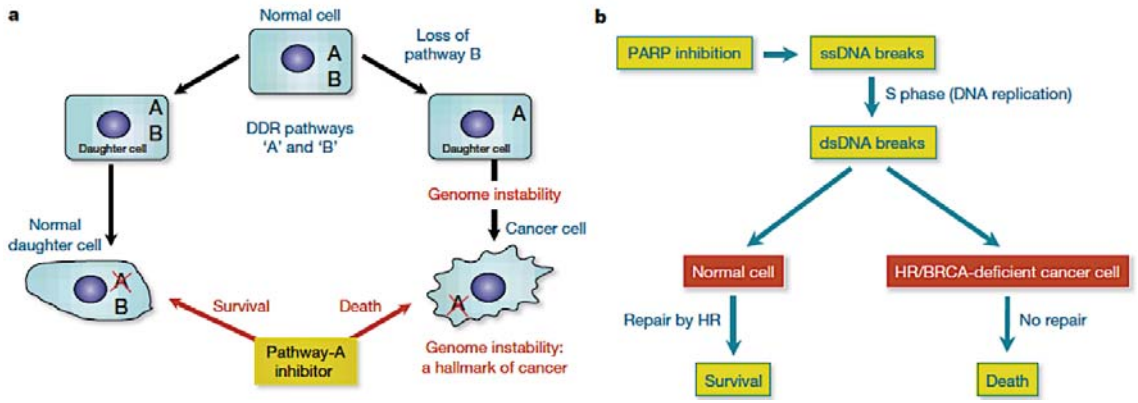

Figure 8. Explotation of DDR pathways to enhance therapeutic responses. a) Model in which normal cells have two DDR pathways, A and B. Elimination of one results in genomic instability, which enhances the development of the cancer cell. Addition of an inhibitor targeting the second pathway leads to cell death. b) Treatment with a PARP inhibitor selectively kills HR/BRCA-deficient cells. PARP inhibition impairs the repair of SSBs, which are converted to DSBs in S phase. Such DSBs are effectively repaired by HR in non-cancerous cells but not in BRCA-deficient cancer cell (taken from [10])

1.1.17 Acquired resistance.

The major problem of DNA damage-creating therapies are side effects due to lack of specificity and lack of efficacy due to acquire resistance. In general, adquire resistance can be divided into two groups depending on its causes:

Tumors that are defective in DNA repair pathways, which are characterized by a high degree of genomic instability, may readily acquire mutations in genes that confer resistance to therapy. In many cases, chemotherapy resistance is caused by reduced drug action because of changes in drug metabolism and/or transport[137,138] In this sense, there is an evident intrinsic resistance because of limited tumour-specific uptake.

Therapy resistance of DDR-deficient tumours may also be caused by partial reactivation of mutated alleles. Hypomorphic mutations can be sufficiently active to reactivate tumor growth. In case mutations lead to the total inactivation of the mutated allele (null allele), chemotherapy may select for new mutations that revert the original defect or select for mutations in other DDR pathway.

4. The Tousled like kinases link chromatin status and the DDR

4.1. Identification of the Tousled Kinase

The Tousled kinase (TSL) was initially described in Arabidopsis thaliana as a Ser/Thr kinase that, when mutated, is responsible for aberrant floral organ and leaf development. TSL mutants exhibited flowering time defects and altered leaf morphology. Flowers in tsl mutants consistently lack the normal complement of floral organs, although the particular organs that are missing vary from flower to flower, suggesting stochastic effects in null mutants. In addition, the sexual organs fail to fuse completely, and lack a complete style and stigma. Microscopy of tsl mutants revealed poorly coordinated cell division resulting in impaired growth and development. Altogether, these observations suggested that TSL was a developmentally important gene [139,140].

4.2. Tsl homologs in other species.

Homologous proteins in other species, named Tousled-like kinases, show high level of similarity to TSL, suggesting a conserved role during evolution. Indeed, the catalytic region is highly conserved between species: *Drosophila melanogaster* TLK, *Caenorhabditis elegans* TLK, mouse TLK1 and TLK2 and human hTLK1 and hTLK2 show a high degree of conservation in the kinase domain, with an average of 70% similarity between them. Interestingly, although TLKs are present in plants, animals and many microorganisms, they are apparently absent in yeast.

TLKs have been implicated cell division with special relevance to S-phase progression and mitosis. In *D. melanogaster*, TLK is an essential gene for nuclear divisions and cell viability. Nuclear defects are detected in early embryos lacking TLK, where the nuclei proceed through rapid DNA replication without successful nuclear divisions, forming a DNA mass of disordered chromatin[141]. In *C.elegans*, TLK is also an essential gene for embryonic development, although in this model, the lack of TLK not only leads to impaired chromosome segregation, but also problems in transcriptional regulation. This process is affected by an inappropriate posttranslational modification in RNAPII and deficient chromatin assembly[142,143].

Figure 9: Evolutionary tree of TLKs in model organisms (www.treefam.org). Lower organisms, such as *D. melanogaster* (fruit fly) or *C. elegans* present only one TLK. Rodents and humans carry two TLKs, TLK1 and TLK2. Zebra fish has three copies.

Importantly, mammalian cells harbor two TLK genes, TLK1 and TLK2, instead the single TLK gene present in lower organisms. The two mammalian genes share 80% sequence identity; their catalytic domains share 94% identity [144] [145]. These kinases were shown to be nuclear proteins whose maximal activity was linked to ongoing DNA replication during S-phase [144,145]. Importantly, TLKs are ubiquitously expressed amongst tissues and the protein levels of this kinase remain consistent throughout the cell cycle in cultured cells.

4.3. TLK functional domains.

The TLKs are serine/threonine kinases with a C-terminal catalytic kinase domain and an N-terminal regulatory domain that contains two coiled coil domains that are necessary for oligomerization [146].

The catalytic kinase domain of TLK constitutes its own branch in the human kinome but is closely related to the calcium/calmodulin-dependent kinase family (CAMK) and the Protein kinase A, G, C family (AGC). Further analysis of the TLK kinase domain revealed a non-canonical evolutionary conserved loop next to the ATP binding pocket. This motif is likely to be an activation loop and several serine residues have been identified as plausible phospho-residues that could regulate TLK activity (further discussed in the results of this thesis).

Two coiled coil domains placed in the N-terminal part of the protein are essential for TLK oligomerization. In humans and mice, both TLKs, TLK1 and TLK2, are able to homo and heteromerize through the coiled coil domains. However, the total stoicheometry and the ratios between TLK1 and TLK2 present in the heteromers is still a matter of study.

There is also strong evidence that TLK1 is regulated in a checkpoint dependent manner. Indeed, Chk1 can phosphorylate TLK1 in Ser 695 and block its activity upon genotoxic stress[97]. It's still not clear whether TLK2 has checkpoint-dependent modulation.

In silico analysis of TLK1 structure revealed a potential SNF domain in the N-terminus of the protein, similar to the yeast SWI/SNF complex, capable of altering the position of nucleosomes along DNA. The functional relevance of this domain is still unclear.

Interestingly, TLKs show a regulatory region in the N-terminus characterized by potentially phosphorytable residues (Ser and Thr residues, in red in figure 10). No potential upstream regulator for this region has been identified, and it is still unclear its functional relevance. The localization of the different domains is shown in figure 10.

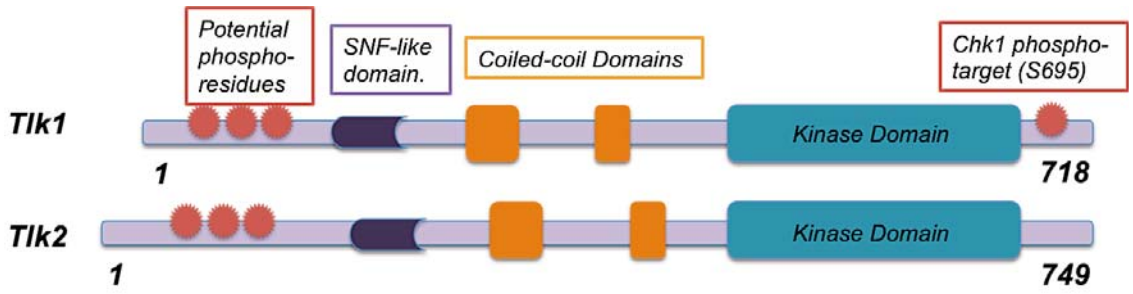

Figure 10. Tlk1 and Tlk2 functional domains. Single residues in red are potential phosphorylation sites. In purple a predicted SNF domain. In orange, two coiled coil domains required for oligomerization. In green the catalytic kinase domain. The total number of residues is shown.

4.4. TLK activity and regulation.

Despite TLKs were discovered 20 years ago and they show high level of evolutionary conservation, there is not much knowledge about their cellular function and regulation.

Mammalian TLKs, TLK1 and TLK2 are ubiquously expressed and show nuclear localization. They show constant protein and mRNA levels during the cell cycle, despite they show maximal activity is during S-phase. The peak in TLKs activity corresponds with a phosphorylated form of these proteins, recognized by a retarded electrophoretic mobility. There are not known substrates that are able to phosphorylate TLKs. In contrast, both TLKs interact with and phosphorylate each other and are capable of autophosphorylation [145,147], which is thought to be responsible of TLKs activation.

It has been suggested that TLKs activities are linked to ongoing DNA replication. According to, aphidicolin or HU treatment decrease TLKs activity[145]. The link between TLKs and DNA replication is belive to be the chromatin assembly factor Asf1 [141,142,148-150]. Additional substrates that have been suggested but not independently confirmed are, histone H3 serine 10 [149,151], the DEAD-box RNA helicase p68 [152] and the RAD9 DNA repair protein [153]. As both TLK1 and TLK2 interact with and phosphorylate Asf1, these Ser/Thr kinases have been proposed to regulate chromatin remodeling during DNA replication and transcription. These data is consistent with the fact that C.elegans TLK null mutants display problems in chromatin condensation and transcription. Even more, in this organism TLK has been propose to regulate the mitotic kinase Aurora B through phosphorylation.

Owing to the lack of knowledge about the substrates or the relative importance of TLK1 or TLK2 to any cellular function, it is difficult to speculate on the effect of TLK suppression in regulating cellular responses.

1.1.18 Link to replication and DDR.

TLKs are S-phase active kinases, which most reported substrate is the histone chaperone Asf1, a highly conserved histone chaperone among eukaryotes that assembles and disassembles chromatin during transcription, replication and repair [81,154-156]. In mammals, there are two forms of Asf1, namely Asf1a and Asf1b. Both proteins contribute to nucleosome deposition, but Asf1a has been related to replication-independent assembly (mainly transcription) while Asf1b is important in replication fork progression. It is also reflected in the complexes they interact with, as

Asf1a interacts with HIRA, a factor involved in transcription [83,157], but Asf1b has never been reported to be associated with transcription machinery. In addition, Asf1b is the only isoform required for cell proliferation and its expression levels have prognostic value in breast cancer [158]. Further evidence of Asf1b participation in DNA replication comes from unpublished work from our collaborators in Anja Groth's laboratory. They have recently shown that TLK phosphorylation of Asf1 promotes its binding to histones and facilitates their delivery during DNA replication [159]. In this regard, TLK1 localizes to replication sites and targets histone-free Asf1 in its C-terminus. This phosphorylation stimulates the association of Asf1 with histones and the ability of transfer this histones to CAF1, promoting the supply of histones to the nascent DNA.

It has been established that TLK activity is inhibited in the presence of DSB, UV-induced DNA damage, and after blocking ongoing DNA replication [97,147,148]. Direct phosphorylation of TLK by Chk1 results in TLK inhibition, and this phosphorylation is dependent on the upstream ATM checkpoint kinase rather than the canonical Chk1 activator, ATR [97]. The inhibition of TLK activity results, ultimately, in Asf1 inhibition after genotoxic stress. But the significance of this inhibition is still unknown. Further more, loss of ASF1 in yeast leads to spontaneous DNA damage, increased frequencies of genome rearrangements [160,161], and sensitivity to a number of genotoxic agents that damage DNA during replication [162]. However, while Asf1 does not appear to play a direct role in the repair process, it is critical for the replacement of nucleosomes that are lost as a result of DNA resection before repair. Following repair, cells lacking Asf1 maintain nucleosome free regions and remain arrested through signaling pathways that have not yet been identified [75].

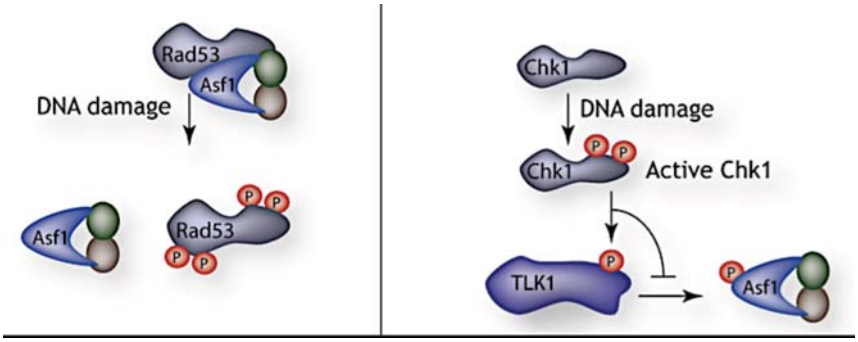

Figure 11. In yeast (left) Asf1 interacts with Rad53, but in mammals (right) there is no a direct interaction between Asf1 and Chk1 (homologous to Rad53). In mammals, Asf1 interacts with TLKs.

How Asf1 exchange nucleosomes during DNA repair is still an open question. In yeast, Asf1 interacts with the checkpoint kinase Rad53 and this association is perturbed in response to DNA damage, although the significance of this remains unclear (Figure 11) [161-163]. In mammalian cells, the primary cell cycle checkpoint kinase analogous to Rad53 is Chk1, but a direct association between Asf1 and Chk1 has not been identified. However, in response to replication blockage or DNA damage, activated Chk1 negatively regulates TLK1 activity, which forms complexes with its homolog TLK2 and these proteins can interact with and phosphorylate Asf1 (Figure 11) [148]. In fact, TLKs are the only known kinases that phosphorylate Asf1.

In addition, yeast Asf1 interacts with some other factors including histone modification enzymes and modification-recognizing proteins. For example, Asf-1 directly activates the HAT activity of Rtt109 that acetylates histone H3 at lysine 56 via its role in presenting H3/H4 dimers to Rtt109 [121,164,165]. Interestingly, a non-acetylable H3K56R mutant in yeast showed a phenotype in DNA damage similar to that of the mutant lacking Asf1 (asf1Δ mutant) [166] and an H3K56Q mutant that mimics the acetylated state of H356K was found to suppress this defect in DNA damage [164]. But how H3K56 acetylation contributes DDR is still not well established. Some studies argue that H3K56 is rapidly deacetylated after damage, and that Asf1- mediated acetylation is rapidly recovered after DNA repair [167]. This acetylation would be important for γH2AX dephosphorylation and the recovery of checkpoint arrest.

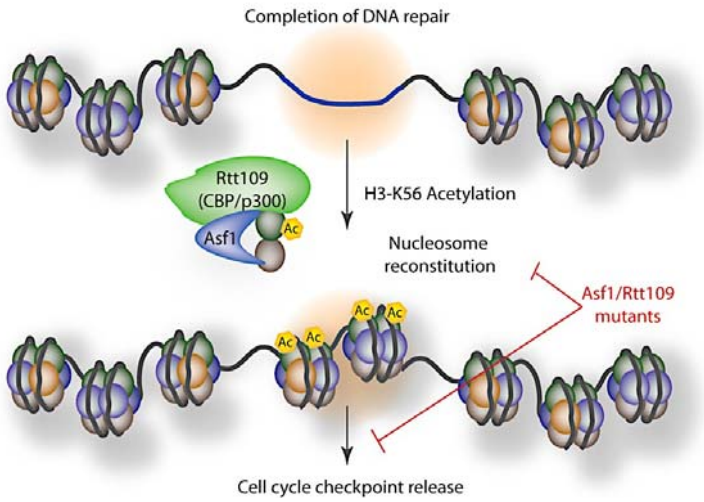

Figure 12. Asf-1 directly activates the HAT activity of Rtt109 which acetylates histone H3 at lysine 56 via its role in presenting H3/H4 dimers to Rtt109. Asf1 or Rtt109 mutant are deficient in reconstituting chromatin composition after completion of the repair

Given the critical role of Asf1 in cellular processes and the severe phenotypes of TLK depletion in lower organisms, is likely that TLK1 and TLK2 are critical regulators of histone transactions, which would make these genes key players in development and disease. Supporting this, recent work has proposed that TLK2 expression levels have predictive value in glioblastoma patients [168]. This finding suggests that reduction of TLK activity will impair the function of Asf1, thus affecting key cellular processes that maintain genome integrity, proliferative capacity and cellular identity (Figure 13).

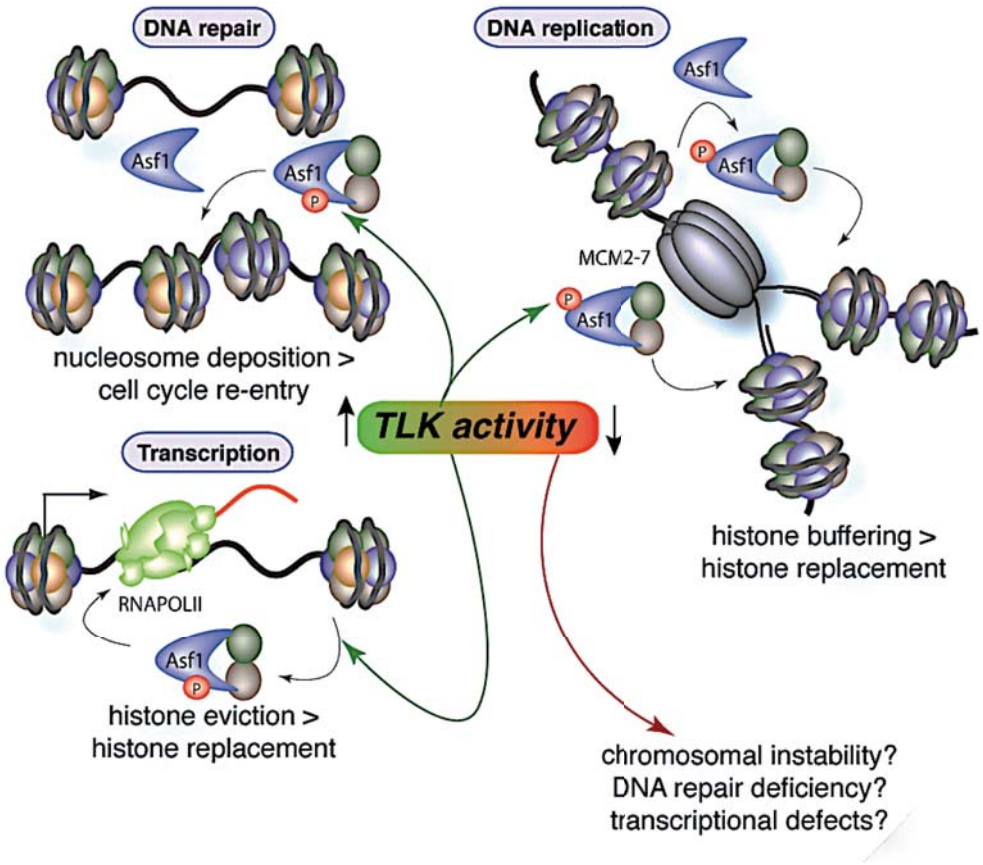

Figure 13. Reduction in TLK activity will impair key Asf1 functions in DNA replication, DNA repair and transcription. This will impair genome integrity and cellular function. These consequences may promote cancer development but could also represent a vulnerability that could be exploited for therapeutic intervention.

Hypothesis and objectives

Hypothesis

We hypothesize that diminished Tousled like kinase activity will compromise the regulation of chromatin modifications and will therefore lead to chromosomal instability, DNA damage sensitivity, activated DNA damage responses, impaired development and impaired cancer progression.

Objectives

1. Generation of genetrap mouse models to determine the functions of Tlk1 and Tlk2 in primary cells and *in vivo*.
2. Phenotypic characterization of primary and transformed cells lacking Tlk1, Tlk2 or both in the presence or absence of DNA damage.
3. Phenotypic characterization of cells overexpressing TLK1 or TLK2 and its kinase dead mutants.
4. Analysis of protein-protein interactions of TLK1 and TLK2.
5. Analysis of TLKs role in tumour progression.

Material and methods

1. Generation of a TLK1 and TLK2 deficient mouse model

Design and construction of a TLK1 and TLK2-targeting vector, ES cell transfection, identification of correctly targeted cell clones, ES microinjection into pre-implantation stage mouse embryos and chimera generation were done by Mouse Mutant Core Facility at IRB Barcelona.

1.1. Generation and screening of TLK1 and TLK2 targeting constructs

Mouse embryonic stem (ES) cells containing a gene-trap cassette between exons 1 and 2 of the TLK1 gene were purchased from the German Genetrap Consortium (clone ID E067A02) and ES cells with a gene-trap cassette between exons 1 and 2 of the TLK2 gene were purchased from Bay Genomics (DTM063). Cells were injected into 3.5-day old mouse blastocysts derived from C57B6/j mice. Approximately 12-15 ES cells were injected into each blastocyst, and injected blasts were re-implanted back into the oviduct of 2.5-day pseudo-pregnant foster mice (CD1s). Chimeras born from these injections were scored for chimerism by coat colour analysis, and the chimeras showing the highest contribution from the ES cells were mated with C57B6/j wild-type mice. Agouti offspring obtained from these test-matings were screened for the presence of the mutation. Subsequent pups were screened for the zygosity of the mutation (Tlk1) or the presence of the genetrap (Tlk2) using specific primers (Table 2). Subsequent genotyping was performed using quantitative real time PCR primers designed by Transnetyx.

1.2. Genotyping strategy

For the purpose of genotyping we have designed primers for PCR that allowed us to distinguish with high accuracy wild type and gene-trap alleles based on unique amplification products. Primer sequences are provided in Table 1.1. and PCR reaction conditions in Table 1.2. Genomic DNA used for genotyping was isolated from the tails of the mice and extracted by digestion with proteinase K over night at 56ºC, followed by isopropanol precipitation. The buffer used for genomic DNA extraction has next

composition: 0.1M Tris/HCl, 200mM NaCl, 0.2% SDS and 5mM EDTA.

Table 2. Tlk1 and Tlk2 genetrap genotyping primers

Allele	Primer	Primer sequence	Product (bp)
Tlk1^{Trap} (5' side)	Tlk1-A02-F	ACTGAGTGTGTTATGCCCTTCGCA	971
Tlk1^{Trap} (5' side)	B32 diagnostic	GGGAGGATTGGGAAGACAAT	971
Tlk1^{Trap} (3' side)	Tlk1-A02-R	GCGTACACATGTGCGTGTGAGTAT	1870
Tlk1^{Trap} (3' side)	GT2 diagnostic	GGGAGGATTGGGAAGACAAT	1870
Tlk1^{+}	Tlk1-A02-F	ACTGAGTGTGTTATGCCCTTCGCA	400
Tlk1^{+}	Tlk1-A02-R	GCGTACACATGTGCGTGTGAGTAT	400
Tlk2^{Trap}	Bgal probe F	TTATCGATGAGCGTGGTGGTTATGC	681
Tlk2^{Trap}	Bgal probe R	GCGCGTACATCGGGCAAATAATATC	681

1.1.19 Real time PCR based assessment of gene expression levels

In order to assess the endogenous transcript levels in gene trap and knock out mice as well as in siRNA experiments, we have developed a quantitative Real Time-PCR (qRT-PCR) assay for both the human and mouse *TLK1 and TLK2* genes. qRT-PCR was performed using comparative CT method and a Step-One-Plus Applied Biosystems Instrument. Amplification was performed using SYBR Green Expression Assay or TaqMan assays using commercial Applied Biosystem probes. Primer sequences are given in Table 3. and qRT-PCR reaction conditions are given in the Table 4. All assays were done in triplicates and Gapdh primers were used as an endogenous control for normalization. Data are means ± standard deviation of at least 3 experiments.

Table 3. Genotyping primers for cDNA (by qPCR)

Tested gene	Sequence
TLK1 (exon3-5)	Fw: 5' GGCAGTTGCAGTGTTGGAGCTAAA 3' Rv: 5' TACCAGGGTGGAAATGGCTCAAGT 3'

Gapdh	Fw: 5' GCACAGTCAAGGCCGAGAAT 3' Rv: 5' GCCTTCTCCATGGTGGTGAA 3'
TLK1 (Taq Man probe)	**ABIMm00554286** ACAGATACGTTTTGTACA(EX15-16)
TLK2 (TaqMan Probe)	**ABIMm01246220** TGACTCGTTTTG (EX17)
Gapdh (TaqMan probe)	**ABIMm99999915** CGTGCCGCCTGGAGAAACCTGCC

Table 4. qPCR conditions

Step	Temperature	Time
Holding stage	95ºC	10min
Cycling stage **(40x)**	95ºC 60ºC	15sec 1min
Melt Curve Stage	95ºC 60ºC 95ºC	15sec 1min 15sec

2. Cultured human and mouse cell methods

2.1. Cell cultures

The cell media, supplements, and antibiotics, were purchased from Gibco Invitrogen. Cell culture flasks, plates, dishes, and cryotubes were purchased from Nunc and BD Falcon. All cells were grown in a 37ºC incubator with a humidified atmosphere containing 5 % CO2.

1.1.20 Human cell lines

Human embryonic kidney HEK293 cells were cultured in Dulbecco's modified Eagle Medium (DMEM, Invitrogen) supplemented with 10 % (v/v) foetal calf serum (FCS) and 100 U/ml penicillin/streptomycin (Gibco).

1.1.21 Preparation of mouse embryonic fibroblasts (MEFs)

Mouse embryonic fibroblasts were isolated from pregnant females at E14.5. Uterine horns were removed and placed into a petri dish with PBS. Intact embryos were taken out from uterine horns into fresh PBS, embryos were then released from yolk sac and placenta and moved to fresh PBS. Heads and viscera were removed and tails were taken for the genotyping. Carcasses were washed in fresh PBS and kept over night at 4ºC in the 5ml trypsin in 15ml Falcon tubes. Upon obtaining genotyping results, selected embryos were processed further. Trypsin volume was reduced in tubes and carcasses were incubated in 1ml of remaining trypsin at 37ºC for 20 minutes. 5ml of DMEM media was added to each carcass and they were minced by pipetting up and down with a 5ml serological pipette. The supernatant containing cells were plated in 3 x 10 cm plates and further propagated as necessary.

1.1.21.1 Culture of primary MEFs

Primary MEFs (p0-p5) were cultured in Dulbecco's modified Eagle Medium (DMEM) supplemented with 10 % (v/v) foetal calf serum (FCS), 2mM L-glutamine and 100 U/ml penicillin. Cells were used for experiments until passage 5 while still in the log phase of growth.

1.1.21.2 Generation and culture of transformed MEFs

Primary MEFs were transformed in two ways.

a) The primary mouse embryonic fibroblast cells were replated every 3 days at the rigid density of 1 x 10^6 cells per 10-cm dish. The spontaneously immortalized cells with a stable growth rate were established after 20-30 generations in culture.

b) The primary MEFs were transfected with linearized p129 plasmid (origin-less SV40 genome) using the AMAXA nucleofector (MEF solution 2) protocol. Immortalized cells were selected after 3-5 passages.

3T3 and SV40 transformed cells were cultured in Dulbecco's modified Eagle Medium (DMEM) supplemented with 10 % (v/v) foetal calf serum (FCS) and 100 U/ml penicillin.

1.1.22 Neurosphere cell culture

Neural precursors were obtained from dissociated e14.5 forebrains of WT, *Tlk2*$^{+/Trap}$ and *Tlk2*$^{Trap/Trap}$ embryos. Neurospheres were grown in DMEM/F12 supplemented with B27 (Invitrogen) using previously described methods[169] in the presence of 10 ng/ml EGF (human recombinant; Peprotech) and 20 ng/ml bFGF (human recombinant; Peprotech). Primary neurospheres al passage 0 were harvested after 7 days in culture, dissociated into single cells and plated at 2x10^4 cells/ml. Fresh medium was added to the cultures 3 days after replating. Primary neurospheres (passage 1) were counted, harvested and trypsinized every week for later passages. Neurospheres were dissociated in 0.25% trypsin (Invitrogen) for 10 minutes and subsequent mechanical dissociation in L15 Medium (Sigma) supplemented with 1 mg/ml trypsin inhibitor (Sigma) and 0.8 mg/ml DNase I (Roche).

2.2. Growth, cell cycle and sensitivity assays

1.1.23 3T3 Proliferation assay

Primary MEFs were continuously replated every 3 days at rigid density of 1 x 10^6 cells per 10-cm dish. The cells were counted each passage until spontaneous immortalization. For analysis of long-term growth, total cell numbers in each passage was plotted on a log scale, against passage numbers on a linear scale.

1.1.24 Clonogenic survival assay

The ability of SV40 immortalized MEFs to form colonies upon damage was tested by clonogenic colony forming assay (CFA). Cells were plated either after the treatment (X-irradiation induced damage) or before the treatment (UVC, etoposide). Cells were plated on 6 cm plates in duplicates. The number of cells for seeding was adjusted to the plating efficiency and the toxicity of the treatment. The details are provided in the Table 5. Cells were kept in a CO_2 incubator at 37°C for 10 days until cells in control plates formed visible colonies (50 cells per colony is the minimum for scoring). Colonies were stained with crystal violet (Sigma-Aldrich) and counted. Based on the colony number, plating efficiency (PE=number of colonies formed/number of colonies seeded x 100%) and surviving fraction (SF=number of colonies formed after

treatment/number of cells seeded x PE) were calculated and plotted.

1.1.25 DNA damaging agents and drug treatments

UV-C irradiation at 254 nm was performed with a germicidal lamp using a Stratalinker. Cells plated in dishes were aspirated of their medium, washed with PBS, and with no liquid present in the dish and lid removed, exposed to the desired dose of UV-C radiation. Pre-warmed media was then added to the cells before returning to the incubator for the appropriate recovery time. Exposure of cells to ionising radiation was performed with 200 kV X-rays at 4.5 mA with a dose rate of 0.025 Gy/s. Cells were irradiated in suspension and plated following damage. Camptothecin stock solution was dissolved in DMSO to 1mM stock concentration and added to cell medium to a final concentration of 40, 80 or 120 nM for 24 hours for the clonogenic assay (CFA). Etoposide was dissolved in DMSO to 50mM stock concentration and added to cell medium to a final concentration of 50, 150 or 300 nM for 24 hours for CFA. MMS was applied for 24hrs at final concentration of 2, 4 or 8 µg/ml (CFA). Aphidicolin was prepared in DMSO and added to cell medium to a final concentration of 300 nM for 36 hours (metaphase spreads).

Table 5. Colony forming assay plating conditions and doses of damaging agents.

Etoposide	**CPT**	**X-IR**	**UVC**	**Cells/6cm plate**
Mock	Mock	Mock	Mock	500
50nM	40nM	2Gy	10J/m^2	1000
150nM	80nM	5Gy	20J/m^2	2000
300nM	120nM	8Gy	30J/m^2	5000

1.1.26 Senescence-associated (SA) β-Galactosidase

Frozen tissue sections and primary WT and *Ercc1*-/- MEFs were fixed in 0.25% gluteraldehyde and 2% paraformaldehyde for ten minutes at room temperature. Following three rinses in PBS, SA-β-Gal staining was performed at pH 6.0 as previously described [170].

1.1.27 Metaphase spreads

A mitotic population of primary MEFs in logarithmic phase growth was enriched by colcemid treatment for 1 or 2 hours at $2x10^{-7}$M concentrations. Cells were harvested, swollen with 0.075M KCL for 15 minutes at 37ºC and fixed over night with dropwise added ice-cold methanol: glacial acetic acid (3:1). Cells were resuspended in 300 µl of fixative and 30ul was spread over the glass slide that was then inverted over 80ºC water bath for 7 seconds and dried on the hot lid. Slides were stained in 5% Giemsa solution for 10 minutes and examined under oil immersion at 100X magnification, using a white light source. 50 spreads were counted per sample and the number of chromosomes per spread and aberrations per spread were recorded.

3. Isolation of proteins and nucleic acids

3.1. Genomic DNA isolation:

MEFs were plated at 10cm plates at 10^6 cells/plate density. Next day cells were washed by PBS and harvested with 500 µl of buffer containing: 75mM of NACl, 50mM EDTA, 0.2% SDA and 0.4mg/ml of Proteinase K. Cells were incubated over night at 50ºC and next day isopropanol precipitated, resuspended in 200ul of TE and stored at -20ºC for further usage.

3.2. mRNA Isolation:

This protocol was used for primary MEFs and sorted HSC. RNA was isolated by TRIZOL (Invitrogen)- Chloroform. In the case of small samples (less than 10.000 cells), 2µl of Pellet Paint (Novagen #69049-3) were added per 300µl of TRIZOL. RNA was precipited in isopropanol, washed with 75% ethanol twice and resuspended in DEPC water. Ethanol precipitation was carried out by adding 3 M NaOAc pH 5.5 (to a final concentration of 0.3 M) and 2.5 volumes of ice-cold 100% ethanol to the RNA. After washing with 75% etanol, RNA was resuspended in comercial RNase free water and stored in -80ºC. In the case of further cDNA generation, 4 µg of total RNA from each sample were used for Reverse Transcription using the “High Capacity RNA-to-cDNA Kit”, Applied Biosystems.

3.3. Total protein extraction and western blotting

Cells were lysed with a TNG-150 buffer containing 50mM Tris/Hcl, 150mM NaCl, 1% Tween-20, 0.5%NP-40, 1x Sigma protease and phosphatase inhibitors. Protein samples were quantified using The Bio-Rad *DC* Protein Assay, separated by standard SDS-PAGE on 6%, 8%, 12% or 15% polyacrylamide gel (90V, 20min + 120 V, 90 min) and transferred (1hr, 95V) to PVDF membrane (Immobilon-P, Millipore). The antibodies used are listed in the Tables 6 and 7.

Table 6. List of primary antibodies

Antibody	Species	Source	Dilution
H2AXg (S139)	Mouse	Millipore (05-636)	WB 1:1000, IF 1:500, IHC 1:600
Chk1 (FL-476)	Rabbit	Santa Cruz (sc7898)	WB 1:500
p-Chk1 (s345)	Rabbit	Cell Signaling (2341S)	WB 1:500
actin	Mouse	Sigma (T5168)	WB 1:3000
LC8	Mouse	ABCAM (AB51603)	WB 1:2000
Asf1	Mouse	Sigma (A5236)	WB 1:800
BrdU	Mouse	B. Dickinson (347580)	FACS 1:50
Histone3 serine10	Rabbit	Milipore (06-570)	FACS 1:200
TLK1	Rabbit	Cell signaling (#4125)	WB 1:1000
TLK1 Ct	Rabbit	Bethyl (A301-253A)	WB 1:1500
TLK1 Nt	Rabbit	Bethyl (A301-252A)	WB 1:1500
TLK2	Rabbit	Bethyl (A301-257A)	WB: 1:2000
FLAG	Mous	Cosmo Bio Co (NMDN002)	WB 1:20

Table 7. List of secondary antibodies

Antibody	Source	Dilution
Rabbit HRP	Thermo Scientific	WB 1:30000
Mouse HRP	Thermo Scientific	WB 1:30000
Rabbit Alexa Fluor 488 (green)	Invitrogen	IF 1:500
Mouse Alexa Fluor 488 (green)	Invitrogen	IF 1:500
Mouse Alexa Fluor 594 (red)	Invitrogen	IF 1:500
FITC-Anti Rabbit IgG (H+L)	ImmunoResearch	FACS 1:200

1.1.28 Isolation of soluble and insoluble cellular fractions

The fractionation protocol was modified from Groth et al, 2008. Fractionation of HEK293 cells over-expressing TLK1, TLK2 and its kinase dead isoforms required two confluent 15 cm dish per condition in order to detect chromatin bound to Tousled-like kinases. Plates were washed 2 times in ice cold PBS and incubated at 4ºC for 10 minutes in 10 ml of buffer E without phospho or protease inhibitors, containing 20mM HEPES-KOH, 5mM Potassium Acetate, 0.5mM $MgCl_2$, 0.5mM DTT. In this step cells will get swollen. The buffer gets removed and replaced with fresh cold buffer E containing phosphatase and protease inhibitors and cells are incubated additional 10 minutes at 4ºC. After incubation is over, buffer is removed and plates are drained. Cells are scraped and transferred into Wheaton 1ml douncer where they get homogenized by pestle (25-30 strokes/sample). The disrupted cells are transferred then to tubes and centrifuged for 5minutes at 1500g. Pellet contains nuclei while the supernatant can be cleared by additional spinning at 13.000g for 15min and used as cytosolic fraction that contains cytoplasmic and soluble nuclear proteins. Nuclear pellet is further resuspended in buffer N that contains buffer E, 540mM NaCl and 10% Glycerol. Chromatin and nuclear bound proteins are extracted by end-over-end rotation for 90 min at 4ºC. Afterwards samples are spun at maximum speed for 15 minutes and the supernatant is used for further analysis of chromatin bound proteins.

1.1.29 Purification of Strep-Flag tagged mouse TLK1 and TLK2 from human cultured cells

Tandem affinity purification (TAP) combines two sequential steps of affinity-purification. As a result, TAP can significantly reduce the background caused by nonspecific binding of proteins.

The Strep/FLAG tandem affinity purification (SF-TAP) tag combines a tandem Strep-tag II and a FLAG tag, resulting in a small 4.6 kDa tag[171]. First, SF-TAP fusion protein is eluted from the Strep-Tactin with desthiobiotin and then flag peptide is used for elution of the SF-TAP fusion protein from the anti-FLAG M2 affinity matrix.

Protein extracts were incubated with 100µlpre-washed streptactin superflow resin (IBA) for 2 h at 4ºC using an overhead tumbler. Resin was spin down (7,000 g, 30 s) and transferred to microspin columns (GE Healthcare). Resin was washed 3 times with 500 µl washing buffer (30 mM Tris pH 7.4, 150 mM NaCl, 0.1% NP-40, protease inhibitor cocktail (Roche) and phosphatase inhibitors (Sigma)). SF-TAP fusion proteins were eluted from the Strep-Tactin matrix with 500 µl of desthiobiotin elution buffer (IBA) (30 mM Tris pH 7.4, 150 mMNaCl, 1mM EDTA, 2 mM desthiobiotin, protease and phosphatase inhibitors) for 10 min on ice. 150 µl were stored as “IP STREP”.

The eluted fractions were equilibrated with 0.5% NP-40 and 1% Tween-20 and were incubated with 120 µl pre-washed anti-FLAG-M2 magnetic beads at 4ºC overnight in the over head tumbler. Beads were washed with 500 µl wash buffer and twice with 500 µl of TBS buffer (30 mM Tris pH 7.4, 150 mM NaCl, protease and phosphatase inhibitors). For elution of the SF-TAP fusion protein from the anti-FLAG-M2 magnetic beads, 400 µl of Flag elution buffer (30 mM Tris pH 7.4, 150 mM NaCl, 200 µg/mL flag peptide (Sigma)) were used for 6h at 4ºC in the over head tumbler. Remaining proteins bound to the magnetic beads were recovered with 60 µl sample buffer (250 mM Tris HCl pH 6.8, 8% SDS, 40% glycerol) for 5 min at 95ºC.

The different aliquots retained during the experiment and the final TAP fractions were quantified using the Bradford reagent (BioRad).

*Strep or Flag purifications: in some cases, one-step purifications were performed. Strep purification was performed as described previously without the Flag purification sequential step. Flag purification was performed directly from the protein extracts as described previously.

4. Subcloning of TLK1 and TLK2 in retroviral vector

Human cDNA isoforms of TLK1 and TLK2 were subcloned in pENTR223 (from Invitrogen) using Bam HI and Xho I sites. From this vector hI was subcloned by LR clonase reaction (Invitrogen) into PLPC backbone or PcDNA3.0-*Strep*-FLAG (provided by Dr. Ueffing's laboratory, Helmholtz Zentrum Munchen). They were used for transient or stable transfections.

4.1. Mutagenesis

The TLK2 kinase dead (TLK2 KD) mutant and TLK2 autophosphorylation mutants were generated using the QuickChange site-directed mutagenesis kit (Stratagene). The PCR reactions were prepared with 5 µl of 10x reaction buffer, 100 ng of SF-TAP-TLK2 (destination vector), 125 ng primer sense, 125 ng primer antisense, 1 µl of dNTPs mix, 1.5 µl QuikSolution reagent, ddH_20 to a final volume of 50 µl and 1 µl QuickChange Lightning Enzyme. The mutagenesis primers used are outlined in Table 8.

Table 8: Sequences of the primers used in site-directed mutagenesis reactions to generate TLK2 kinase dead protein (in red) and TLK2 autophosphorylation mutants (in blue).

MUTANT		Sequence
Kinase dead Q703A	Sense	5'-CACCATGATGGAAGAATTGCATAGCCTGG-3'
	Antisense	5'AATATTACCTGGTTTGAGGACATAGTGTATGATGGGAGG-3'
TLK2 S569A	Sense	5'-GGAGAAAGAGGCCCGGGCCATTATCATGCAGAT-3'
	Antisense	5'-ATCTGCATGATAATGGCCCGGGCCTCTTTCTCC-3
TLK2 S617A	Sense	5'GATAAAAATTACAGATTTTGGTCTTGCGAAGATCATGGATGATGATAG-3'
	Antisense	5'CTATCATCATCCATGATCTTCGCAAGACCAAAATCTGTAATTTTTATC-3'
TLK2 S635A	Sense	5'-TGGCATGGAGCTAACAGCACAAGGTGCTGGTAC-3
	Antisense	5'-GTACCAGCACCTTGTGCTGTTAGCTCCATGCCA-3'
TLK2 S686A	Sense	5'-CTTTTGGCCATAACCAGGCTCAGCAAGACATCCTA-3'
	Antisense	5'-TAGGATGTCTTGCTGAGCCTGGTTATGGCCAAAAG-3'

Each reaction was cycling using the cycling parameters described in Table 9

Table 9: Cycling parameters for the QuikChange Lightning Site-Directed Mutagenesis Method.

Segment	Cycles	Temperature	Time
1	1	95°C	2 minutes
2	18	95°C	20 seconds
		60°C	10 seconds
		68°C	4 minutes
3	1	68°C	5 minutes

The parental supercoiled dsDNA were digested by 2 µl of DpnI restriction enzyme (Stratagene) for 5 minutes at 37ºC. X-Gold Ultracompetent Cells (45 µl) were transformed with DpnI-treated DNA (5 µl). The transformation reactions were done using the heat-shock method. LB media was added (500 µl) and the tubes were incubated at 37ºC for 1 hour. The transformation reaction was dispersed on agar plates (kanamycin resistance) and plates were incubated at 37ºC for 16 h.

Mutant plasmids were purified from the positive clones using The PureLink® Quick Plasmid Miniprep Kit (Invitrogen) as described previously. All constructs were sequenced after generation using the primer (5'-TCAGGCCCCTCCTGCAACCA-3') (Macrogen, Amsterdam, The Netherlands). Plasmids with the mutation were purified using PureYield™ Plasmid Maxiprep System (Promega) as described previously.

4.2. Retroviral overexpression

For production of retrovirus, HEK293t packaging cells were transfected with the gene of interest subcloned in pLPC backbone and with retroviral vectors (VSVG and GagPol) using PEI (1mg/ml) and NaCl (150mM). Viral supernatants were harvested 48 and 72 hours post transfection, filtered (0.45um) and placed directly on fresh split HEK293 cells. Infection was done in presence of polybrene (10 µg/ml) for 24 hours in 2

cycles. Cells were then recovered with fresh media and selected with 10 µg/ml of puromycin for several days.

5. Mass spectrometry

Experiments were performed in the IRB Mass Spectrometry core facility. Samples (200 µg) were digested with trypsin following FASP protocol [172] The nano-LC-MS/MS set up was as follows. Digested peptides were diluted in 1% FA. Samples were loaded to a180 µm × 2 cm C18 Symmetry trap column (Waters) at a flow rate of 15 µl/min using a nanoAcquity Ultra Performance LCTM chromatographic system (Waters Corp., Milford, MA). Peptides were separated using a C18 analytical column(BEH130™ C18 75 mm × 25 cm, 1.7 µm, Waters Corp.) with a 80 min run, comprising three consecutive steps with linear gradients from 1 to 35% B in 60 min, from 35 to 50% B in 5 min, and from 50 % to 85 % B in 3 min, followed by isocratic elution at 85 % B in 10 min and stabilization to initial conditions (A= 0.1% FA in water, B= 0.1% FA in CH3CN). The column outlet was directly connected to an Advion TriVersa NanoMate (Advion) fitted on an LTQ-FT Ultra mass spectrometer (Thermo). The mass spectrometer was operated in a data-dependent acquisition (DDA) mode. Survey MS scans were acquired in the FT with the resolution (defined at 400 m/z) set to 100,000. Up to six of the most intense ions per scan were fragmented and detected in the linear ion trap. The ion count target value was 1,000,000 for the survey scan and 50,000 for the MS/MS scan. Target ions already selected for MS/MS were dynamically excluded for 30s. Spray voltage in the NanoMate source was set to 1.70 kV. Capillary voltage and tube lens on the LTQ-FT were tuned to 40 V and 120 V. Minimal signal required to trigger MS to MS/MS switch was set to 1000 and activation Q was 0.250.The spectrometer was working in positive polarity mode and singly charge state precursors were rejected for fragmentation. At least one blank run before each analysis was performed in order to ensure the absence of cross contamination from previous samples.

A database search was performed with Proteome Discoverer software v1.3 (Thermo) using Sequest search engine and SwissProt database (Human, release 2012_03). Searches were run against targeted and decoy databases to determine the false discovery rate (FDR). Search parameters included trypsin enzyme specificity, allowing for two missed cleavage sites, carbamidomethyl in cysteine as static modification and methionine oxidation as dynamic modifications. Peptide mass tolerance was 10 ppm

and the MS/MS tolerance was 0.8 Da. Peptides with a q-value lower than 0.1 and a FDR < 1% were considered as positive identifications with a high confidence level.

For phosphoproteomic analysis phosphopeptides were selectively enriched for on TiO2 colum. The peptides are eluted and analyzed as described above. Sequest peptide sequences were manually confirmed to ensure correct sequence identification. For MS3 scans, search parameters were almost the same as those for MS2 scans, with the following changes: loss of water in ST was included as dynamic modification and precursor ion mass tolerance was 1.8 Da. Positive identifications were filtered by setting up a XCorr higher than 2 for charge state 2, higher than 2.25 for charge state 3 and higher than 2.5 for charge state 4.

6. Knockdown assays

6.1. Short hairpin RNA-mediated knockdown

We used an online shRNA prediction tool: 'Designer of Small Interfering RNAs—DSIR' (http://biodev.extra.cea.fr/DSIR/DSIR.html) to predict the sequence of high confidence shRNA that could downregulate TLK2. We cloned and tested 8 high-confidence shRNAs, following the strategy published by Lukas E. Dow [173]. Once cloned into the tTRMP viral vector, HEK293t were transfected with the shRNA and retrotiviral vectors (VSVG, RSV and RRE) using PEI (1mg/ml) and NaCl (150mM). Viral supernatants were harvested 48 and 72 hours post transfection, filtered (0.45um) and placed directly on fresh split SV40 transformed MEFs. Infection was done in presence of polybrene (10 µg/ml) for 24 hours in 2 cycles. Cells were then recovered sorting GFP positive populations. The sequence of the shRNAs tested are listed in table 10.

Table 10. List of eight target sites in TLK2 cDNA and the sequence of the respective oligonucleotides used to produce shRNA.

Name	Target site	97bpOligo
Tlk2.1189	CAGCAAAAGATGCTAGAGAAA	TGCTGTTGACAGTGAGCGCCAGCAAAAGATGCTAGAGAAATAGTGAAGCCACAGATGTATTTCTCTAGCATCTTTTGCTGTTGCCTACTGCCTCGGA
Tlk2.1424	CACAGAGAGAAGAGATAGAAA	TGCTGTTGACAGTGAGCGCCACAGAGAGAAGAGATAGAAATAGTGAAGCCACAGATGTATTTCTATCTCTTCTCTCTGTGATGCCTACTGCCTCGGA

Tlk2.882	CATGTCAGTGATGTTAGCAAA	TGCTGTTGACAGTGAGCGCCATGTCAGTGATGTTA GCAAATAGTGAAGCCACAGATGTATTTGCTAACATC ACTGACATGATGCCTACTGCCTCGG
Tlk2.1194	AAAGATGCTAGAGAAATACAA	TGCTGTTGACAGTGAGCGCAAAGATGCTAGAGAAA TACAATAGTGAAGCCACAGATGTATTGTATTTCTCT AGCATCTTTTTGCCTACTGCCTCGGA
Tlk2.1188	ACAGCAAAAGATGCTAGAGAA	TGCTGTTGACAGTGAGCGCACAGCAAAAGATGCTA GAGAATAGTGAAGCCACAGATGTATTCTCTAGCATC TTTTGCTGTTTGCCTACTGCCTCGGA
Tlk2.1217	AACGATTAAATAGATGTGTCA	TGCTGTTGACAGTGAGCGAAACGATTAAATAGATGT GTCATAGTGAAGCCACAGATGTATGACACATCTATT TAATCGTTCTGCCTACTGCCTCGGA
Tlk2.1695	AAGGATACATAATGAAGACAA	TGCTGTTGACAGTGAGCGCAAGGATACATAATGAA GACAATAGTGAAGCCACAGATGTATTGTCTTCATTA TGTATCCTTTTGCCTACTGCCTCGGA
Tlk2.1941	CAGGATAGTGAAGCTGTATGA	TGCTGTTGACAGTGAGCGACAGGATAGTGAAGCTG TATGATAGTGAAGCCACAGATGTATCATACAGCTTC ACTATCCTGGTGCCTACTGCCTCGG

Positive GFP cells were cultured in the presence of Doxicline and TLK2 RNA levels were measured 48 and 72 hours after Doxicicline addition. Cells with efective shRNAs were growth for further experiments.

6.2. Small interfering RNA-mediated knockdown

Small interfering (si)RNA duplexes targeting TLK2 mRNA were designed using tools found at the http://sirna.wi.mit.edu/ web site and they were manufactured by Invitrogen as Stealth RNAi siRNA. For each gene at least 3 primer sets were tested for the most efficient downregulation. The sequences of the siRNA duplexes are detailed in the table 1.5. SV40 transformed MEFs were transfected using Lipofectamine RNAiMAX (Invitrogen); 7.5 µl RNAiMAX was added to a well of a 6-well plate containing 350 µl OPTI-MEM medium (Invitrogen) with 10 nM siRNA duplex (final concentration). To this a 400 µl suspension of 3 x 10^5 cells was added and returned to the incubator. Twenty-four hours later a transfection mix composed of 350 µl OPTI-MEM, 7.5 µl RNAiMAX, and 10 nM siRNA (final) was added to the well before returning to the incubator. Usually, a well became confluent 48 hours after seeding and initial transfection, and required passaging into an appropriate size dish; experiments were typically performed

the following day (72 hours from the starting point). The number of wells seeded was scaled up as required. Mock transfections that contained water instead of siRNA were performed alongside as a control.

Table 11. siRNA oligonucleotide sequences

Exon	Fw siRNA oligonucleotide	Rv siRNA oligonucleotide
TLK2ex13	GGCCUAUCGAAAGGAAGAU [dT] [dT]	AUCUUCCUUUCGAUAGGCC [dT] [dT]
TLK2ex11	CCACCAAAGAUCUCAAAUA [dT] [dT]	UAUUUGAGAUCUUUGGUGG[dT] [dT]

7. Flow cytometry

7.1. BrdU labeling for G_1/S checkpoint assay

$1x10^6$ primary passage 2 MEFs were plated on 10 cm plates. Media was removed and they were exposed to varying doses of UVC ($5J/m^2$, $10J/m^2$ or $15J/m^2$) using a Stratalinker (Stratagene). 14 hours after UVC exposure, MEFs were pulsed with 10uM BrdU (Sigma) for 4 hours. Cells were washed in PBS, trypsinized and fixed over night with 70% ethanol. Cells were washed in PBS and DNA was denaturated by incubation in 0.1M HCl and by 100ºC heat. Cells were stained with BrdU-FITC antibody (Sigma) and were resuspended in 300ul of PBS with 10 µg /ml of propidium iodide (PI) and 10 µg /ml of RNaseA. The percentage of S-phase cells was determined by flow cytometry and normalized to untreated cells (S-phase ratio).

7.2. G2/M Checkpoint Assay

Primary MEFs in passage 2 were mock treated or damaged with $15J/m^2$ of UVC. 1 hour after damage, cells were harvested in PBS and fixed over night with 70% ethanol. Cells were washed and stained for one hour at room temperature with rabbit anti-H3ser10 at 1:200 dilution (table 1.3). Following several washes they were incubated 1 hour with secondary anti- IgG-FITC at 1:200 dilution. All washes and incubations with primary and secondary antibodies were done in dilution buffer containing 1% FBS and 0.1% Triton X-100 in PBS. Cells were resuspended in 300ul of PBS with the addition of 10ug/ml of propidium iodide (PI) and 10ug/ml of RNaseA. The percentage of mitotic

cells was determined by flow cytometry and normalized to untreated cells (G2M-phase ratio).

7.3. γ-H2AX staining

Cells were harvested and washed with PBS, resuspended in 500 µl of PBS and fixed in 5 ml of ice-cold 70% ethanol, drop-wise to the tube walls. Incubate at -20 ºC at least for 2h. Samples were centrifugated at 400 g for 5 min at 4 ºC to remove ethanol, and washed with PBS+0,2% TritonX100. Incubated with γ -H2AX antibody diluted 1:200 in 1% BSA + PBS-TritonX100 0.2% overnight at 4ºC. Next day, cells were washed with 1ml of 1% BSA + PBS-TritonX100 0.2% and incubated with the Alexa Fluor-488 conjugated secondary antibody diluted 1:200 for 1 h at RT. Cells were resuspended in 20 µg/ml of PI and analyzed by FACs.

7.4. Isolation of thymocytes for the analysis of differentiation and apoptosis

The thymus was isolated from 8 week old mice. The organ was ground in media chilled on ice with a 5ml syringe barrel and splenocytes were segregated by pipetting through a 40 µM filter into a 50 ml conical tube. 10^6 of cells in 100ul volume of media were plated in the wells of a 96-well plate in RPMI-1640 media enriched with 15% FBS. For assessment of T-cell differentiation, cells were stained for CD4, CD8 and CD3 markers and analyzed by flow cytometry. Additional cells were damaged with different doses of X-irradiation (1.25 Gy, 2.5 Gy and 5 Gy), incubated for an additional 16 hours and stained for apoptotic marker Annexin V and propidium iodide (PI). Cells were analyzed by flow cytometry to determine the number of viable (double negative) cells.

7.5. Haematopoietic Stem Cell Sorting

To obtain HSC, embryos were dissected from sacrificed pregnant mice at E14.5. Fetal livers were disaggregated, pipeting up and down (1 ml of PBS+5% FBS) in a 1.5 eppendorff with a p1000 until fully single-cell suspended. Cells were resuspend in 200ul PBS+5% FBS with primary antibody mix, on ice 20 minutes and dark. Cells were washed with 1ml PBS+5% FBS, spin 5' 300 g at 4ºC and resuspended in 200 ul PBS+5% FBS Strep. antibody 20 min. on ice. Cells were washed with 1ml PBS+5% FBS, spin 5' 300 g at 4º and resuspend in a final volume of 400 ul PBS+5% FBS+DAPI before transfer to FACs tube. Stained cells were analyzed and sorted using

a FACSAria cell sorter (BD Biosciences).

The following monoclonal antibodies were used for flow cytometry and cell sorting: anti-c-Kit (2B8, BD Pharmingen), anti-Sca-1 (D7, BD Pharmingen), anti-CD48 (HM48-1, BD Pharmingen), anti-CD150 (9D1, BD Pharmingen), anti-B220 (RA3-6B2, BD Pharmingen), anti-TER-119 (TER-119, eBioscience), anti-Gr-1 (RB6-8C5, BD Pharmingen), anti-CD3e (145-2C11).

1.1.30 Single lineaje marker staining

Cell isolation was performed as previously described. In this case, whole cell suspension was stained with single linage markers: anti-Ter119 for erythrocytes, anti-B220 for B-cells, anti-CD3e for T-cells and anti-Gr1 for myeloid differentiation. The samples were analyzed in FACs Galios

8. Microscopy

8.1. Immunofluorescence microscopy

Primary and secondary antibodies used in this thesis for immunofluorescence analysis are detailed in Tables 1.3 and 1.4 respectively. Cells were grown on glass cover slips, which for primary MEFs cells were poly-L-lysine coated (Invitrogen), in typically 3.5cm dishes with 2-3 cover slips per dish. Cell medium was removed and cells washed in PBS before fixing in 4 % formaldehyde (in PBS) for 10 minutes at room temperature. Following fixation, dishes of fixed cells were often stored at 4ºC in PBS until immunofluorescent staining. Cells were permeabilised with 0.2 % Triton X-100 (in PBS) for 5 minutes, then washed with PBS before blocking with 3 % BSA (in PBS) for at least 30 minutes. Primary antibodies were diluted in blocking buffer and added dropwise to the surface of the cover slips, and incubated for at least 1 hour at room temperature. Cells were then washed with PBS before incubation with the secondary antibody and 4',6-diamidino-2-phenylindole (DAPI) also diluted in blocking buffer, for at least 30 minutes in the dark. Following further washes with PBS, the excess PBS was removed from the cover slip before mounting onto a glass slide with Prolong Gold anti-fade (Invitrogen). Nail varnish was then used to coat the edge of the cover slips to create a seal and the slides were stored at 4^{o}C until analysis. If slides were to be scored, they were analysed on a Leica spectral confocal microscope (SPE) with a 40x and 63x oil immersion objective.

8.2. Selective Plain Ilumination Microscopy (SPIM)

We obtained whole embryos at E14.5. Embryos were transferred to PFA 4% for 1 day at 4ºC. The sample was prepared embebing the embryo in a 0.8% agarose block, dehydrated them in methanol 100% during 48h (adding fresh metanol every 12h). The whole sample was transferred into a clearing solution of 1 part benzylalcohol (Sigma) in 2 parts benzylbenzoat (Sigma) for at least 2 days at room temperature before imaging. Generally we observed the transparency of all preparations by eye during clearing to start imaging as soon as clearing was complete.

Microscopy: The specimen was illuminated with a planar sheet of light, formed by cylinder lenses and slit apertures. For fluorescence observation we coupled the light of an argon-ion laser (Innova 90, Coherent; l . 488 nm) via a single mode glass-fiber into the setup, allowing illumination from one or two sides. Illumination intensity was 1.5 mWper mm light sheet (for example, 15 mWfor a 10 mm wide light sheet). We observed the specimen from above with a modified macroscope (Leica) or microscope (Zeiss), which was oriented perpendicular to the light sheet. For autofluorescence imaging, a bandpass filter was positioned (pass band: 505–530 nm; Zeiss) above the objective. For specimens labeled with CY3 secondary antibody we used a rhodamine filter (pass band 496–576 nm; Chroma Technologies). The images were recorded with a CCD camera (CoolSnap Cf, 1392 _1040 pixels, Roper Scientific or Retiga EXi, 1,024 _ 1,024 pixels, Quantum Imaging).

8.3. Immunohistochemistry analysis.

Embryos were harvested and whole body and/or placentas were fixed in 4% paraformaldehide over night at 4ºC and paraffin embedded. For BrdU staining, embryos were harvested 3 hours after injecting the pregnant female 10ul of BrdU (10mM) per 10g of weight. Sections were made at 3 um thickness and staining for hematoxylin and eosin (H&E), Ki67, BrdU and γH2AX was performed in the facility for immunohistochemistry at IRB Barcelona. Pictures were taken using E600 Nikon epifluorescence microscope equipped with 40x NA 0.75 objective lens and a charge-coupled Olympus DP72 device camera.

9. Peptide microarray

A peptide microarray was carried out by LC Sciences (Houston, TX, USA). The array chip containing 3738 10-mer peptide probes was blocked overnight at 4°C in blocking buffer (1% BSA, 0.05% Tween-20, 0.05% TX-100 in TBS, pH 7.0). The array was washed in 1 ml of TBS and scanned at 532 nm and PMT400. The array was washed with 1 ml kinase reaction buffer (50 mM HEPES, 200 µM ATP, 10 mM $MgCl_2$, 2.5 mM DTT, 10% glycerol, 0.01% TX-100, pH 7.4) for 20 minutes. It was then incubated with 10 µg/ml TLK2 in kinase reaction buffer at 25°C for 1 hour. The array was washed 0.2 ml kinase reaction buffer followed by 1 ml of TBS (pH 7.0). The array was washed with deionized water for 5 minutes and incubated with 1 ml of 5X diluted ProQ staining buffer at 25°C for 30 minutes, washed with deionized water for 5 minutes and then incubated with 1 ml of ProQ destaining buffer at 25°C for 30 minutes. Images were scanned on an Axon GenePix 4000B microarray scanner at 532 nm and PMT400. Full length TLK2 was purified in the laboratory of Guillermo Montoya (CNIO) by Ana Garrote.

10. Library of inhibitors

The InhibitorSelect™ 96-Well Protein Kinase Inhibitor Library III consists of 84 protein kinase inhibitors, the majority of which are cell-permeable and ATPcompetitive. They are supplied in a 96 well-plate format at a concentration of 10 mM in DMSO. Their target pathways are specified in Table **12**.

Table 12 Pathways targeted by The InhibitorSelect™ 96-Well Protein Kinase Inhibitor Library III

Targeted kinases			
AK	DNA-PK	MLCK	PKG
Akt	eEF2	Myt1	Plk
Aurora	GSK-3	p90RSK	Ras/Rac
c-Abl	IKK	PAK	Rho
CaMK	IP3K	PI3K	RIPK1
Cdks	Lck	PIKfyve	Src
CK1,2	MEK	PIM	Ste11
c-kit	MAPK	PKA	Tpl2
Chk1	MAPKAPK2	PKC	Wee1

Results

1. Characterization of TLK1 knockout mice and cell cultures

Chapter Summary

To gain insight into Tlk1 activity in vivo and its role in tissue homeostasis and chromosomal stability, we have generated mice lacking expression of Tlk1. Surprisingly, we found that they developed normally, showed no pathology and aged normally over 18 months. Examination of developmental processes, such as lymphocyte maturation, revealed no abnormalities, and DNA replication and cell cycle progression were normal, even in response to DNA damage. Sensitivity to DNA damage and the spectrum of chromosome aberrations were also normal, in contrast to published work using siRNA depletion of Tlk1 [174]

1.1. Strategy and design of *Tlk1* genetrap mice.

To investigate Tlk1 function in vivo, we generated animals lacking Tlk1 expression due to a genetrap cassette inserted by retrovirus infection between exons 2 and 3. Embryonic stem cell lines with the mapped genetrap insertion were obtained from the German Genetrap Consortium (GGTC). The genetrap cassette consists of a promoterless reporter and selectable genetic marker, Bgeo, flanked by an upstream 5' splice site (splice acceptor; SA) and a downstream transcriptional termination sequence (polyadenylation sequence; polyA). The cassette, integrated downstream of Tlk1 exon2, is transcribed from the endogenous promoter of that gene in the form of a fusion transcript in which the exons upstream of the insertion site is spliced in frame to the reporter/selectable marker gene (Figure 14.A). Since transcription is terminated prematurely at the inserted polyadenylation site, the processed fusion transcript encodes a truncated and non-functional version of the cellular protein and the selectable marker. The genetrap cassette was flanked by multiple, inverted FRT and LoxP sequences to allow the orientation of the trapping cassette to be manipulated by Flp and Cre recombinase expression. This allows recovery of gene expression if necessary, as well as conditional inactivation of the gene in particular tissues or developmental stages depending on the Cre line used (Figure 14.A).

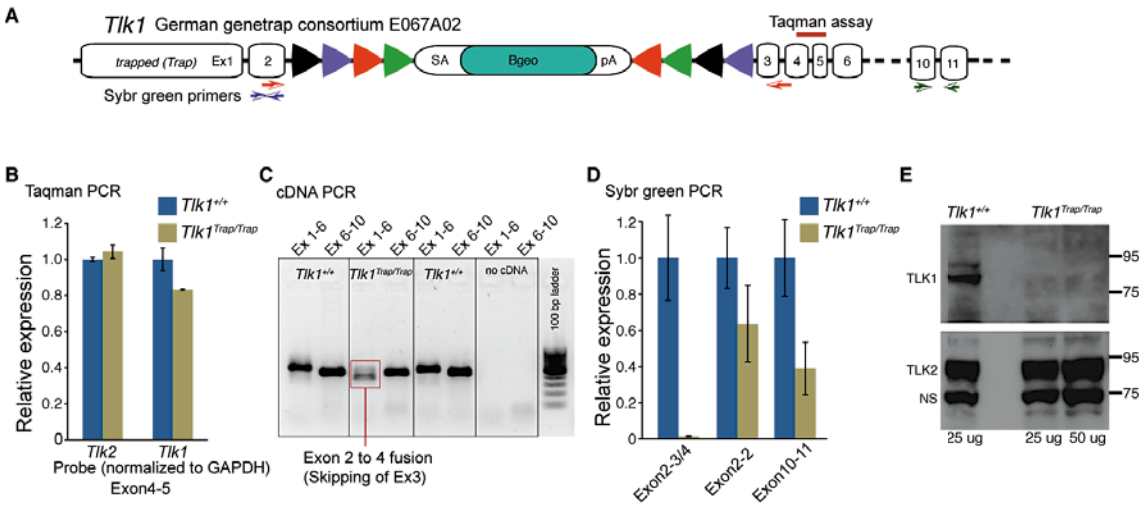

Figure 14. Characterization of *Tlk1* genetrap mice and cells. A) Gene Trap with FlpO vector. B-geo is a fusion gene, with b-gal and neoR activity. SA is a splicing site acceptor. pA is a polyadeyilation tail. B) Q-PCR for Tlk1 expression using Applied TaqMan probe. C) RT-PCR analysis of cDNAs obtained from wild type and Tlk1$^{Trap/Trap}$ mice. Primers were specific from pairs of Tlk1 exons. D) Q-PCR for Tlk1 expression using Sybr Green and three combinations of primers. D)Western Blot analysis of protein extracts obtained from wild type and Tlk1$^{Trap/Trap}$ livers.

To check the efficiency of the trapping cassette in our mice, we obtained RNA from mouse tissues in order to measure the expression levels of *Tlk1*. Using a commercial TaqMan probe (ABI Mm00554286), we could not detect any decrease in the levels of *Tlk1* (Figure 14.B). Using primers between upstream exons and the trap, we could confirm that the Tlk1 gene was trapped. We will refer to this allele subsequently as *Tlk1*^{Trap}. As splicing can sometimes take place around genetrap insertions, leading to expression of full length or truncated mRNAs, we used exon specific primers to map the mRNA that was produced (Figure 14.C). It was apparent that the product generated from PCR of Exons 1 to 6 was smaller than in wild type samples. To determine the composition of the mRNA, we cloned the PCR products and sequenced them after plasmid purification. This revealed that Exon 3 was skipped during transcription of the trapped allele. This was corroborated by Q-PCR using sybr green to ensure that the exon skipping was complete and that no wild type product was produced (Figure 1C). Importantly, TLK1 protein levels were not detectable in cells from the genetrap mice using 3 different antibodies against TLK1 (cell signaling, Bethyl Nt and Bethyl Ct) (Figure 14.E). These results confirmed that the genetrap efficiently blocked *Tlk1* mRNA and protein expression.

As mammals encode two highly similar *TLK* genes, *Tlk1* and *Tlk2* in mice, we wanted to address whether *Tlk1* suppression could increase the expression levels of *Tlk2* as a compensatory mechanism. We analyzed by Q-PCR and WB the levels of *Tlk2* in wild

type and *Tlk1*$^{Trap/Trap}$ cells (Figure 14 B and E). Our results indicated that both *Tlk2* mRNA and protein levels were unaffected after *Tlk1* depletion.

1.2. TLK1 genetrap mice develop normally.

To determine the consequences of the total depletion of *Tlk1* activity *in vivo*, we interbred *Tlk1*$^{+/Trap}$ mice to generate *Tlk1*$^{Trap/Trap}$ mice. These mice were viable, born at predicted Mendelian frequencies and had no obvious developmental abnormalities (Figure 2A). Both male and female *Tlk1*$^{Trap/Trap}$ mice were fertile and litter sizes did not differ significantly from wild-type (WT) littermate mice. In addition, no anatomic abnormalities were observed in embryos isolated at E14.5 for the generation of primary cell cultures.

1.2.1.TLK1 deficiency did not affect viability, fertility or lifespan.

To determine if development progressed normally, we measured the weights of mice during the first month of life.

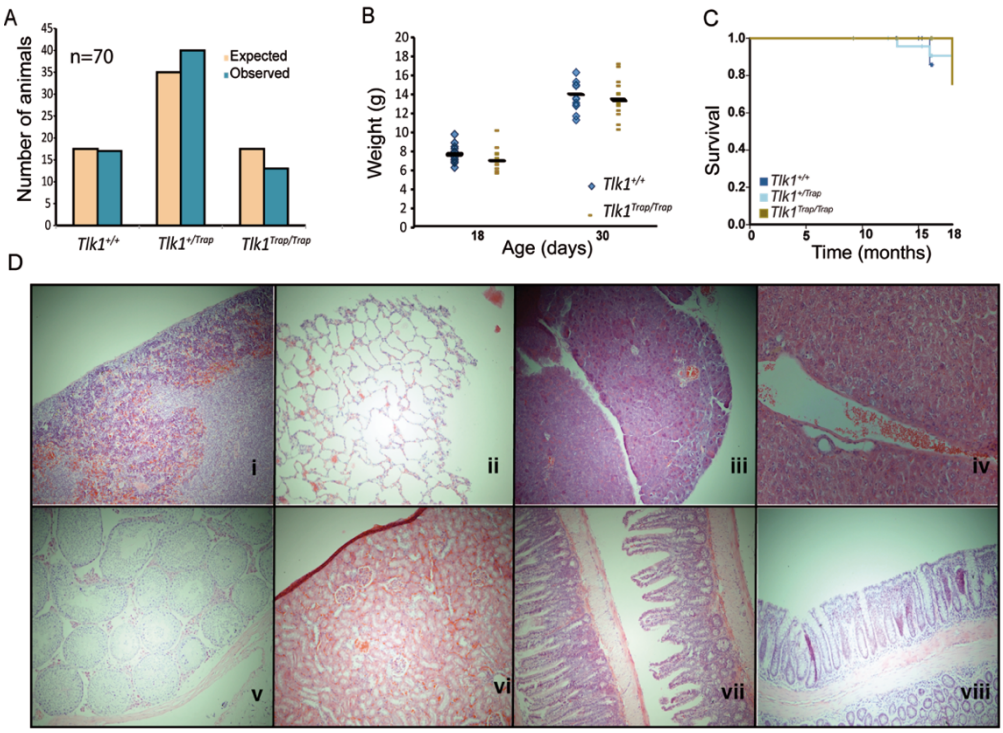

Figure 15: Lack of Tlk1 doesn't affect mice development. A) Mendelian ratios from a total of 70 pups borned in interbreeding of *Tlk1*$^{+/Trap}$ mice. B) Wild type and in TLK1$^{Trap/trap}$ weigh at 18 and 30 days after birth. C) Kaplan Meier curve for wild type, Wild type and in TLK1+$^{/trap}$ and TLK1$^{Trap/trap}$ animals. Animals aged normally over 18 months. D)Samples of tissues of TLK1$^{Trap/trap}$ mice. i. Spleen; ii. Lung; iii. Pancreas; iv. Liver; v. Testis; vi. Kidney; vii. Intestine; viii. Colon. No pathologies were found.

There was no significant difference observed in the weights between wild type (WT or *Tlk1*$^{+/+}$) and *Tlk1*$^{Trap/Trap}$ animals at 18 and 30 days old (Figure 15B). Mutant animals developed normally through puberty, showing normal size and weight (Figure 15B) and exhibited no signs of pathology over 18 months (Figure 15C). Several tissues, including spleen, lung, pancreas, liver, intestine and colon, were examined in the aging population and, showed no obvious abnormalities (Figure 15D).

1.2.2.TLK1 loss did not affect immunological development

We next examined developmental processes that can be affected when DNA repair pathways are impaired, such as fertility and lymphocyte maturation. During gametogenesis, meiotic crossover formation involves the repair of programmed DNA double-strand breaks (DSBs) through homologous recombination. To check if this process was affected in genetrap mice, we bred *Tlk1*$^{Trap/Trap}$ with wild type and *Tlk1*$^{+/Trap}$ animals. Both sexes were fertile, suggesting no major abnormalities in spermatogenesis nor oogenesis.

During T-lymphocyte maturation, that occurs in the thymus, DNA is cleaved and repaired during V(D)J recombination. V, D and J regions are joined together by non-homologous-end-joining (NHEJ) to create a variable region in T-cell receptor genes. Lack of any of NHEJ factors can affect TCR recombination events and cause aberrant distribution of T cell subsets. To check the efficiency of this process in our mutant mice, we analyzed the development of T cells in the thymus of 7-week old mice (**Figure 16**). The distribution of subsets was comparable in *Tlk1*$^{Trap/Trap}$ mice and wild type littermates, indicating that TLK1 does not have a role in NHEJ. Together, these results suggested that Tlk1 was not required for either major DSB pathway, homologous recombination or NHEJ.

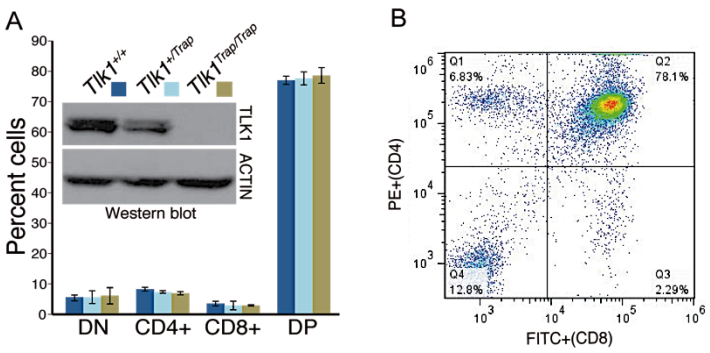

Figure 16. NHEJ is not affected in *Tlk1*$^{Trap/Trap}$ mice A) Percent cells of double negative (DN), double positive (DP), CD4+ and CD8+ in the thymus of wild type, TLK1$^{+/Trap}$ and TLK1$^{Trap/Trap}$.. The data plotted represent the average of 3 mice of each genotype. B) FACS profile of T cell analysis. Q1-CD4+; Q2-DP; Q3-CD8+; Q4-DN.

1.3. Generation and characterization of *Tlk1*$^{Trap/Trap}$ Mouse Embryonic Fibroblasts

1.3.1. Proliferation and cell cycle regulation is not impaired in TLK1 depleted cells

Previous studies showed that *TLK* depletion in *D. melanogaster* and *C. elegans* caused mitotic catastrophe and DNA fragmentation, affecting directly the progression through the cell cycle. To determine if Tlk1 deficiency had an effect on cell proliferation, primary MEFs were replated for at least 25 passages until spontaneous immortalization. Primary MEFs were prepared from E13.5-15.5 mouse embryos of interbred *Tlk1*$^{+/Trap}$ mice (see material and methods). We observed normal growth rates of cells lacking Tlk1 compared to their WT littermates (Figure 5). These results suggested that Tlk1 was not required for normal mammalian cell cycle progression.

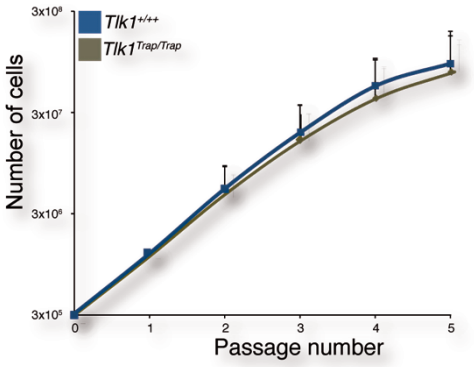

Figure 17: 3T3 growth curve for Tlk1$^{+/+}$ and Tlk1$^{Trap/Trap}$ primary MEFs. Cell cultures showed no difference in proliferation. Results from 3 representative experiments performed in triplicates are shown. Error bars indicate standard deviation mean.

To address if *Tlk1* deficiency affected cell cycle progression following DNA damage , we have analyzed cell cycle distribution in *Tlk1*$^{Trap/Trap}$ primary MEFs by propidium iodide incorporation (PI) following treatment with ionizing radiation (IR). PI stains nuclear DNA and provides a cell cycle profile in which G1, S and G2 phases are distinguishable and quantifiable. Cell cycle distribution in untreated cells and at different time points after 5Gy of damage are plotted in

Figure 18B. No difference in cell cycle distribution was observed between *Tlk1*$^{Trap/Trap}$ and their WT littermates.

We next examined the G2/M checkpoint response in *Tlk1* deficient cells as the resolution of this DNA-damage-dependent checkpoint could be potentially regulated by TLK activity,. To distinguish between cells in G2 and mitosis (M) we performed the G2/M checkpoint assay using the marker for M phase cells, phospho-histone 3, serine 10 (H3-S10). Mitotic cells were defined by 4N DNA content (PI) and positivity for H3-

S10. Briefly, cells were fixed and incubated with an antiphospho histone H3 (Ser10) antibody (Cell Signalling). Positive cells were identified using a FITC-conjugated secondary antibody and the percentage of positive cells was determined using flow cytometry (see materials and Methods). As can be observed in figure 18, *Tlk1*$^{Trap/Trap}$ cells show the same ability to arrest and progress through the cell cycle as their WT counterparts. We could detect a slight but not significant increase in the speed of recovery of mitotic rates after IR treatment (Fisher's exact test p=0,97).

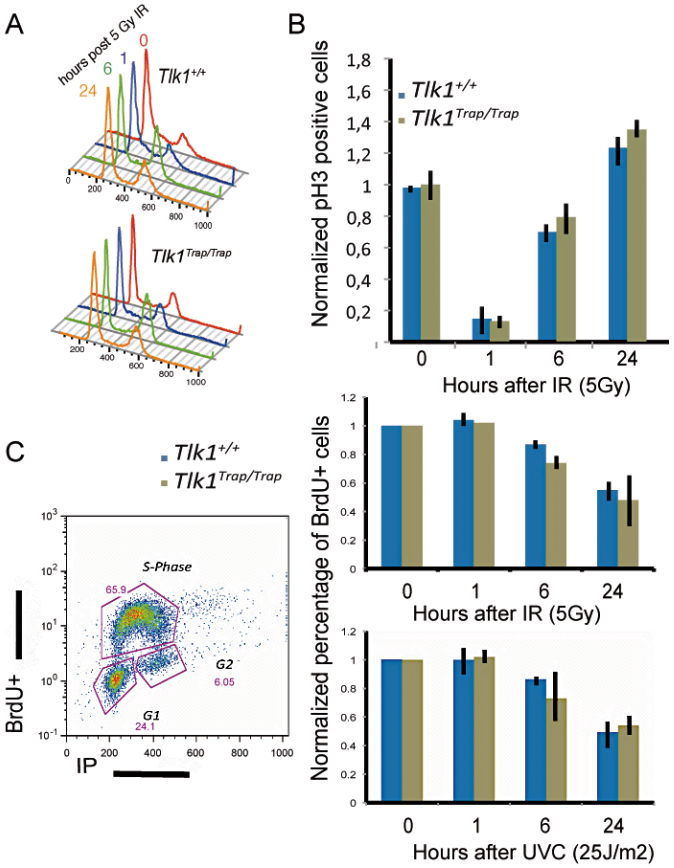

Figure 18. Cell cycle progression in cells lacking Tlk1.A) Cell cycle profiles of wild type and TLK1$^{Trap/Trap}$ primary MEFs labeled with propidium iodide (PI). Cell cycle profiles were analyzed by flow cytometry and plotted as cell count vs. DNA content. Cells were either undamaged or damaged with 5Gy of X-Ray and let recover 1, 6 and 24 hours. B) Normalized levels of positive pH3 cells after 5Gy of X-radiation. The plotted values represent four independent experiments made in duplicates (p=0,97). Error bars denote SD.C) G1/S checkpoint in SV40 transformed MEF cultures. S-phase ratios (%BrdU+ cells in ionizing radiation or mock treated samples/average %BrdU+ in mock treated samples) are plotted. Results are the average of one experiment performed in triplicate for each genotype. Error bars denote SD.

As TLK1 could be involved in S-phase progression, potentially controlling histone exchange at the replication fork, we analyzed S-phase progression and G1/S checkpoint responses to IR in *Tlk1*$^{Trap/Trap}$ MEFs. To examine the G1/S checkpoint, exponentially growing SV40 transformed MEFs were exposed to 5 Gy of IR and the percentage of cells in S phase 1, 6 and 24h post-treatment was measured by BrdU incorporation. No significant differences were found in the levels of BrdU incorporation compared to untreated cells in the response to DNA damage (Figure 18)

These results indicated that the lack of Tlk1 was not affecting the progression of the replication fork in transformed MEFs. As Tlk1 was shown to have maximal activity during S-phase, and we coul not identify a significant phenotype in MEFs lacking this kinase, we considered that some redundant functions may compensate for its absence.

1.3.2.Loss of TLK1 does not affect sensitivity to DNA damage.

In order to determine if TLK1 influenced the sensitivity of MEFs to DNA damage, we used the clonogenic survival assay. This reveals the ability of a cell to survive a particular cytotoxic threat and continue to proliferate indefinitely, forming a large colony (>50 cells) visible to the naked eye following contrast staining. Cells were plated the day before damage treatment and the number of colonies was normalized to those in the non-treated plates to control for plating efficiency. The percentage of survival of those cells was determined by dividing the number of colonies that arose after irradiation with the number in the non-irradiated plate.

The loss of Tlk1 did not exacerbate sensitivity to the double strand break inducing agent IR or to UVC that introduces bulky base lesions and some single and double strand breaks, indicating that TLK1 does not modulate DNA damage sensitivity as has been previously reported[174,175]

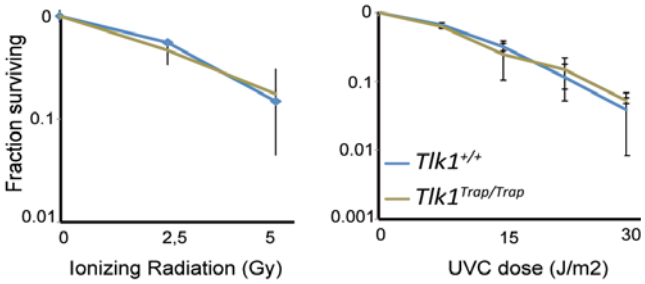

Figure 19: Lack of Tlk1 doesn't increase sensitivity to DNA damage. *Tlk1*$^{Trap/Trap}$ surviving fraction after exposure to X-rays or ultraviolet C radiation. The data are represented as the means and standard errors of three different experiments performed in duplicates.

1.3.3.Genome instability is not increased in Tlk1 deficient MEFs.

To determine if the loss of TLK1 influenced chromosome stability, we examined spreads from primary fibroblasts and examined metaphase aberrations in the presence of absence of damage. We scored four different classes of aberrations that were apparent in the spreads: chromatid breaks, chromosome breaks, fusions or rearrangements and fragments. DSBs can occur spontaneously in cultured MEFs, appearing as a chromatid breaks if the DSB occurred during or after S-phase or as a chromosome break if it occurred during G1. Following the analysis, we could not identify any increase in the number of chromosomal aberrations, suggesting that TLK1 deficiency did not influence chromosome stability (**Figure 20**).

We next wanted to determine if TLK1 was required under situations of replication stress. To address this we used aphidicolin that is a selective inhibitor of DNA polymerase alpha and induces DNA breaks during S-phase by fork stalling due to

replisome dissociation. TLK1 has been shown to be active during S-phase, potentially regulating the exchange of nucleosomes, and we considered its absence could be problematic during DNA synthesis. Our results show that the aberrations provoked by aphidicolin were not increased in absence of TLK1 (**Figure 20**).

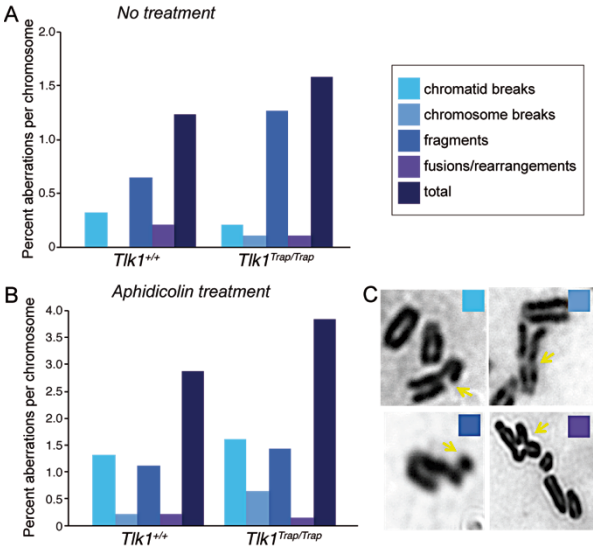

Figure 20: *Tlk1*$^{Trap/Trap}$ MEFs show normal genomic stability. Metaphase chromosome analysis of primary MEFs of the indicated genotype with percentages of chromatid (cd) and chromosome (Ch) breaks, fusions, fragments and total aberrations per chromosome.

2. TLK1 and TLK2 have redundant roles in the DDR.

Chapter Summary

To begin to address the role of TLK activity in development and the DDR, we have generated mice lacking TLK1 protein expression. To our surprise, these mice developed normally, had no increased tumor incidence and were not sensitive to DNA damage. We reasoned that a likely explanation was that TLK2 could provide a redundant function. To test this, we depleted TLK2 in cells using siRNA and analyzed cell cycle and survival following IR treatment. We found that cells with reduced TLK1/2 activities showed impaired checkpoint recovery and reduced survival after damaging treatment. This data suggests that a higher threshold of TLK1/2 activity is required for cells to tolerate DNA damage and transiently reduced TLK activity was not toxic for cells over the course of several days.

2.1. Depletion of total TLK activity impairs cell cycle recovery.

As already described, mice lacking Tlk1 expression were phenotypically indistinguishable from wild type mice and developmental processes affected by DNA repair defects, were normal. In addition, our results showed that loss of expression of

Tlk1 does not affect the viability or checkpoint responses of primary MEFs after DNA damage.

In the introduction, we discussed that loss of TLK causes severe chromosomal instability phenotypes in dividing cells of lower organisms that have a single TLK gene [141,143,176]. As we could not detect any of these previously reported phenotypes, we speculated that some functional redundancy exists in mammals.

In mice cells there are two structurally similar Tlks, Tlk1 and Tlk2, and both are shown to be cell cycle-regulated kinases with maximal activities during S phase [145]. and both are regulated after treatment with inhibitors of DNA replication [97]. Tlk1 is phosphorylated by Chk1 on Ser 695 after DNA damage [97] while Tlk2 does not appear to be a target of Chk1. However, Tlk2 interacts directly with Tlk1 and is able to phosphorylate Asf1 as well. Tlk1 and Tlk2 share 86% similarity at the amino acid level and even higher levels, 94%, in their kinase domains. Thus, Tlk2 is a clear candidate for a redundant activity in Tlk1 deficient cells.

Figure 21: Scheme of experimental design for siRNA mediated downregulation of TK2. *Tlk1*$^{Trap/Trap}$ and WT immortalized MEFs were plated at 3x105 per well on a 6 well plate. After 2 transfections with siRNAs at designated time points, cells were plated for G2/M checkpoint or clonogenic assays. Cells were treated with damaging agents 16 hours after plating. Protein levels were measured on the day of plating.

To test this hypothesis, we used small interfering RNAs (siRNA) to downregulate Tlk2 in both wild type and *Tlk1*$^{Trap/Trap}$ MEFs. These cells were subsequently plated for sensitivity or checkpoint assays after DNA damage as illustrated in Figure 21. Briefly, we transfected cells with siRNA against Tlk2 twice, and the experiments were made 48h after the second transfection, when Tlk2 expression was the lowest. The downregulation was efficient and reduced Tlk activity was not toxic for untreated cells over the course of several days.

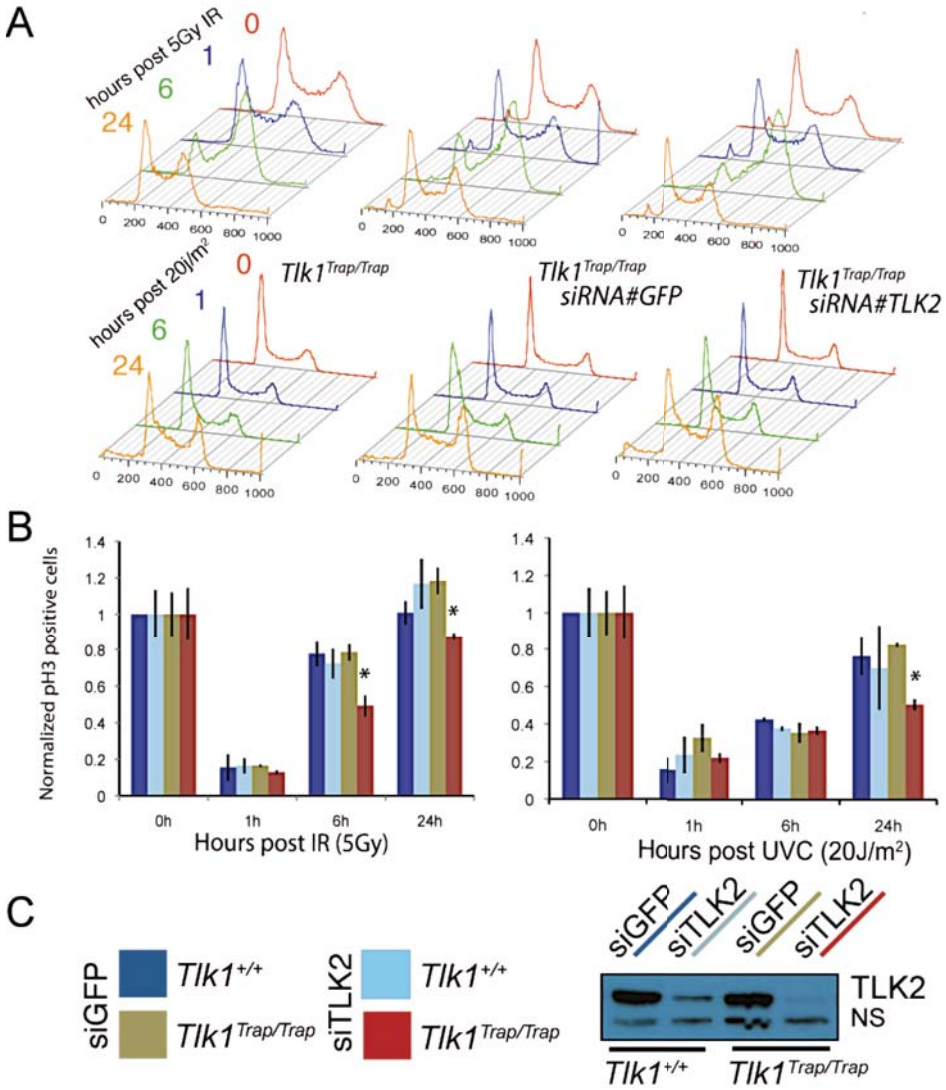

Figure 22. *Tlk1* and *Tlk2* play redundant roles in cell cycle recovery. A. Histograms of cell cycle distribution in transformed MEFs labeled with propidium iodide (IP). Cell cycle profiles were analyzed by flow cytometry and plotted as cell count vs. DNA content. Cells were either undamaged or damaged with 5Gy X-Ray or 20J/m^2 UVC and let them recover for 1, 6 and 24h. B. G2/M checkpoint responses of exponentially growing transformed MEFs. Normalized mitotic ratios (percentage of H3ser10 positive) are plotted for untreated cells and cells treated with UVC treated cells (15J/m^2) or X-Ray treated cells (5Gy) and let them recover 1, 6 and 24h. Fisher test *p<0.1. C.Western Blot against TLK2 showing the efficiency of downregulation by TLK2 siRNA.

After reducing Tlk2 expression in cells lacking Tlk1, we did not observe any clear differences in the cell cycle profile of untreated cells (**Figure 22**A). However, when analyzing the ability of cells to resume cell cycle arrest after damaging treatments with UVC or X-Ray, we found that cells with reduced TLK1/2 activities showed impaired checkpoint recovery. As this effect was not observed with the single depletion of TLK1, it suggested that TLK2 may indeed play a redundant role during cell cycle resumption

2.2. TLK1 and TLK2 have redundant roles in sensitivity to DNA damage.

To further test if TLK activity is involved in the DDR, we also analyzed survival after DNA damaging treatments. After siRNA transfection we plated the cells at low density and let them recover over night. At the moment of DNA damaging treatment, levels of *TLK2* were measured by WB. We observed that TLK2 downregulation was not sufficient to increase the sensitivity of WT cells. In contrast, TLK2 downregulation strongly increased the sensitivity of *Tlk1*$^{Trap/Trap}$ cells after damaging treatments. The result for clonogenic survival after UVC, X-Ray and Etoposide are plotted in **Figure 23**. In contrast, no increase in sensitivity was observed following campthothecin (CPT) or mitomycin C (MMC) exposure. The decreased survival; of *Tlk1*$^{Trap/Trap}$ cells with reduced TLK2 activity suggested that a higher threshold of TLK1/2 activity is required for cells to tolerate some types of DNA damage than is needed to support normal cell growth and viability.

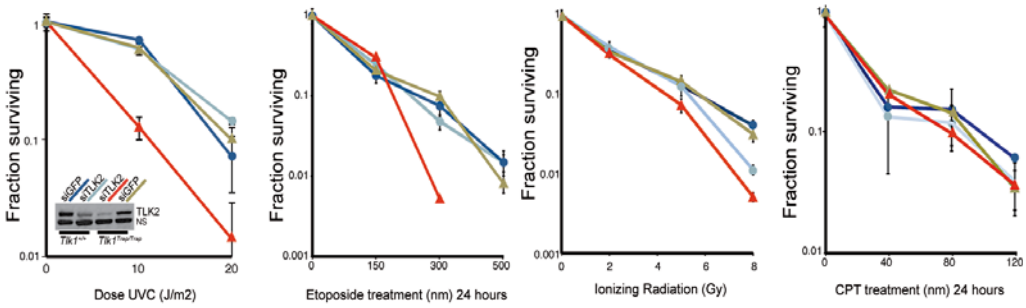

Figure 23. ***Tlk1* and *Tlk2* play redundant DDR.** Sensitivity to UVC, etoposide, IR and CPT was determined by clonogenic survival assay. SV40-transformed MEF cultures were plated for colony formation as described. The western Blot shows protein levels of TLK2 at the moment of damage of control samples treated by siRNAs against GFP or samples treated with siRNA against TLK2. The plots show that TLK2 inhibition is not sufficient to synthetize cells to DNA damage. When TLK2 downregulation is done in a TLK1 null background a clear increase in the sensitivity to several types of damage is detected.

The main limitation that we had to face is that siRNA gives a transient mRNA downregulation which can affect the reproducibility of our experiments, specially if we take into account that we are measuring cell cycle recovery after several hours and survival after several weeks. During this time, we know that the levels of TLK2 are eventually recovered in all the samples, potentially masking more severe phenotypes. To solve this problem, we generated switchable shRNA retrovirus vectors using technology recently developed and reported by Scott Lowe's laboratory [173].

We designed 8 oligos to target TLK2 and cloned them into tTRMPVIR retrovirus vectors that express shRNA under a doxycycline inducible promoter (see materials and methods).

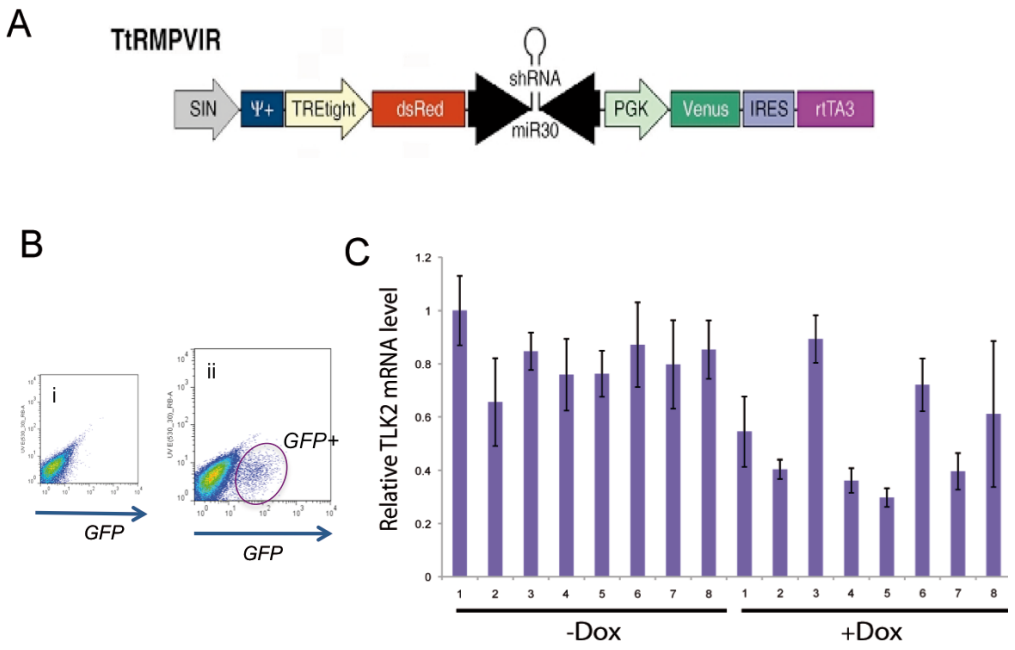

Figure 24. Desing of shRNA retrovirus vectors A) Map of TtRMPVIR vector. The shRNAs were cloned using EcoRI and XhoI. The constitutive expression of Venus is under the control of PGK promoter. Only after Doxycycline addition, reverse tetracycline-controlled transactivator (rtTA3) becomes active, activating the expression of the shRNA, which is linked to the expression of a red fluorescence promoter (dsRed). B) Effectiveness of transdiction. i. SV40 transformed MEFs before TtRMVIR infection and ii) after infection. C) TLK2 mRNA levels of 8 cell populations infected with different shRNAs. After doxycycline addition, some shRNAs produced a downregulation in TLK2 mRNA levels.

We used 293T cells to produce retrovirus, that was used to infect SV40 transformed MEFs of different genotypes. As the TtRMPVIR vector carries a constitutive Venus fluorescence marker, we could visualize the transduction efficiency using a flow cytometer. We sorted the Venus positive cells from the infections with 8 different shRNA vectors and grew them for a week. We then extracted mRNA to test their efficiency in TLK2 downregulation in SV40 transformed MEFs using Q-PCR at different time-points after adding doxycycline. Effective TLK2 downregulation was achieved with 4 out of the 8 shRNAs (numbers 2, 4, 5 and 7) 48 hours after adding doxycycline (**Figure 24**).This stable system will be used in future experiments to confirm previous results obtained using siRNA. Thus, we will perform DNA damage sensitivity experiments and examine cell cycle recovery after DNA damage. Effective hairpins can then be used in a number of genetic backgrounds in order to downregulate TLK2 in a stable manner, which will be discussed in section 6.

3. TLK2 is an essential gene during mouse development. Characterization of TLK2 knockout mice and cell cultures

Chapter Summary

According to our siRNA results, depletion of total Tlk activity results in an increased sensitivity to DNA damage and impaired cell cycle progression. In order to study these effects in vivo we wanted to generate mice lacking Tlk1 and Tlk2 expression. To reach this objective, we have generated mice lacking expression of Tlk2. In contrast to Tlk1, no liveborn homozygous mutants have been observed and embryos isolated for MEFs were severely runted, displayed heterogeneous defects, including failure to close the neural tube, limb patterning defects, hemorrhaging, and hematopoietic failure. Further, primary MEFs lacking Tlk2 exhibited increased spontaneous chromosomal instability, markedly slower growth and premature senescence. These data indicated that Tlk1 and TLK2 do not play equivalent roles during development and that Tlk2 is an essential gene.

3.1. Strategy and design of Tlk2 genetrap mice.

According to siRNA experiments, the depletion of both Tlk activities caused sensitivity to DNA damaging agents and an impairment of checkpoint recovery. To test this phenomenon *in vivo*, we decided to generate a double Tlk mutant, which would lack expression of both Tlk1 and Tlk2. Our experimental strategy was to generate a Tlk2 genetrap mouse that could be crossed with $Tlk1^{Trap/Trap}$ mice in order to deplete total Tlk activity. To generate the gene-trapped allele, we obtained an ES cell line from Bay Genomics (DTM063) with a retroviral genetrap insertion after exon 1 of *Tlk2* (Figure 25)

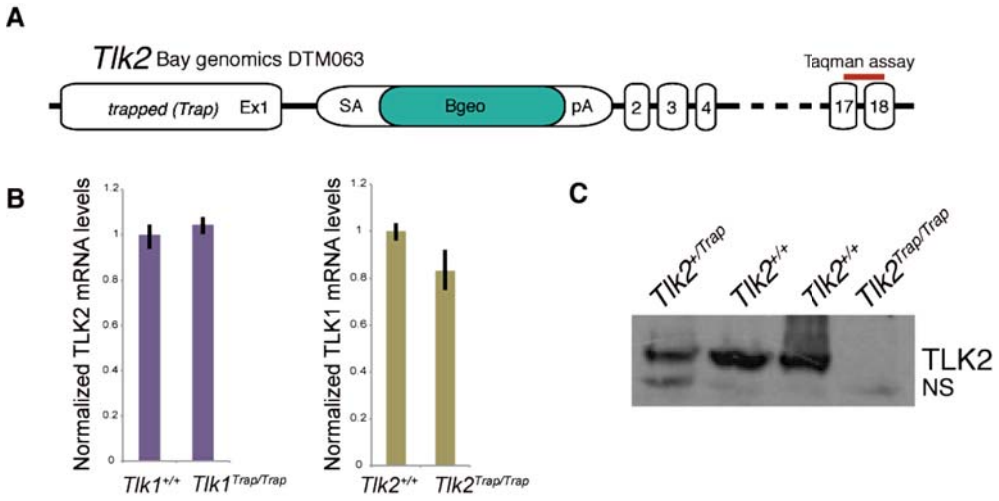

Figure 25: Tlk2 genetrap generation. A) TLK2 Gene Trap strategy. B-geo is a fusion gene, with b-gal and neoR activity. SA is a splicing site acceptor. pA is a polyadeyilation tail. B) Real time PCR using commercial Taqman probes C) Western Blot anti-TLK2 of littermates at e14.5.

The efficiency of the trapped gene was tested by western blotting with an antibody against TLK2, and by q-PCR, with a Taqman (ABI # Mm01246220) probe for this gene. We did not detect mRNA or protein expression in the mutant embryos. Interestingly, the depletion of TLK2 did not affect the expression levels of TLK1 (Figure 25B)

3.2. Tlk2 genetrap mice have embryonic developmental defects.

3.2.1. Loss of TLK2 is embryonically lethal

To determine the consequences of total depletion of TLK2 activity in vivo, we interbred *Tlk2*$^{+/Trap}$ to generate *Tlk2*$^{Trap/Trap}$ mice. As *Tlk1*$^{Trap/Trap}$ mice were viable, we speculated that *Tlk2*$^{Trap/Trap}$ would also lack severe phenotypes. To our surprise, no liveborn homozygous animals were observed. Heterozygous mice were viable and appeared to develop normally, and the ratio between WT and *Tlk2*$^{+/Trap}$ was about 1:1.5 (39.6% to 60.4%, **Figure 26**). This demonstrated that *Tlk2* expression was required for embryonic development and viability.

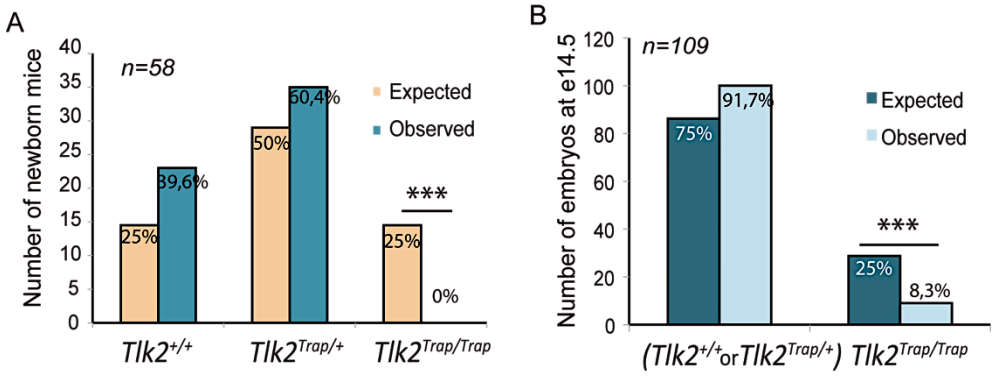

Figure 26. Tlk2 genetrap Mendelian ratios. A. Mendelian ratios from a total of 58 pups borned in interbreeding of *Tlk2*$^{+/Trap}$ mice. B. Mendelian ratios embryonic stage 14.5.

We started a morphological analysis of the embryos to elucidate the cause of premature death. At e10.5, *Tlk2*$^{Trap/Trap}$ embryos showed several aberrant phenotypes that were characterize by brain development failure and deficient neural tube closure (Figure27)but these phenotypes did not appear at later developmental stages. Overall, of nine e10.5 embryos that were analyzed, one presented with an open neural tube (spina bifida) and one with a large brain hemorrhage. This suggested that some *Tlk2*$^{Trap/Trap}$ embryos were potentially reabsorbed at earlier stages. However, to corroborate this hypothesis we need to analyze more embryos to study the frequencies of different phenotypes at e10.5 in larger numbers.

At later stages, from e12.5 to e15.5, the phenotype was more consistent, characterized by a general developmental delay, smaller size, pale coloration, an apparent reduction in angiogenesis and smaller livers. At these stages, every *Tlk2*$^{Trap/Trap}$ embryo exhibited the same phenotype (*Tlk2*$^{Trap/Trap}$ embryos analyzed: e12.5 n=3; e14.5 n=9; e16.5 n=4). A beating heart was apparent at e14.5, in some cases with weaker contractions, but absent by e15.5, indicating that the time of premature death is between these two embryonic days. In addition, at e14.5 the number of observed *Tlk2*$^{Trap/Trap}$ is significantly reduced compared to the expected Mendelian frequencies (**Figure 26**A, Chi^2 $p<0.001$) which may indicate stochastic death of some embryos at earlier stages. This is consistent with the fact that the most severe phenotypes seen at e10.5 did not appear at later stages. In future experiments we will analyze more e10.5 embryos to measure the frequencies of each genotype and relate them with the observed Mendelian ratios at e14.5.

No obvious developmental abnormalities were detected for the heterozygous embryos at any stage, suggesting that just one *Tlk2* allele is sufficient to maintain normal embryonic development. In agreement, new born and adult *Tlk2*$^{+/Trap}$ mice developed normally.

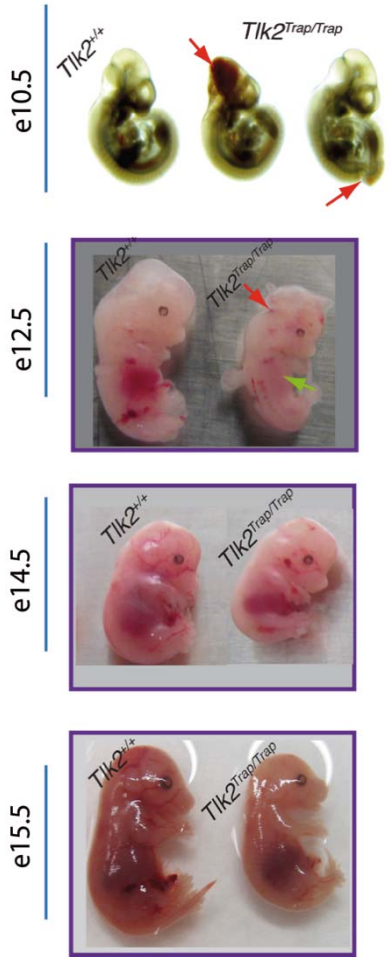

Figure 27: *Tlk2*$^{Trap/Trap}$ embryonic morphology. External appearance of WT (+/+) and mutant *Tlk2*$^{Trap/Trap}$ embryos at different embryonic stages.

By e10.5 *Tlk2*$^{Trap/Trap}$ embryos show bleedings in the ventricle system of the brain and they display problems in the closure of the neural tube (arrowheads).

Tlk2$^{Trap/Trap}$ embryos are retarded in growth compared to WT littermates at e12.5. In some cases they present closure tube problems (red arrowhead) and, in every case, smaller liver (green arrowhead).

In further developmental stages they appear paler, and major blood vessels are often not clearly visible.

If an embryo survives implantation but fails to progress to live birth, , it can indicate that there is some form of lethal cardio-vascular defect. A number of embryonic organ and body systems, including the central nervous system, gut, lungs, urogenital system, and musculoskeletal system appear to have little or no contribution to survival *in utero* [177]. Cardiovascular abnormalities include the failure to establish adequate yolk-sac vascular circulation, which results in early lethality (E8.5-10.5); poor cardiac function (E9.0-birth), inadequate establishment of the cardiac conduction system (E12.0-birth), and impaired flow of oxygen and nutrients through the placenta (E8.5-birth).

3.2.2. Morphological and histological study of *Tlk2*$^{Trap/Trap}$ embryos

To visualize the morphology of the whole embryo specimens and examine whether the heart and vasculature system were compromised during embryonic development, we

performed Single Plain Illumination Microscopy (SPIM). This technique is performed by a special procedure to clear tissue and allow optical sectioning of the fixed mouse. We obtained three-dimensional (3D) images of whole embryos at e14.5, allowing us to visualize details of the anatomy by imaging autofluorescence. We considered that 3D volumetric imaging was optimal for analyzing mouse embryo morphological characteristics [178] particularly when used as a primary phenotypic screen, because of its whole embryo coverage.

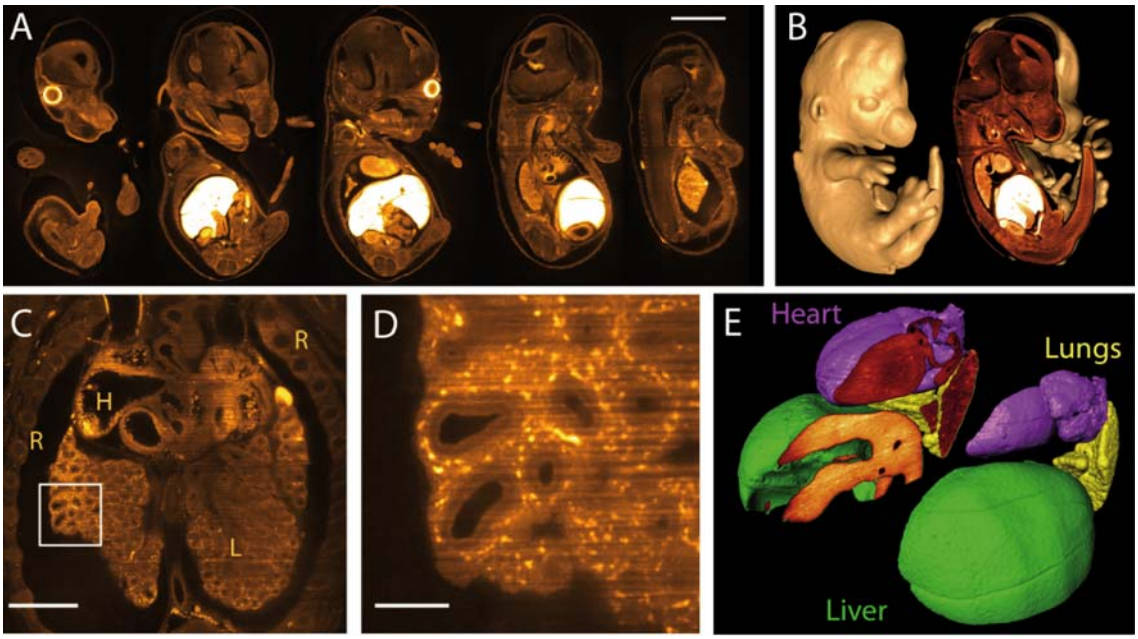

Figure 28. SPIM analysis. A. Single Plain Illumination Microscopy (SPIM) of several seccions of e14.5 *Tlk2*$^{Trap/Trap}$ embryo. B. 3D reconstruction of the whole embryo. C. Detailed visualization of the heart (H), lungs (L) and ribs (R). D. Higher magnification of the lungs. E. 3D reconstruction of heart, lungs and liver. No gross abnormalities were detected.

As a first approach, we used embryonic autofluorescence to have a whole image of the specimen, as represented in Figure 28 A and B. We could easily discern strongly autofluorescent structures, such as liver, lungs and heart (Figure 28 C and D). In the analysis of these images, we could not detect any major abnormality in organ morphology, and all the differences seen were consistent with normal embryonic variability.

We then performed a more specific histological analysis of the embryos at e14.5 using immunohistochemistry (IHC). The whole specimen was fixed in 4% paraformaldehyde for 48h, embedded in parafin and processed for staining with four markers. Haematoxilin & Eosin (H&E) was used to have a general view of tissue architecture; DNA synthesis was measured by bromodeoxyuridine (BrdU) and Ki67 staining of sections and CD31 staining was performed to reveal the status of endothelial cells and vasculature.

As shown in **Figure 29**, *Tlk2*$^{Trap/Trap}$ embryos were smaller, but no gross histological problems were found with any of these four staining. Surprisingly, given the smaller size and the developmental delay in *Tlk2*$^{Trap/Trap}$ embryos, there was no evident differences in BrdU or Ki67, suggesting that *Tlk2* deficiency caused no obvious defects in cell proliferation at the time of lethality.

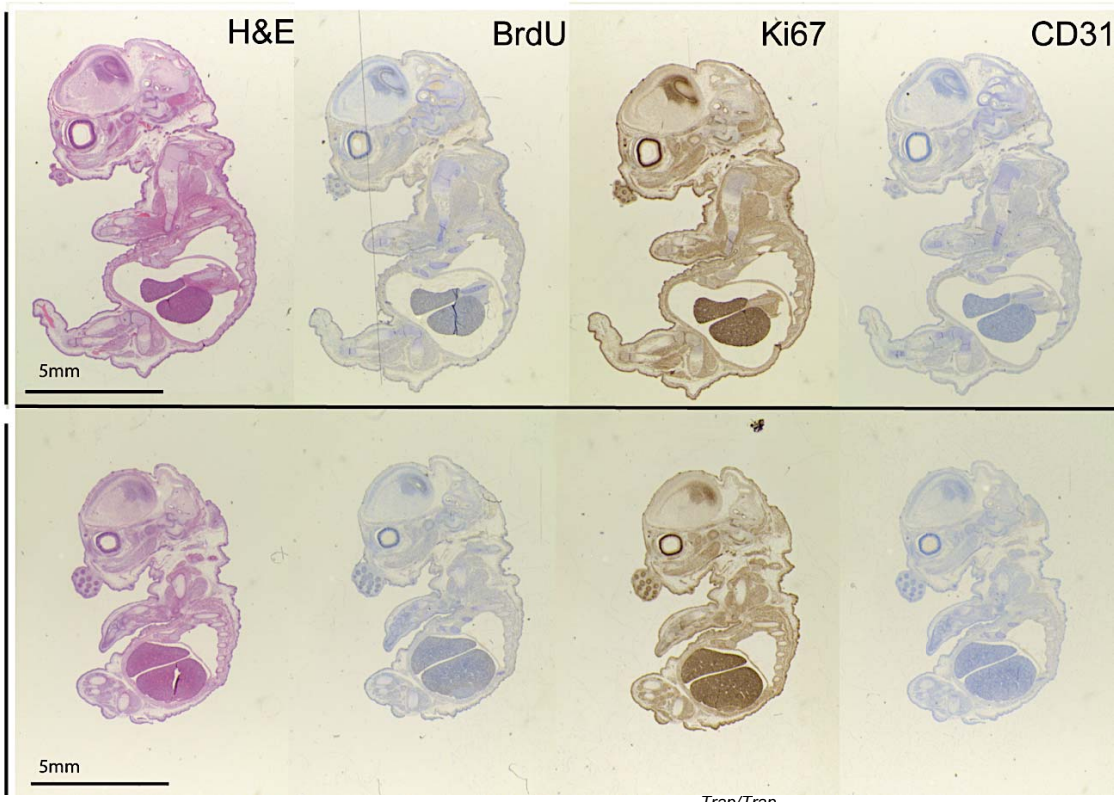

Figure 29: Histological analysis of WT (upper) and *Tlk2*$^{Trap/Trap}$ (lower) whole embryos at e14.5. No relevant pathologies were found in H&E, BrdU, Ki67 nor CD31 staining. Although the smaller size in the mutants, BrdU staining shows equally abundant S phases in *Tlk2*$^{Trap/Trap}$ and control siblings.

3.2.3. Analysis of Hematopoietic system and blood cell development.

The noticeable developmental delay and pale coloration of the mutant embryos was consistent with a possible deficiency in the blood supply that did not correspond with obvious heart or endothelial cell related developmental problems. Available data indicated that, in the adult hematopoietic system, stem cells (HSCs) exhibited higher mRNA levels of TLK2 than its homolog TLK1 (GEO datasheet, Figure 30). To determine if lack of TLK2 could compromise HSC function during embryonic development analyzed the cellular composition of the fetal liver where HSCs appear at day E11.5 (Figure 31).

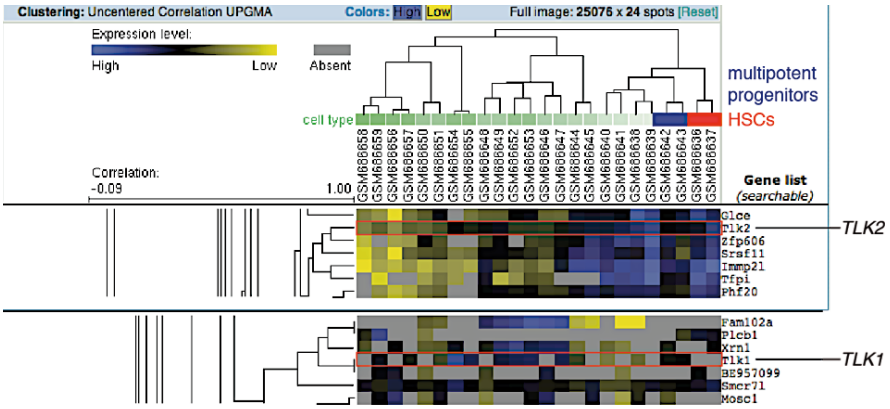

Figure 30. Expression level GEO DataSet cluster analysis TLK1 and TLK2 expression levels are clustered for different compartments in the hematopoietic system.

At day E12.5, the fetal liver becomes the main hematopoietic organ during embryonic development, both for HSC expansion and production of definitive blood cells. The HSCs expand dramatically in the fetal liver microenvironment until day E15.5-16.5. The fact that the *Tlk2*$^{Trap/Trap}$ embryos appear pale by e12.5, they had smaller livers and at e14.5 they started to die, led us to hypothesize that maybe there was a defect in the production of HSCs in the fetal liver of mice lacking TLK2.

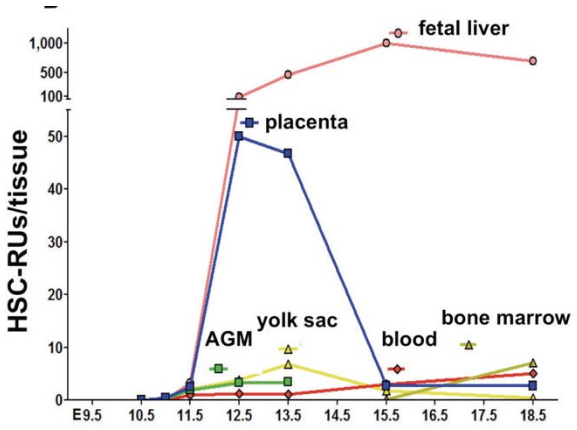

Figure 31. Kinetics of HSC-Repopulating Units (RU) at each hematopoietic site during mouse development. HSC-RUs are calculated from the frequency of reconstituted recipients at 10–12 weeks after transplantation, divided by the transplanted cell dose (in embryo equivalents). The figure has been adapted from Mikkola et al., 2005.

HSC lack the expression of cell surface molecules that appear on lineage-specific mature cells, and are therefore Lin$^-$. In mouse models, HSCs usually express stem cell antigen 1 (Sca1$^+$) and c-Kit (Kit$^+$, CD117), a trans-membrane tyrosine kinase that serves as a receptor for stem cell factor. Thus, we used the established Lin$^-$ Sca1$^+$Kit$^+$ (LSK) combination to identify HSCs. Surprisingly, quantification of HSCs in *Tlk2*$^{Trap/Trap}$ embryos revealed no significant difference from their WT littermates.

However, the total number of HSCs does not give us information about the pluripotency of these cells. Hematopoiesis is organized as a hierarchy of cells with decreasing self-renewal and differentiation potential. Long-term (LT) HSCs, the most primitive cell in this hierarchy, can give rise to all blood lineages and have unlimited

capacity to self-renew. LT-HSCs produces short-term (ST) HSCs that are still multipotent, but are limited in their self-renewal capacity. ST-HSCs differentiate further into lineage-committed progenitor cells that are responsible for the large-scale production of mature blood cells. To identify if there could be some problem in the renewal or commitment of fetal HSCs, we used an additional two markers that can discriminate between LT and ST-HSCs: CD150 and CD48.

As shown in **Figure 32**, none of these cellular populations were altered in *Tlk2*$^{Trap/Trap}$ embryos, suggesting that the embryonic problems were not due to a failure in the HSC compartment.

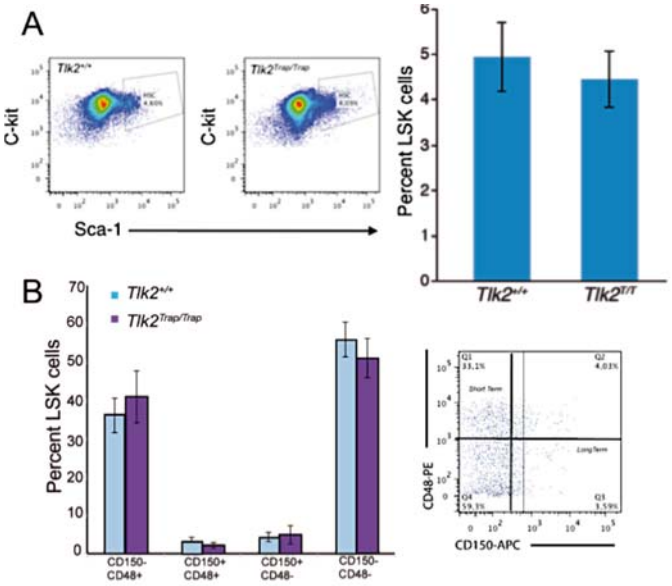

Figure 32. LSK cells are not affected in *Tlk2*$^{Trap/Trap}$ embryos A. Flow cytometer analysis of LSKcells from fetal liver. The average percentage of LSK population is plotted. Bars represent standard deviation. B. Bar graph showing the percentage of LT and ST-HSC using CD48 and CD150.

In addition, we analyzed the development and commitment of other blood cell populations. We performed a specific staining for the erythroid linage using Ter119 and c-kit cellular markers; myeloid linage, using Gr-1; and lymphoid linage using B220. All the stainings were done from cells in the fetal liver, showing no significant differences between genotypes. Cell distribution of erythroid development in fetal liver at e14.5 using c-Kit and Ter119 is shown in figure 33.

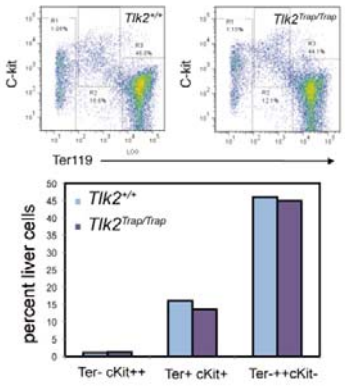

Figure 33. Flow cytometer analysis of erythroid lineage in fetal liver at E14.5. The average percentage of three developmental stages is plotted. Erythroid maturation flows from Ter119-c-kit+ to Ter119-c-kit+. Bars represent standard deviation.

3.2.4. Neural development is not compromise in *Tlk2*$^{Trap/Trap}$ embryos.

At e10.5 and 12.5 some of the *Tlk2*$^{Trap/Trap}$ embryos exhibit problems in the clousure of the neural tube, which lead us to think that Tlk2 could be acting in the development of the neural system. We asked if Tlk2 signalling constitutes a requirement for the maintenance of neural stem cells. To address this question, we tested the capacity of neural stem cell self-renewal in WT, *Tlk2*$^{+/Trap}$ and *Tlk2*$^{Trap/Trap}$ neurosphere cell populations. We predicted that lack of Tlk2 signalling could disrupt chromatin organization and may lead to gene deregulation and differentiation problems, resulting in the premature attrition of stem cell pools.

Neural stem cells were obtained from perinatal forebrain germinal zones of WT, *Tlk2*$^{+/Trap}$ and *Tlk2*$^{Trap/Trap}$ embryos and grown in vitro in the presence of EGF and FGF-2 as multipotent neurospheres with self-renewing capacity (Ciccolini and Svendsen, 1998; Tropepe et al., 1999; Zhu et al., 1999b). The total number of neurospheres determines the capacity of stem cell maintenance and differentiation (Reynolds and Weiss, 1996).

Our results indicates that loss of Tlk2 does not impair neural stem cell self-renewal as assessed by neurosphere

formation over several passages. No difference was found in number of neurospheres between different genotypes at passages (p) 0, p1 and p2 in the presence of 10 ng/ml of EGF and 20 ng/ml of FGF-2 (**Figure 34**). The absence of a significant reduction of recombined neurospheres over several passages suggests that Tlk2 is not essential for maintenance of neural stem cells.

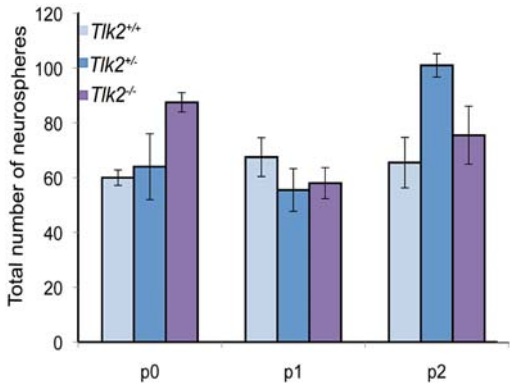

Figure 34: Neurosphere formation is not impaired. Neurospheres formation in WT, *Tlk2*$^{+/Trap}$ and *Tlk2*$^{Trap/Trap}$ embryos show no differences, suggesting that Tlk2 is not an essential gene in neural system development.

3.2.5. Placental development is impaired in *Tlk2*$^{Trap/Trap}$ embryos.

The placental vasculature provides the main site for the exchange of nutrients and waste between the mother and the fetus, via a network of maternal sinusoids that run along fetal blood vessels. A disruption in the placental architecture can lead to

developmental delays and embryonic lethality, as we have seen in *Tlk2*$^{Trap/Trap}$ embryos. As we could not identify any consistent disruption in organ development or in the hematopoietic system in *Tlk2*$^{Trap/Trap}$ embryos, we decided to next analyze placental formation at different stages.

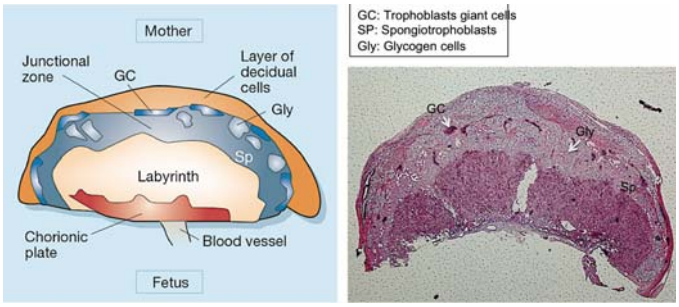

Figure 35. Schematic illustration of placental layers. Decidua, Junctional and labyrinth zone. The junctional zone is divided in trophoblast (gigant and glycogen cells) and sphingotrophoblast cells (Scheme taken from Tycko et al, 2002)

There are three layers in the mature placenta that allow communication and transfer of nutrients, ions, gases and water between the mother and the fetus. The zone nearest to the chorionic plate (inner membrane) is the labyrinth. Within this zone, maternal and fetal circulation occur in close proximity and this represents the principal site for nutrient and waste exchange. Maternal blood is separated from the fetal blood by a selectively permeable barrier. Surrounding the labyrinth there is a layer comprised of fetal spongiotrophoblast cells and trophoblast cells, subdivided in trophoblast glycogen and giant cells. Together they represent the junctional zone of the mouse placenta. The role of this zone is not well understood, but in its absence, the embryo cannot survive[179]. Initial invasion of the mouse blastocyst into the maternal uterus is controlled in part by the trophoblast giant cells (TGC). Initially, these appear as a continuous layer at e12.5. These cells represent the most distal fetal component of the mouse placenta and are in contact with the maternal decidua.

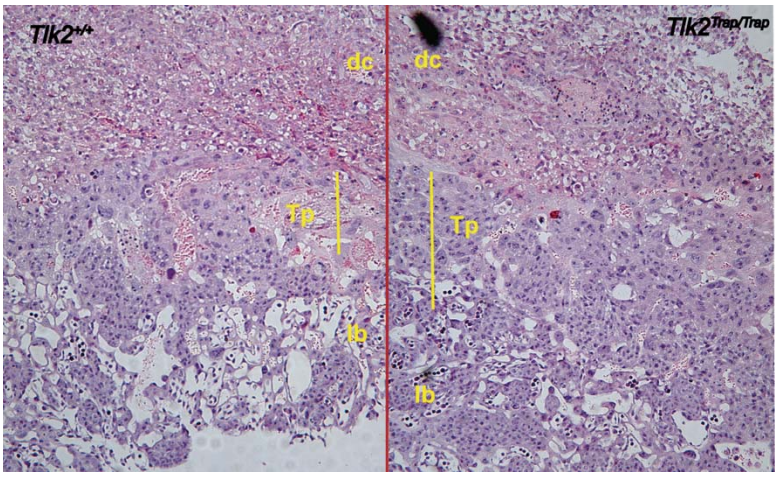

Figure 36: H&E staining of placental sections from e10.5 WT and *Tlk2*$^{Trap/Trap}$. Chorionic plate (ch), labyrinthine (lb), trophoblast (Tp) and maternal decidual layer (dc) are indicated in the image.

We decided to analyze placental formation by IHC at different developmental stages. As *Tlk2*$^{Trap/Trap}$ embryos die shortly after e14.5, we decided to start the study at early stages, aiming to detect the origin of the problem. Analysis at e10.5 revealed a mild hyperproliferation in the trophoblast layer (Figure 36), resulting in a wider trophoblast zone.

By e14.5, there is an evident impairment in the global *Tlk2*$^{Trap/Trap}$ placental morphology. Mutant placentas were smaller and thinner than those of the WT. Surprisingly, when dissecting placentas at e14.5, we detected a reduction in the size and complexity of the umbilical cord in all the mutant embryos processed (Figure 37B-C). This could account for the apparent impairment in circulation between the embryo and maternal tissue. By e16.5, placental problems were much more severe as *Tlk2*$^{Trap/Trap}$ placentas were clearly more pale and smaller in size than WT placentas (Figure 37C). At this stage *Tlk2*$^{Trap/Trap}$ embryos were dead with a severe hypoxic phenotype.

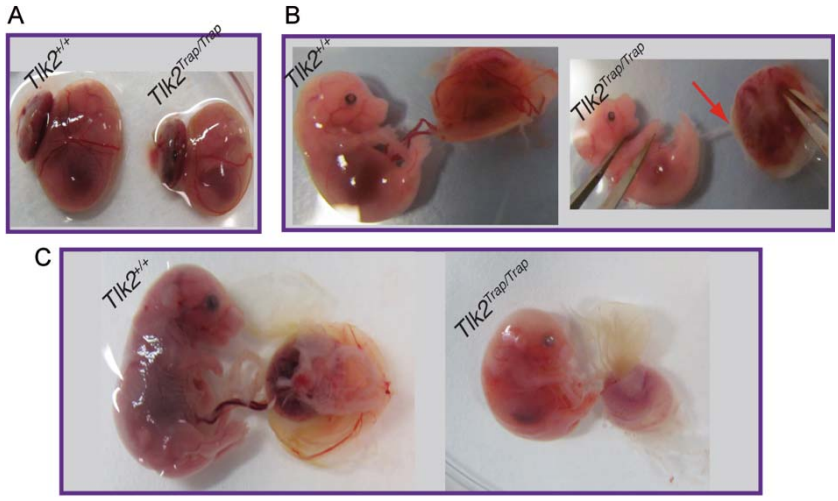

Figure 37:. A. The vascular structure of the yolk sac appeared normal at e14.5. B. Lack of umbilical cord circulation at e14.5. C. Died embryos at e16.5, with evident lack of circulation also in the extraembryonic tissues.

H&E sections of *Tlk2*$^{Trap/Trap}$ placentas at e14.5 revealed a marked reduction in the thickness of the labyrinthine and trophoblast layers (Figure 38) that resembled the phenotypes already reported in Rb and cyclin E1 and E2 mutants[180,181]. Very few polynucleated trophoblast giant cells (TGC) were identifiable in *Tlk2*$^{Trap/Trap}$ placentas by H&E staining. During differentiation of trophoblast stem cells into TGCs, multiple rounds of DNA synthesis occur without mitotic division (endoreplication) leading to increases in DNA content up to 1000N and to a parallel increase in nuclear size[182,183]. The choice to undergo endoreplication instead of mitosis to form polynucleated cells is a decision that is made in the G2/M checkpoint. According to previous work relating TLK2 to DNA synthesis and mitosis, it could suggest a deregulation of the G2/M

checkpoint that leads cells to enter mitosis instead of endoreplicate. This observation is consistent with the hyperproliferation already seen in the trophoblast at e10.5, suggesting an accelerated cell cycle that may impair endoreplication.

In addition, the IHC study revealed a significant decrease in the vascular space in *Tlk2*$^{Trap/Trap}$ placentas and an acute reduction in the presence of blood cells. To confirm this, we stained placental sections with the endothelial marker CD31 (Figure 38). We could observe that blood vessels in the labyrinth layer were collapsed, with only residual blood circulation. This phenotype was even stronger in e16.5 placentas. Indeed, at this stage, blood cells are almost absent and blood vessels collapsed, as was evident when staining the cells with the endothelial marker CD31.

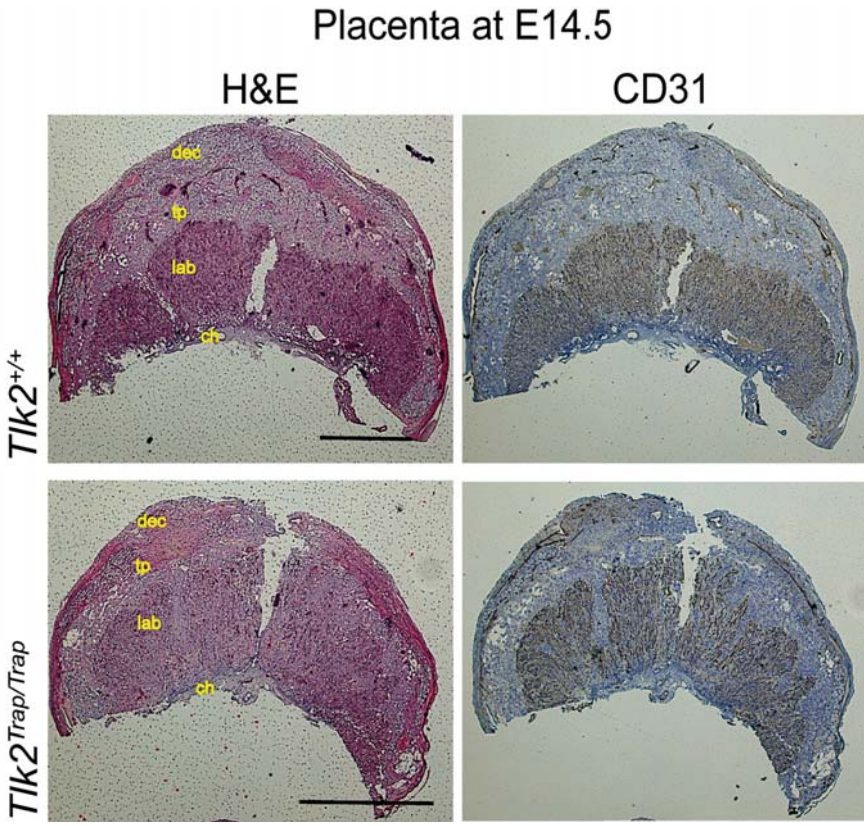

Figure 38: Morphology and histology of WT and *Tlk2*$^{Trap/Trap}$ placentas. H&E stained radial sections of WT and *Tlk2*$^{Trap/Trap}$ placentas at e14.5. All characteristic layers are present in the mutant placenta (de, maternal decidual tissue; tp, trophoblast layer; la, labyrinth layer; ch, chorionic plate). The trophoblast of the mutant placenta is significantly decreased in thickness, with cell infiltration in the labyrinth whereas the mutant labyrinth layer is not markedly reduced in size but present reduced intravascular spaces. Bars, 2.0 mm.

A closer look into the trophoblast and labyrinth revealed excessive proliferation of trophoblast cells, with evident infiltrations into the labyrinth (Figure 39, yellow arrows) and a severe disruption of the normal labyrinth architecture in the placenta. This

analysis confirms a decrease in the vascular spaces as the blood vessels are collapsed. However, the decrease in the vascular density is not highly pronounced which lead us to think that a primary vascular defect is unlikely.

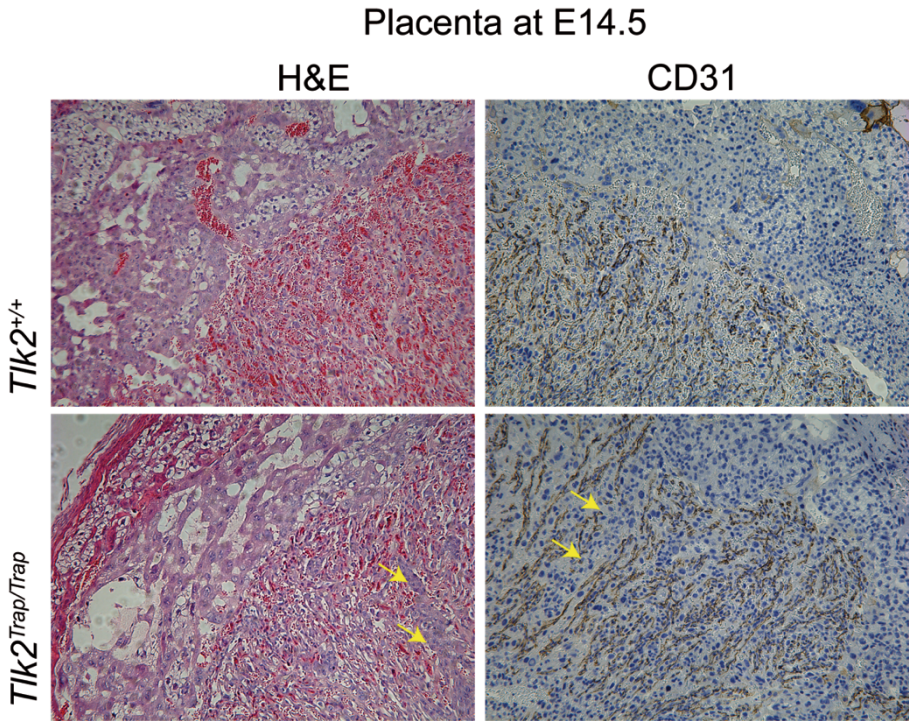

Figure 39: H&E staining of placental sections from e14.5 WT and *Tlk2*$^{Trap/Trap}$. Labyrinth layer shows a decrease in the vascular spaces and gross infiltrations of throphoblast cells (yellow arrows).

An evident BrdU hyper-incorporation in the labyrinth was also seen in *Tlk2*$^{Trap/Trap}$ placentas, which may suggest several possibilities: a higher proliferation rate, as there are more cells in S-phase or a burst of compensatory proliferation due to the circulation defects. Interestingly, at e16.5 there was an accumulation of γH2AX, a marker of DSBs, in trophoblast layer, suggesting increased DNA damage in this zone.

Altogether, these data suggest that a placental defect is responsible for the embryonic death in *Tlk2*$^{Trap/Trap}$ mice. The trophoblast cells are likely to be the cells primarily affected, disrupting the membrane that allows a fetal-maternal exchange. Accordingly, the fetal blood vessels in the labyrinth collapse due to lack of maternal water and oxygen. This fact is manifested in the absence of blood circulation in the umbilical cord. Further studies are needed to understand the potential role of TLK2 in trophoblast proliferation and endoreplication.

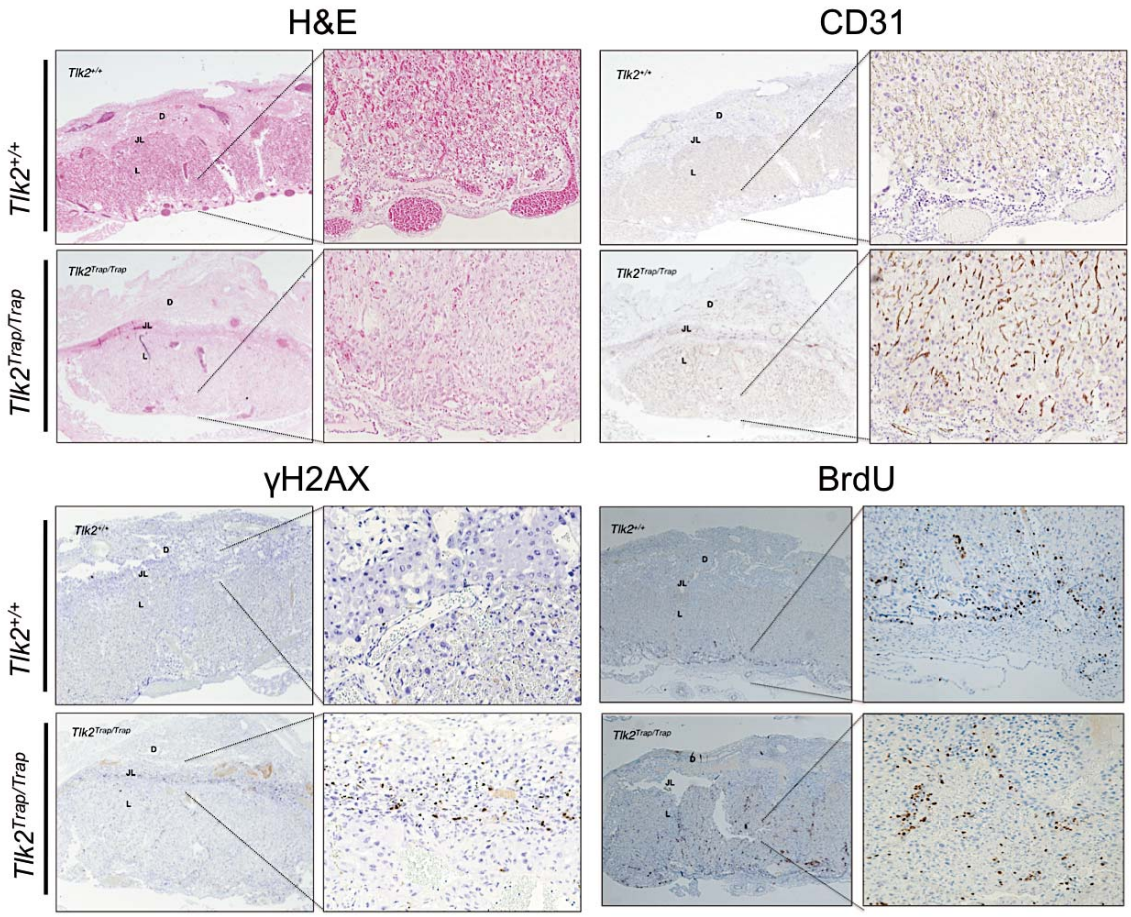

Figure 40: H&E staining of placental sections from e16.5 WT and *Tlk2*$^{Trap/Trap}$ animals. The boxed areas in the left are shown at higher magnification in the right. Noticeable lack of blood and blood vessel collapse in the labyrinth are obvious in H&E and CD31 staining in *Tlk2*$^{Trap/Trap}$ placentas. Acumulation of γH2AX in the spingotrophoblast and BrdU through all the layers can be observed in *Tlk2*$^{Trap/Trap}$

3.3. TLK2 is haploinsufficient in the absence of TLK1.

Our previous cellular data suggested that Tlk1 and Tlk2 were functionally redundant. It was therefore surprising that only Tlk2 loss led to placental defects. To determine if Tlk1 could also contribute to development, we examined the effects of reduced dosage of *Tlk2*, which on its own does not lead to developmental defects, on the *Tlk1*$^{Trap/Trap}$ background. Through interbreeding, we generated double heterozygous mice, *Tlk1*$^{+/Trap}$ *Tlk2*$^{+/Trap}$, that seem to develop normally, with no altered longevity or fertility. By interbreeding these animals, we then generated *Tlk1*$^{Trap/Trap}$ *Tlk2*$^{+/Trap}$ animals. These mice were born but, interestingly, developed severe developmental defects and died within the first month (n=3). These results indicated that one allele of *Tlk2* was not sufficient for normal development in the absence of *Tlk1*. Further studies are required

to elucidate the origin of the systemic failure observed in *Tlk1*$^{Trap/Trap}$ *Tlk2*$^{+/Trap}$ but we speculate the cause is not related with placental defects.

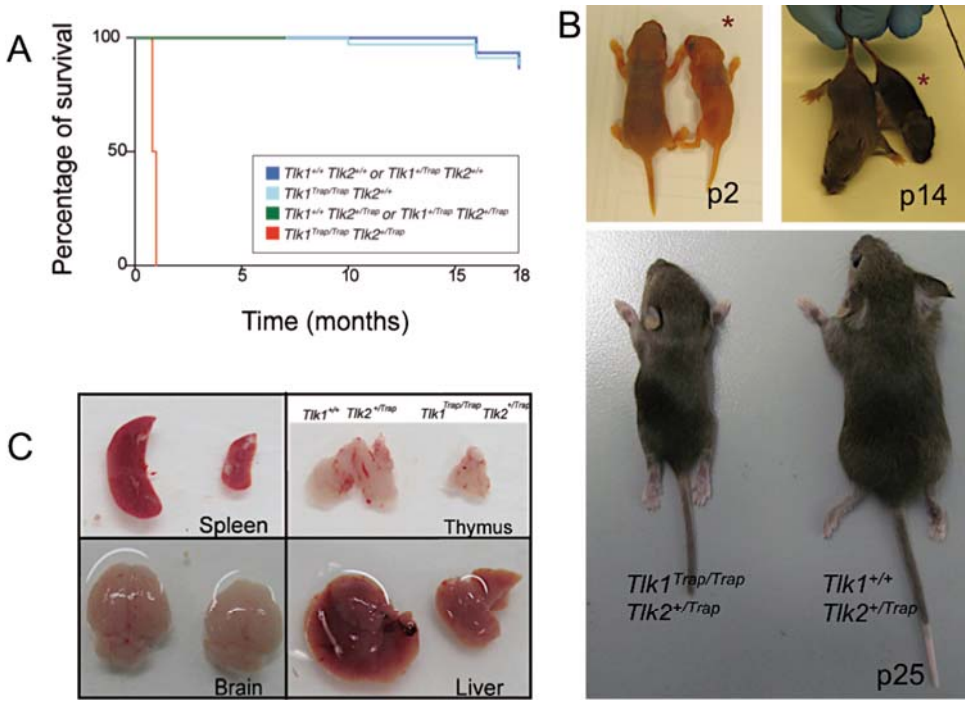

Figure 41: TLK2 is haploinsufficient in the absence of TLK1. A) Survival rate of a series Tlk genetrap phenotypes. *Tlk1*$^{Trap/Trap}$ *Tlk2*$^{+/Trap}$ die within a month. B) Phenotypical comparation of *Tlk1*$^{Trap/Trap}$ *Tlk2*$^{+/Trap}$ and *Tlk1*$^{+/+}$*Tlk2*$^{+/Trap}$. Growth retardation is noticeable since the birth (p= day post-partum). C) Several organs show severe growth retardation. Liver also exhibit paleness.

3.4. Generation and analysis of *Tlk2*$^{Trap/Trap}$ MEFs.

3.4.1.Loss of TLK2 affects cell proliferation.

To determine if loss of *Tlk2* affected the growth or viability of primary cells, primary MEFs were prepared from E13.5-15.5 mouse embryos of interbred *Tlk2*$^{+/Trap}$ mice (see material and methods). To determine if *Tlk2* deficiency had an effect on cell proliferation, primary MEFs were replated following a classical 3T3 growth assay. At first passages, we observed a significant reduction in the growth rates of cells lacking TLK2 compared to their WT littermates (**Figure 42**A). All *Tlk2*$^{Trap/Trap}$ cells became senescent between passage 7 and 9, we were unable to obtain spontaneously immortalized lines (**Figure 42**B).

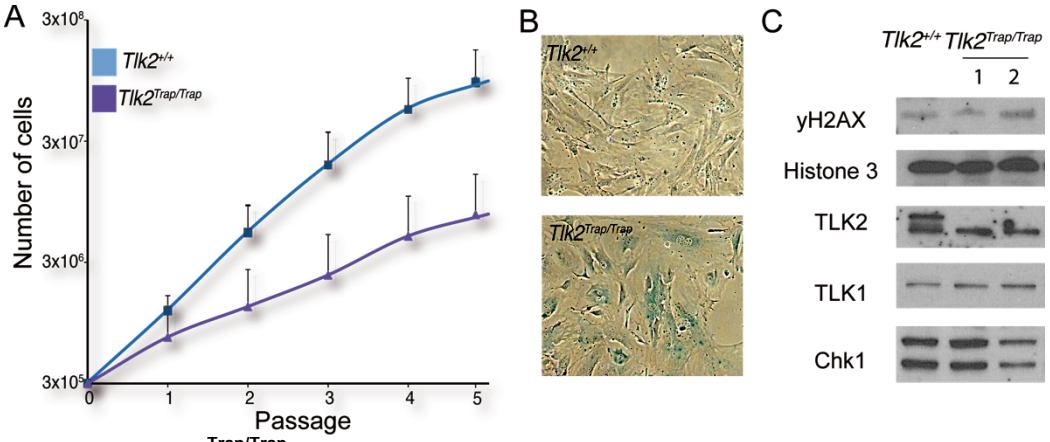

Figure 42: Tlk2$^{Trap/Trap}$ MEFs show premature senescence. A) 3T3 growth curve for Tlk2$^{+/+}$ and Tlk2$^{Trap/Trap}$ primary MEFs for the 5 first passages. Cell cultures showed significative differences in cell proliferation. Results from 3 representative experiments performed in triplicates are shown. Error bars indicate standard deviation mean. B) SA-*β*-gal staining of Tlk2$^{+/+}$ and *Tlk2*$^{Trap/Trap}$ primary MEFs at passage 8. Evident senescent is seen in TLK2 null cells. C) Whole protein extraction of *Tlk2*$^{+/+}$ and *Tlk2*$^{Trap/Trap}$ primary MEFs at passage 3. Two cell lines of Tlk2$^{Trap/Trap}$ were analyze for TLK1, Chk1, γH2AX and H3 as loading control.

Since Chk1 has been shown to regulate Tlk1 activity, it was of interest to examine whether a reciprocal relationship exists such that Tlk2 might affect the levels or activity of Chk1. Using *Tlk2*$^{Trap/Trap}$ primary MEFs at passage 3, we analyzed Chk1, Tlk1 and γH2AX levels. These protein levels did not show major changes at early passages, demonstrating that TLK2 did not affect Chk1 or Tlk1 protein levels and that there was not high levels of DDR signaling (**Figure 42**C).

3.4.2.Loss of TLK2 increases senescence in primary fibroblast.

Tlk2$^{Trap/Trap}$ primary MEFs displayed premature senescence at passage 6-7, evidenced by SA-*β*-gal staining. Persistent activation of the DDR is important for the establishment and maintenance of cellular senescence, so we analyzed the activation status of DDR pathways in MEFs. We have analyzed whether there was accumulation of DSBs in undamaged primary *Tlk2*$^{Trap/Trap}$ MEFs by measuring γH2AX. By IF, we only could see a mild increase in the number of γH2AX foci when visualizing MEFs at early passages (p2). This increase was more pronounce at later passages (p7), in accordance with the premature senescence already seen by SA-*β*-gal. We corroborated this phenotype using flow cytometry analysis for γH2AX.

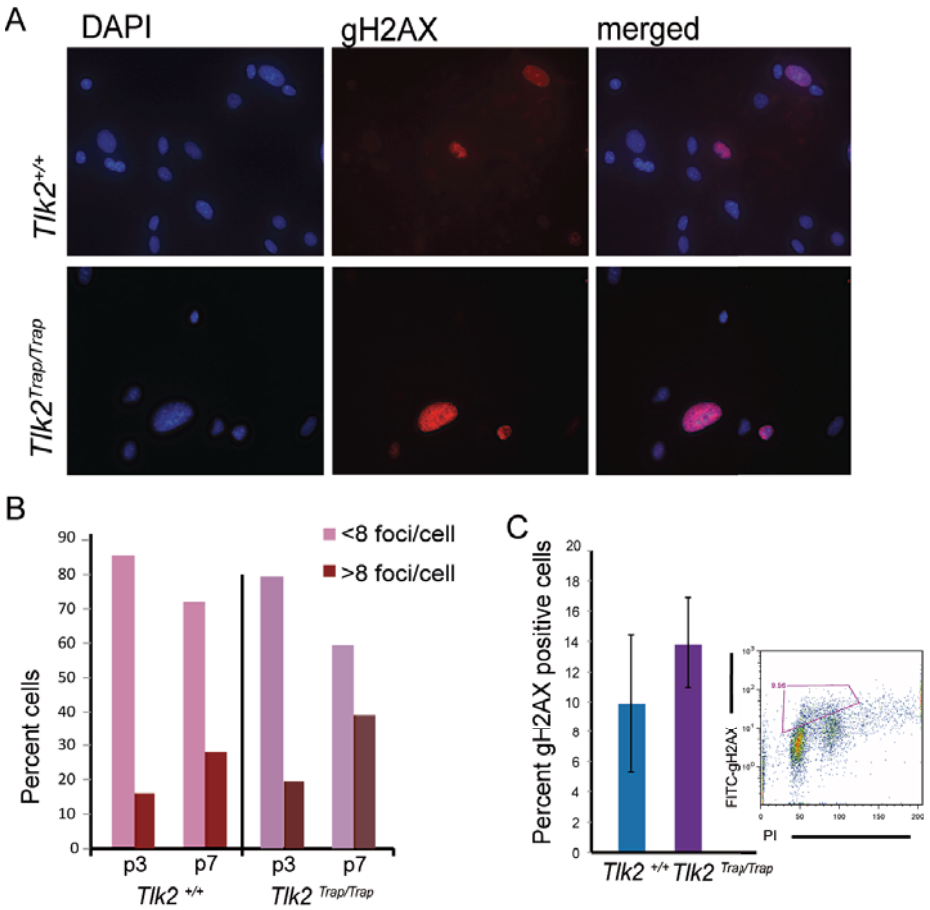

Figure 43: γH2AX levels are increased in primary MEFs. A. Immunofluorescence for γH2AX of primary MEFs at passage 7. B. Percentage of cells with more than 8 γH2AX foci per cell. Results for MEFs in passage 2 and passage 7 are plotted. 200 cells were scored. C. FACs analysis of γH2AX positive cells for the illustrated genotypes. The percentages of positive cells are plotted. 2 representative experiments performed in duplicates are shown.

Persistent activation of the DDR due to cellular senescence can contribute to an increase in the levels of phosphorylation of p53 and an increase in the total levels of the Cyclin dependent kinase inhibitor (CDKi), p21. Further experiments will be done to address p53 and p21 activation status in these cells.

3.4.3.The number of cells in S-phase is lower in *Tlk2*$^{Trap/Trap}$ primary MEFs.

Tlks have been implicated in chromatin exchange during DNA synthesis. To analyze the effect of TLK2 during this process, we measured levels of BrdU incorporation in *Tlk2*$^{Trap/Trap}$ primary MEFs. A significant decrease was evident in the levels of BrdU incorporation in cells lacking TLK2 (Figure 44), corroborating a potential role during S-phase. Our collaborators in the lab of Anja Groth also could observe this phenotype using siRNA against TLK2 in U2OS cells. In future experiments we will analyze if this

situation is exacerbated in double mutant MEFs, which will shed light on the potential role of Tlk1/2 in facilitating replication fork progression.

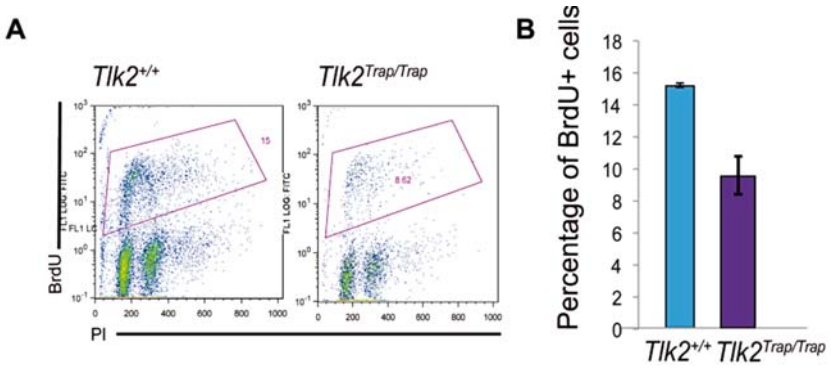

Figure 44: BrdU incorporation is decreased in primary MEF cultures. S-phase ratios (%BrdU+ cells) are plotted. Results are the average of one experiment performed in triplicate for each genotype. Error bars denote SD

3.4.4.Cell cycle arrest in TLK2 depleted cells is impaired.

To determine if *Tlk2* deficiency affected cell cycle progression following DNA damage, especially after IR, we analyzed cell cycle distribution in *Tlk2*$^{Trap/Trap}$ primary MEFs by PI incorporation. Cell cycle distribution in untreated cells did not show any clear difference (Figure 45A). We next examined the G2/M checkpoint response in *Tlk2* deficient cells by staining for the mitotic marker H3-S10 (you have already defined this). First, we noticed a decrease in the number of mitotic cells in basal conditions without any damaging treatment, which is consistent with the slower growth rate detected previously (1.6% in WT cells vs 0.9 in *Tlk2*$^{Trap/Trap}$ cells). After IR damage, as can be observed in Figure 45, *Tlk2*$^{Trap/Trap}$ cells showed a higher frequency in mitosis than the WT cells, suggesting an impaired ability to arrest cell cycle after damage, with partial loss of G2/M checkpoint arrest or impaired mitotic exit.

3.4.5.Loss of TLK2 does not affect sensitivity to DNA damage.

As TLK activity is regulated after DNA damage, and depletion of TLK2 in TLK1 mutant cells sensitized them to damage, we wanted to explore the potential role of TLK2 in the DDR. To do this, we tested the sensitivity of MEFs to IR, UVC and Etoposide using clonogenic survival assays.

Surprisingly, the loss of TLK2 did not caues sensitivity to IR, UVC, or Etoposide. Taken together with the sensitivity assays using siRNA, again suggested that there is a redundant role between TLK1 and TLK2 in DDR (Figure 45C).

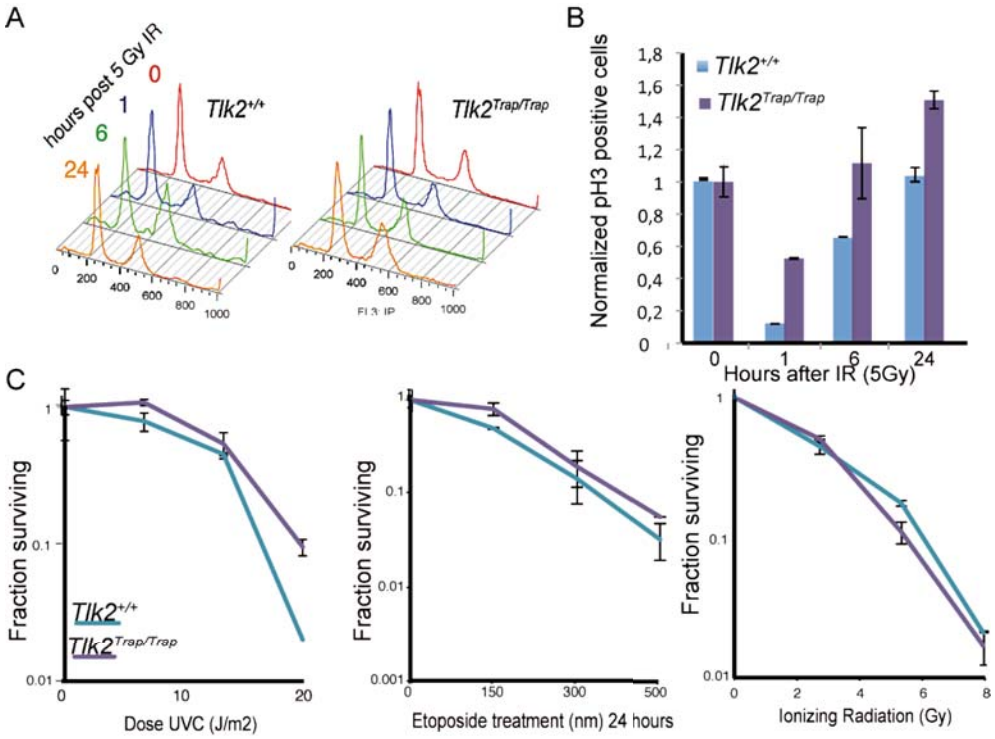

Figure 45: Cell cycle recovery in and Tlk2$^{Trap/Trap}$ primary MEFs A) Cell cycle profiles of WT and Tlk2$^{Trap/Trap}$ primary MEFs labeled with propidium iodide (PI). Cell cycle profiles were analyzed by flow cytometry and plotted as cell count vs. DNA content. Cells were either undamaged or damaged with 5Gy of X-Ray and let recover 1, 6 and 24 hours. B) Normalized levels of positive pH3 cells after 5Gy of X-radiation. TLK2$^{Trap/Trap}$ primary MEFs showed impaired G2/M arrest after damaging treatment, showing a 5 fold increase levels of cells in mitosis after 1 hour of IR compaired with WT control MEFs (Fisher test $p<0.1$). The data represent two independent experiments using duplicates. C. Sensitivity to DNA damage treatments in cells lacking TLK2. Surviving fraction after exposure to X-rays, Etoposide or ultraviolet C radiation. The data are represented as the means and standard errors of 3 different experiments performed in duplicates.

3.4.6.Loss of TLK2 affects chromosomal stability.

We examined spreads from primary fibroblasts derived from both genotypes of embryos at passage 6 to determine if increased chromosomal instability was evident. Similarly to what was done with TLK1, we scored four different aberrations that were apparent in the spreads: chromatid breaks, chromosome breaks, fusions/rearrangements and fragments. After scoring around 50 metaphases we could detect an increase in the number of spontaneous aberrations, especially chromatid breaks, in the case of *Tlk2*$^{Trap/Trap}$ MEFs. This result indicated that, in cells lacking *Tlk2* expression, there is an increase in spontaneous DSBs. Due to the nature of the break, that only affects one chromatid, its likely that these cells accumulated breaks during or after replication of DNA (S/G2) when each chromosome has two sister chromatids.

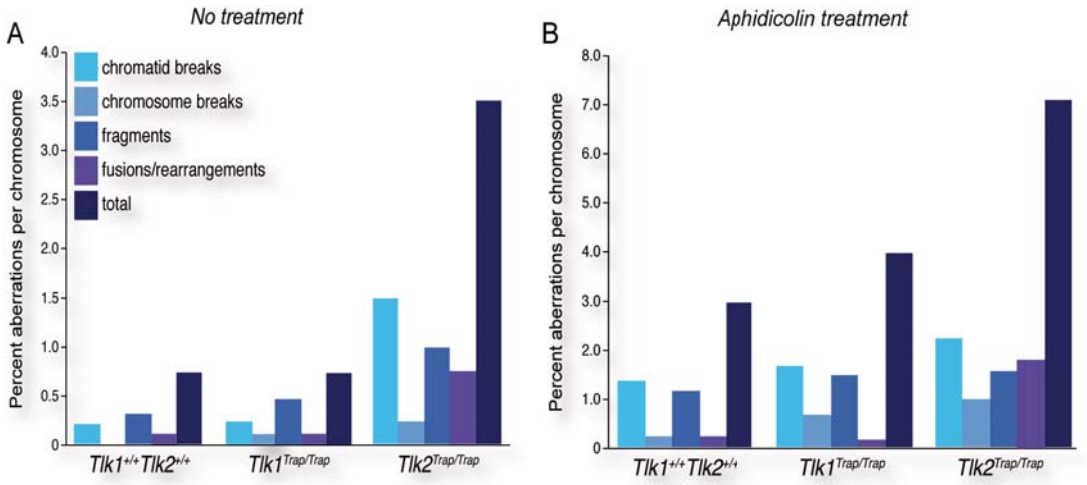

Figure 46: *Tlk2*$^{Trap/Trap}$ cells show genomic instability. Metaphase chromosome analysis of primary MEFs (p6) of the indicated genotype with percentages of chromatid (cd) and chromosome (Ch) breaks, fusions, fragments and total aberrations per chromosome A. without treatment and B. after aphidicolin treatment.

We have also observed a substantially higher frequency of aberrant metaphases in *Tlk2* deficient MEFs compared to WT controls, after 36 hours of treatment with low dose (300nM) aphidicolin (**Figure 46** B). Aphidicolin inhibits polymerase α, causing the dissociation of leading and lagging strands and the accumulation of underreplicated DNA at low doses or the complete inhibition of replication at higher doses. Aphidicolin induces chromatid breaks at high levels in fragile sites (CFS) that have repetitive DNA or potential secondary structures. After aphidicolin all types of aberrations were expressed at higher frequencies in *Tlk2*$^{Trap/Trap}$ cells compared to WT, specially chromatid breaks and fusions. These results indicated that Tlk2 may play important roles during DNA replication, particularly at CFS sites.

4. Consequences of wild type and Kinase-Dead overexpression.

Chapter Summary

Several previous publications implicated TLK1 in the DDR and chromosome stability using overexpression approaches. As we did not detect similar phenotypes, unless both *Tlk1* and *Tlk2* were impaired, we speculated that overexpression might result in dominant phenotypes. To address this, we cloned the cDNA of human *TLK1* and *TLK2* in an expression vector derived from pcDNA3 in order to overexpress them in 293T cells. Using site-directed mutagenesis, we mutated an essential residue in the kinase domain, Aspartic Acid 622 with Alanine, to generate the kinase-dead (KD) mutants. We

speculated that expression of a dominant negative form might override the endogenous TLK1/2 and suppress their specific functions. Our results show that cells expressing any of the kianse dead mutants showed increased sensitivity to IR and deficient cell cycle reentry after damage.

4.1. TLK1 KD overexpression led to minor effects in cell cycle regulation.

TLKs forms complexes and their kinase dead isoforms act as dominant negative. Interestingly, a good deal of data has emerged in the last 2-3 years showing that sustained TLK activation can exert a tumorigenic effect and speed cell cycle progression.

Thus, our aim was to elucidate the effect of TLK1/2 (gain of function) and TLK1/2 kinase-dead (loss of kinase function) overexpression in mammalian cells in order to characterize the cellular role of TLK when is overexpressed. For this purpose, we transiently overexpressed TLK1/2 and the kinase dead forms in human 293T cells to study their role in cell cycle progression and DDR.

The KD mutants were generated by replacing the Aspartic Acid 622 with Alanine. Aspartic acid is an essential amino acid for the kinase activity, as it binds the magnesium required for stabilizing ATP in the catalytic domain.

We constructed expression vectors with TLK1, TLK2, and their KD forms, fused to a Strep-FLAG tag. We obtained the vector pcDNA3.0 with Strep II-FLAG tags from Dr. Ueffing's laboratory, Helmholtz Zentrum Munchen. The human cDNAs of these proteins were cloned in frame with tandem Flag and Strep-Tag II epitopes that were fused at C-terminus. This construct was ligated into an expression vector to generate the constructs pLPC-hTLK1, pLPC-hTLK2, pLPC-hTLK1KD, and pLPC-hTLK2 KD-FLAG-Strep-Tag II.

As a first attempt, we used retroviral transduction to stably express TLK1 and TLK1 KD in 293T cells. 293T cells were transfected with these constructs and retroviral production vectors (VSV-G, RRE and REV). Retrovirus was produced in the supernatant and target cells were subsequently infected and puromycin-selected. To our surprise most of the cells under selection (Puromycin 2 μg/ml) were dead 48 h later (Figure 47), suggesting that stable expression of these proteins was lethal or that TLK1 overexpression impaired viral production.

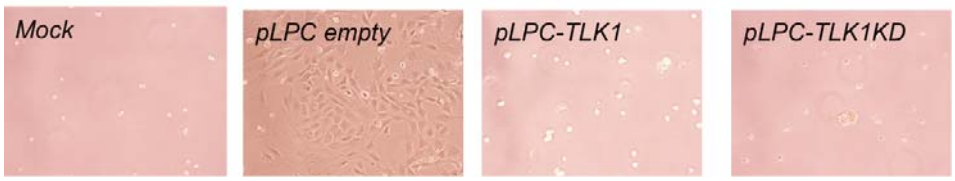

Figure 47: TLK1 and TLK1 KD cannot be stably overexpressed in HEK293 cells. Cells were infected by the retrovirus expressing TLK1/TLK1 KD for 48 h. After 24 h for recovery, puromycin (2 μg/ml) was added to select infected cells stably overexpressing TLK1/TLK1 KD. Pictures were taken after 48 h of puromycin selection. No cells were viable.

Indeed, upon treatment of latent herpesvirus-infected cells with siRNAs targeting TLKs, there is a robust viral reactivation, suggesting that TLK is important for viral latency[184]. It's likely that overexpression of these kinases inhibit the viral production in host cells.

As we could not generate stable cell lines, we studied the role of human TLK1 and TLK2 overexpression in cell lines following a transient transfection strategy. The expression of these proteins peaked 48 h post-transfection (Figure 48). Thus, all the experiments were performed in the time period between 36 and 72 h.

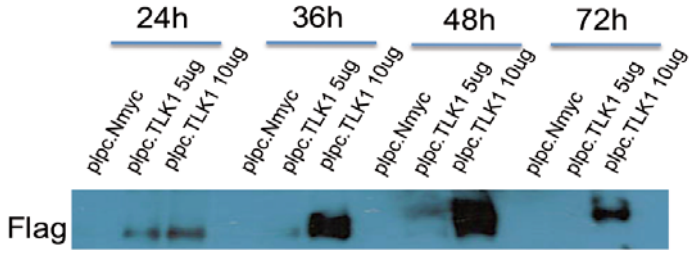

Figure 48: TLK1 shows a peak of expression at 48h. The expression of TLK1 was detected by Western blotting using an antibody to Flag. The maximal peak of expression corresponds to 48 h post-transfection.

To assess the effects of the overexpression of either an active or a kinase dead isoform of TLK1 to the growth of transfected cells, growth assays were performed with cells expressing empty pLPC, TLK1, and TLK1 KD cDNAs. $3x10^5$ cells were seeded in 6-cm plates 36 h after transfection. At various times (1 and 2 days post-seeding), cell counts were performed to determine the total cell number (Chapter 2: Materials and Methods, Section 3T3). Cell growth changes were not evident in TLK1-overexpressing cells. However, the growth rate of those overexpressing TLK1 KD was slightly lower than their control counterparts (Figure 49A). These results indicated that the activity of TLK1 influenced cell proliferation and suggested that the TLK1 KD may have dominant negative effects when overexpressed.

To study whether TLK1 overexpression could impair cycle recovery after DNA damage, we measured the capacity of transfected cells to reenter the cell cycle after checkpoint activation by IR. First, we analyzed the cell cycle profiles of PI-stained cells at various

time-points after DNA damage (Figure 49B). The profiles obtained showed no major differences between mock and TLK1- or TLK1 KD-overexpressing cells, with no evident accumulation of cells in any phase (G1-S-G2).

To measure the ability of cells to recover from mitotic arrest, cells were irradiated with 5 Gy and mitotic cells were scored 1, 6 and 24h after IR. Overall, undamaged cells overexpressing TLK1 or TLK1 KD showed, on average, the same proportion of cells in M phase (1.4 % and 1.3 % respectively) compared with mock cells (1.6 %). Interestingly, while cell cycle arrest was normal in TLK1-overexpressing cells, overexpression of TLK1 KD caused a defective reentry into mitosis, reducing the amount of cells that reenter mitosis 24h later by 3.5 fold. Thus, disruption of TLK complex activity caused a defective G2 checkpoint. This observation corroborates previous observations with cells lacking TLK activity that indicated that TLK kinases participate in checkpoint resumption and mitotic progression.

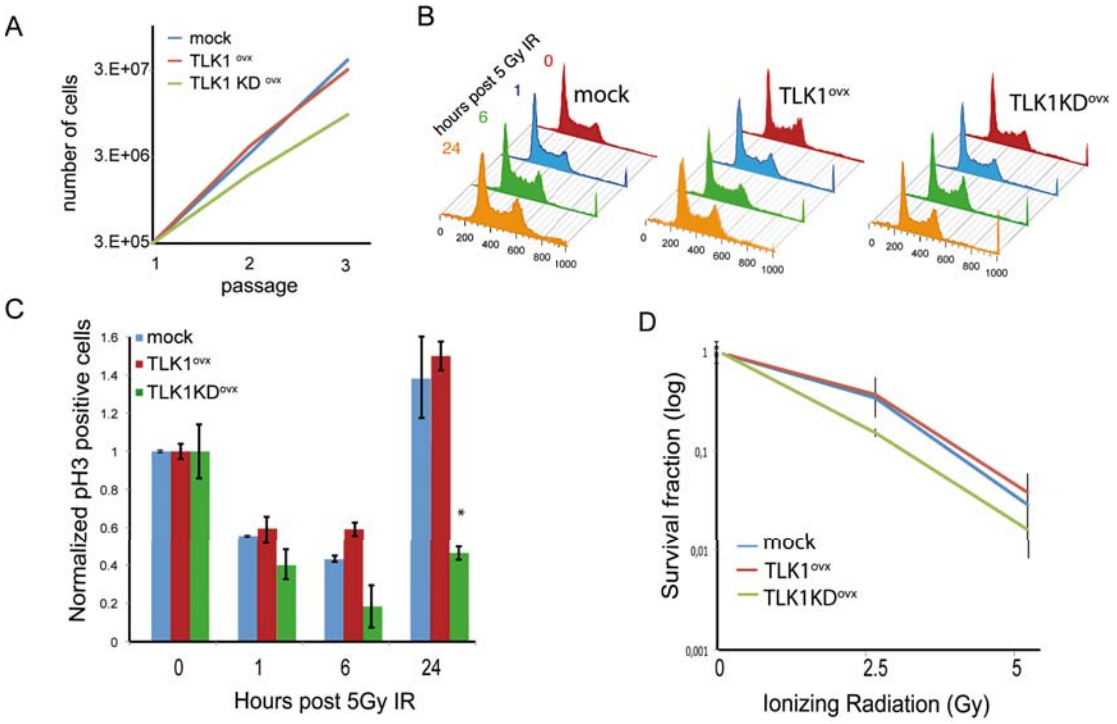

Figure 49: Growth ratio, cell cycle recovery and damage sensitivity in TLK1 and TLK1-KD overexpressing cells A. 3T3 growth assay in TLK1- and TLK1 KD- overexpressing cells. In the first passage $3x10^5$ cells were plated 36 h after transfection and cells counts were performed every 24 h.B. Cell cycle profiles of transiently transfected mock and TLK1/TLK1 KD cells after 5 Gy of ionizing radiation. C. Normalized mitotic ratio (pH3-positive cells) of mock and TLK1/TLK1 KD cells after 5 Gy of ionizing radiation (Fisher test <0.05). 2 representative experiments performed in duplicates are plotted D. Clonogenic survival assays of transiently transfected cells exposed to the indicated dose of ionizing radiation. The data represent one experiment made in duplicates.

We next wanted to determine if suppression of TLK complex activity using a KD isoform rendered cells more sensitive to DNA damaging agents, as was observed when total TLK activity was depleted. To determine whether overexpression of TLK1 or TLK1 KD caused increased or reduced sensitivity of cells to radiation, cells were irradiated with 0, 2 or 5 Gy and then plated for clonogenic survival assays.

The results are plotted in Figure 49, which showed that TLK1 KD-overexpressing cells are slightly more radio-sensitive than mock and TLK1- overexpressing cells after IR at 2 Gy and 5 Gy, although this data is not statistically significant. In conclusion, the presence of high levels of the inactive form of TLK1 resulted in a mild increase of sensitivity to IR. A similar result has been reported using TLK1B KD isoform [185].

4.2. TLK2- KD overexpression renders cells more sensitive to DNA damage and delays cell growth.

The transient overexpression of TLK1 protein had no major effect on cell cycle regulation, but the overexpression of its KD form caused mild growth retardation and cell cycle resumption problems that are reflected in a mild increased sensitivity to DNA damage. In this regard, the KD mutant likely acts as a dominant negative form. TLK2 shares 84% identity at the amino acid level with TLK1 and both have been reported to interact to form heteromers. Our hypothesis was that overexpression of TLK1 KD led to inhibition of endogenous TLK1 and TLK2 containing complexes. We therefore predicted that TLK2 KD overexpression should cause similar effects. To test this, we followed the same strategy as with TLK1, namely transient transfection of cells with wild type and kinase dead TLK2 and performing experiments between 36 and 72 h.

The first effect we observed during the routine handling of the transfected cells was obvious differences in their growth characteristics. Those overexpressing TLK2 KD showed a clear retardation in growth, as revealed by a senescent appearance under the microscope. We measured growth by means of a 3T3 assay and considering the first passage as that occurring 24 h after transient transfection (Figure 50)

We then examined cell cycle recovery after 5 Gy of ionizing radiation. In contrast to TLK1 KD, cells carrying TLK2 KD showed, on average, reduced populations of cells in M phase (1.3 % and 0.6 % respectively) compared with mock cells (1.5 %). The results of mitotic recovery are normalized and plotted in Figure 50. Similar to what was observed with TLK1, overexpression of wild-type TLK2 had almost no effect on the population of cells in M phase when compared to mock treated cells.

We measured the mitotic ratio of TLK2- and TLK2 KD-overexpressing cells after 1 h, 6 h and 24 h post-IR. The data presented represents the combined results of 2 separate experiments performed in duplicates. Interestingly, in cells overexpressing TLK2 KD, cell cycle arrest was deficient, as only half of the cells showed G2-M arrest. In addition, the kinase-dead form also caused defective checkpoint resumption, in a similar way to that of TLK1 KD-overexpressing cells. In contrast, overexpression of the active form, TLK2, had almost no effect on the cells.

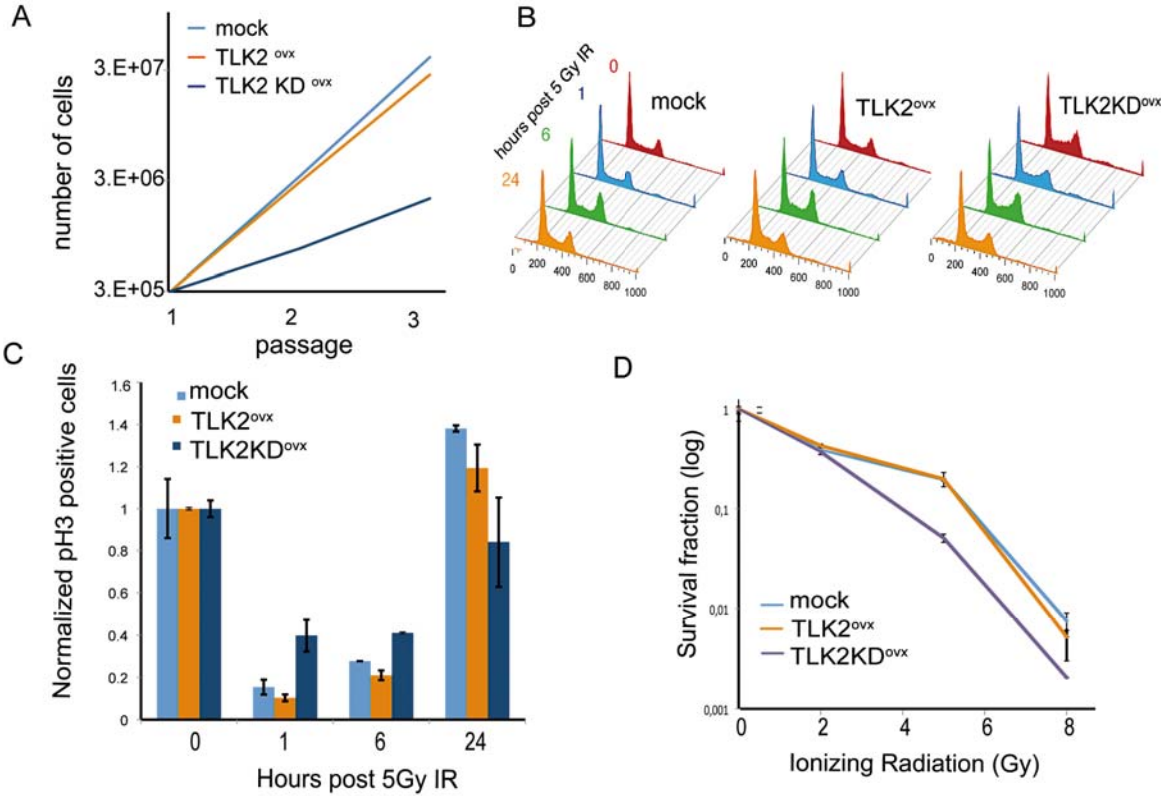

Figure 50: Growth ratio, cell cycle recovery and damage sensitivity in TLK and TLK2-KD overexpressing cells. A. 3T3 growth assay in TLK2- and TLK2 KD- overexpressing cells. In the first passage $3x10^5$ cells were plated 36 h after transfection, and the total number of cells was measured every 24 h. B. Cell cycle profiles of transiently transfected mock and TLK1/TLK1 KD cells after 5 Gy of ionizing radiation. C. Normalized mitotic ratio (pH3-positive cells) of mock and TLK1/TLK1 KD cells after 5 Gy of ionizing radiation. 2 representative experiments performed in duplicates are plotted D. Clonogenic survival assays of transiently transfected cells exposed to the indicated dose of ionizing radiation.

We next examined the effects of TLK2 and TLK2 KD expression on sensitivity to DNA damage. To determine the percentage of survival in TLK2- and TLK2 KD-overexpressing cells after IR, the number of colonies in the non-irradiated control plates were first counted and set as 100% survival. The results are plotted in Figure 6B, which shows that TLK2 KD-overexpressing cells are more radio-sensitive than

mock and TLK2-overexpressing ones after IR at high doses (5 Gy and 8 Gy); however, we did not detect increased sensitivity at 2 Gy.

Thus, disruption of TLK1 or TLK2 kinase activity by the overexpression of kinase dead forms caused defects in the number of cells in mitosis and sensitivity to DNA damage. These data suggest that TLK1 KD and TLK2 KD act as a dominant negative proteins able to poison endogenous TLK1/2 activity or compete for key substrates such as Asf1.

5. Identification of substrates and regulators of TLK1 and TLK2.

Chapter Summary

A major limitation in the interpretation of our phenotypic data from mice and cells with reduced or elevated TLK activity is the lack of knowledge regarding the substrates of TLK1 and TLK2. To address this, we have performed tandem affinity purification (TAP) and LC-MS/MS from cells transiently expressing TLK1 or TLK2 to identify interacting proteins that could represent substrates of regulators. These experiments validated previous data, as Asf1a and Asf1b, H4 and the TLKs themselves were identified as the top ranking interactors. Additionally, we identified a number of new putative interacting proteins that are involved in a range of cellular functions, such as DNA replication, assembly of multiprotein complex formation, and cytoskeletal integrity. These observations support the notion that TLKs may participate in additional cellular processes besides those regulated by Asf1.
In parallel, we have performed a peptide microarray using purified, full-length TLK2. While this approach identified over 100 peptides specifically targeted by TLK2 activity, no clear consensus motif emerged. We hypothesize that the TLK1/2 kinases play a much wider role in governing histone exchange beyond Asf1, and our data indicate that *in silico* prediction of TLK targets will not be trivial, thus more direct biochemical methods will be required to identify bona fide substrates.

5.1. Identification of TLK regulators and substrates using tandem affinity purification

To identify TLK1 and TLK2 interacting proteins, we generated expression constructs for wild-type TLK1 and TLK2 with an C-terminal Strep-FLAG tag for tandem affinity purification (TAP). As TLK2 deficiency resulted in a more severe phenotype, we focused on identifying the possible interactors of TLK2 in preference to TLK1. We also

considered that kinase-substrate interactions may be quite transient and for this this reason we included TLK2 kinase dead (TLK2-KD) in the TAP analysis. This mutant prevents TLK2 kinase activity and could result in higher affinity for some substrates [186].

Using a single tag or both tags, we purified these proteins from whole-cell extracts or nuclear fractions derived from HEK293T cells transiently overexpressing the TLK1, TLK2 or TLK2-KD proteins (Figure 51). Strep-Flag-TLK2 protein was detected in overexpressed cells using anti-Flag antibody, but it was not found in the controls (non-transfected cells and mock) or in the supernatant, thereby indicating that both one-step purification and TAP worked efficiently. It is noteworthy that after two sequential steps of purification, we could only recover TLK2 protein using high salt treatment in the last step (see material and methods). As this would potentially disrupt interactions, we primarily used one-step purifications for the experiments.

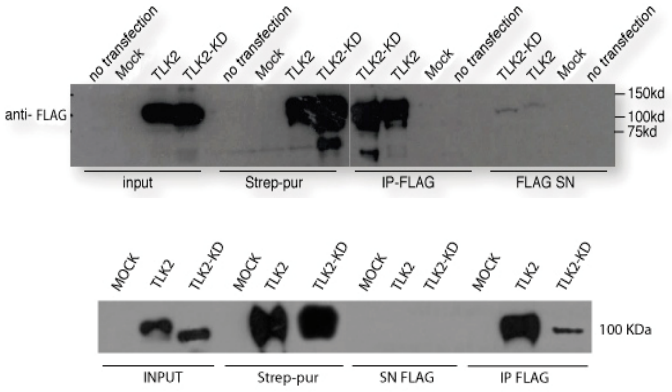

Figure 51: TLK2 purification. One-step purification (Strep and FLAG tag purifications) (upper) and tandem affinity purification (lower) were performed using Strep-tactin resin and/or anti-Flag (M2) magnetic beads. Purifications were done from nuclear extracts derived from HEK293T overexpressing Mock, TLK2 and TLK2 KD and analyzed by Western Blot with anti-FLAG antibody

5.1.1.LC-MS/MS analysis identifies potential TLK2 interacting proteins

To identify TLK1 and TLK2 partners, we analyzed purification experiments (one-step purification) from nuclear fraction by LC-MS/MS. The criteria used to select the potential TLK1-TLK2 interactions was the identification of the protein in more than one experiment and absence of the protein in the mock (control) samples of all experiments. Following these criteria, we selected a number of proteins that are described in table 13, together with the number of experiments in which the proteins were identified.

Protein name	IP TLK2 (n = 4)	IP TLK2 KD (n=4)	IP TLK1 (n=1)	GO category
Tousled-like kinase 2	4	4	1	Chromatin regulation
Tousled-like kinase 1	2	2	1	Chromatin regulation

Dynein light chain 1 (LC8)	2	0	1	Motor activity / Assembly and disassembly of protein complexes
Histone H4	1	1	1	Chromatin architecture
Histone chaperone ASF1B	1	2	1	Chromatin organization
Tubulin β-4B	1	2	0	Structural constituent of cytoskeleton
Histone chaperone ASF1A	0	2	0	Chromatin organization
Tubulin α-1B	1	1	0	Structural constituent of cytoskeleton / Microtubule-based process
MOB	2	1	0	Kinase regulator
PP1C	2	1	0	Protein Phosphatase subunit C
MCM	2	0	0	DNA replication

Table 13. Potential interactors of TLK2, TLK2 KD and TLK1 identified by mass spectrometry from TLK2/TLK1 one-step purifications and TAP. Four purifications were performed in the case of TLK2 and TLK2 KD. Just one for TLK1. Numbers correspond to the times each protein was identified by LC-MS/MS. The proteins shown fulfilled the selection criteria (presence in more than one experiment and absence in the control). Some of the proteins are related to chromatin regulation functions.

Among proteins interacting with the TLKs, were some related to chromatin regulation (Asf1a, Asf1b, Histone 4), thus emphasizing the contribution of TLKs to this process and validating our system. However, other identified proteins are involved in various cellular functions, such as calcium signaling, dimerization or disassembly of complex formation, and cytoskeleton integrity. Together, these results suggest that TLKs participate in additional cellular processes.

5.1.2.TLK2 KD interacts with TLK1 and Asf1 and may act as a dominant negative form.

Our results confirmed the previously reported interactions between TLK1 and TLK2 and both of them with Asf1a and Asf1b[145,148] (Figure 52). Surprisingly, Asf1 was detected only in TLK2 KD overexpression, as a result of an increased affinity for the TLK2 KD protein[141], while TLK1 was identified in both TLK2 and TLK2 KD purifications. These observations suggest that TLK1 and TLK2 do not interact through their kinase domains and support the notion that TLKs act as dimers/oligomers, interacting through their coiled coil domains [97,145].

Previous studies determined the sequence (R/K)R(I/A/V)x(L/P) as an Asf1-interacting protein box in Rad53 kinase [187]. As there is no direct association between Asf1 and Chk1 (homologous of Rad53) in humans, we looked for evidence of this motif in TLKs. We found a potential Asf1 binding motif in TLK2 upstream of the kinase domain (Figure 53C in red). This result suggests that TLK2 could interact with Asf1 through this site in order to enhance the specificity and efficiency of its phosphorylation by the kinase domain.

The TLK2-KD allele contains a single amino-acid replacement (D to A, position 703) responsible for magnesium binding. Thus, the TLK2 KD protein is not able to transfer the phosphate from ATP to substrates, and as a consequence its kinase activity is abrogated. This observation suggests that the TLK2 KD protein interacts longer with substrates, thus improving their purification, as we observed with Asf1. Strikingly, TLK2 KD decreased the phosphorylation status and mobility of endogenous TLK1, and Strep-Flag-TLK2-KD also ran with increased mobility compared to the WT. These results indicated that TLK1 is a TLK2 target and that TLK2 is autophosphorylated (Figure 52) In previous experiment using TLK2 KD overexpression in 293T cells, we observed cellular outcomes similar as the ones observed in cells lacking TLK2. Taking these findings together, we conclude that TLK2-KD acts as a dominant negative protein.

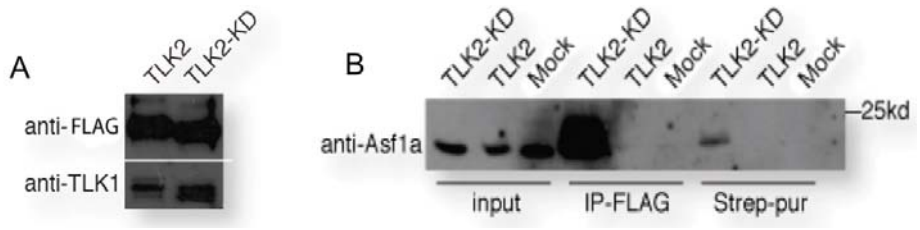

Figure 52: A) Anti-Flag immunoprecipitation from 293T cells transfected with TLK2 or TLK2-KD. TLK2 showed a retarded electrophoretic mobility when compared with their inactive form, suggesting a phosphorylated status. B) Anti-Flag immunoprecipitation followed by Strep purification from 293T cells transfected with TLK2 or TLK2-KD and immunoblotted against Asf1.

5.1.3.TLK2 interacts with LC8 but not with Nek9

In order to gain insight into the relevance of potential new interactors with TLK2, we validated one of the proteins identified by LC-MS/MS that was unrelated to chromatin regulation. One of the most consistent hits was the Dynein light chain like 1 (DYNLL1 or LC8), that was detected in all experiments performed to date.

The LC8 family members (DYNLL1 and DYNLL2 in vertebrates) are highly conserved ubiquitous eukaryotic homodimers. In addition to interacting with dynein and myosin 5a

motor proteins, LC8 molecules promotes the assembly or disassembly of a large (and still incomplete) number of proteins involved in diverse biological functions [188,189]. Interestingly, LC8 was previously implicated in the regulation of the NEK9 kinase that also multimerizes through coiled coil domains (ref). Given this potential LC8 function and that TLKs probably act as heteromultimers, we checked whether LC8 was a *bona fide* TLK2 interactor. TLK2 and TLK2 KD purifications were transferred to a membrane and probed using an anti-LC8 antibody (Figure 53).

LC8 was identified in TLK2 pull-downs, and it showed higher affinity with TLK2-KD-overexpressing cells, as we expected. These results confirmed LC8 as a novel TLK2 interactor.

Two protein sequence motifs are recognized by LC8 on its target proteins: $[K/R]_{-3}X_{-2}T_{-1}Q_0T_1$ and $G_{-2}[I/V]_{-1}Q_0V_1D_2$ (where X is any amino acid) [189]. The motifs are found in disordered segments of the LC8-binding proteins and are often flanked by coiled-coil or other potential dimerization domains [190]. We looked for a TLK2 sequence that conformed to the previously described LC8 recognition motifs. In this regard, we identified two putative binding motifs, one of them near a coiled-coil domain (Figure 53C) thereby pointing to a potential site for a direct interaction between TLK2 and LC8.

We tested whether Nek9 participates in the LC8-TLK2 interaction. TLK2 and TLK2 KD purifications were probed using a Nek9 antibody. We observed unspecific signals for Nek9 (Figure 53 B) thus indicating that Nek9 does not interact with TLK2 and that its interactions with LC8 are independent of the TLKs.

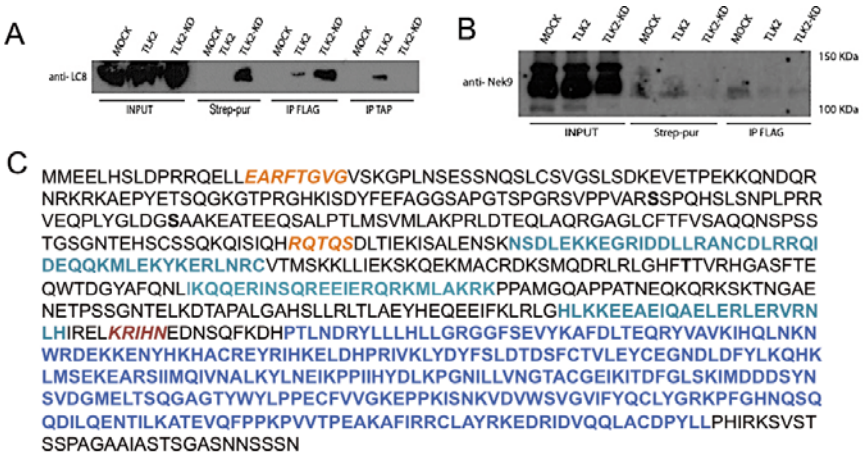

Figure 53. TLKs don't interact with Nek9. anti-Flag immunoprecipitated and Strep purified from HEK293T cells transfected with TLK2 and TLK2-KD were immunoblotted with anti-LC8 antibody (A) and anti-Nek9 antibody (B). C) TLK2 amino acid sequence. The coiled-coil domains are shown in green, the putative LC8 binding motifs in orange, the putative Asf1 binding domain in red, and the kinase domain in blue.

5.2. Identification of TLK2 autophosphorylation sites

5.2.1.TLK2 S635 could be required for TLK2 autophosphorylation.

On the basis of the results obtained with TLK2 immunoprecipitation from TLK2 and TLK2-KD overexpression using anti-Flag antibody TLK2 likely undergoes autophosphorylation, a common mode of regulation amongst kinases. This is evident in the electrophoretic retardation of TLK2 KD but not TLK2 (Figure 52). Even more, previous work using ^{32}P incorporation into TLK proteins in vitro also revealed TLK autophosphorylation[98,145]. However, it remains unknown what residue(s) are autophosphorylation targets.

Data from our collaborators in the laboratories of Guillermo Montoya (CNIO) and Anja Groth (BRIC) using different expression methods identified four putative TLK2 autophosphorylation sites (Figure 54A). In order to test whether any of these putative sites is responsible for TLK2 activity, we generated three mutants (we are still working on the GLSKIM mutant) by site-directed mutagenesis: TLK2 S569A (EAR**S**Y), TLK2 S635A (MELT**S**Q) and TLK2 S686A (Q**S**QQDI). We analyzed the effect on their mobility by Western Blot from whole-cell extract derived from HEK293T cells transfected with the three putative autophosphorylation mutants (Figure 54B). The replacement of Serine to Alanine in position 635 produces a decreased mobility, similar to that observed in TLK2 KD (Figure 52A). Thus, these results suggest that the residue S635, located in the TLK2 activation loop, could be required for TLK2 autophosphorylation and activity.

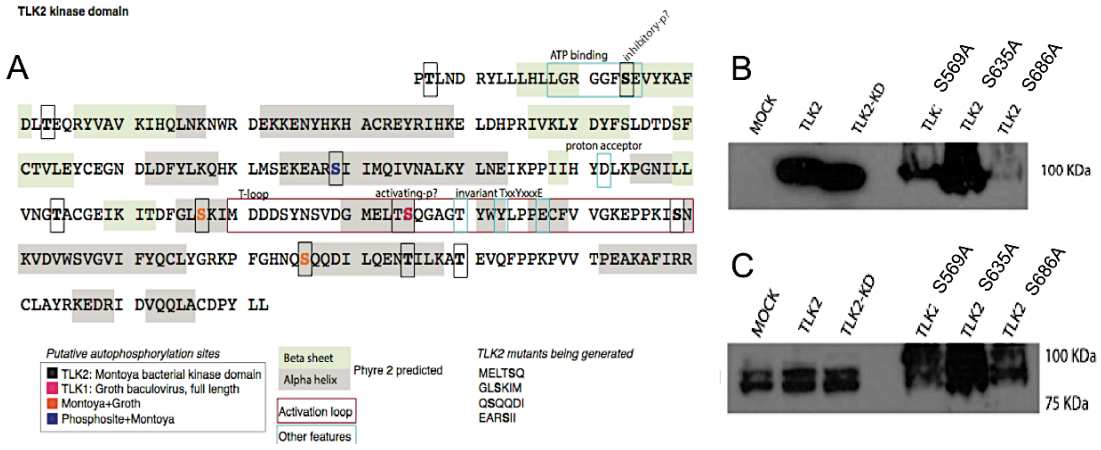

Figure 54: TLK2 S635 could be required for TLK2 autophosphorylation. A) TLK2 kinase domain sequence. Four putative autophosphorylation sites are shown (colored residus). TLK2 mutants being generated are: MELTSQ (TLK2 S569A), QSQQDI (TLK2 S635A) and EARSII (TLK2 S686A) (GLSKIM (TLK2 S617A) was not generated). B) 293T cells transfected with TLK2, TLK2 KD, TLK2 S569A, TLK2 S635A and TLK2 S686A were immunoblotted with anti-Flag.

TLK2 autophosphorylation could have an impact on TLK2 activity, so its loss could prevent TLK1/2 activity. An indirect but rapid way to assess this is by analyzing the mobility of TLK1 in SDS-PAGE by co-immunoprecipitation from HEK293T cells transfected with the three putative autophosphorylation mutants and controls (Figure 54C). The TLK2 S635A mutant also caused decreased mobility of endogenous TLK1, indicating that this mutant could act as an inactive TLK2 protein. Together, these results suggest that S635 is a crucial TLK2 autophosphorylation site. However, further cellular assays are required to validate its functional relevance.

5.3. TLK2 does not have consensus target-phosphosites

In order to try to identify a consensus sequence for TLK2 activity, we performed a peptide microarray. An array chip spotted with peptides containing a phosphorylateable residue (S, T or Y) and a corresponding control with the target residue mutated to alanine. The array was incubated with full length TLK2 under conditions to facilitate kinase activity. The chip was then stained with ProQ diamond that generates fluorescence signal when it interacts with phosphorylated residues and scanned on an imager to quantify the signal of each peptide. The chip contained 550 known phosphorylation sites in 10 residue peptides and corresponding alanine controls. In addition, we included 100 custom probes that contained known target residues from TLK1/2 and Asf1a/b as well as predicted targets from the Phosphosite database based on the Asf1 consensus site generated from comparing Asf1 homologues across species: [DE][NQ][ST][LM] (**¡Error! No se encuentra el origen de la referencia.**A). In addition to Asf1a/b, this search identified 74 predicted targets in human and mouse that have been shown to be experimentally modified on this consensus site (**¡Error! No se encuentra el origen de la referencia.**B).

Notably, MCM4, a known interactor of Asf1a/b, as well as several proteins related to chromatin modifications were predicted including CHD4, PICH and SMARCA1 (**¡Error! No se encuentra el origen de la referencia.**B, blue). Other subunits of the MCM helicase, MCM2 and MCM3, were identified as copurified proteins with TLK2 in MS experiments described in section 5.1.1. Also predicted by the *in silico* analysis was PPP1R7, a subunit of protein phosphatase 1 that plays important roles in cell cycle progression. PPP1CA, a catalytic subunit of PPP1 was identified as a TLK2 interactor in MS experiments. MCM4, several of the chromatin modifiers and selected Asf1 peptides were among the highest scoring hits in the array (**Figure 55**) while H3S10, a previously reported target of TLK1 did not score. However, it is also worth noting that

one of the Asf1 peptides containing the predicted target site used to generate the consensus motif was not modified in the array (Asf1b_003)

A

Hs/Mm/Xt Asf1a	ENSL
Hs/Mm Asf1a	LQSL
Hs/Mm Asf1a	DNTE
Xt Asf1a	EDSN
Hs/Mm/Xt Asf1b	ENSM
Dm Asf1	ENSN
Dm Asf1	DNSL

[DE][NQ][ST][LM]

B

Protein	Organism	Accession	MW	Matches	Start	End	Mod. Sites	On array	Validated
ABCA2	mouse	UP:P41234	270509	DQsL	1325	1328	S1327-p	+	+
ACCN4	mouse	UP:Q7TNS7	59216	EQsL	26	29	S28-p	-	
ALK2	human	UP:Q04771	57153	DNsL	499	502	S501-p	-	
ASF1A	human	UP:Q9Y294	22969	ENsL	190	193	S192-p	+	++
ASF1B	human	UP:Q9NVP2	22434	ENsM	196	199	S198-p	-	
ataxin-2L	human	UP:Q8WWM7	113374	ENsL	561	564	S563-p	+	+
BKR2	human	UP:P30411	44461	ENsM	364	367	S366-p	-	
BSG	mouse	UP:P18572	42445	DQtL	356	359	T358-p	-	
C14orf106	mouse	UP:Q80WQ8	113956	DNsL	476	479	S478-p	-	
CdGAP	mouse	GP:NP_064656	155276	ENsL	270	273	S272-p	-	
CEP97	human	UP:Q8IW35	96981	DNsL	768	771	S770-p	-	
ChaK1	human	UP:Q96QT4	212697	ENtL	1469	1472	T1471-p	+	+
CHD-4	human	UP:Q14839	217991	ENsL	1568	1571	S1570-p	+	+
CNKSR2	mouse	UP:Q80YA9	117396	ENsL	465	468	S467-p	-	
CNR1	human	UP:P21554	52858	DNsM	423	426	S425-p	+	-
CPEB	human	UP:Q9BZB8	62595	DNsL	41	44	S43-p	+	++
DNA-PK	human	UP:P78527	469089	DNsM	3203	3206	S3205-p	+	-
eIF2B-epsilon	human	UP:Q13144	80380	EQsM	530	533	S532-p	-	
eplin	human	UP:Q9UHB6	85226	ENsL	329	332	S331-p	-	
ESCO2	mouse	UP:Q8CIB9	67273	ENsL	307	310	S309-p	-	
FAM130A2	human	UP:Q8WYN3	64900	ENsL	559	562	S561-p	-	
FBN1	mouse	UP:Q61554	312266	DNsL	2707	2710	S2709-p	-	
FCP1	human	UP:Q9Y5B0	104297	DQsM	573	576	S575-p	-	
FNBP1	human	UP:Q96RU3	71307	DNsL	297	300	S299-p	+	+
GAPDH	human	UP:P04406	36053	DNsL	141	144	S143-p	+	+
Grb10	mouse	UP:Q60760	70585	ENsL	456	459	S458-p	-	
Grb7	mouse	UP:Q03160	59959	DNtL	372	375	T374-p	-	
HNRPUL2	mouse	UP:Q00PI9	85000	DQtL	240	243	T242-p	-	
IL18RAP	human	UP:O95256	68310	DQtL	399	402	T401-p	-	
JNK2	human	UP:P45984	48139	EQtL	402	405	T404-p	+	+
K18	mouse	UP:P05784	47538	ENsL	314	317	S316-p	-	
K32	human	UP:Q14532	50319	ENtL	337	340	T339-p	-	
KIF4A	human	UP:O95239	139881	EQsM	1036	1039	S1038-p	-	
KIF4B	human	UP:Q2VIQ3	140035	EQsM	1036	1039	S1038-p	-	
Krt31	human	UP:Q15323	47237	ENtL	297	300	T299-p	-	
KRT33A	human	UP:O76009	45940	ENtL	297	300	T299-p	-	
Kv7.2	mouse	UP:Q9Z351	84450	DQsL	442	445	S444-p	-	
LOC676542	mouse	GP:XP_996040	56831	ENsL	365	368	S367-p	-	
MAGI3	human	UP:Q5TCQ9	165608	DQsL	1278	1281	S1280-p	+	+
MAP1B	human	UP:P46821	270620	EQsL	1655	1658	S1657-p	-	
MCM4	human	UP:P33991	96558	EQsL	143	146	S145-p	+	++
NAP1L4	mouse	UP:O88701	42679	ENsL	3	6	S5-p	-	
NCAPD3	human	UP:P42695	168891	DNtL	428	431	T430-p	-	
PHF3	mouse	GP:NP_001074549	225542	ENsL	1580	1583	S1582-p	-	
PICH	human	UP:Q2NKX8	141103	ENsL	978	981	S980-p	-	
PLEKHA5	mouse	UP:Q8CIA7	96338	DQtM	279	282	T281-p	-	
PPP1R7	human	UP:Q15435	41564	EQsL	45	48	S47-p	-	
RASAL3	mouse	UP:Q8C2K5	114782	ENsM	191	194	S193-p	-	
RILP	mouse	UP:Q5ND29	41139	EQsL	191	194	S193-p	-	
SEMA4D	human	UP:Q92854	96150	EQsL	786	789	S788-p	-	
SETD2	mouse	GP:NP_001074809	285663	ENsM	1860	1863	S1862-p	-	
SLK	human	UP:Q9H2G2	142695	ENsL	328	331	S330-p	+	+
SMARCA1	human	UP:P28370	122605	EQsL	723	726	S725-p	+	++
SNX29	mouse	UP:Q9D3S3	53184	DQsL	305	308	S307-p	-	
SR-A1	mouse	UP:Q5U4C3	133842	DNsL	300	303	S302-p	-	
STARD3NL	mouse	UP:Q9DCI3	26811	ENtL	9	12	T11-p	-	
STIM1	human	UP:Q13586	77492	EQsL	255	258	S257-p	-	
TCF12 iso1	human	UP:Q99081	72965	ENsL	390	393	S392-p	-	
UGP2	mouse	UP:Q91ZJ5	56979	ENsL	380	383	S382-p	-	
VCIP135	mouse	UP:Q8CDG3	134503	ENsM	1194	1197	S1196-p	-	
VPS13C	human	UP:Q709C8	422390	DQtL	622	625	T624-p	-	
WDR9	mouse	UP:Q921C3	259026	DQsL	1684	1687	S1686-p	-	
ZBP-89	human	UP:Q9UQR1	88976	DNsL	309	312	S311-p	-	

Gene ID	Peptide	Intensity
PLXND1	KDNTLGRV	995.34
NFAT2	ENSMRAV	746.72
SMARCA1	IEQSLYKF	677.02
PICH	EKENSLCGS	622.97
ARID1B	RDNTLVTL	613.96
ASF1A_010	NLQSLLST	627.44
ASF1A_008	PNLQSLLS	654.44
ABCA10_001	HDNSLKFL	596.73
BRDT	RENTNEAS	523
PCNXL2	NYNTRRVD	486
CPEB1	ILDNSLDF	474.94
MCM4	EQSLGQKL	474.86
MKP-5	DENTNEPS	474.4
ASF1A_001	EYTETELR	444.04
MBD4	EENSLVKK	419.25
CSRNP3	PAENSLSL	416.5
ATAD5	EMENSLSD	407.25
GAPDH_002	DNSLKIIS	387.6
HSPH1	TAENSLKK	385.75
ATXN2L_002	LQPSSSPE	377.34
ASF1B_002	PLNCTPIK	373.28
GAPDH_001	YDNSLKII	371.36
OSBP	KCENSLEQ	350.93
CSDE1	PDNSMGFG	317.64
FNBP1	VSDNSLSN	302.25
MAX	SDNSLYTN	296.75
OLFML2A	ADNTLQGT	296.6
FAS	IENSNFRN	290.75
ATXN2L_003	PENSLDPF	281.5
ACVR1	IDNSLDKL	277.33
CYP39A1	DNSMTLLQ	272.86
MAGI3	SADNTLER	268.7
ASF1A_002	TSENSLNV	262.04
SPATA6	FENSMDKM	256.8
NCAPD3	VDNTLSLE	248.2
CPEB2	LNMHSLEN	247.28
ASF1A_009	LLSTDALP	240.75
SLK	TENSLPIP	236.61
CHD4	IEENSLKE	228.47
ChaK1	NNNTSENT	224.8
BDKRB2	QMENSMGA	220.11
ATXN2L_001	QPSSSPEN	0
ATXN2L_004	PENALDPF	0
ABCA10_002	QENSLWPK	0
CLIC4	IDENSMED	0
CNR1	PLDNSMGD	0
BCL7C	NDENSNQA	0
CASP8AP2	EDENSLLV	0
CDC45L	EENTLSVD	0
L1TD1	LDNTNEYN	0
MPHOSPH10	PENSLLEE	0
Nedd4-BP2	LENSNSPV	0
OSTM1	ANIQENSN	0
OXR1	HENSLHQE	0
PRKDC_001	EDNSMNVD	0
PRKDC_002	EDNAMNVD	0
PUS3	EEENTNLE	0
ASF1A_003	TSENALNV	0
ASF1A_004	WEDNTEKL	0
ASF1A_006	DAESSNPN	0
ASF1B_003	PENSMDCI	0

Figure 55: Custom peptides ranked by score using the same color scheme as Figure 55: Known interactors are shown in yellow, additional kinases in purple and chromatin modifiers in blue.

Scanning and analysis of the peptide microarray showed that purified TLK2 modified many peptides with high specificity. Using the most stringent cutoffs, we identified 69 S/T containing peptides that showed no signal in the corresponding alanine control and were thus considered positive. In addition, we found 61 Y containing peptides that were specifically modified by TLK2. 125 S/T and 64 Y containing peptides were unmodified and considered negative. A third class of peptide gave signal in both the S/T/Y and A containing peptides suggesting a non-specific signal. This could be due to an affinity for TLK2 with these residues as the active kinase would be heavily phosphorylated and generate signal if retained on the peptide following the washes.

In order to try and identify a target motif for TLK2, we compared the sequences of S/T containing peptides. As TLK2 is predicted to be a serine-threonine kinase, and no tyrosine phosphorylation has been observed in mass spectrometry experiments to date, we did not extensively analyze the Y containing peptides. As a first approach we aligned all of the phosphorylated S/T peptides and used a motif generating software (http://weblogo.berkeley.edu/logo.cgi) to determine if we could identify enriched residues. We first generated a motif using the -4 to +2 positions of 65 of the positive peptides. 3 peptides were excluded from the analysis due to the irregular spacing of the target site. The resulting motif (Motif-100) suggested a preference for S over T but did not clearly identify enriched adjacent residues (Figure 57A). We next applied an arbitrary cutoff of 300 for the signal intensity to select the 17 highest scoring peptides in the array (top 25%: Motif-25). Motif-25 showed serine as the exclusive target residue and suggested a preference for E in the +1 and +2 positions as well as a preference for K/D/N and L/G/I at the -2 and -1 sites respectively (Figure 57B). E and A were enriched at the -4 and -3 sites respectively, but a motif generated from all of the negative peptides (Motif-neg) showed enrichment of these residues as well, suggesting that they are not likely to be major determinants of specificity (Figure 57D). We next generated a motif from the bottom 75% of the positive peptides (Motif-75) that scored with a similar intensity range (Figure 57C). This motif again showed E enriched at the -4 position and K/G/R at the -3 position. R was also enriched in motif-25 at -3 but enrichment for K at -3 was apparent in motif-neg.

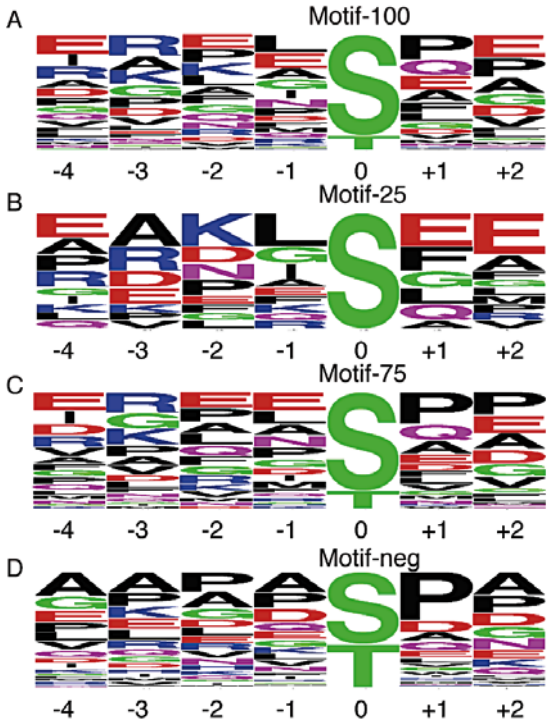

Figure 56: Generation of motifs from peptide array targets. A. Motif from generated from all of the S/T positive peptides (Motif-100). B. Motif generated from the top 25% of the S/T positive peptides (Motif-25). C. Motif generated from the bottom 75% of the positive peptides (Motif-75). D. Motif generated from the S/T negative peptides (Motif-neg).

Notably, D, which shares the acidic character of E, was enriched in the +1 and +2 sites of the negative peptides, suggesting that an aspect other than charge selects for E at the +1/2 sites. P was enriched at the +1 site in both the positive and negative motifs but absent from the top 25%. S/TP is a common target site of both CDK and MAPKs. Q was also enriched to some extent at the +1 site of the positives. These results suggest that TLK2 could be responsible for some phosphorylation events attributed to the CDK, MAPK and PI3K like kinases (PIKKs).

As the sites adjacent to the phosphorylated residue often influence substrate specificity, we examined the frequency of each amino acid in the -4 to +2 position surrounding the S/T residue in the positive peptides. As the library was not unbiased, these are plotted as a heatmap, with the number indicating the percentage of peptides with the indicated residue in that position that were positive (Figure 58). The target site is omitted as it is always S or T. We did not observe a preference for L/M at +1 as used in our predicted motif with F and K being frequently found at the +1 site. There seemed to be little preference for any amino acid at the -1 and -4 sites and the predicted D/E preference at -2 was also not clearly observed. The clearest enrichments were for C and F at the +2 and N and F at the -3 and -2 sites respectively. However, few peptides contained F and C residues so this may reflect a jackpot effect.

	pos -4	pos -3	pos -2	pos -1	pos +1	pos +2
A	18.8	26.7	28.0	24.1	47.4	28.6
C	25.0	50.0	0.0	33.3	0.0	100.0
D	45.5	53.8	25.0	31.8	46.2	33.3
E	48.0	14.3	52.9	50.0	53.3	58.3
F	57.1	33.3	85.7	42.9	85.7	100.0
G	25.0	53.3	33.3	42.9	50.0	33.3
H	50.0	0.0	0.0	50.0	0.0	0.0
I	53.8	28.6	0.0	55.6	0.0	
K	28.6	40.9	54.5	22.2	100.0	0.0
L	23.1	20.0	43.8	63.2	45.5	50.0
M	40.0	20.0	50.0	60.0	50.0	40.0
N	33.3	100.0	36.4	45.5	50.0	7.7
P	31.3	28.6	30.0	22.7	24.6	36.7
Q	33.3	33.3	50.0	23.1	47.4	11.1
R	70.0	59.1	38.5	40.0		50.0
V	35.7	55.6	27.3	12.5	37.5	66.7
W				0.0	20.0	0.0

Figure 57: Frequency of particular residues adjacent to the TLK2 target site. The percentage of positives when the indicated residue was at the indicated site are plotted with colors indicating frequency (blue high, red low). For example, if 10 peptides had a G at the +1 site and 5 were positive, this would score as 50%.

We reasoned that as there was no clear requirement for amino acids adjacent to the target residue, TLK2 may use more complex combination motifs that would be obscured by this type of simple analysis. We next used clustering analysis of the positive motifs to identify more complex subsets within the positive pool (data not shown). This identified subpopulations based on amino acid character but again, no clear preference for TLK2 phosphorylation emerged from this analysis.

In conclusion, despite the confirmation that some known targets were phosphorylated in the array, we were unable to generate a detailed consensus sequence from our data that would allow the de novo prediction of new targets. It is likely that distant sites, 3D configurations or other modifications may dictate the specificity of TLK2 for its targets and this will require more sophisticated affinity purification and mass spectrometry based approaches such as those described in Section 5.1.1.

6. TLK activity as a potential chemotherapeutic target

Chapter Summary

Inhibition of TLK1/2 kinase activity represents an unexplored approach in radio/chemosensitization. The fact that TLK is a kinase, and not a critical repair protein per se, and its activities are not specific for a particular type of DNA damage, suggests it may be applicable to a number of different chemotherapeutic agents. This approach could also take advantage of the fact that somatic mutations in either TLK1 or TLK2 [191,192] occur in human cancers, thus lowering the threshold of activity to target and allowing the sensitization of tumor cells versus normal tissue.

Our aim is to identify compounds that exhibit specificity towards TLK1 or TLK2 deficient cells in normal growth conditions or in the presence of ionizing radiation induced damage. We monitored the growth and survival of mouse embryonic fibroblasts in 96 well plates 24h post mock or IR treatment using Resazurine (Alamar Blue). This experiment would identify both potential TLK2 inhibitors, as we expect from our siRNA studies that this will severely impair cell growth after IR, and synthetic lethalities with TLK1/2 loss.

6.1. Expression of TLKs in cancer.

As TLK1/2 could affect a wide variety of cellular processes through Asf1 regulation, it is not surprising that the expression and copy number of these kinases is frequently altered in human cancers (Figure 58, from the MSKCC cBIO portal). Data from human patient samples showed that TLK2, but not TLK1 expression levels, were significantly reduced in a large cohort of colon cancer patients (Figure 59). This reduction was even more dramatic in samples from metastatic lesions. These results indicated that loss of TLK2 may provide some specific advantages for colon cancer growth and metastasis. In contrast, we found that copy numbers and mRNA expression of either TLK1 or TLK2 are increased in nearly 30% of patients (266 of 950, TGCA) with invasive breast carcinomas (Figure 59, from the MSKCC cBIO portal).

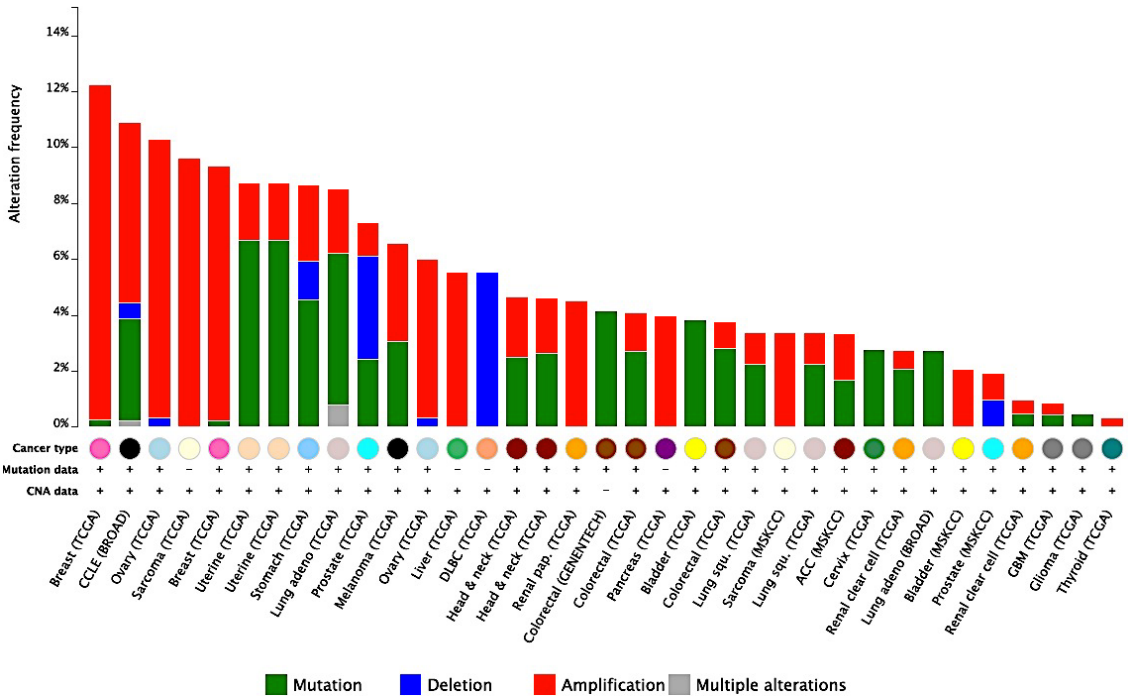

Figure 58. Cancer alteration summary for TLK1-TLK2. The histogram shows the alteration frequency detected for TLK1 and TLK2 genes in several cancer studies.

Interestingly, the majority of copy number increases in TLK1 or TLK2 are mutually exclusive, which suggested that in some breast lesions, increased TLK general activity and this may provide an advantage to tumour cells.

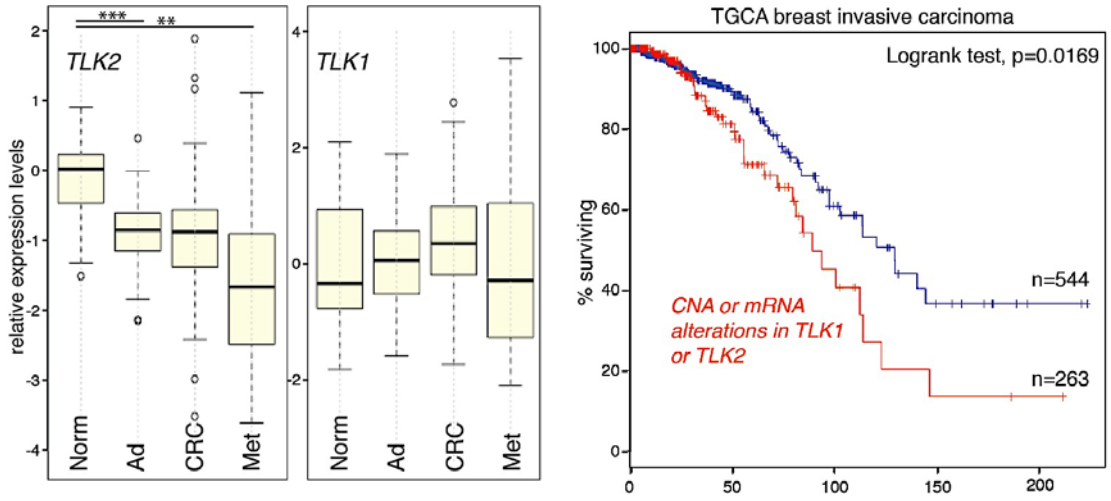

Figure 59. Left: Relative expression levels of TLK1-TLK2 expression in human colorectal cancer. Normal colon (Norm), adenomas (Ad), colorectal cancer (CRC) and liver metastasis (met). Data sets represent over 500 patients. ***p<0,001, **p<0,01. Right: TLK1-TLK2 copy number alterations and expression significantly correlate with survival in invasive breast carcinoma.

Even more, alterations of TLK1/2 predicts reduced survival in a large cohort of patients with invasive breast cancer (Figure 59, right panel). These data are statistically significant but a conclusive role for TLKs in cancer predisposition or progression is still not clear. However, they suggest that TLK activity may influence different cancer types in a distinct manner, as TLK2 reduction correlates with colon cancer progression and TLK1 or TLK2 copy number or expression increases are observed in a high percentage of invasive breast cancers.

6.2. TLK activity as a chemotherapeutic target: screen for potential TLK inhibitors.

TLK1 has been suggested to be an attractive therapeutic target and a splice variant, TLK1B, that confers radioresistance in some human cancer cell lines, is being tested as a therapeutic intervention via gene delivery methods [193,194]. Our previous results suggested that TLK activity promotes genomic stability and is therefore important to prevent genomic alterations that could promote tumorigenesis in some cancer types. On the other hand, increased TLK activity may support the rapid growth of aggressive lesions by facilitating histone exchange during DNA replication or transcription. Given that we see an acute response to DNA damage under conditions where total TLK activity is reduced and it is unlikely that cells lacking all TLK activity can support proliferation, we believe that the modulation of TLK activity represents a potentially valuable therapeutic approach

To identify compounds that affect TLK activity, we screened a kinase inhibitor library for the sensitization of TLK1 or TLK2 deficient cells. In these experiments we aimed to identify compounds that exhibit specificity towards TLK deficient cells that could be potential TLK inhibitors, or cause synthetic lethality withTLK1 loss.

We analyzed 84 chemical inhibitors that target at least 36 different cell signaling pathways. Based on siRNA experiments, we anticipated that we would see bigger changes in cell survival under cytotoxic conditions, as TLK1 null cells with TLK2 downregulation responded more strongly to IR, UV and etoposide than untreated or those treated with siRNA against TLK2 (chapter 0). Thus, we decided to compare untreated cells with cells treated with 5Gy of IR. Therefore, we performed the screening in both WT and *Tlk1*$^{Trap/Trap}$ cell lines measuring cell viability with resazurin with no radiation or after 5Gy IR treatment. We performed the screening twice, plating 10000 cells per well, and after calculating the fold changes of cell viability relative to the WT cells.

Surprisingly, we didn't detect differences in the screen with or without IR treatment. In addition, *Tlk1*$^{Trap/Trap}$ cells showed the same rates of survival as the WT cells in the presence of inhibitors, and only iKK and Wee1 inhibitors could decrease around 20% the survival rate of *Tlk1*$^{Trap/Trap}$ cells compared to WT. Based on these data, although further characterization of these observation needs to be done, iKK and Wee1 kinase inhibitors could be considered as putative synthetic lethal compounds in TLK1 deficient cells.

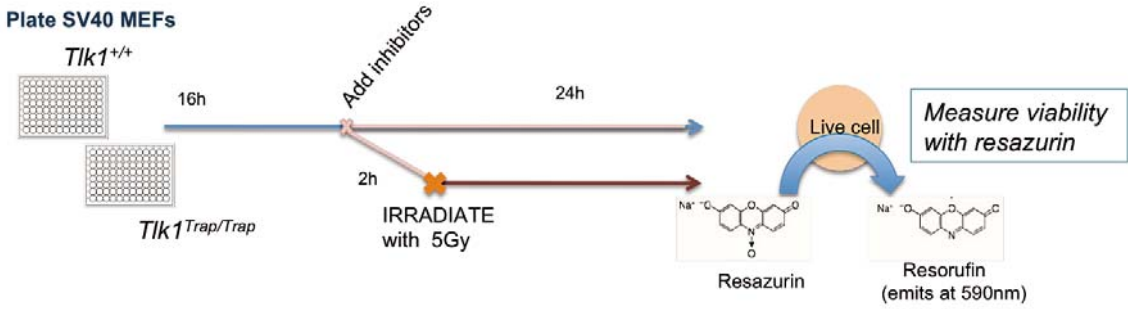

Figure 60: Library inhibitor experimental procedure: The indicated transformed MEFs were treated for 24 hours with a library of inhibitors. The experiment was performed with or without ionizing radiation as source of DNA damage. Resazurin was used to determine the remaining viable cells

We repeated this approach using *Tlk2*$^{Trap/Trap}$ immortalized MEFs. Again, we did not detect differences in the screen with or without IR. But in this experiment, we identified four kinase inhibitors that exhibited specificity towards TLK2 deficient cells, reducing their viability by more than 80%: Cdk2 inhibitor II, PI3-ky/CKII inhibitor , H-8 dihidrochloride, and KT5720. The last two can both specifically inhibit cAMP-dependent kinases (PKA). The experiment was done once in duplicates, and the data should be considered as preliminary results that can be used for further validation of the possible synthetic lethality.

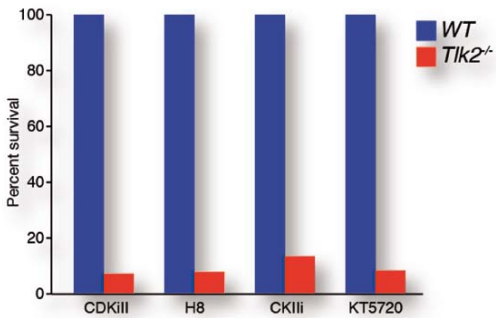

Figure 61: TLK2 synthetic lethalities. *Tlk2*$^{Trap/Trap}$ immortalized MEFs were treated for 24 hours with a library of inhibitors. Cell viability was measured by Resazurin.

6.3. Loss of TLK activity influences tumor progression.

To explore the importance of TLK activity in tumor development and progression, we perform a pilot experiment which could guide us in future approaches. In this proof of principle experiment, we injected 1×10^6 WT or *Tlk1*$^{Trap/Trap}$ SV40 transformed MEFs into the abdominal mammary gland of eight-week-old female NOD/SCID mice. Two females injected in both abdominal mammary glands were used per genotype. The experimental procedure is illustrated in Figure 62A. We followed tumor growth until the size was 20mm, in which case the mice were sacrificed. Unexpectedly, tumor growth was clearly faster when we injected *Tlk1*$^{Trap/Trap}$ SV40 transformed MEFs than with WT (Figure 62B). This data could be controversial, as almost all mutations in breast cancer patients are duplications of TLK1/2 genes. However, different types of cancer respond in a distinct manner to altered TLK activity and there is strong evidence that colorectal, urinary and prostate cancer normally harbor decreased levels of TLKs.

We then analyzed whether the depletion of *Tlk2* in *Tlk1*$^{Trap/Trap}$ MEFs at the time of injection could be relevant for the initiation and growth of the tumor. We knocked down transiently *Tlk2* expression using siRNA that we previously validated (Figure 62C). In this case tumors started to grow before controls, but the ongoing growth rate was similar. However, as expected, at final point the levels of *Tlk2* were recovered to normality, as our siRNA give a transient downregulation. These data suggested that in the context of transformed MEFs, reduced *Tlk* levels were beneficial to tumor growth and initiation. However, this needs to be further validates in multiple cell lines.

As transformed MEFs are not a reliable model for breast cancer, we have interbred mice expressing the middle T-antigen of polyoma virus under the control of the MMTV promoter (MMTV PyMT mice) with mice lacking *Tlk1.* Mice expressing PyMT spontaneously develop breast tumors [195]. We then isolated and cultured tumors from wild type mice and those lacking *Tlk1,* which can then be reinjected in nude mice to follow cancer development. Here we can assess the effects of *Tlk1* depletion in untreated tumor growth or in the context of a chemotherapeutic agent.

Thus, when depleting also *Tlk2* activity in *Tlk1* null cells, the ability to settle and start developing a tumor is increased. Taken all together, this data suggests that TLK activity may have a positive role in fibroblast driven tumor growth. Though, this data is

not conclusive and more experiments need to be done in order to have a strong support for this hypothesis.

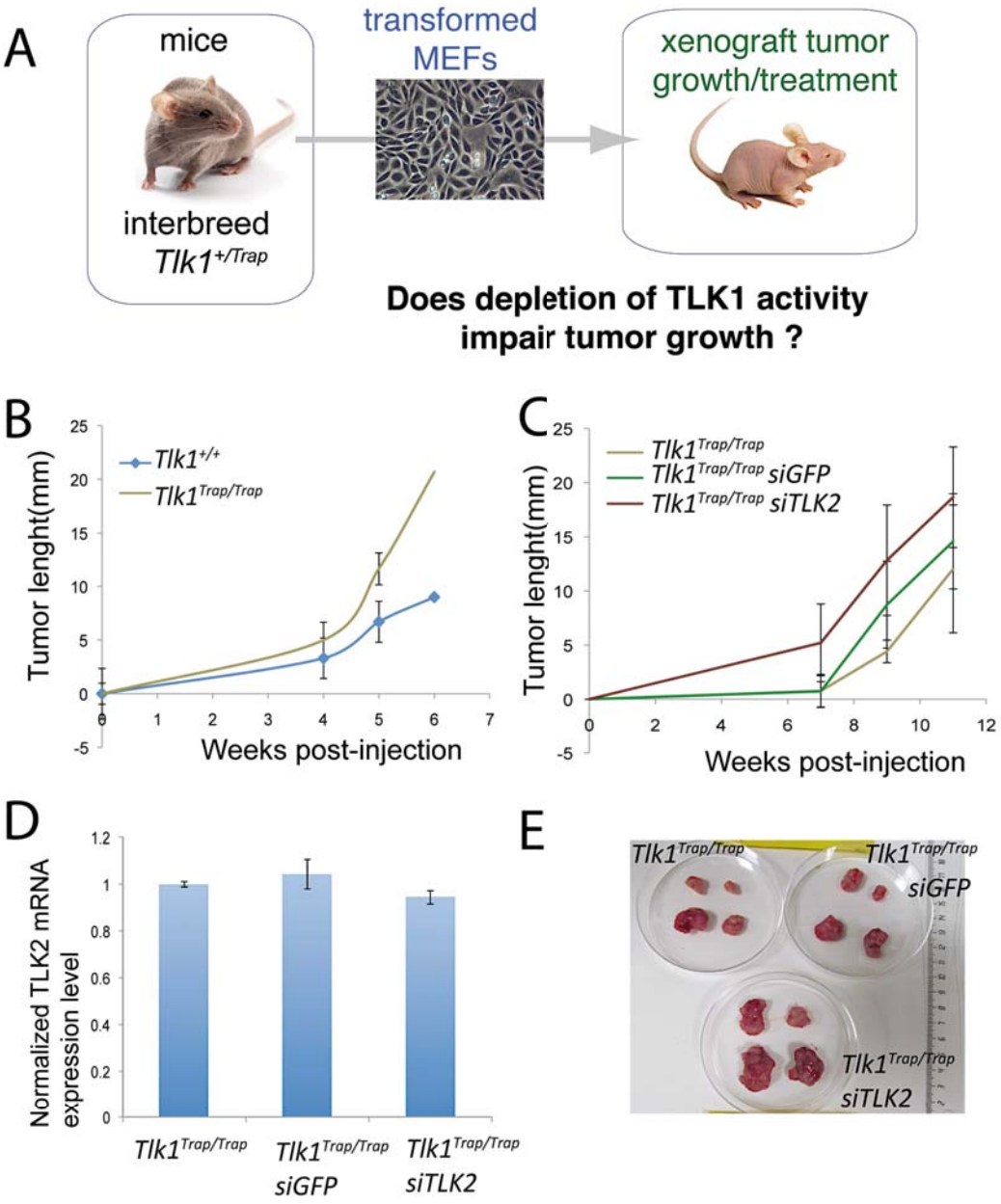

Figure 62: Role of TLK in tumor progression. A) Graphical summary of the experimental approach. B. TLK1 depletion boosts tumor growth. C. TLK2 downregulation enhances tumor ability to settle and grow. For B) And C) SV40 transformed MEFs were inoculated in the mammary glands of nude mice. Tumor growth was measured every week until reach 20mm length. D) Expression levels of TLK2 at the final point of tumor growth inoculating siRNA treated cells. As expected, TLK2 recover basal levels after transient siRNA downregulation.. E) Tumors extracted from mammary glands of nude mice. The genotype of the tumoral cells is indicated. Two mice were injected per genotype in two mammary glands. The four formed tumors are shown.

Our next step is to infect these PyMT breast cancer cells with retroviruses expressing shRNAs against *Tlk2* (section 2). Upon successful validation of *Tlk2* knockdown, we will inject these lines into mice and monitor tumor development. Here we can assess the effects of *Tlk2* downregulation in untreated tumor growth or in the context of a chemotherapeutic agent such as etoposide. This will directly test whether *Tlk1/2* inhibition alone, or in combination with chemotherapy can effectively impair tumor proliferation and provide rationale for pursuing inhibitor development.

Discussion

It has become clear that a major function of the DNA damage response is to promote chromatin assembly and disassembly in order to facilitate the regulation of transcription, signaling and repair. For example, the activation and signaling of the central transducer of the DDR to DSBs, ATM, plays a central role in the relaxation of heterochromatic regions as well as the maintenance of transcriptional silencing[68]. The perturbation of these processes leads to DNA damage sensitivity, cell cycle checkpoint defects, chromosomal instability and predisposes to developmental disorders and cancer[196].

The process of checkpoint resolution following DNA repair is poorly understood. In yeast, a central component of cell cycle resumption following G2 arrest is the reestablishment of nucleosomes on repaired regions that have been rendered nucleosome free due to resection and repair processes. The histone chaperone Asf1 is required for cell cycle resumption as it promotes the incorporation of acetylated H3 and H4 in newly repaired regions. The dynamic interaction of Asf1 with Rad53, the canonical checkpoint kinase in yeast, is disrupted after DNA damage[80]. This process has been suggested to control histone pools during DNA repair to prevent the potential toxic effects of non-deposited histones during fluctuations in replication rates[117,197].

In mammals, it has been shown that Chk1 does not interact directly with Asf1 but targets the Asf1 interacting Tousled like kinase 1 (TLK1) for inactivation [97,98]. In addition, the related kinase, TLK2 interacts and oligomerizes with both TLK1 and Asf1, indicating that it also may play a role in chromatin regulation in response to damage. Collectively, this regulation of TLKs by damage-induced kinases suggests a mechanism that could coordinate repair with the deposition of chromatin and facilitate checkpoint resolution. Thus, a more complex regulatory system exists in mammals than in yeast that may ensure that Asf1 is regulated precisely in response to DNA damage to prevent precocious histone deposition at repair sites.

A surprising aspect of our work was the observation that *Tlk1* appears to be dispensable for mammalian development and DNA damage responses. These data are contradictory with previous published work in which siRNA depletion of TLK1 in MCF-7 cell lines led to mitotic abnormalities and a failure in chromosomal segregation[174] as well as work that suggests TLK1 is important for repair and radiosensitivity by regulating DNA repair factors such as Rad9[97,159].

A plausible explanation is that the siRNAs used in previous studies provoked off-target effects that led to the observed phenotypes, possibly targeting TLK2. However, despite the high similarity in the amino-acid sequence, TLK1 and TLK2 share very little similarity at the DNA sequence level making this possibility unlikely. A more plausible scenario is that the genetic background of MCF-7 and other cell types used select for alterations that lead to a higher dependence on TLK1 dependent pathways, leading to phenotypes that are not representative of primary cells. According to available clinical data, high percentages of breast cancers (~30%) harbor amplifications of TLK1 or TLK2, indicating a higher reliance on TLK activity.

Depletion of the single TLK in lower organisms leads to severe phenotypes. In mammalian cells, the absence of a strong phenotype when depleting Tlk1 suggested redundancy. Thus, we explored biological redundancy between *Tlk1* and *Tlk2* by examining the outcome under genotoxic stress after depleting both simultaneously. Using *Tlk1*$^{Trap/Trap}$ MEFs, we downregulated *Tlk2* by siRNA, obtaining a reduction of total TLK activity. In this scenario, cells exhibited an increased sensitivity to damaging agents such as UV, IR and Etoposide. The fact that both IR and UV lesions affect cell sensitivity when TLK activity is diminished confirms that TLKs are playing a role in the DDR. Asf1 is recruited to UV and IR-damaged DNA both *in vitro* and *in vivo*. In line with these observations, it is clear that histones H3 and H4 are incorporated following the repair of UV and IR lesions [94,198,199]. The increased sensitivity when depleting TLK activity could be due to Asf1 deregulation, which can impair histone shuttling to newly repaired chromosomal regions.

The most dramatic effect observed on DNA damage sensitivity was in cells treated with Etoposide, an inhibitor of topoisomerase II. Interestingly, no sensitivity was found following treatment with CPT, an inhibitor of topo I. DNA topoisomerases are enzymes used for resolving the unique problems of DNA entanglement that occur during unwinding and rewinding the DNA helix in replication, transcription, recombination, repair, and also chromatin remodeling. These enzymes perform topological transformations by providing a transient DNA break, formed by a covalent adduct with the enzyme, through which strand passage can occur. Topo I acts by solving DNA supercoils preferentially in G1 during origin firing and transcription, and ahead the replication fork in S-phase by making SSBs. TopoII plays a role behind the replication fork and in G2 introducing DSB into the DNA (**Figure 63**). As cells with reduced TLK activity showed an increased sensitivity to Topo II but not Topo I inhibitors, we speculate that in the absence of TLKs, cells rely on the action of Topo II in a greater manner. A plausible explanation is that the absence of correct nucleosome

redistribution in the naked DNA provokes topological problems that need to be solved by Topo II.

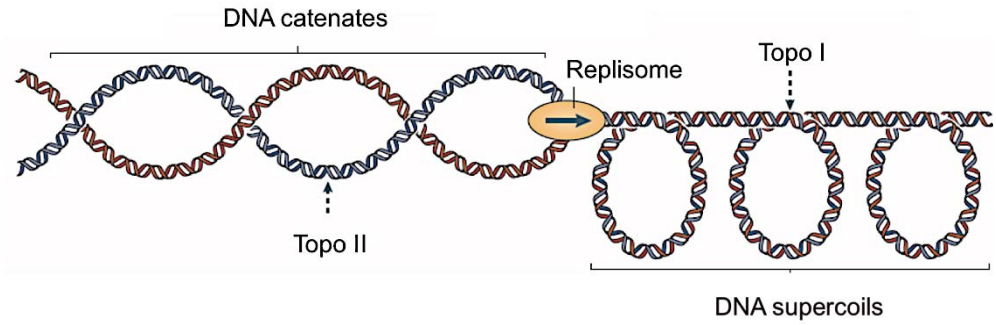

Figure 63: Topoisomerase functions during DNA replication. Topological problems that arise during DNA replication. The names of the topoisomerases that resolve these superstructures are listed. Topoisomerase action is indicated by a dashed arrow. As a replisome progresses, positive supercoils form ahead of the fork, and newly replicated form behind it. If unresolved, precatenanes can give rise to tangled or catenated DNAs that lead to abnormal DNA segregation on entry into cell division. Unresolved positive supercoils can impede fork progression and terminate DNA replication prematurely.

Many drugs targeting Topo II have been in clinical use for years, including Etoposide and its variants. In most cases, the use of Topo II inhibitors has been combined with additional drugs targeting repair pathways. Especially relevant has been the combination of Topo II and DNA-PKs inhibitors[200]. However the accurate mechanism by which inhibition of these two molecules provokes a cooperative effect is still not clear. In accordance, inhibition of TLK2 could represent a chemotherapeutic target in combination with Topo II inhibitors. Further experiments *in vivo* for validation of this hypothesis have already started in our lab (further discussed).

Our results have revealed for the first time that *Tlk1* is not an essential gene in mammals and that *Tlk2* is sufficient to provide the levels of activity required for DNA replication and repair in cultured fibroblasts. These data also suggested that different thresholds of TLK activity are required for normal cell division and sensitivity to DNA damage as untreated, but not UV, IR or etoposide treated cells, could tolerate transient depletion of *Tlk2* without a profound reduction in viability.

We next generated mice with constitutively impaired expression of TLK2. When comparing the amino-acid sequence, TLK2 showed higher similarity to the single TLKs in lower organisms than TLK1. Similar to the requirement for TLK in lower organisms, TLK2 is essential for viability in mammals. We found that *Tlk2*$^{Trap/Trap}$ animals were embryonically lethal. Indeed, in contrast to homozygosity of the *Tlk1* genetrap, no live-

born homozygous *Tlk2* mutants have been observed. To elucidate the cause of the premature death, we analyzed several embryonic developmental stages. Some *Tlk2*$^{Trap/Trap}$ embryos isolated at e10.5 were severely runted, displaying heterogeneous defects including failure to close the neural tube and hemmoraging. These patterns were not observed at later stages, suggesting that some embryos may be reabsorbed. However, at e14.5 we can still detect live *Tlk2*$^{Trap/Trap}$ embryos with a frequency of about 30% of expected. At e15.5 all the *Tlk2*$^{Trap/Trap}$ embryos were dead, indicating that they begin to die around e15. Future experiments that are started in our lab will analyze a higher number of e10.5 embryos to measure frequencies of each genotype and relate them with the observed Mendelian ratios at e14.5.

At e14.5, *Tlk2*$^{Trap/Trap}$ embryos displayed the same phenotypes, characterized by smaller size and pale coloration, due to problems in placental development. The blood vessel space in the labyrinth is severely reduced in *Tlk2*$^{Trap/Trap}$ embryos, being much more dramatic at e16.5, when the embryo was already dead. The trophoblast layer showed evident hyperproliferation at e10.5 and infiltration into the labyrinth by 14.5, with clusters of densely packed trophoblast cells at the expenses of fetal blood spaces. This abnormal phenotype was observed in all the placentas analyzed at e14.5 (n=3), and it is shared with embryos lacking essential cell cycle genes such as Rb[180] and cyclins E1 and E2[181]. Furthermore, BrdU staining at e16.5 provides evidence of an increase in DNA synthesis in the labyrinth layer, consistent with hyperproliferation and infiltration of the trophoblast cells.

The hyperproliferation of trophoblast cells and the decrease in the blood spaces in the labyrinth indicates restricted nutrients and oxygen exchange between the mother and the fetus, which is consistent with the lack of blood irrigation seen in the embryo and likely to be the cause of the premature death. It is tempting to speculate that Tlk2 could be affecting endoreplication that is undergone by cells in the trophoblast. This also would explain the hyperproliferation in this layer, as cells would undergo mitosis instead of repetitive S-phase cycles used to become polyploid cells. More over, during endoreplication, there is an overactivation of cyclins involved in the progression through S-phase, such as cyclin E1 and E2 and, importantly, depletion of these cyclins also leads to endoreplication failure in TGCs. It has been published that overexpression of TLK or Asf1 in flies disrupts salivary-gland chromosomal architecture and inhibits endoreplication, reinforcing the idea that TLKs could be required for this process. To analyze the potential role of TLK2 in endoreplication, we will derive Trophoblast Stem Cells (TSCs) from *Tlk2*$^{Trap/Trap}$ blastocysts[201]. The trophoblasts committed to the TGC lineage adhere to the plate more tightly than the other cells and

can be enriched by light trypsinization[202]. The analysis of DNA content can be performed by flow cytometry, visualizing how many time the cells require to duplicate their DNA content. This approach has been followed in several TGC endoreplication studies[181,201,202].

Despite the embryonic lethality, we could collect *Tlk2*$^{Trap/Trap}$ MEFs from embryos at e14.5 and analyze primary cells in the absence of *Tlk2*. These cells showed increased chromosomal instability, characterized by a higher percentage of chromatid breaks. Chromatid breaks are indicative of lesions that occur in the S or G2 phases of the cell cycle and can indicate fragile site expression. The expression of common fragile sites (CFS), regions linked to genomic instability, is correlated with a higher probability of cancer incidence [99,203]. CFSs are characterized as “hot spots” where double strand breaks, translocations and sister chromatid exchanges occur more frequently than in any other part of the genome [35,204]. Fragile site expression can be enhanced using low doses of polymerase inhibitor, aphidicolin. Indeed, after low dose aphidicolin treatment, the percentage of aberrations in *Tlk2*$^{Trap/Trap}$ cells increased compared to WT, with chromatid breaks and rearrangements being the most common aberrations identified in both cases. These observations indicated that most chromosomal abnormalities in Tlk2 depleted cells are likely to be replication dependent. These results lead us to speculate that Tlk2 might be required for the stability of CFS.

Interestingly, loss of Asf1, the main target of TLK activity, also provoked increased genomic instability. Cells lacking Asf1 showed higher rates of sister chromatid exchange (SCE), affecting chromosomal stability[161]. In this regard, loss of TLK2, an Asf1 upstream regulator, could mimic the effects of Asf1 loss, increasing genomic instability due to defects in chromatin distribution that would normally suppress hyperrecombination and fragile site breakage.

Defects in chromatin structure, as well as changes in the levels particular histone marks and histone chaperones have all been correlated with ageing. In this regard, several lines of evidence indicate that loss of TLK2 promotes premature cellular senescence, as primary MEFs derived from *Tlk2*$^{Trap/Trap}$ embryos exhibited a markedly slower growth, were enriched in SAβ-galactosidase activity and showed a flat morphology, all of which are typical of senescent cells. At the same passages WT control cells are were still growing exponentially with little SAβ-galactosidase activity. In addition, at between 6 and 8 passages, the levels of γH2AX increased compared to WT cells, consistent with the observed premature senescence. However, according to our previous results, when the embryos are harvested for MEFs production, at e14.5, they already displayed signs of reduced circulation due to placental defects, and they

are easily distinguishable by their characteristic paleness. Lack of oxygen in the embryo could promote a stress response that may predispose to premature senescence when these MEFs are cultured *in vitro*.

To address the question of whether loss of *Tlk2* promoted ageing related phenotypes or its only a result of impaired oxygen exchange in the placenta, we will bypass this defect with the ERT2-Cre transgene to induce *Tlk2* deletion in 2 month old WT and *Tlk1* deficient animals. In these mice, Cre recombinase is under the regulation of an estrogen inducible promoter and is expressed following tamoxifen administration. A cohort of each genotype will be monitored following tamoxifen administration for health and signs of ageing (ex. greying hair, alopecia, reduced mobility, tumorigenesis and reduced lifespan). At one year, mice will be sacrificed to analyze parameters associated with premature ageing (ex. bone marrow hematopoietic stem cell pool (LSK cells), thymic involution, dermal thickness, skeletal abnormalities (kyphosis by X-ray), bone density (CT scan) and spermatogenesis). These experiments will directly test if impaired Tlk2 activity may drive premature ageing as would be predicted from some cellular data.

As we could not detect any defect in the development of mice with a *Tlk1* null background, our siRNA experiments shed light to the redundant roles of *Tlk1* and *Tlk2* in the DDR. These results prompted us to think that reduced *Tlk2* levels on a $Tlk1^{Trap/Trap}$ background could have consequences in development and/or tissue homeostasis. To address this, we generated an allelic series to give rise to a gradient of Tlk1/2 activity. So far, we can state that total depletion of *Tlk1* is not relevant for mouse development, unless *Tlk2* is haploinsufficient, as in the genotype $Tlk1^{Trap/Trap}Tlk2^{+/Trap}$. These mice displayed several developmental and motor problems and the newborn mice were smaller, weaker and paler than their littermates until their premature death, usually before 1 month of age. An open issue is to determine whether these represent cellular responses triggered by the loss of TLK activity or that this is due to less severe placental defects that in full knockouts of *Tlk2*. We hypothesize that reducing *Tlk1/2* activity below a certain threshold will cause widespread defects in DNA replication and repair, transcription and cell division but have to consider that these phenotypes would also be consistent with impaired placental function.

Lower organisms lacking TLK activity show lethality because of mitotic catastrophe. In flies, Tlk is essential for nuclear divisions in early embryos and lack of Tlk leads to underreplicated DNA and problems in chromosomal architecture that lead to the inhibition of the nuclear cleavage and increased apoptosis[141]. In worms, depletion of

TLK activity resulted in an altered nuclear morphology and chromosome-segregation defects[142]. However, neither in whole *Tlk2*$^{Trap/Trap}$ embryos nor in primary cells, we could detect any of these effects. As long as in these organisms there is only one TLK, total depletion of TLK activity in mammalian cells is required to observe mitotic disruption. Indeed, unpublished data from our collaborators in the Groth laboratory using siRNA showed that a greater downregulation of TLK1/2 activity gives a stronger cell-cycle arrest, so that the effect is correlated with TLK levels. In this sense, the use of MEFs from our allelic series as a system to analyze the minimal level of TLK that can recapitulate the effects in lower organisms could be useful. Our next aim is to analyze cell cycle progression in the presence and absence of DNA damage and determine if cells undergo premature senescence, as they do when *Tlk2* is lost, exhibit karyotypic aberrations or problems in chromosomal dynamics during mitosis. As Asf1 also regulates transcription, we will perform transcriptomal profiling of isolated total RNA to see changes in gene expression levels, splicing and the inappropriate transcription of silenced regions such as telomeres, transposons or heterochromatin.

Up until now, a major limitation in the interpretation of phenotypic data from mice with reduced TLK activity is the lack of knowledge regarding the substrates of TLK1 or TLK2. Both have been reported to interact with each other and the only clearly reliable substrates of their activity are Asf1a and Asf1b[148]. Even more, in flies, overexpression of a kinase dead TLK leads to chromosomal aggregation problems but can be rescued by overexpression of Asf1. Thus, Asf1 appears to be a main target of TLK[141]. In our experiments overexpressing TLK1/2-KDs we observed a deficient mitotic entry after DNA damage, which could be explained by defects in Asf1 that lead to inefficient chromatin restoration after DNA repair. In this regard, unpublished work in the Groth Laboratory, revealed that TLKs binding to Asf1 required an intact histone-binding pocket and TLKs can compete with histones for Asf1 binding in a mutually exclusive interaction[205]. TLK-KDs form a stable complex with Asf1[148], recruiting this histone chaperone leading to a inefficient histone supply.

However, despite Asf1 appearing to be the main target of TLKs, there is evidence that TLK activity can also depend on other modulators and substrates. For instance, in *C. elegans* TLK activity during chromosomal condensation depends on Aurora kinase control, suggesting additional pathways of TLK regulation. To fully understand the cellular effects of TLK depletion in mammalian cells, we have tried to identify interacting proteins that could be substrates or regulators of TLK1/2 by quantitative LC-MS/MS. Validating our approach, we found that Asf1a and Asf1b were the top hits, present in every experiment performed to date. In addition, we identified and validated

the known kinase regulator LC8 in all experiments[189]. LC8 is a small (8 KDa) and unrelated chromatin protein that interacts with multiple partners, modulating protein complex formation. LC8 act as dimers and its dimerization is disrupted by phosphorylation, which releases LC8 from its partners and destabilizes the protein complex. Several consensus domains have been described for LC8 binding and we have located the previously described motif ([KR]XTQT) next to a coiled-coil domain in TLK2 which may suggest that LC8 is not a TLK2 substrate but a TLK complex-regulator. It is tempting to speculate that the phosphorylation of LC8 could play a role in TLK oligomerization. Many other proteins need LC8 to form active complexes, some of them involved in mitosis and damage recovery such as Astrin and SKAP[206]. Even more, LC8 has been shown to interact with kinetochores during mitosis, modulating the location of their interacting proteins.

In addition, from the MS experiments we generated a shortlist of interesting hits currently being validated, including MOB2 and PP1C that are potential positive and negative regulators of TLK activity respectively. Members of MOB family have been shown to regulate mitosis, cell proliferation, apoptosis and centrosome biology through the regulation of the activity of effector kinases. Even more, MOB is a key member in the Hippo pathway, defined as a tumor suppressor cascade and frequently deregulated in cancer cells. PP1C, is a subunit of Protein Phosphatase 1 (PP1) that is crucial for mitotic exit as it allows the orderly dephosphorylation of mitotic phospho-proteins. Importantly, in 10 independent purifications we have not identified the previously implicated repair protein Rad9[207], or any other proteins that play a direct role in DNA repair or checkpoint regulation, supporting the idea that TLK activity exerts its functions primarily through chromatin regulation.

Given the critical role of TLKs in replication and DNA damage responses, it is likely that these kinases are playing a role in cancer progression. The most striking result when analyzing TLKs status in human cancer is the differences in expression in not related cancers. While breast cancers frequently have an increased copy number of *TLK1* or *TLK2*, being both mutually exclusive, many colon cancers show a decrease in *TLK2* expression, which suggest that TLK activity may influence different cancer types in a distinct manner. According to our previous results using cultured primary MEFs, we proposed that TLK activity promotes genomic stability and is therefore important to prevent genomic alterations that could promote tumorigenesis in some cancer types. On the other hand, increased TLK activity may support the rapid growth of aggressive lesions by facilitating histone exchange during DNA replication.

Our pilot experiment, injecting transformed MEFs in the mammary glands, suggested

that lack of *Tlk1* enhanced tumor aggressiveness. In addition, when also depleting TLK2 activity in *Tlk1* null cells prior to injection, tumor initiation was reduced but not progression rate once tumors were formed. Taken together, this data suggests that lack of TLK activity may have a positive role in fibroblast driven tumor growth. However, we could not detect an increase in genome instability using primary *Tlk1*$^{Trap/Trap}$ MEFs. On the other hand, MEF immortalization using SV40 T antigen involves p53 inhibition. We can speculate that in a p53 null background, the absence of *Tlk1* could drive genomic instability that could stimulate tumor progression. In this regard, if these results are further corroborated, it will be essential to study the interactions between p53 and TLK1 pathways.

As the injection of transformed MEFs injection in the mammary gland is not the best cancer model for future studies we have begun developing additional systems. We crossed mice expressing an MMTV driven polyoma middle-T antigen transgene (MMTV-Pymt) onto our WT and *Tlk1* deficient backgrounds. MMTV-Pymt mice will rapidly develop mammary carcinomas that can be cultured, manipulated and spontaneously transformed for subsequent allografting in recipient mice. To complement this, we have generated switchable shRNA retrovirus vectors to target *Tlk2* under a doxycycline inducible promoter. Tumor cells from WT or *Tlk1* mutant animals will be transduced with retroviruses and injected in the mammary gland of nude animals for tumor formation. A cohort of these mice will be treated with dox via food supplements to induce *Tlk2* shRNA and this system will be used to address the role of TLKs in tumorigenesis.

Our previous results using siRNA against *Tlk2* in a *Tlk1* null background and the observed mouse phenotypes, suggest two thresholds for TLK activity. While partial inhibition of TLK activity seemed to enhance genome instability and increase fibroblast-tumor growth, a lower threshold of TLK activity impaired development and sensitized cells to damaging agents. Given that we see an acute response to DNA damage under conditions where total TLK activity is reduced, and it is unlikely that cells lacking all TLK activity can support proliferation, we believe that the modulation of TLK activity represents a potentially valuable therapeutic approach. Taking into account that there are somatic mutations in either TLK1 or TLK2 in human cancers (colorectal, prostate, bladder and uterine) lowering the threshold of activity with a TLK inhibitor, will allow the sensitization of tumor cells versus normal tissue. In fact, TLK1 has already been suggested to be an attractive therapeutic target and a splice variant, TLK1B, that confers radioresistance in some human cancer cell lines, is being tested as a therapeutic intervention via gene delivery methods[193,194]. To identify potential TLK

inhibitors, we are currently testing several panels of kinase inhibitors that could exhibit specificity towards *Tlk1* or *Tlk2* deficient cells in normal growth conditions or in the presence of IR induced damage. With this experiment we will identified both, potential TLK1/2 inhibitors and synthetic lethalities with TLK1/2 loss. Until now, we did not identify any compound that showed inhibition of cell growth in the absence of TLK1, with or without IR treatment. However four kinase inhibitors exhibited specificity towards *Tlk2* deficient cells, reducing their viability by more than 80%: Cdk2 inhibitor II, PI3-ky/CKII inhibitor, H-8 dihidrochloride, and KT5720. The last two can both specifically inhibit cAMP-dependent kinases (PKA). These inhibitors are unlikely *Tlk1* inhibitors, as the decrease in cell growth is shown without damaging treatments, and results after IR are comparable. More probably, they lead to synthetic lethalities. These inhibitors could potentially be used in cancer therapy with cancer patients that expressed lower *Tlk2* levels.

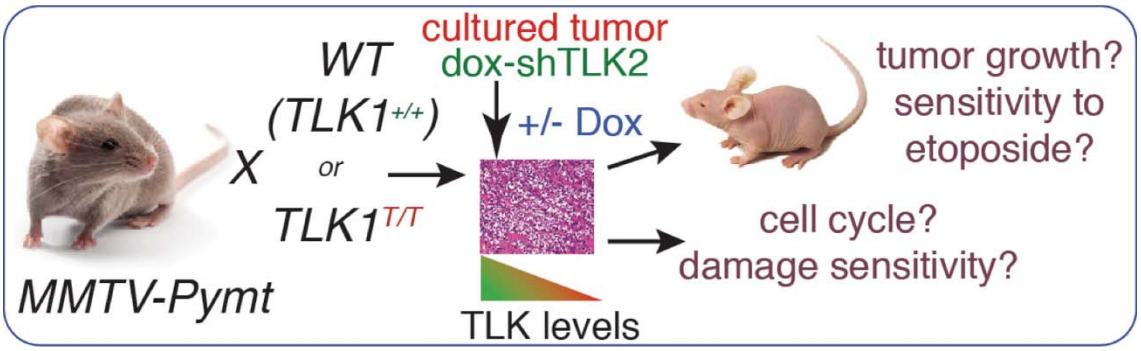

Figure 64: Conditional depletion of Tlk2 by Dox administration in WT or Tlk1 deficient mammary tumor cells in culture or in allografts. Tumor-bearing animals will be treated with vehicle or etoposide. Cultured cells will be analysed for proliferation and responses to DNA damage.

The main focus of this dissertation was the functional characterization of the mammalian TLKs. When the project was initiated, no reports were published regarding the *in vivo* function of this protein in mammalian organisms, only the *in vitro* analysis using tumor cell lines that could be reflect abnormal TLK regulation. The data collected to date firmly establishes a role for TLKs in tissue homeostasis, mammalian development and the DDR. TLK1 and TLK2 form complexes and play redundant roles in DDR but not in mammalian development. In this sense, *Tlk2* is an essential gene during embryonic development, due to placental formation, while *Tlk1* is not. In the same line, lack of *Tlk2* in primary MEFs leads to premature senescence and increased genomic instability, effects that are not observed when depleting *Tlk1* activity.

However, *Tlk1* becomes an essential gene when Tlk2 activity is reduced. This statement is corroborated by the phenotype of our mice and the increased sensitivity to damaging agents observed in our siRNA experiments. Overall, there exist two thresholds of activity for mammalian TLKs and a higher threshold is required to support cellular viability in situations where DNA is damaged. This fact could be highly relevant to cancer treatment and chemotherapy. Indeed, one of the main future goals of this project will be deciphering the ability of TLK inhibition to prevent tumor growth or augment chemotherapy. Collectively, the work I have presented represents a significant advance in our understanding of TLK function in cells and in mammalian development and supports the possibility that TLKs represent a potentially valuable target for the treatment of human disease.

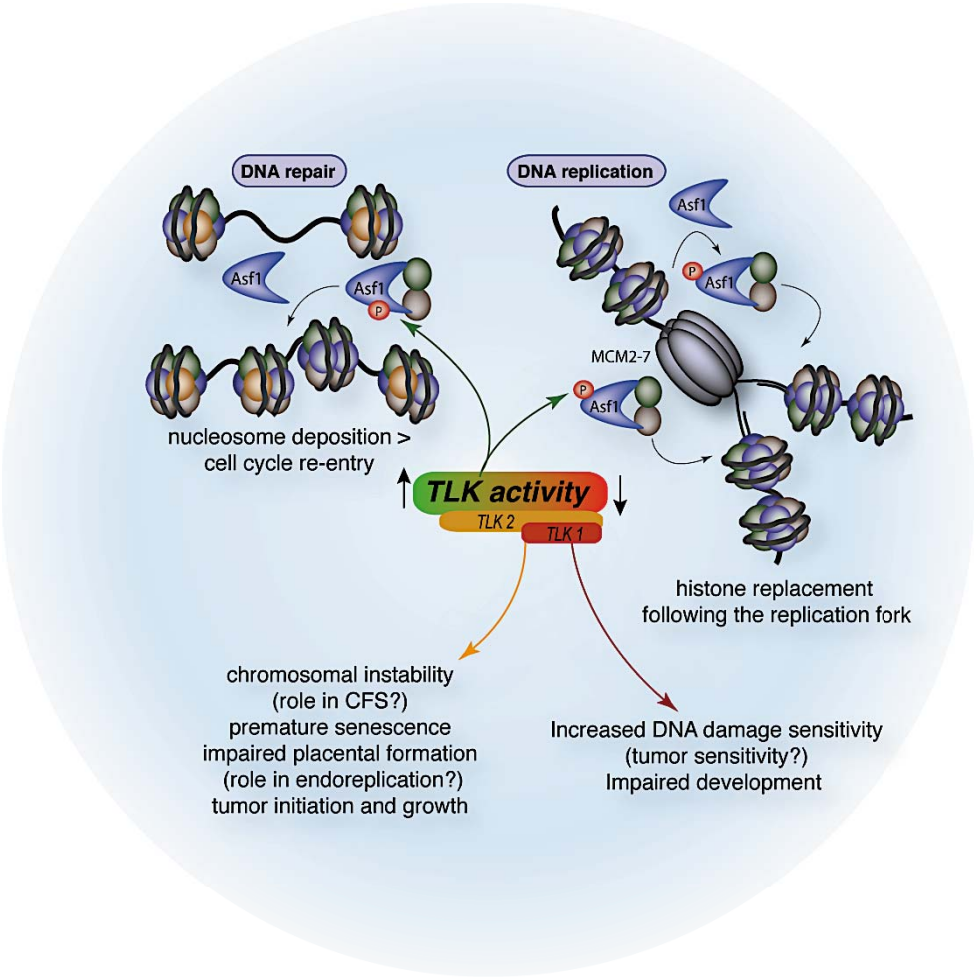

Figure 65. TLK model of action. Two thresholds of activity in TLKs regulation.

Conclusions

1. TLK1 is not an essential gene for cell cycle progression, the DNA damage response or organism development.
2. A higher threshold of total TLK activity is required for DNA damage tolerance.
3. TLK1 and TLK2 both contribute to normal DNA damage sensitivity and checkpoint recovery.
4. TLK2 is required for embryonic development.
5. Loss of TLK2 increases chromosomal instability and drives premature senescence in primary cells.
6. TLKs have additional interacting proteins besides Asf1 that may represent additional targets.
7. Lack of TLK1 can enhance tumour development.

Resumen en castellano

1. Introducción

El mantenimiento de la integridad del genoma es esencial para la supervivencia celular. Por ello, para luchar contra el daño al ADN, las células han desarrollado mecanismos de respuesta al daño en el ADN (DDR). La DDR mantiene la integridad genómica coordinando del reconocimiento del daño en el ADN con las vías de señalización que controlan el comportamiento celular. Defectos en la DDR son característicos de enfermedades neurológicas e inmunes tipos de enfermedades y síndromes y ocurren con frecuencia en células cancerosas. Diversos estudios apuntan la importancia del control de la transición G2/M en la supresión tumoral, pero los mecanismos que regulan este punto de control del ciclo celular todavía se desconocen [41]. La transición G2/M está controlada por las quinasas ATM y ATR, que potencialmente modifican cientos de sustratos para regular el comportamiento celular. Dentro de estos sustratos se encuentran enzimas capaces de modificar el empaquetamiento de la cromatina, proceso de crucial importancia para la reparación del ADN.

El papel de TLK1/TLK2 en la integridad genómica después del daño al ADN

Una de las lesiones más importantes que puede sufrir el ADN son las roturas de doble cadena (DSB) ya que pueden resultar en la muerte celular o en una amplia variedad de alteraciones genéticas incluyendo deleciones, translocaciones, pérdida de heterozigosidad y pérdida de cromosomas. Durante la fase G2 del ciclo celular, la reparación de DSB requiere una resección del ADN de doble cadena hasta ADN monocatenario mediante la acción de múltiples nucleasas. El ADN monocatenario activa las quinasas ATR y Chk1 las cuales regulan la parada del ciclo celular y la reparación del ADN. Durante la resección los nucleosomas deben eliminarse, y volver a colocarse en el ADN una vez reparado, para constituir de nuevo la fibra de cromatina que contiene la información epigenética, de vital importancia para la célula. Diversos estudios en levadura, señalan que la chaperona de histonas Asf1 es la responsable del ensamblaje de nucleosomas tras la reparación del ADN [208], lo cual permite la progresion del ciclo cellular. Asf1 es regulada mediante la unión a Rad53, quinasa que controla la parada del ciclo celular en levaduras. En mamíferos también se ha comprobado la necesidad de Asf1 para una correcta reparación del ADN y la

progresión del ciclo celular. TLK1 y TLK2 son Ser/Thr quinasas capaces de fosforilar y activar Asf1, y éstas, a su vez, pueden ser inactivadas por Chk1 tras el daño al ADN (Figura 1), funcionando como eslabón entre la DDR y el empaquetamiento de la cromatina [97].

En este proyecto nos hemos centrado en entender en detalle el papel de TLK1 y TLK2 posiblemente implicadas en procesos clave en la transición G2/M así como en patologías humanas. El objetivo de esta tesis es esclarecer la función de TLK1 y TLK2 en la transición G2/M, contribuyendo así a nuestra comprensión de la etiología de la enfermedad humana y sugiriendo protocolos de tratamiento dirigidos a esta transición en la terapia contra el cáncer.

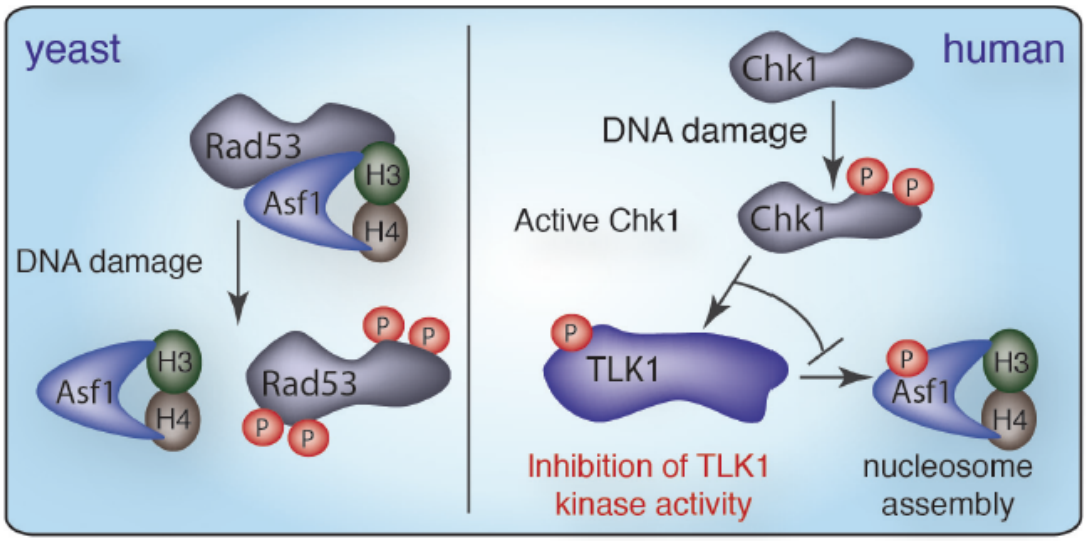

Figura 1: Regulación de Asf1 por la DDR. En levadura Asf1 se asocia con Rad53 (Chk1) hasta que se detecta un daño en el ADN, cuando es requerida para la resolución del checkpoint. En humanos, Chk1 regula Asf1 mediante una fosforilación indirecta mediante TLKs. TLK1 fosforila Asf1 y promueve la recolocación de nucleosomas tras la reparación del ADN.

2. Hipótesis y objetivos

Nuestra hipótesis es que una actividad de las TLKs disminuida da lugar a fallos en la formación de la cromatina que conllevan inestabilidad genómica, problemas en el desarrollo e inhibición del desarrollo tumoral.

Objetivos

1. Generar ratones genetrap para eliminar as funciones de Tlk1 y Tlk2 in vivo.
2. Caracterización fenotípica de células primarias y transformadas carentes de Tlk1, Tlk2 o ambas en presencia o ausencia de daños al ADN.
3. Caracterización fenotípica de células que sobreexpresan TLK1, TLK2 o sus mutantes con el dominio kinasa no fncional.
4. Análisis de las interacciones proteína-proteina de TLK1 y TLK2.
5. Análisis del papel de las TLKs en el desarrollo y crecimiento tumoral.

3. Resultados

Tlk1 no es esencial para el desarrollo ni para la DDR

Para comprender el papel de TLK1 in vivo y su función en el desarrollo y en la estabilidad genómica, hemos generado ratones que carecen de la expresión de Tlk1 debido a una secuencia *genetrap* insertada entre los exones 2 y 3 ($Tlk1^{Trap/Trap}$). Inesperadamente, estos ratones se desarrollan normalmente, alcanzando los 18 meses de edad sin manifestar patologías. Examinando de manera más detallada procesos que se podrían ver afectados por una ineficiente DDR como son la formación de gametos o la maduración linfoide, no pudimos encontrar ninguna anomalía. En el estudio de fibroblastos derivados de embriones (MEFs) de esta línea de ratones y, por lo tanto, carentes de la expresión de Tlk1, no observamos un aumento en la sensibilidad al daño al ADN, aumento en la inestabilidad genómica o fallo en regular el ciclo celular.

TLK1 y TLK2 tienen funciones redundantes en la DDR.

Una explicación para la ausencia de fenotipo tanto en ratones como en MEFs carentes de Tlk1 es la redundancia debida a Tlk2. Para comprobarlo, hemos generado varios siRNA para inhibir la expresión de Tlk2 en células $Tlk1^{Trap/Trap.}$

Las células que presentan una reducción el la actividad total de las Tlks, es decir, Tlk1 y Tlk2, presentan un aumento en la sensibilidad a diversos agentes que dañan el ADN, como la irradiación X, el UVC y el Etopósido (Figura 2). A su vez, presentan problemas en la regulación del ciclo celular. Sin embargo, estas células no presentan disfunciones evidentes en condiciones normales, sin presencia de daño al ADN. Estos datos sugieren que existen dos umbrales de acción de las Tlks, y que para tolerar el daño celular se necesita un umbral mayor de actividad.

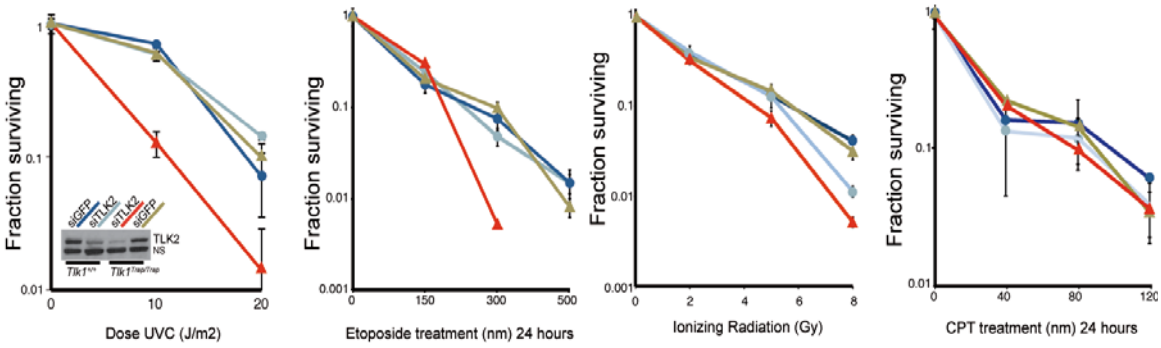

Figura 2: Sensibilidad a UVC, etopósido, IR y camptotecin determinado mediante ensayo de supervivencia celular. El Western Blot (WB) muestra los niveles de TLK2 en el momento de dañar las células. Los gráficos muestran que la inhibición de Tlk2 no es suficiente para sintetizar las células ante el daño al ADN y que se necesita la inibición simultánea de Tlk1.

Tlk2 es esencial para el desarrollo embrionario.

Teniendo en cuenta los resultados utilizando siRNA frente a Tlk2, la inhibición total de la actividad de Tlk2 in vivo debería resultar en problemas de homeostasis tisular, una sensibilidad mayor al daño al ADN que desemboque en un posible desarrollo tumoral. Para corroborarlo, nos propusimos generar ratones carentes de la expresión de Tlk2 mediante genetrap (*Tlk2*$^{Trap/Trap}$). Nuestra hipótesis era que estos ratones, al igual que *Tlk1*$^{Trap/Trap}$, se desarrollarían de manera normal, y solo cuando las funciones de ambas Tlks estuvieran comprometidas se manifestaría el fenotipo. Sin embargo, para nuestra sorpresa, los ratones *Tlk2*$^{Trap/Trap}$ no llegaban a nacer y la ausencia de Tlk2 era letal a nivel embrionario. Un estudio detallado de los distintos estadios embrionarios puso de manifiesto que la edad a la que los embriones morían era a día 14.5 post-coitum (e14.5). A este estadio de desarrollo los embriones presentaban un menor tamaño y una coloración pálida que nos llevó a pensar en la posibilidad de un fallo vascular o hematopoyético (Figura 3). Estudios subsiguientes del desarrollo vascular del embrión y de la formación de células sanguíneas descartó estas dos hipótesis. Dado que la placenta es el órgano responsable del intercambio de oxígeno y nutrientes entre la madre y el feto, estudiamos el desarrollo de este órgano encontrando un fallo en el desarrollo del tropoblasto, capa que separa la decidua

(materna) del laberinto (fetal) y que es la capa responsable del intercambio de nutrientes y gases. El trofoblasto presenta una hiperproliferación celular a día e10.5 que se manifiesta en una invasión de células del trofoblasto al laberinto a día e14.5, reduciendo los espacios vasculares de la parte fetal de la placenta, llegando al colapso (Figura 4). Esto conlleva la ausencia de irrigación sanguínea de la parte fetal de la placenta, lo cual puede ser corroborado por la ausencia de sangre en el cordón umbilical. Por tanto, se pone de manifiesto que la causa de la muerte embrionaria de los ratones *Tlk2*$^{Trap/Trap}$ es debida a un de comunicación entre la madre y el feto.

Una cuestión que queda por resolver es la causa que lleva a la hiperproliferación del trofoblasto. En esta capa existen células poliploides que siguen múltiples ciclos de endoreplicación. Dada la posible función de las Tlks en la transición G2/M es lógico pensar que el proceso que lleva a la edoreplicación esté fallando. Se necesitan más estudios para poder corroborar esta hipótesis.

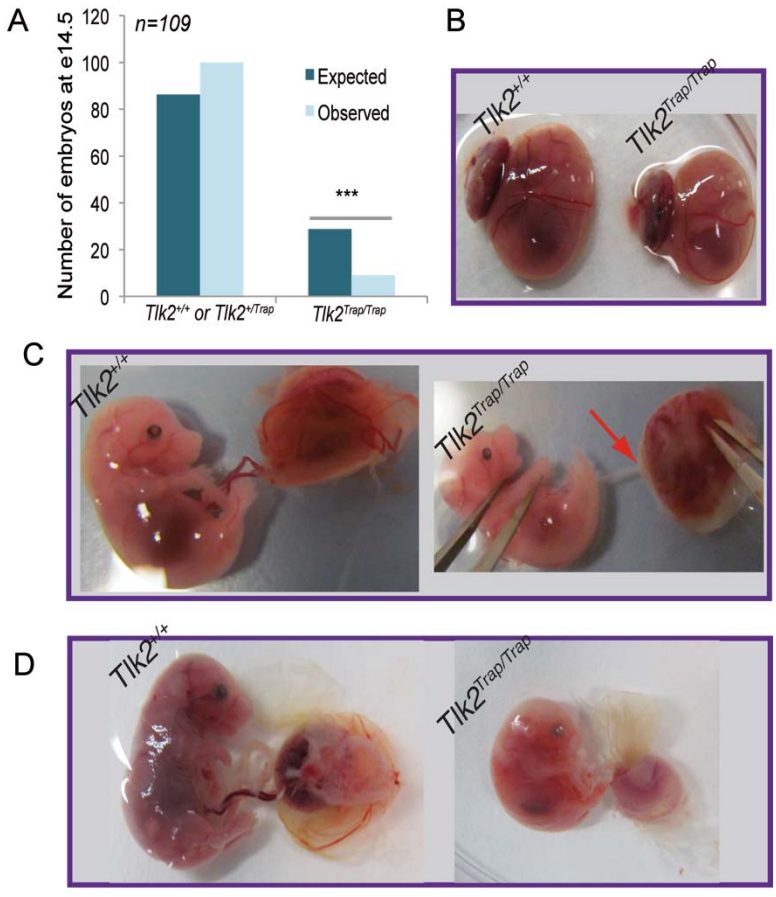

Figura 3: Los ratios mendelianos están alterados a e14.5. B. La vasos sanguíneos del saco embrionario no está afectada. C. Ausencia de circulación en el cordón umbilical a e14.5. D. Embriones a e16.5 con una evidente falta de circulación sanguínea.

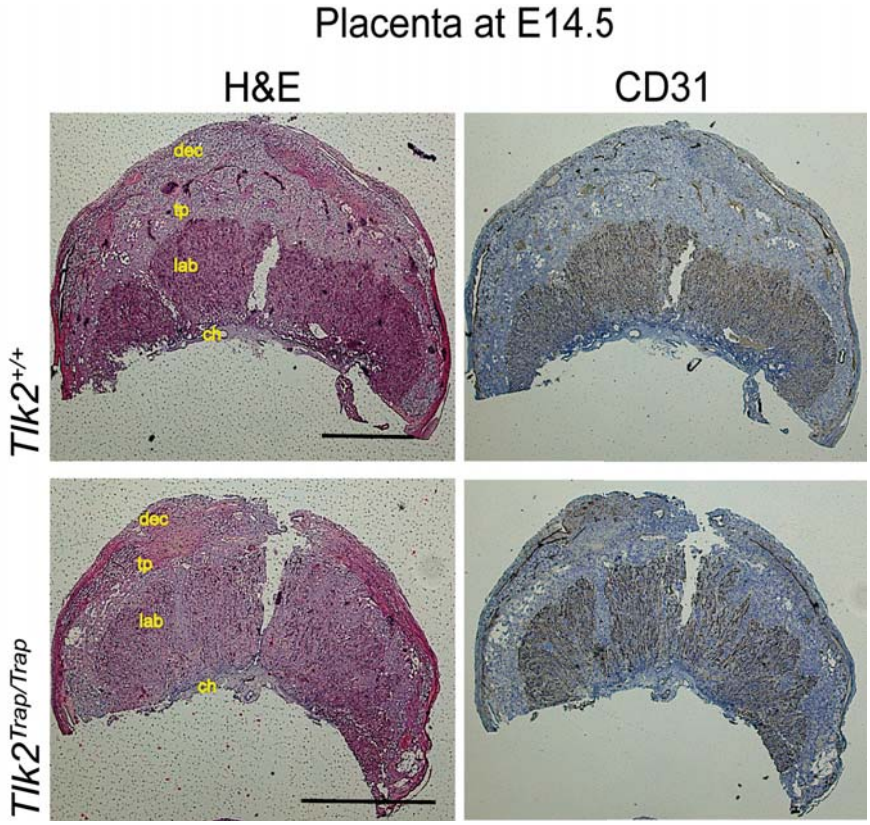

Figura 4: Tinción H&E para el estudio histológico de las placentas WT y *Tlk2*$^{Trap/Trap}$ a e14.5. Las distintas capas de la placenta están señaladas: Dec: Decidua; tp: trofoblasto; lab: laberinto; Ch: corion. Se observa una infiltración cellular en el laberinto que reduce significativamente los espacios vasculares, llegando a perder la irrigación sanguinea.

Tlk2 es haploinsuficiente en ausencia de Tlk1

Nuestros resultados con siRNA confirmaron la redundancia de Tlk1 y Tlk2, por lo que fue sorprendente encontrar que la ausencia de únicamente Tlk2 fuera letal a nivel embrionario. Para determinar si Tlk1 podía contribuir también al desarrollo de los ratones, quisimos examinar el efecto de una dosis reducida de Tlk2 (*Tlk2*$^{+/Trap}$,que por sí mismo no tiene efecto en el desarrollo) en un background sin Tlk1. Mediante cruces seriados generamos ratones *Tlk1*$^{Trap/Trap}$ *Tlk2*$^{+/Trap}$ los cuales podían nacer. Sin embargo el desarrollo se vió altamente comprometido muriendo en menos de un mes (Figura 5).

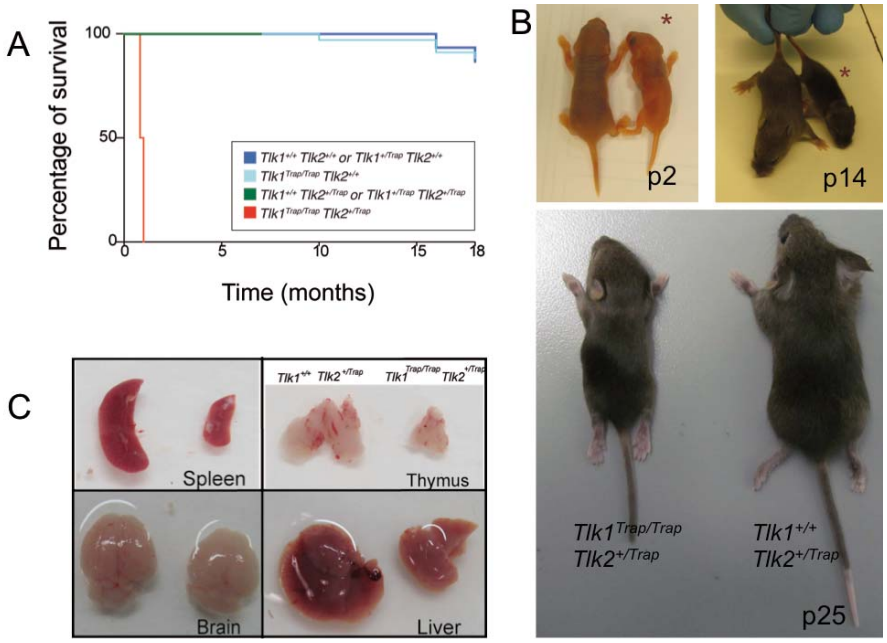

Figura 5: A. Supervivencia de diversas series de fenotipos Tlk-genetrap. B. Comparación fenotípica de *Tlk1*$^{Trap/Trap}$ *Tlk2*$^{+/Trap}$ y *Tlk1*$^{+/+}$*Tlk2*$^{+/Trap.}$El retraso en el crecimiento es obvio. C. Varios órganos presentan un severo retraso en el desarrollo.

La pérdida de Tlk2 afecta al crecimiento celular in vitro, produce inestabilidad genómica y senescencia prematura.

Para determinar si la pérdida de Tlk2 afecta al crecimiento o al a viabilidad de células en cultivo, obtuvimos *Tlk2*$^{Trap/Trap}$ MEFs y analizamos su comportamiento. La pérdida de Tlk2 se traduce en una disminución del crecimiento celular debido a una senescencia prematura (Figura 6). A su vez, existe un aumento en la inestabilidad genómica pero no se traduce en un aumento en la sensibilidad a agentes que dañan el ADN.

Sin embargo, dado que los MEFs son obtenidos de embriones a e14.5 y en este estadío de desarrollo presentan falta de irrigación sanguínea, puede ser que este fenotipo sea una consecuencia del estrés producido por la falta de oxígeno. Para clarificarlo, hemos generado ratones condicionales en los que la expresión de Tlk2 se anula solo en presencia de la recombinasa Cre. De este modo podremos Tlk2 después que tener los MEFs en cultivo.

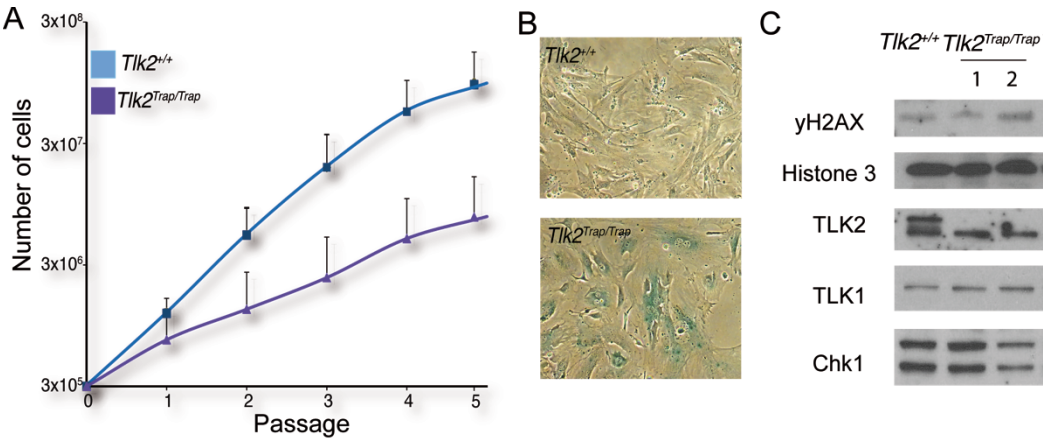

Figura 6: A. Curva de crecimiento 3T3 para los 5 primeros pases. B. Tinción SA-*β*-gal de MEFs primaries en el pase 8. Se muestra una senescencia prematura en ausencia de Tlk2. C. Análisis de los niveles de TLK1, Chk1, γH2AX y H3 (control de carga) en MEFs primaries a pase 3.

Consecuencias de la sobreexpresión de TLKs y sus respectivas Kinase-Dead (KD).

Con estos experimentos quisimos explorar cuál era el efecto de la ganancia y pérdida de función kinasa en las TLKs y cómo eso afectaba a ciclo celular. Nuestros resultados señalan que la sobreexpresión de las formas sin función kinasa (KD) provocan en las células una disminución en el crecimiento, aumento de la sensibilidad a agentes que dañan el ADN y problemas en el restablecimiento del ciclo celular tras el daño (Figuras 7 y 8). Estos efectos pueden ser explicados por el arresto de Asf1 en las formas KD, lo que ocasiona una incorrecta deposición de los nucleosomas que da lugar a los efectos antes señalados.

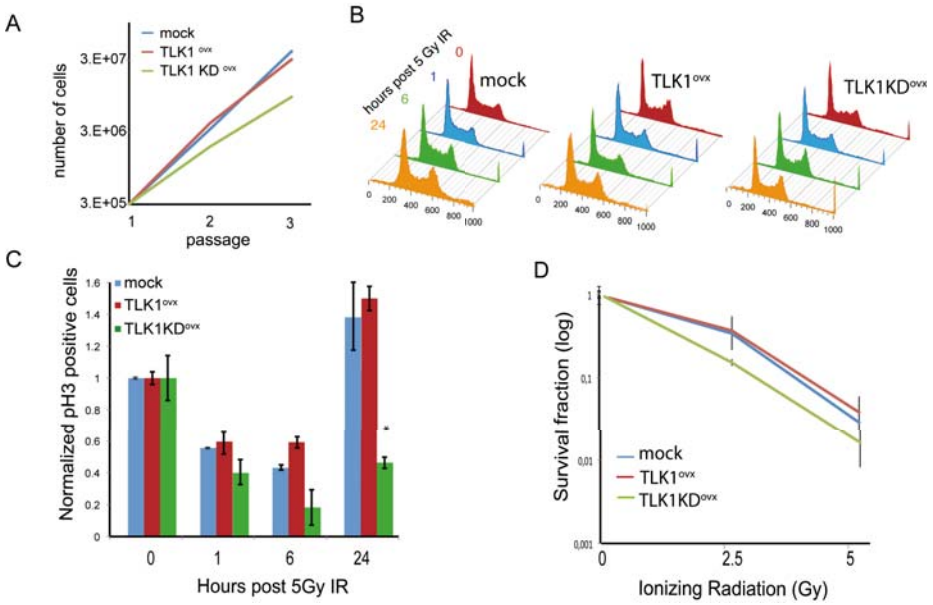

Figura 7. Ensayo de crecimiento celular 3T3 con la sobreexpresión de TLK1 y TLK1 KD. B. Perfiles de ciclo celular tras la irradiación con 5Gy. C. Datos normalizados de número de células en mitosis (positivas para pH3) tras una irradiación de 5Gy en células con sobreexpresión de TLK1 y TLK1 KD (Fisher test <0.05). D. Ensayo de supervivencia celular de células expuestas a distintas dosis de radiación ionizante.

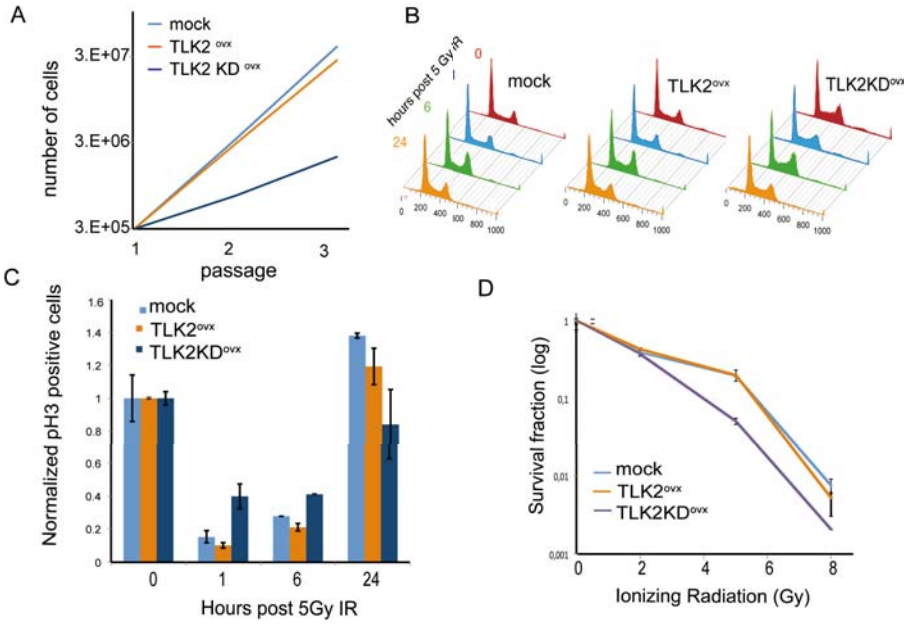

Figura 8. Ensayo de crecimiento celular 3T3 con la sobreexpresión de TLK2 y TLK2 KD. B. Perfiles de ciclo celular tras la irradiación con 5Gy. C. Datos normalizados de número de células en mitosis (positivas para pH3) tras una irradiación de 5Gy en células con sobreexpresión de TLK2 y TLK2 KD. D. Ensayo de supervivencia celular de células expuestas a distintas dosis de radiación ionizante.

Identification of sustrates and regulators of TLK1 and TLK2

Una de las principales limitaciones con la que contamos para interpretar el fenotipo de los ratones genetrap es la falta de conocimiento acerca de los sustratos y reguladores de las TLKs. En un intento de conocer nuevas proteínas que interaccionan con TLK1 y TLK2 hemos realizado una purificación de afinidad en tándem (TAP) seguida de la identificación de las proteínas que unen a TLKs mediante espectrometría de masas (MS). Estos experimentos validaron sustratos que ya habían sido identificados en otros estudios como Asf1 o H4 y las propias TLKs (ya que forman oligómeros). Adicionalmente, hemos identificado un número elevado de proteínas que pueden interaccionar con las TLKs y que se relacionan con la síntesis de ADN, la regulación del citoesqueleto y la formación de complejos multiproteicos (Tabla1). De ellas, hasta la fecha, hemos validado LC8, una proteína de apenas 8KDa implicada en la oligomerización de complejos multiproteicos.

Protein name	IP TLK2 (n = 4)	IP TLK2 KD (n=4)	IP TLK1 (n=1)	GO category
Tousled-like kinase 2	4	4	1	Regulación de la cromatina
Tousled-like kinase 1	2	2	1	Regulación de la cromatina
Dynein light chain 1 (LC8)	2	0	1	Ensamblaje de complejos proteicos
Histone H4	1	1	1	Ensamblajede la cromatina
Histone chaperone ASF1B	1	2	1	Organización de la cromatina
Tubulin β-4B	1	2	0	Constituyente del citoesqueleto
Histone chaperone ASF1A	0	2	0	Organización de la cromatina
Tubulin α-1B	1	1	0	Procesos que conllevan microtubules
MOB	2	1	0	Activador de kinasas
PP1C	2	1	0	Protein Fosfatasa
MCM	2	0	0	Replicación del ADN

Tabla1: Lista de posibles interactores de TLK1 y TLK2.

En paralelo hemos realizado un microarray peptídico usando TLK2 purificada. Con este experimento hemos identificado más de 100 péptidos que pueden ser fosforilados por TLK2, sin embargo no hemos podido identificar ninguna secuencia consenso. Este resultado apunta a que debe existir una regulación mucho más amplia más allá de Asf1, por lo que se requerirán nuevos métodos para identificar nuevos sustratos fiables.

TLKs como dianas quimioterapéuticas.

La inhibición de las TLKs presenta un camino aún no explorado en quimioterapia. El hecho de que las TLKs sean kinasas, y no una proteína de reparación del ADN per sé, y que sus actividades no son específicas de un único tipo de daño al ADN, sugiere que puede ser aplicada en combinación de otros fármacos quimioterapéuticos. Además, existe la ventaja de que varios tipos de cáncer presentan mutaciones en TLKs, lo que disminuye su umbral de actividad, haciendo la una diana que podría sintetizar de manera más eficiente las células tumorales con respecto a las sanas. Datos provenientes de pacientes con cáncer de colon muestran que los niveles de TLK2, pero no TLK1, se veían significativamente reducidos y que esta reducción era más dramática en lesiones metastáticas.

Nuestro objetivo es encontrar compuestos químicos que muestren especificidad por las células carentes de TLK1 o TLK2 en condiciones normales o tras tratamiento con irradiación. Para ello, monitorizamos la supervivencia de MEFs carentes de algunas de estas dos proteínas frente a una librería de inhibidores. Este experimento identificó 4 compuestos capaces de disminir la supervivencia de MEFs *Tlk2*$^{Trap/Trap}$ en más del 80%. Estos compuestos son Cdk2 inhibitor II, PI3-ky/CKII inhibitor , H-8 dihidrochloride, y KT5720. Los últimos dos son inhibidores de kinasas dependientes de cAMP (PKA) (Figura 9). Estos inhibidores puedan actuar sobre Tlk1 (según nuestros experimentos usando siRNA) o bien representar letalidades sintéticas con la pérdida de TLK1/2.

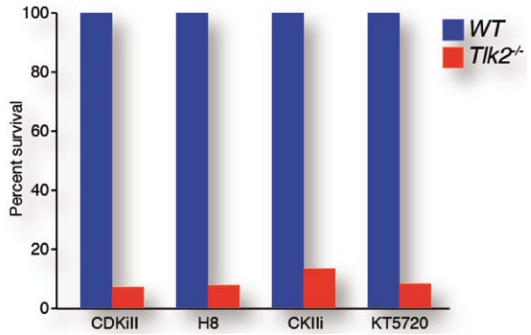

Figura 9. *Tlk2*$^{Trap/Trap}$ MEFs fueron tratados durante 24 horas con una librería de inhibidores . La viabilidad cellular fue medida con Resazurina.

La pérdida de TLK tiene influencia en el desarrollo tumoral.

Para explorar la importancia de la actividad de TLK en el desarrollo tumoral, inyectamos 1×10^6 WT o *Tlk1*$^{Trap/Trap}$ MEFs inmortalizados en la glándula mamaria abdominal de un ratón NOD/SCID. Dos ratones fueron usados para cada genotipo. El crecimiento tumoral fue mayor en los tumores *Tlk1*$^{Trap/Trap}$, lo que puede suponer que la falta de Tlk1 dentro de un contexto tumoral (la inmortalización fue llevada a cabo mediante la inhibición de p53) puede potenciar la inestabilidad genómica y el desarrollo tumoral. Sin embargo, se requieren nuevos experimentos y nuevas líneas tumorales para validar esta hipótesis.

A su vez, analizamos si la inhibición de Tlk2 en los tumores inducidos carentes de Tlk1 podría tener un efecto en la reversión del crecimiento tumoral. Usamos siRNA en el momento de la inyección para downregular de manera no estable Tlk2. Los resultados fueron contrarios a lo esperado, ya que los tumores en los que utilizamos siRNA comenzaron a crecer a estadios más tempranos que los controles (Figura 10), sugiriendo que la actividad de TLKs sea, quizás, necesaria para la implantación tumoral.

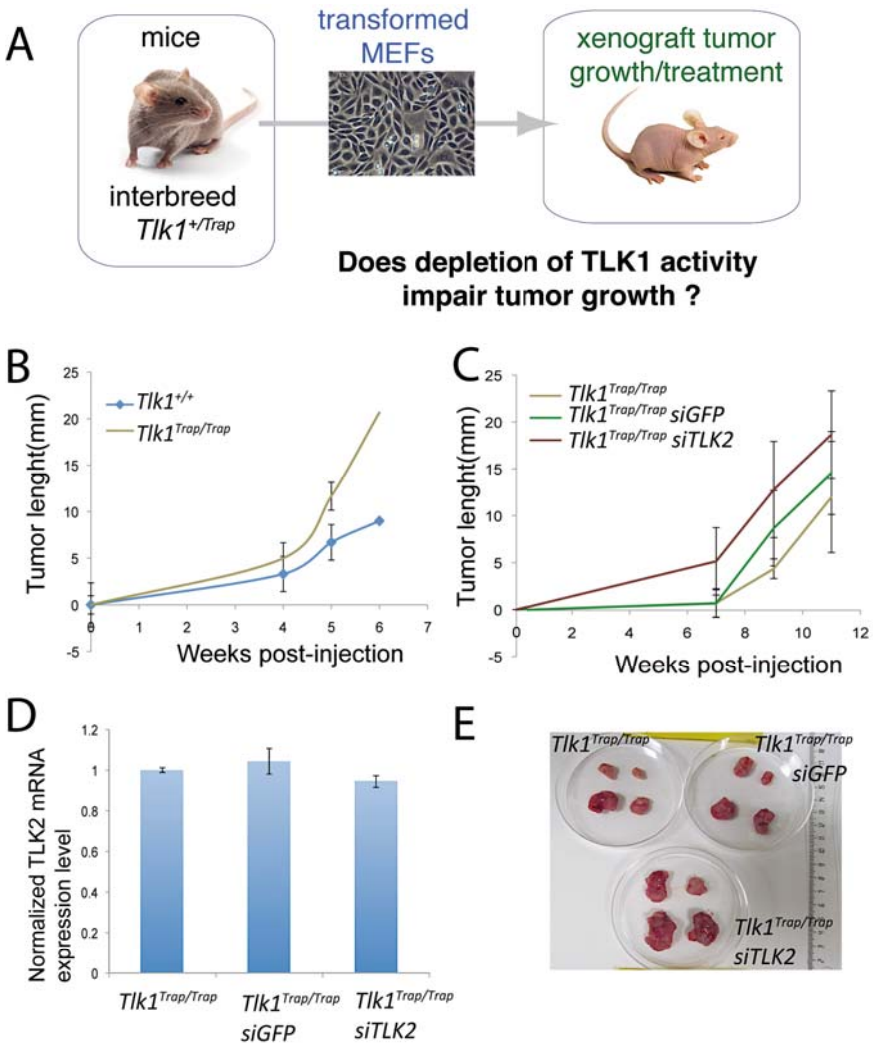

Figura 10. Papel de TLKs en el desarrollo tumoral. A) Gráfico del plan experimental. B. La carencia de Tlk1 aumenta el desarrollo tumoral. C. Tumores con Tlk2 downregulation aumentan la capacidad de comenzar a crecer . Para B) y C) se inocularon MEFs inmortalizados en las glándulas mamarias de ratones nude. El crecimiento fue medido semanalmente hasta que se alcanzaron los 20mm de diámetro. D) Niveles de expresión de Tlk2 en el punto final del desarrollo tumoral de los tumores tratados con siRNA. Como esperábamos, los niveles de Tllk2 se recuperaron tras el tratamiento no estable con siRNA. E) Tumores extraídos de la glándula mamaria de ratones nude. Los genotipos están indicados en cada caso. Dos ratones fueron inyectados en dos glándulas mamarias por cada genotipo. Se muestran los cuatro tumores.

4. Discusión

Un aspecto sorprendente de esta investigación ha sido comprobar que Tlk1 es prescindible tanto para el desarrollo en mamíferos como para la DDR, especialmente teniendo en cuenta que la inhibición de TLK en organismos inferiores lleva a la muerte embrionaria debido, fundamentalmente a problemas de compactación cromosómica. Así, examinamos la posibilidad de redundancia. Mientras en

organismos inferiores existe sólo una proteína TLK, en mamíferos hay dos: Tlk1 y Tlk2, las cuales comparten el 84% de similaridad, 95% en su dominio kinasa. Así, downregulamos la expresión de Tlk2 en $Tlk1^{Trap/Trap}$ MEFs. En este escenario las células mostraban un incremento en la sensibilidad a diversos agentes genotóxicos, como IR y UV. Esto corrobora la redundancia de Tlk1 y Tlk2 en la DDR. El hecho que más sorprendente encontramos es que estas células eran sensibles a Etopósido (inhibidor de TopoII) pero no a Camtotecina (inhibidor de TopoI), lo cual indica que en ausencia de Tlks, las células dependen de la función de TopoII, quizá debido a una incorrecta deposición de las histonas que ocasiona mayor entrelazado del ADN.

En quimioterapia se han utilizado drogas que inhiben TopoII, incluyendo el Etopósido. En la mayoría de ocasiones, estas drogas se han usado junto con otras capaces de inhibir otras rutas de reparación del ADN. Así, la inhibición de Tlk2 puede llegar a ser una estrategia quimioterapéutica en combinación con inhibidores de TopoII.

La falta de Tlk2, pero no de Tlk1, ocasiona muerte embrionaria. La causa reside en a capa de trofoblastos de la placenta. En esta capa, las células comienzan a hiperproliferar, infiltrándose en el laberinto y disminuyendo los espacios vasculares. Esto ocasiona un incorrecto intercambio de gases y nutrientes y los embriones terminan muriendo por hipoxia a e14.5.

En la capa de trofoblasto las células llevan a cabo una endorreplicación que las convierte en células diploides. Podemos especular que la ausencia de Tlk2 ocasiona fallos de endoreplicación y las células entran en mitosis en lugar de repetir varias fases S seguidas, lo cual explicaría la hiperproliferación. Se requieren más estudios para corroborar el papel de Tlk2 en endorreplicación.

Pese a la muerte embrionaria, pudimos obtener embriones a e14.5 para formar MEFs. Los $Tlk2^{Trap/Trap}$ MEFs presentan crecimiento lento y senescencia prematura, sin embargo es difícil diferenciar si este fenotipo es debido a la ausencia de Tlk2 per sé o a que a e14.5 los embriones están comenzando a morir y los MEFs están en condiciones de estrés replicativo. Para dilucidar si la ausencia de Tlk2 provoca en realidad senescencia prematura y envejecimiento, evitaremos el efecto placentario mediante un trasgén ERT2-Cre que induce la deleción de Tlk2 sólo en presencia de tamoxifén.

Pese a no poder detectar ningún defecto en el desarrollo de los ratones carentes de Tlk1, nuestros experimentos con siRNA frente a Tlk2 ponen de manifiesto que ambas proteínas tienen funciones redundantes en la DDR. Esto nos llevó a pensar que una

actividad reducida de *Tlk2* en un background *Tlk1*$^{Trap/Trap}$ podría tener consecuencias en el desarrollo de los ratones. Por ello generamos series alélicas, comprobando la haploinsuficiencia de Tlk2 en ausencia de Tlk1, ya que el genotipo *Tlk1*$^{Trap/Trap}$*Tlk2*$^{+/Trap}$ muestra severos problemas de desarrollo y ataxia motora. Nuestra hipótesis es que disminuyendo la actividad de Tlk por debajo de cierto umbral aparecen problemas en la replicación del ADN, en la transcripción y un incremento en la inestabilidad genómica causante de los genotipos observados.

Hasta ahora, una de las mayores limitaciones para interpretar el fenotipo de ratones y células carentes de Tlks, es la falta de conocimiento acerca de sus sustratos y proteínas reguladoras. Se ha comprobado que Tlk1 y Tlk2 son capaces de interaccionar entre sí y de unirse y fosforilar Asf1, chaperona de histonas que parece ser el principal efector de las Tlks. Sin embargo, existe evidencia de que las Tlks pueden estar inplicadas en otras rutas de señalización. Por ello, realizamos una LC-MS para identificar nuevas proteínas que pueden interaccionar con las Tlks. Identificamos y validamos la interacción de las TLKs con LC8, una pequeña proteína de 8KDa implicada en la estabilización de complejos multiproteicos. LC8 es un importante regulador de proteínas que intervienen en mitosis, como Astrin y SKAP, modulando su localización en los cinetocoros en las distintas fases de la mitosis. Nuestra hipótesis es que LC8 puede modular la actividad y la localización de las TLKs durante el ciclo celular.

Además, en nuestros experimentos de MS obtuvimos MOB y PPC1 como posibles proteínas capaces de unirse a TLKs. Estas proteínas son importantes reguladores de varias kinasas, por lo que, de validarse la interacción, podría implicar a las TLKs en otras rutas de señalización.

Las TLKs son una diana quimioterapéutica aún no explorada.

Dado el importante papel de las TLKs en replicación del ADN y DDR, es muy posible que jueguen un papel en el desarrollo de cáncer. El resultado más chocante cuando analizamos datos provenientes de pacientes, es que el comportamiento de las TLKs es distinto en diferentes tipos de cáncer. Por ejemplo, más del 30% de los pacientes con cáncer de mama presentan amplificación de TLK1 ó TLK2, siendo ambos excluyentes. Sin embargo, en CRC, existe una disminución en la expresión de los genes TLKs. Este distinto comportamiento nos llevó a estudiar cómo es el desarrollo tumoral en ausencia de TLK. Nuestros resultados señalaron que los tumores *Tlk1*$^{Trap/Trap}$ crecían de manera más acelerada que los tumores con niveles normales de Tlk1. Es más, si en un *Tlk1*$^{Trap/Trap}$ background inhibimos la expresión de Tlk2

mediante siRNA, los tumores se iniciaba antes. Así, podemos concluir que la ausencia de Tlks aumenta la capacidad de desarrollo tumoral en nuestro modelo de estudio, quizá debido a un aumento de la inestabilidad cromosómica en estas células.

Nuestros datos de supervivencia celular en células con depleción global de la actividad Tlk (*Tlk1*$^{Trap/Trap}$ +siTlk2) señalan que estas células son más sensibles a tratamientos que dañen el ADN. Teniendo en cuenta que hay tumores que muestran una disminución en la expresión de TLK1 ó 2, el uso de inhibidores frente al otro homólogo puede sintetizar las células tumorales con preferencia a las del resto del organismo. Hasta ahora no hemos identificado ningún compuesto que inhiba el crecimiento celular preferentemente en células sin Tlk1. Sin embargo, hemos encontrado cuatro inhibidores que tienen especificidad frente a células deficientes en Tlk2, reduciendo su viabilidad hasta en un 80%: Cdk2 inhibidor II, PI3-ky/CKII inhibidor, H-8 dihidroclorido y KT5720. Estos cuatro inhibidores pueden estar inhibiendo Tlk1, disminuyendo la actividad total de Tlks y por lo tanto disminuyendo la supervivencia celular. O bien pueden ser letalidades sintéticas que estén actuando en otras rutas aún por descubrir.

Los datos obtenidos durante el desarrollo de esta tesis doctoral establecen un papel de las Tlks en el desarrollo de mamíferos, el la homeostasis tisular y en la DDR. Tlk1 y Tlk2 tienen dos umbrales de actividad, y se necesita un umbral mayor bajo condiciones de estrés que pueda dañar el ADN. Este hecho puede ser explotado en quimioterapia. Así, uno de los retos que abre este proyecto es el de descifrar la habilidad de TLKs en prevenir el desarrollo tumoral o aumentar la eficiencia de la quimioterapia.

5. Conclusiones.

1. TLK1 no es un gen esencial para el desarrollo embrionario ni para la DDR.

2. Existen dos umbrales de actividad para TLK. Se requiere un umbral mayor en presencia de daño al ADN. Tanto TLK1 como TLK2 se necesitan para hacer frente al daño al ADN y para un correcto funcionamiento de los checkpoint celulares.

3. TLK2 es esencial para un correcto desarrollo embrionario

4. TLK2 es haploinsuficiente en ausencia de TLK1.

5. La pérdida de TLK2 aumenta la inestabilidad cromosómica y da lugar a senescencia prematura en cultivos primarios.

6. Las TLKs pueden regular rutas metabólicas además de las relacionadas con Asf1.

7. La pérdida de TLK1 pòdría potenciar el desarrollo tumoral.

Bibliography

1 Harper, J. W. & Elledge, S. J. The DNA damage response: ten years after. *Molecular cell* **28**, 739-745, doi:10.1016/j.molcel.2007.11.015 (2007).

2 Keeney, S., Giroux, C. N. & Kleckner, N. Meiosis-specific DNA double-strand breaks are catalyzed by Spo11, a member of a widely conserved protein family. *Cell* **88**, 375-384 (1997).

3 Schwarz, K. *et al.* RAG mutations in human B cell-negative SCID. *Science* **274**, 97-99 (1996).

4 Nicolas, N. *et al.* A human severe combined immunodeficiency (SCID) condition with increased sensitivity to ionizing radiations and impaired V(D)J rearrangements defines a new DNA recombination/repair deficiency. *The Journal of experimental medicine* **188**, 627-634 (1998).

5 van der Burg, M. *et al.* A DNA-PKcs mutation in a radiosensitive T-B- SCID patient inhibits Artemis activation and nonhomologous end-joining. *The Journal of clinical investigation* **119**, 91-98, doi:10.1172/JCI37141 (2009).

6 Lahdesmaki, A., Taylor, A. M., Chrzanowska, K. H. & Pan-Hammarstrom, Q. Delineation of the role of the Mre11 complex in class switch recombination. *The Journal of biological chemistry* **279**, 16479-16487, doi:10.1074/jbc.M312796200 (2004).

7 van Engelen, B. G. *et al.* Decreased immunoglobulin class switching in Nijmegen Breakage syndrome due to the DNA repair defect. *Human immunology* **62**, 1324-1327 (2001).

8 Tycko, B. & Sklar, J. Chromosomal translocations in lymphoid neoplasia: a reappraisal of the recombinase model. *Cancer Cells* **2**, 1-8 (1990).

9 Chatterji, M., Tsai, C. L. & Schatz, D. G. New concepts in the regulation of an ancient reaction: transposition by RAG1/RAG2. *Immunological reviews* **200**, 261-271, doi:10.1111/j.0105-2896.2004.00167.x (2004).

10 Jackson, S. P. & Bartek, J. The DNA-damage response in human biology and disease. *Nature* **461**, 1071-1078, doi:10.1038/nature08467 (2009).

11 Lengauer, C., Kinzler, K. W. & Vogelstein, B. Genetic instability in colorectal cancers. *Nature* **386**, 623-627, doi:10.1038/386623a0 (1997).

12 Kennedy, R. D. & D'Andrea, A. D. DNA repair pathways in clinical practice: lessons from pediatric cancer susceptibility syndromes. *Journal of clinical oncology : official journal of the American Society of Clinical Oncology* **24**, 3799-3808, doi:10.1200/JCO.2005.05.4171 (2006).

13 Ripperger, T., Gadzicki, D., Meindl, A. & Schlegelberger, B. Breast cancer susceptibility: current knowledge and implications for genetic counselling. *European journal of human genetics : EJHG* **17**, 722-731, doi:10.1038/ejhg.2008.212 (2009).

14 Nelson, H. D., Huffman, L. H., Fu, R. & Harris, E. L. Genetic risk assessment and BRCA mutation testing for breast and ovarian cancer susceptibility: systematic evidence review for the U.S. Preventive Services Task Force. *Annals of internal medicine* **143**, 362-379 (2005).

15 Zhou, B. B. & Elledge, S. J. The DNA damage response: putting checkpoints in perspective. *Nature* **408**, 433-439, doi:10.1038/35044005 (2000).

16 Kuntz, K. & O'Connell, M. J. The G(2) DNA damage checkpoint: could this ancient regulator be the Achilles heel of cancer? *Cancer biology & therapy* **8**, 1433-1439 (2009).
17 Lindahl, T. & Barnes, D. E. Repair of endogenous DNA damage. *Cold Spring Harbor symposia on quantitative biology* **65**, 127-133 (2000).
18 Nitiss, J. L. DNA topoisomerase II and its growing repertoire of biological functions. *Nature reviews. Cancer* **9**, 327-337, doi:10.1038/nrc2608 (2009).
19 Hendriks, G. *et al.* Transcription-dependent cytosine deamination is a novel mechanism in ultraviolet light-induced mutagenesis. *Current biology : CB* **20**, 170-175, doi:10.1016/j.cub.2009.11.061 (2010).
20 Azvolinsky, A., Giresi, P. G., Lieb, J. D. & Zakian, V. A. Highly transcribed RNA polymerase II genes are impediments to replication fork progression in Saccharomyces cerevisiae. *Molecular cell* **34**, 722-734, doi:10.1016/j.molcel.2009.05.022 (2009).
21 Stracker, T. H. & Petrini, J. H. The MRE11 complex: starting from the ends. *Nature reviews. Molecular cell biology* **12**, 90-103, doi:10.1038/nrm3047 (2011).
22 Zou, L. & Elledge, S. J. Sensing DNA damage through ATRIP recognition of RPA-ssDNA complexes. *Science* **300**, 1542-1548, doi:10.1126/science.1083430 (2003).
23 Lempiainen, H. & Halazonetis, T. D. Emerging common themes in regulation of PIKKs and PI3Ks. *The EMBO journal* **28**, 3067-3073, doi:10.1038/emboj.2009.281 (2009).
24 Furuno, N., den Elzen, N. & Pines, J. Human cyclin A is required for mitosis until mid prophase. *The Journal of cell biology* **147**, 295-306 (1999).
25 Sancar, A., Lindsey-Boltz, L. A., Unsal-Kacmaz, K. & Linn, S. Molecular mechanisms of mammalian DNA repair and the DNA damage checkpoints. *Annual review of biochemistry* **73**, 39-85, doi:10.1146/annurev.biochem.73.011303.073723 (2004).
26 Helt, C. E., Wang, W., Keng, P. C. & Bambara, R. A. Evidence that DNA damage detection machinery participates in DNA repair. *Cell Cycle* **4**, 529-532 (2005).
27 Batinac, T. *et al.* Protein p53--structure, function, and possible therapeutic implications. *Acta dermatovenerologica Croatica : ADC* **11**, 225-230 (2003).
28 Friedberg, E. C. Suffering in silence: the tolerance of DNA damage. *Nature reviews. Molecular cell biology* **6**, 943-953, doi:10.1038/nrm1781 (2005).
29 Levine, A. J. p53, the cellular gatekeeper for growth and division. *Cell* **88**, 323-331 (1997).
30 Alberts, B., Johnson, A., Lewis, J., Raff, M., Roberts, K., and Walter, P. *Molecular Biology of the Cell*. (Garland Science, New York, NY., 2002).
31 Nurse, P. A long twentieth century of the cell cycle and beyond. *Cell* **100**, 71-78 (2000).
32 Flatt, P. M., Tang, L. J., Scatena, C. D., Szak, S. T. & Pietenpol, J. A. p53 regulation of G(2) checkpoint is retinoblastoma protein dependent. *Molecular and cellular biology* **20**, 4210-4223 (2000).
33 Malumbres, M. & Barbacid, M. Cell cycle, CDKs and cancer: a changing paradigm. *Nature reviews. Cancer* **9**, 153-166, doi:10.1038/nrc2602 (2009).
34 Blow, J. J. & Gillespie, P. J. Replication licensing and cancer--a fatal entanglement? *Nature reviews. Cancer* **8**, 799-806, doi:10.1038/nrc2500 (2008).

35 Durkin, S. G. & Glover, T. W. Chromosome fragile sites. *Annual review of genetics* **41**, 169-192, doi:10.1146/annurev.genet.41.042007.165900 (2007).
36 Sandell, L. L. & Zakian, V. A. Loss of a yeast telomere: arrest, recovery, and chromosome loss. *Cell* **75**, 729-739 (1993).
37 Toczyski, D. P., Galgoczy, D. J. & Hartwell, L. H. CDC5 and CKII control adaptation to the yeast DNA damage checkpoint. *Cell* **90**, 1097-1106 (1997).
38 Lee, S. E. *et al.* Saccharomyces Ku70, mre11/rad50 and RPA proteins regulate adaptation to G2/M arrest after DNA damage. *Cell* **94**, 399-409 (1998).
39 Peng, C. Y. *et al.* Mitotic and G2 checkpoint control: regulation of 14-3-3 protein binding by phosphorylation of Cdc25C on serine-216. *Science* **277**, 1501-1505 (1997).
40 Lopez-Girona, A., Furnari, B., Mondesert, O. & Russell, P. Nuclear localization of Cdc25 is regulated by DNA damage and a 14-3-3 protein. *Nature* **397**, 172-175, doi:10.1038/16488 (1999).
41 Stracker, T. H., Couto, S. S., Cordon-Cardo, C., Matos, T. & Petrini, J. H. Chk2 suppresses the oncogenic potential of DNA replication-associated DNA damage. *Molecular cell* **31**, 21-32, doi:10.1016/j.molcel.2008.04.028 (2008).
42 Chapman, J. R., Taylor, M. R. G. & Boulton, S. J. Playing the end game: DNA double-strand break repair pathway choice. *Molecular cell* **47**, 497-510, doi:10.1016/j.molcel.2012.07.029 (2012).
43 Rothkamm, K., Kruger, I., Thompson, L. H. & Lobrich, M. Pathways of DNA double-strand break repair during the mammalian cell cycle. *Molecular and cellular biology* **23**, 5706-5715 (2003).
44 Jankovic, M., Nussenzweig, A. & Nussenzweig, M. C. Antigen receptor diversification and chromosome translocations. *Nature immunology* **8**, 801-808, doi:10.1038/ni1498 (2007).
45 Bassing, C. H., Swat, W. & Alt, F. W. The mechanism and regulation of chromosomal V(D)J recombination. *Cell* **109 Suppl**, S45-55 (2002).
46 Li, X. & Heyer, W. D. Homologous recombination in DNA repair and DNA damage tolerance. *Cell research* **18**, 99-113, doi:10.1038/cr.2008.1 (2008).
47 Bothmer, A. *et al.* 53BP1 regulates DNA resection and the choice between classical and alternative end joining during class switch recombination. *The Journal of experimental medicine* **207**, 855-865, doi:10.1084/jem.20100244 (2010).
48 Bunting, S. F. *et al.* 53BP1 inhibits homologous recombination in Brca1-deficient cells by blocking resection of DNA breaks. *Cell* **141**, 243-254, doi:10.1016/j.cell.2010.03.012 (2010).
49 Chapman, J. R., Sossick, A. J., Boulton, S. J. & Jackson, S. P. BRCA1-associated exclusion of 53BP1 from DNA damage sites underlies temporal control of DNA repair. *Journal of cell science* **125**, 3529-3534, doi:10.1242/jcs.105353 (2012).
50 Shiotani, B. & Zou, L. Single-stranded DNA orchestrates an ATM-to-ATR switch at DNA breaks. *Molecular cell* **33**, 547-558, doi:10.1016/j.molcel.2009.01.024 (2009).
51 Huen, M. S. & Chen, J. Assembly of checkpoint and repair machineries at DNA damage sites. *Trends in biochemical sciences* **35**, 101-108, doi:10.1016/j.tibs.2009.09.001 (2010).

52 Tsukuda, T., Fleming, A. B., Nickoloff, J. A. & Osley, M. A. Chromatin remodelling at a DNA double-strand break site in Saccharomyces cerevisiae. *Nature* **438**, 379-383, doi:10.1038/nature04148 (2005).
53 Goodarzi, A. A. *et al.* ATM signaling facilitates repair of DNA double-strand breaks associated with heterochromatin. *Molecular cell* **31**, 167-177, doi:10.1016/j.molcel.2008.05.017 (2008).
54 Ayoub, N., Jeyasekharan, A. D., Bernal, J. A. & Venkitaraman, A. R. HP1-beta mobilization promotes chromatin changes that initiate the DNA damage response. *Nature* **453**, 682-686, doi:10.1038/nature06875 (2008).
55 Ayoub, N., Jeyasekharan, A. D. & Venkitaraman, A. R. Mobilization and recruitment of HP1: a bimodal response to DNA breakage. *Cell Cycle* **8**, 2945-2950 (2009).
56 Micheva-Viteva, S. *et al.* High-throughput screening uncovers a compound that activates latent HIV-1 and acts cooperatively with a histone deacetylase (HDAC) inhibitor. *The Journal of biological chemistry* **286**, 21083-21091, doi:10.1074/jbc.M110.195537 (2011).
57 Burma, S., Chen, B. P., Murphy, M., Kurimasa, A. & Chen, D. J. ATM phosphorylates histone H2AX in response to DNA double-strand breaks. *The Journal of biological chemistry* **276**, 42462-42467, doi:10.1074/jbc.C100466200 (2001).
58 Yuan, J., Adamski, R. & Chen, J. Focus on histone variant H2AX: to be or not to be. *FEBS letters* **584**, 3717-3724, doi:10.1016/j.febslet.2010.05.021 (2010).
59 Chen, W. T. *et al.* Systematic identification of functional residues in mammalian histone H2AX. *Molecular and cellular biology* **33**, 111-126, doi:10.1128/MCB.01024-12 (2013).
60 Murr, R. *et al.* Histone acetylation by Trrap-Tip60 modulates loading of repair proteins and repair of DNA double-strand breaks. *Nature cell biology* **8**, 91-99, doi:10.1038/ncb1343 (2006).
61 Keogh, M. C. *et al.* A phosphatase complex that dephosphorylates gammaH2AX regulates DNA damage checkpoint recovery. *Nature* **439**, 497-501, doi:10.1038/nature04384 (2006).
62 Shogren-Knaak, M. *et al.* Histone H4-K16 acetylation controls chromatin structure and protein interactions. *Science* **311**, 844-847, doi:10.1126/science.1124000 (2006).
63 Tamburini, B. A. & Tyler, J. K. Localized histone acetylation and deacetylation triggered by the homologous recombination pathway of double-strand DNA repair. *Molecular and cellular biology* **25**, 4903-4913, doi:10.1128/MCB.25.12.4903-4913.2005 (2005).
64 Li, X. *et al.* MOF and H4 K16 acetylation play important roles in DNA damage repair by modulating recruitment of DNA damage repair protein Mdc1. *Molecular and cellular biology* **30**, 5335-5347, doi:10.1128/MCB.00350-10 (2010).
65 Botuyan, M. V. *et al.* Structural basis for the methylation state-specific recognition of histone H4-K20 by 53BP1 and Crb2 in DNA repair. *Cell* **127**, 1361-1373, doi:10.1016/j.cell.2006.10.043 (2006).
66 Miller, K. M. *et al.* Human HDAC1 and HDAC2 function in the DNA-damage response to promote DNA nonhomologous end-joining. *Nature structural & molecular biology* **17**, 1144-1151, doi:10.1038/nsmb.1899 (2010).

67 Tjeertes, J. V., Miller, K. M. & Jackson, S. P. Screen for DNA-damage-responsive histone modifications identifies H3K9Ac and H3K56Ac in human cells. *The EMBO journal* **28**, 1878-1889, doi:10.1038/emboj.2009.119 (2009).
68 Shanbhag, N. M., Rafalska-Metcalf, I. U., Balane-Bolivar, C., Janicki, S. M. & Greenberg, R. A. ATM-dependent chromatin changes silence transcription in cis to DNA double-strand breaks. *Cell* **141**, 970-981, doi:10.1016/j.cell.2010.04.038 (2010).
69 Huen, M. S. & Chen, J. ATM Creates a veil of transcriptional silence. *Cell* **141**, 924-926, doi:10.1016/j.cell.2010.05.035 (2010).
70 Nakamura, K. *et al.* Regulation of homologous recombination by RNF20-dependent H2B ubiquitination. *Molecular cell* **41**, 515-528, doi:10.1016/j.molcel.2011.02.002 (2011).
71 Adam, S., Polo, S. E. & Almouzni, G. Transcription recovery after DNA damage requires chromatin priming by the H3.3 histone chaperone HIRA. *Cell* **155**, 94-106, doi:10.1016/j.cell.2013.08.029 (2013).
72 Clapier, C. R. & Cairns, B. R. The biology of chromatin remodeling complexes. *Annual review of biochemistry* **78**, 273-304, doi:10.1146/annurev.biochem.77.062706.153223 (2009).
73 Smeenk, G. & van Attikum, H. The chromatin response to DNA breaks: leaving a mark on genome integrity. *Annual review of biochemistry* **82**, 55-80, doi:10.1146/annurev-biochem-061809-174504 (2013).
74 Morrison, A. J. *et al.* INO80 and gamma-H2AX interaction links ATP-dependent chromatin remodeling to DNA damage repair. *Cell* **119**, 767-775, doi:10.1016/j.cell.2004.11.037 (2004).
75 Chen, C. C. *et al.* Acetylated lysine 56 on histone H3 drives chromatin assembly after repair and signals for the completion of repair. *Cell* **134**, 231-243, doi:10.1016/j.cell.2008.06.035 (2008).
76 Costelloe, T. *et al.* The yeast Fun30 and human SMARCAD1 chromatin remodellers promote DNA end resection. *Nature* **489**, 581-584, doi:10.1038/nature11353 (2012).
77 Burgess, R. J. & Zhang, Z. Histone chaperones in nucleosome assembly and human disease. *Nature structural & molecular biology* **20**, 14-22, doi:10.1038/nsmb.2461 (2013).
78 Tyler, J. K. Chromatin assembly. Cooperation between histone chaperones and ATP-dependent nucleosome remodeling machines. *European journal of biochemistry / FEBS* **269**, 2268-2274 (2002).
79 Eitoku, M., Sato, L., Senda, T. & Horikoshi, M. Histone chaperones: 30 years from isolation to elucidation of the mechanisms of nucleosome assembly and disassembly. *Cellular and molecular life sciences : CMLS* **65**, 414-444, doi:10.1007/s00018-007-7305-6 (2008).
80 Emili, A., Schieltz, D. M., Yates, J. R. & Hartwell, L. H. Dynamic interaction of DNA damage checkpoint protein Rad53 with chromatin assembly factor Asf1. *Molecular cell* **7**, 13-20 (2001).
81 English, C. M., Adkins, M. W., Carson, J. J., Churchill, M. E. & Tyler, J. K. Structural basis for the histone chaperone activity of Asf1. *Cell* **127**, 495-508, doi:10.1016/j.cell.2006.08.047 (2006).
82 Green, E. M. *et al.* Replication-independent histone deposition by the HIR complex and Asf1. *Current biology : CB* **15**, 2044-2049, doi:10.1016/j.cub.2005.10.053 (2005).

83 Tagami, H., Ray-Gallet, D., Almouzni, G. & Nakatani, Y. Histone H3.1 and H3.3 complexes mediate nucleosome assembly pathways dependent or independent of DNA synthesis. *Cell* **116**, 51-61 (2004).
84 Huang, S. *et al.* Rtt106p is a histone chaperone involved in heterochromatin-mediated silencing. *Proceedings of the National Academy of Sciences of the United States of America* **102**, 13410-13415, doi:10.1073/pnas.0506176102 (2005).
85 Bortvin, A. & Winston, F. Evidence that Spt6p controls chromatin structure by a direct interaction with histones. *Science* **272**, 1473-1476 (1996).
86 Andrews, A. J., Downing, G., Brown, K., Park, Y. J. & Luger, K. A thermodynamic model for Nap1-histone interactions. *The Journal of biological chemistry* **283**, 32412-32418, doi:10.1074/jbc.M805918200 (2008).
87 Park, Y. J., Sudhoff, K. B., Andrews, A. J., Stargell, L. A. & Luger, K. Histone chaperone specificity in Rtt109 activation. *Nature structural & molecular biology* **15**, 957-964 (2008).
88 Selth, L. A. *et al.* An rtt109-independent role for vps75 in transcription-associated nucleosome dynamics. *Molecular and cellular biology* **29**, 4220-4234, doi:10.1128/MCB.01882-08 (2009).
89 Leung-Pineda, V., Ryan, C. E. & Piwnica-Worms, H. Phosphorylation of Chk1 by ATR is antagonized by a Chk1-regulated protein phosphatase 2A circuit. *Molecular and cellular biology* **26**, 7529-7538, doi:10.1128/MCB.00447-06 (2006).
90 Huh, J. & Piwnica-Worms, H. CRL4(CDT2) targets CHK1 for PCNA-independent destruction. *Molecular and cellular biology* **33**, 213-226, doi:10.1128/MCB.00847-12 (2013).
91 Smerdon, M. J. DNA repair and the role of chromatin structure. *Current opinion in cell biology* **3**, 422-428 (1991).
92 Huyen, Y. *et al.* Methylated lysine 79 of histone H3 targets 53BP1 to DNA double-strand breaks. *Nature* **432**, 406-411, doi:10.1038/nature03114 (2004).
93 Sanders, S. L. *et al.* Methylation of histone H4 lysine 20 controls recruitment of Crb2 to sites of DNA damage. *Cell* **119**, 603-614, doi:10.1016/j.cell.2004.11.009 (2004).
94 Polo, S. E., Roche, D. & Almouzni, G. New histone incorporation marks sites of UV repair in human cells. *Cell* **127**, 481-493, doi:10.1016/j.cell.2006.08.049 (2006).
95 Lan, L. *et al.* In situ analysis of repair processes for oxidative DNA damage in mammalian cells. *Proceedings of the National Academy of Sciences of the United States of America* **101**, 13738-13743, doi:10.1073/pnas.0406048101 (2004).
96 Mousson, F., Ochsenbein, F. & Mann, C. The histone chaperone Asf1 at the crossroads of chromatin and DNA checkpoint pathways. *Chromosoma* **116**, 79-93, doi:10.1007/s00412-006-0087-z (2007).
97 Groth, A. *et al.* Human Tousled like kinases are targeted by an ATM- and Chk1-dependent DNA damage checkpoint. *The EMBO journal* **22**, 1676-1687, doi:10.1093/emboj/cdg151 (2003).
98 Krause, D. R. *et al.* Suppression of Tousled-like kinase activity after DNA damage or replication block requires ATM, NBS1 and Chk1. *Oncogene* **22**, 5927-5937, doi:10.1038/sj.onc.1206691 (2003).

99 Gorgoulis, V. G. *et al.* Activation of the DNA damage checkpoint and genomic instability in human precancerous lesions. *Nature* **434**, 907-913, doi:10.1038/nature03485 (2005).
100 Bartkova, J. *et al.* DNA damage response as a candidate anti-cancer barrier in early human tumorigenesis. *Nature* **434**, 864-870, doi:10.1038/nature03482 (2005).
101 Bartek, J., Lukas, J. & Bartkova, J. DNA damage response as an anti-cancer barrier: damage threshold and the concept of 'conditional haploinsufficiency'. *Cell Cycle* **6**, 2344-2347 (2007).
102 Bartkova, J. *et al.* Oncogene-induced senescence is part of the tumorigenesis barrier imposed by DNA damage checkpoints. *Nature* **444**, 633-637, doi:10.1038/nature05268 (2006).
103 Hartwell, L. H. & Kastan, M. B. Cell cycle control and cancer. *Science* **266**, 1821-1828 (1994).
104 Ortega, S., Malumbres, M. & Barbacid, M. Cyclin D-dependent kinases, INK4 inhibitors and cancer. *Biochimica et biophysica acta* **1602**, 73-87 (2002).
105 Lengronne, A. & Schwob, E. The yeast CDK inhibitor Sic1 prevents genomic instability by promoting replication origin licensing in late G(1). *Molecular cell* **9**, 1067-1078 (2002).
106 Ozeri-Galai, E. *et al.* Failure of origin activation in response to fork stalling leads to chromosomal instability at fragile sites. *Molecular cell* **43**, 122-131, doi:10.1016/j.molcel.2011.05.019 (2011).
107 Casper, A. M., Nghiem, P., Arlt, M. F. & Glover, T. W. ATR regulates fragile site stability. *Cell* **111**, 779-789 (2002).
108 Feijoo, C. *et al.* Activation of mammalian Chk1 during DNA replication arrest: a role for Chk1 in the intra-S phase checkpoint monitoring replication origin firing. *The Journal of cell biology* **154**, 913-923, doi:10.1083/jcb.200104099 (2001).
109 Pirzio, L. M., Pichierri, P., Bignami, M. & Franchitto, A. Werner syndrome helicase activity is essential in maintaining fragile site stability. *The Journal of cell biology* **180**, 305-314, doi:10.1083/jcb.200705126 (2008).
110 Fundia, A., Gorla, N. & Larripa, I. Non-random distribution of spontaneous chromosome aberrations in two Bloom Syndrome patients. *Hereditas* **122**, 239-243 (1995).
111 Arlt, M. F. *et al.* BRCA1 is required for common-fragile-site stability via its G2/M checkpoint function. *Molecular and cellular biology* **24**, 6701-6709, doi:10.1128/MCB.24.15.6701-6709.2004 (2004).
112 Jiang, Y. *et al.* Common fragile sites are characterized by histone hypoacetylation. *Human molecular genetics* **18**, 4501-4512, doi:10.1093/hmg/ddp410 (2009).
113 Annunziato, A. T. Assembling chromatin: The long and winding road. *Biochimica et biophysica acta* **1819**, 196-210, doi:10.1016/j.bbagrm.2011.07.005 (2012).
114 Campos, E. I. *et al.* The program for processing newly synthesized histones H3.1 and H4. *Nature structural & molecular biology* **17**, 1343-1351, doi:10.1038/nsmb.1911 (2010).
115 Cook, A. J., Gurard-Levin, Z. A., Vassias, I. & Almouzni, G. A specific function for the histone chaperone NASP to fine-tune a reservoir of soluble H3-H4 in the histone supply chain. *Molecular cell* **44**, 918-927, doi:10.1016/j.molcel.2011.11.021 (2011).

116 Jasencakova, Z. *et al.* Replication stress interferes with histone recycling and predeposition marking of new histones. *Molecular cell* **37**, 736-743, doi:10.1016/j.molcel.2010.01.033 (2010).
117 Groth, A. *et al.* Human Asf1 regulates the flow of S phase histones during replicational stress. *Molecular cell* **17**, 301-311, doi:10.1016/j.molcel.2004.12.018 (2005).
118 Jasencakova, Z. & Groth, A. Restoring chromatin after replication: how new and old histone marks come together. *Seminars in cell & developmental biology* **21**, 231-237, doi:10.1016/j.semcdb.2009.09.018 (2010).
119 Park, Y. J. & Luger, K. The structure of nucleosome assembly protein 1. *Proceedings of the National Academy of Sciences of the United States of America* **103**, 1248-1253, doi:10.1073/pnas.0508002103 (2006).
120 Groth, A. Replicating chromatin: a tale of histones. *Biochemistry and cell biology = Biochimie et biologie cellulaire* **87**, 51-63, doi:10.1139/O08-102 (2009).
121 Han, J., Zhou, H., Li, Z., Xu, R. M. & Zhang, Z. Acetylation of lysine 56 of histone H3 catalyzed by RTT109 and regulated by ASF1 is required for replisome integrity. *The Journal of biological chemistry* **282**, 28587-28596, doi:10.1074/jbc.M702496200 (2007).
122 Ask, K. *et al.* Codanin-1, mutated in the anaemic disease CDAI, regulates Asf1 function in S-phase histone supply. *The EMBO journal* **31**, 2013-2023, doi:10.1038/emboj.2012.55 (2012).
123 Helleday, T., Petermann, E., Lundin, C., Hodgson, B. & Sharma, R. A. DNA repair pathways as targets for cancer therapy. *Nature reviews. Cancer* **8**, 193-204, doi:10.1038/nrc2342 (2008).
124 Helleday, T., Lo, J., van Gent, D. C. & Engelward, B. P. DNA double-strand break repair: from mechanistic understanding to cancer treatment. *DNA repair* **6**, 923-935, doi:10.1016/j.dnarep.2007.02.006 (2007).
125 Murga, M. *et al.* Exploiting oncogene-induced replicative stress for the selective killing of Myc-driven tumors. *Nature structural & molecular biology* **18**, 1331-1335, doi:10.1038/nsmb.2189 (2011).
126 McKenna, W. G., Muschel, R. J., Gupta, A. K., Hahn, S. M. & Bernhard, E. J. The RAS signal transduction pathway and its role in radiation sensitivity. *Oncogene* **22**, 5866-5875, doi:10.1038/sj.onc.1206699 (2003).
127 Rainey, M. D., Charlton, M. E., Stanton, R. V. & Kastan, M. B. Transient inhibition of ATM kinase is sufficient to enhance cellular sensitivity to ionizing radiation. *Cancer research* **68**, 7466-7474, doi:10.1158/0008-5472.CAN-08-0763 (2008).
128 Curtin, N. J. DNA repair dysregulation from cancer driver to therapeutic target. *Nature reviews. Cancer* **12**, 801-817, doi:10.1038/nrc3399 (2012).
129 Kao, G. D. *et al.* Histone deacetylase 4 interacts with 53BP1 to mediate the DNA damage response. *The Journal of cell biology* **160**, 1017-1027, doi:10.1083/jcb.200209065 (2003).
130 Bhaskara, S. *et al.* Deletion of histone deacetylase 3 reveals critical roles in S phase progression and DNA damage control. *Molecular cell* **30**, 61-72, doi:10.1016/j.molcel.2008.02.030 (2008).
131 Bhaskara, S. *et al.* Hdac3 is essential for the maintenance of chromatin structure and genome stability. *Cancer cell* **18**, 436-447, doi:10.1016/j.ccr.2010.10.022 (2010).

132 Fan, W. & Luo, J. SIRT1 regulates UV-induced DNA repair through deacetylating XPA. *Molecular cell* **39**, 247-258, doi:10.1016/j.molcel.2010.07.006 (2010).
133 Wang, R. H. *et al.* Impaired DNA damage response, genome instability, and tumorigenesis in SIRT1 mutant mice. *Cancer cell* **14**, 312-323, doi:10.1016/j.ccr.2008.09.001 (2008).
134 Kaidi, A., Weinert, B. T., Choudhary, C. & Jackson, S. P. Human SIRT6 promotes DNA end resection through CtIP deacetylation. *Science* **329**, 1348-1353, doi:10.1126/science.1192049 (2010).
135 Mostoslavsky, R. *et al.* Genomic instability and aging-like phenotype in the absence of mammalian SIRT6. *Cell* **124**, 315-329, doi:10.1016/j.cell.2005.11.044 (2006).
136 Wang, R. H. *et al.* Interplay among BRCA1, SIRT1, and Survivin during BRCA1-associated tumorigenesis. *Molecular cell* **32**, 11-20, doi:10.1016/j.molcel.2008.09.011 (2008).
137 Gottesman, M. M., Fojo, T. & Bates, S. E. Multidrug resistance in cancer: role of ATP-dependent transporters. *Nature reviews. Cancer* **2**, 48-58, doi:10.1038/nrc706 (2002).
138 Olive, K. P. *et al.* Inhibition of Hedgehog signaling enhances delivery of chemotherapy in a mouse model of pancreatic cancer. *Science* **324**, 1457-1461, doi:10.1126/science.1171362 (2009).
139 Roe, J. L., Nemhauser, J. L. & Zambryski, P. C. TOUSLED participates in apical tissue formation during gynoecium development in Arabidopsis. *The Plant cell* **9**, 335-353, doi:10.1105/tpc.9.3.335 (1997).
140 Roe, J. L., Rivin, C. J., Sessions, R. A., Feldmann, K. A. & Zambryski, P. C. The Tousled gene in A. thaliana encodes a protein kinase homolog that is required for leaf and flower development. *Cell* **75**, 939-950 (1993).
141 Carrera, P. *et al.* Tousled-like kinase functions with the chromatin assembly pathway regulating nuclear divisions. *Genes & development* **17**, 2578-2590, doi:10.1101/gad.276703 (2003).
142 Han, Z., Riefler, G. M., Saam, J. R., Mango, S. E. & Schumacher, J. M. The C. elegans Tousled-like kinase contributes to chromosome segregation as a substrate and regulator of the Aurora B kinase. *Current biology : CB* **15**, 894-904, doi:10.1016/j.cub.2005.04.019 (2005).
143 Han, Z., Saam, J. R., Adams, H. P., Mango, S. E. & Schumacher, J. M. The C. elegans Tousled-like kinase (TLK-1) has an essential role in transcription. *Current biology : CB* **13**, 1921-1929 (2003).
144 Yamakawa, A. *et al.* cDNA cloning and chromosomal mapping of genes encoding novel protein kinases termed PKU-alpha and PKU-beta, which have nuclear localization signal. *Gene* **202**, 193-201 (1997).
145 Silljé, H. H., Takahashi, K., Tanaka, K., Van Houwe, G. & Nigg, E. A. Mammalian homologues of the plant Tousled gene code for cell-cycle-regulated kinases with maximal activities linked to ongoing DNA replication. *The EMBO journal* **18**, 5691-5702, doi:10.1093/emboj/18.20.5691 (1999).
146 Roe, J. L. *et al.* TOUSLED is a nuclear serine/threonine protein kinase that requires a coiled-coil region for oligomerization and catalytic activity. *The Journal of biological chemistry* **272**, 5838-5845 (1997).

147 Krause, D. R. *et al.* Suppression of Tousled-like kinase activity after DNA damage or replication block requires ATM, NBS1 and Chk1. *Oncogene* **22**, 5927-5937, doi:10.1038/sj.onc.1206691 (2003).
148 Silljé, H. H. & Nigg, E. A. Identification of human Asf1 chromatin assembly factors as substrates of Tousled-like kinases. *Current biology : CB* **11**, 1068-1073 (2001).
149 Ehsan, H., Reichheld, J. P., Durfee, T. & Roe, J. L. TOUSLED kinase activity oscillates during the cell cycle and interacts with chromatin regulators. *Plant physiology* **134**, 1488-1499, doi:10.1104/pp.103.038117 (2004).
150 Pilyugin, M., Demmers, J., Verrijzer, C. P., Karch, F. & Moshkin, Y. M. Phosphorylation-mediated control of histone chaperone ASF1 levels by Tousled-like kinases. *PloS one* **4**, e8328, doi:10.1371/journal.pone.0008328 (2009).
151 Li, Y., DeFatta, R., Anthony, C., Sunavala, G. & De Benedetti, A. A translationally regulated Tousled kinase phosphorylates histone H3 and confers radioresistance when overexpressed. *Oncogene* **20**, 726-738, doi:10.1038/sj.onc.1204147 (2001).
152 Kodym, R., Henöckl, C. & Fürweger, C. Identification of the human DEAD-box protein p68 as a substrate of Tlk1. *Biochemical and biophysical research communications* **333**, 411-417, doi:10.1016/j.bbrc.2005.05.136 (2005).
153 Sunavala-Dossabhoy, G. & De Benedetti, A. Tousled homolog, TLK1, binds and phosphorylates Rad9; TLK1 acts as a molecular chaperone in DNA repair. *DNA repair* **8**, 87-102, doi:10.1016/j.dnarep.2008.09.005 (2009).
154 Tyler, J. K. & Kadonaga, J. T. The "dark side" of chromatin remodeling: repressive effects on transcription. *Cell* **99**, 443-446 (1999).
155 Le, S., Davis, C., Konopka, J. B. & Sternglanz, R. Two new S-phase-specific genes from Saccharomyces cerevisiae. *Yeast* **13**, 1029-1042, doi:10.1002/(SICI)1097-0061(19970915)13:11<1029::AID-YEA160>3.0.CO;2-1 (1997).
156 Munakata, T., Adachi, N., Yokoyama, N., Kuzuhara, T. & Horikoshi, M. A human homologue of yeast anti-silencing factor has histone chaperone activity. *Genes to cells : devoted to molecular & cellular mechanisms* **5**, 221-233 (2000).
157 Tang, Y. *et al.* Structure of a human ASF1a-HIRA complex and insights into specificity of histone chaperone complex assembly. *Nature structural & molecular biology* **13**, 921-929, doi:10.1038/nsmb1147 (2006).
158 Corpet, A. *et al.* Asf1b, the necessary Asf1 isoform for proliferation, is predictive of outcome in breast cancer. *The EMBO journal* **30**, 480-493, doi:10.1038/emboj.2010.335 (2011).
159 Kamalyukova, I. G., A. *TLK phosphorylation of Asf1 promotes histone delivery during DNA replication.*
160 Myung, K. & Kolodner, R. D. Induction of genome instability by DNA damage in Saccharomyces cerevisiae. *DNA repair* **2**, 243-258 (2003).
161 Prado, F., Cortes-Ledesma, F. & Aguilera, A. The absence of the yeast chromatin assembly factor Asf1 increases genomic instability and sister chromatid exchange. *EMBO reports* **5**, 497-502, doi:10.1038/sj.embor.7400128 (2004).
162 Linger, J. & Tyler, J. K. The yeast histone chaperone chromatin assembly factor 1 protects against double-strand DNA-damaging agents. *Genetics* **171**, 1513-1522, doi:10.1534/genetics.105.043000 (2005).

163 Hu, F., Alcasabas, A. A. & Elledge, S. J. Asf1 links Rad53 to control of chromatin assembly. *Genes & development* **15**, 1061-1066, doi:10.1101/gad.873201 (2001).
164 Recht, J. *et al.* Histone chaperone Asf1 is required for histone H3 lysine 56 acetylation, a modification associated with S phase in mitosis and meiosis. *Proceedings of the National Academy of Sciences of the United States of America* **103**, 6988-6993, doi:10.1073/pnas.0601676103 (2006).
165 Tsubota, T. *et al.* Histone H3-K56 acetylation is catalyzed by histone chaperone-dependent complexes. *Molecular cell* **25**, 703-712, doi:10.1016/j.molcel.2007.02.006 (2007).
166 Masumoto, H., Hawke, D., Kobayashi, R. & Verreault, A. A role for cell-cycle-regulated histone H3 lysine 56 acetylation in the DNA damage response. *Nature* **436**, 294-298, doi:10.1038/nature03714 (2005).
167 Battu, A., Ray, A. & Wani, A. A. ASF1A and ATM regulate H3K56-mediated cell-cycle checkpoint recovery in response to UV irradiation. *Nucleic acids research* **39**, 7931-7945, doi:10.1093/nar/gkr523 (2011).
168 Lee, C. H., Alpert, B. O., Sankaranarayanan, P. & Alter, O. GSVD comparison of patient-matched normal and tumor aCGH profiles reveals global copy-number alterations predicting glioblastoma multiforme survival. *PloS one* **7**, e30098, doi:10.1371/journal.pone.0030098 (2012).
169 Louis, S. A. & Reynolds, B. A. Generation and differentiation of neurospheres from murine embryonic day 14 central nervous system tissue. *Methods Mol Biol* **290**, 265-280 (2005).
170 Dimri, G. P. *et al.* A biomarker that identifies senescent human cells in culture and in aging skin in vivo. *Proceedings of the National Academy of Sciences of the United States of America* **92**, 9363-9367 (1995).
171 Gloeckner, C. J., Boldt, K. & Ueffing, M. Strep/FLAG tandem affinity purification (SF-TAP) to study protein interactions. *Current protocols in protein science / editorial board, John E. Coligan ... [et al.]* **Chapter 19**, Unit19 20, doi:10.1002/0471140864.ps1920s57 (2009).
172 Wisniewski, J. R., Zougman, A., Nagaraj, N. & Mann, M. Universal sample preparation method for proteome analysis. *Nature methods* **6**, 359-362, doi:10.1038/nmeth.1322 (2009).
173 Dow, L. E. *et al.* A pipeline for the generation of shRNA transgenic mice. *Nature protocols* **7**, 374-393, doi:10.1038/nprot.2011.446 (2012).
174 Hashimoto, M., Matsui, T., Iwabuchi, K. & Date, T. PKU-beta/TLK1 regulates myosin II activities, and is required for accurate equaled chromosome segregation. *Mutation research* **657**, 63-67, doi:10.1016/j.mrgentox.2008.09.001 (2008).
175 Sunavala-Dossabhoy, G., Li, Y., Williams, B. & De Benedetti, A. A dominant negative mutant of TLK1 causes chromosome missegregation and aneuploidy in normal breast epithelial cells. *BMC Cell Biol* **4**, 16, doi:10.1186/1471-2121-4-16 (2003).
176 Yeh, C.-H., Yang, H.-J., Lee, I.-J. & Wu, Y.-C. Caenorhabditis elegans TLK-1 controls cytokinesis by localizing AIR-2/Aurora B to midzone microtubules. *Biochemical and biophysical research communications* **400**, 187-193, doi:10.1016/j.bbrc.2010.07.146 (2010).
177 Copp, A. J. Death before birth: clues from gene knockouts and mutations. *Trends in genetics : TIG* **11**, 87-93, doi:10.1016/S0168-9525(00)89008-3 (1995).

178 Nieman, B. J., Wong, M. D. & Henkelman, R. M. Genes into geometry: imaging for mouse development in 3D. *Current opinion in genetics & development* **21**, 638-646, doi:10.1016/j.gde.2011.08.009 (2011).
179 Guillemot, F. *et al.* Genomic imprinting of Mash2, a mouse gene required for trophoblast development. *Nature genetics* **9**, 235-242, doi:10.1038/ng0395-235 (1995).
180 Wu, L. *et al.* Extra-embryonic function of Rb is essential for embryonic development and viability. *Nature* **421**, 942-947, doi:10.1038/nature01417 (2003).
181 Parisi, T. *et al.* Cyclins E1 and E2 are required for endoreplication in placental trophoblast giant cells. *The EMBO journal* **22**, 4794-4803, doi:10.1093/emboj/cdg482 (2003).
182 Varmuza, S., Prideaux, V., Kothary, R. & Rossant, J. Polytene chromosomes in mouse trophoblast giant cells. *Development* **102**, 127-134 (1988).
183 Zybina, E. V. & Zybina, T. G. Polytene chromosomes in mammalian cells. *International review of cytology* **165**, 53-119 (1996).
184 Dillon, P. J. *et al.* Tousled-like kinases modulate reactivation of gammaherpesviruses from latency. *Cell host & microbe* **13**, 204-214, doi:10.1016/j.chom.2012.12.005 (2013).
185 Sen, S. P. & De Benedetti, A. TLK1B promotes repair of UV-damaged DNA through chromatin remodeling by Asf1. *BMC Mol Biol* **7**, 37, doi:10.1186/1471-2199-7-37 (2006).
186 Johnson, S. A. & Hunter, T. Kinomics: methods for deciphering the kinome. *Nature methods* **2**, 17-25, doi:10.1038/nmeth731 (2005).
187 Jiao, Y. *et al.* Surprising complexity of the Asf1 histone chaperone-Rad53 kinase interaction. *Proc Natl Acad Sci USA*, doi:10.1073/pnas.1106023109 (2012).
188 Rapali, P. *et al.* DYNLL/LC8: a light chain subunit of the dynein motor complex and beyond. *The FEBS journal* **278**, 2980-2996, doi:10.1111/j.1742-4658.2011.08254.x (2011).
189 Regue, L. *et al.* DYNLL/LC8 protein controls signal transduction through the Nek9/Nek6 signaling module by regulating Nek6 binding to Nek9. *The Journal of biological chemistry* **286**, 18118-18129, doi:10.1074/jbc.M110.209080 (2011).
190 Rapali, P. *et al.* Directed evolution reveals the binding motif preference of the LC8/DYNLL hub protein and predicts large numbers of novel binders in the human proteome. *PloS one* **6**, e18818, doi:10.1371/journal.pone.0018818 (2011).
191 Ronald, S., Sunavala-Dossabhoy, G., Adams, L., Williams, B. & De Benedetti, A. The expression of tousled kinases in CaP cell lines and its relation to radiation response and DSB repair. *The Prostate*, doi:10.1002/pros.21358 (2011).
192 Stolk, L. *et al.* Meta-analyses identify 13 loci associated with age at menopause and highlight DNA repair and immune pathways. *Nature genetics* **44**, 260-268, doi:10.1038/ng.1051 (2012).
193 Sunavala-Dossabhoy, G. *et al.* TAT-mediated delivery of Tousled protein to salivary glands protects against radiation-induced hypofunction. *International journal of radiation oncology, biology, physics* **84**, 257-265, doi:10.1016/j.ijrobp.2011.10.064 (2012).

194 Palaniyandi, S. *et al.* Adenoviral delivery of Tousled kinase for the protection of salivary glands against ionizing radiation damage. *Gene Ther* **18**, 275-282, doi:10.1038/gt.2010.142 (2011).
195 Lin, E. Y. *et al.* Progression to malignancy in the polyoma middle T oncoprotein mouse breast cancer model provides a reliable model for human diseases. *The American journal of pathology* **163**, 2113-2126, doi:10.1016/S0002-9440(10)63568-7 (2003).
196 Stracker, T. H., Roig, I., Knobel, P. A. & Marjanovic, M. The ATM signaling network in development and disease. *Frontiers in genetics* **4**, 37, doi:10.3389/fgene.2013.00037 (2013).
197 Gunjan, A. & Verreault, A. A Rad53 kinase-dependent surveillance mechanism that regulates histone protein levels in S. cerevisiae. *Cell* **115**, 537-549 (2003).
198 Moggs, J. G. *et al.* A CAF-1-PCNA-mediated chromatin assembly pathway triggered by sensing DNA damage. *Molecular and cellular biology* **20**, 1206-1218 (2000).
199 Mello, J. A. *et al.* Human Asf1 and CAF-1 interact and synergize in a repair-coupled nucleosome assembly pathway. *EMBO reports* **3**, 329-334, doi:10.1093/embo-reports/kvf068 (2002).
200 Hardcastle, I. R. *et al.* Discovery of potent chromen-4-one inhibitors of the DNA-dependent protein kinase (DNA-PK) using a small-molecule library approach. *Journal of medicinal chemistry* **48**, 7829-7846, doi:10.1021/jm050444b (2005).
201 Tanaka, S., Kunath, T., Hadjantonakis, A. K., Nagy, A. & Rossant, J. Promotion of trophoblast stem cell proliferation by FGF4. *Science* **282**, 2072-2075 (1998).
202 Cross, J. C. *et al.* Hxt encodes a basic helix-loop-helix transcription factor that regulates trophoblast cell development. *Development* **121**, 2513-2523 (1995).
203 Tsantoulis, P. K. *et al.* Oncogene-induced replication stress preferentially targets common fragile sites in preneoplastic lesions. A genome-wide study. *Oncogene* **27**, 3256-3264, doi:10.1038/sj.onc.1210989 (2008).
204 Debatisse, M., Le Tallec, B., Letessier, A., Dutrillaux, B. & Brison, O. Common fragile sites: mechanisms of instability revisited. *Trends in genetics : TIG* **28**, 22-32, doi:10.1016/j.tig.2011.10.003 (2012).
205 De Benedetti, A. Tousled kinase TLK1B counteracts the effect of Asf1 in inhibition of histone H3-H4 tetramer formation. *BMC research notes* **2**, 128, doi:10.1186/1756-0500-2-128 (2009).
206 Schmidt, J. C. *et al.* Aurora B kinase controls the targeting of the Astrin-SKAP complex to bioriented kinetochores. *The Journal of cell biology* **191**, 269-280, doi:10.1083/jcb.201006129 (2010).
207 Canfield, C., Rains, J. & De Benedetti, A. TLK1B promotes repair of DSBs via its interaction with Rad9 and Asf1. *BMC Mol Biol* **10**, 110, doi:10.1186/1471-2199-10-110 (2009).
208 Chen, C.-C. *et al.* Acetylated lysine 56 on histone H3 drives chromatin assembly after repair and signals for the completion of repair. *Cell* **134**, 231-243, doi:10.1016/j.cell.2008.06.035 (2008).